1993

Chemistry Of Binuclear And Cluster Complexes Of Ruthenium, Cobalt And Nickel

Hameed A. Mirza

CHEMISTRY OF BINUCLEAR AND CLUSTER COMPLEXES OF Ru, Co AND Ni

By

Hameed A. Mirza

Department of Chemistry

Submitted in partial fulfilment of
the requirement for the degree of
Doctor of Philosophy

Faculty of Graduate Studies
The University of Western Ontario
London, Ontario
September 1992

ISBN 0-315-81271-0

Abstract:

The work described in this thesis is mainly focused on the synthesis, characterization and chemical reactivity of dinuclear and trinuclear phosphine substituted carbonyl complexes of Ru, Co and Ni. The thesis can be broadly classified into three sections. The first section comprising chapters 2 and 3, deals with the chemistry of dinuclear and trinuclear ruthenium complexes with dppm, bis(diphenylphosphino)methane, bridging ligands. The reaction mixture $RuCl_3$/dppm/ $NaBH_4$/CO yielded mainly trans-$[RuCl_2(dppm)_2]$. However, when silver acetate was added to the reaction mixture prior to the reduction with $NaBH_4$, a high yield synthesis of $[Ru_2(\mu\text{-}CO)(CO)_4(\mu\text{-}dppm)_2]$ was achieved. In addition, $[RuH(CO)(dppm)_2]^+$ and the electron rich cluster $[Ru_3(CO)_6(\mu\text{-}dppm)_3]$ were also isolated. Reactions of $[Ru_2(\mu\text{-}CO)(CO)_4(\mu\text{-}dppm)_2]$ with alkynes produced several new products. Structural details of $[Ru_3(CO)_6(\mu\text{-}dppm)_3]$ and its protonated adduct $[Ru_3(\mu\text{-}H)(CO)_6(\mu\text{-}dppm)_3]^+$ are discussed and the mechanism of fluxionality, involving hydride ligand migration in the latter cluster is postulated.

The second section (chapter 4) deals with the synthesis and characterization of di and tetranuclear cobalt complexes with dmpm, bis(dimethylphosphino)methane, ligands. The dinuclear complex $[Co_2(CO)_4(dmpm)_2]$ was found to exist in two isomeric forms, one with two bridging carbonyl ligands, and the other with only terminal carbonyl ligands. The isomers readily interconvert at room temperature. The dynamics of the fluxional processes and thermodynamics of the equilibrium between isomeric forms were investigated using variable temperature FT-IR, ^{31}P, ^{1}H and ^{13}C NMR techniques. The chemistry of $[Co_2(CO)_4(\mu\text{-}dmpm)_2]$ was also explored. Thus,

reaction with $[Cu(MeCN)_4]^+$ gave a novel heptanuclear mixed metal cluster complex, $[Co_4Cu_3(CO)_8(\mu\text{-dmpm})_4]^+$ for which X-ray crystal structure analysis has shown the presence of a central copper atom with unprecedented square planar geometry. The cluster $[Co_4(CO)_8(\mu\text{-dmpm})_2]$ was also prepared and its structure was established by X-ray crystallography.

Chapters 5-7 discuss the synthesis and characterization of mononuclear, dinuclear and trinuclear nickel complexes formed from the Ni(II)/dppm, Ni(II)/dppm/$NaBH_4$/CO, and Ni(II)/dmpm/$NaBH_3CN$/CO reaction systems. The structure of five coordinate $[NiCl_2(\eta^1\text{-dppm})(\eta^2\text{-dppm})]$ was established by X-ray crystallography and represents the first structurally characterized example of a chelating dppm complex of nickel. The reaction of $[Ni_2(\mu\text{-CO})(CO)_2(\mu\text{-dppm})_2]$ with $[NiCl_2(dppm)_2]$ gave a remarkable dinuclear complex $[Ni_2(\mu\text{-CO})Cl_2(\mu\text{-dppm})_2]$ in which, as shown by X-ray diffraction studies, the two phosphorus donors have trans stereochemistry at one nickel atom and cis stereochemistry at the other. The fluxionality, chemical bonding and magnetic properties of this unusual complex are discussed. When $[Ni_2(\mu\text{-CO})Cl_2(\mu\text{-dppm})_2]$ was pyrolysed under vacuum, or when $[Ni_2(\mu\text{-CO})(CO)_2(\mu\text{-dppm})_2]$ was heated in refluxing chlorinated solvents, there was produced a remarkable trinuclear cluster complex $[Ni_3(\mu_3\text{-CO})(\mu_3\text{-Cl})(\mu\text{-dppm})_3]^+$, containing triply bridging carbonyl and chloride ligands on either side of the Ni_3 triangle.

From the reaction mixture of Ni(II)/dmpm/CO/$NaBH_3CN$, two complexes were isolated and their structures were fully established by X-ray crystal structure analysis. The dinuclear $[Ni_2(CN)_4(\mu\text{-dmpm})_2]$, whose formation involves the cleavage

of the B-C bond of BH_3CN^-, is analogous to known Pd and Pt complexes of the type trans, trans-$[M_2(CN)_4(\mu\text{-dppm})_2]$. The second product was a novel trinuclear complex cation $[Ni_3(\mu\text{-CO})(\mu\text{-dmpm})_4]^{2+}$. This was the major product and represents the first example of a nickel cluster stabilized by a diphosphine ligand. This new coordinatively unsaturated $46e^-$ cluster exhibits remarkable fluxionality in which the fourth dmpm ligand migrates rapidly around the Ni_3 triangle. The single crystal X-ray diffraction study shows that it contains a triply bridging carbonyl group.

Acknowledgment

I wish to express my sincere appreciation, gratitude and perhaps above all, admiration to my supervisor Dr. R.J. Puddephatt. His patience, timely encouragement and immeasurable guidance have contributed greatly to this work. I very much appreciate his undivided attention, far-sighted guidance and generous help throughout the course of this work.

I acknowledge gratefully S. England, V. Richardson, J. Vanstone, G. Hall, M. Scheiring, S. McPhee, B. Harwood, D. Hairsine and the other technical and secretarial staff of the department, especially S. Bock, for printing of this thesis and Diane, Shannon and Cheryl for computer help.

Many thanks are also extended to the faculty, staff and graduate students of the chemistry department at the University of Western Ontario for their advice, assistance and friendship; most notably Dr. S. Roy, Dr. G. Jia and E. Kristof.

I would like to express my sincere thanks to Drs. Vittal, Payne, Ferguson and Muir for their crystallographic expertise.

I would also like to acknowledge my parents for their unbounded optimism and unfaltering patience throughout the duration of this thesis.

Finally I must convey my special thanks to my wife Shehla, for her wit, encouragement and moral support (as well as typing this thesis) which allowed me to pursue my graduate studies and research.

I can not forget my "Bundle of Joy" little daughter Hibbat who cherished me through these years.

This thesis is dedicated
to two most revered persons,

Late Hazrat Mirza Nasir Ahmed Sahib M.A.
who inspired me for higher education

and

Hazrat Mirza Tahir Ahmed Sahib
(The supreme head of the Ahmadiyya community)
for his dedication of global peace.

Table of Contents:

Chapter One

Introduction

Chapter Two

The Reactions of Ru(III) Salts with $NaBH_4$ and $NaBH_3CN$ in the Presence of Diphosphines and CO. The Synthesis, Crystal Structure and Chemistry of $[Ru_2(CO)_4(\mu\text{-}CO)(\mu\text{-}dppm)_2]$.

Chapter Three

The Synthesis, Structural Characterization and Reactivity of a 48 Electron Cluster, $[Ru_3(CO)_6(\mu\text{-dppm})_3]$.

Chapter Four

Synthesis of Di and Tetranuclear Cobalt Complexes Stabilized with Bis(dimethylphosphino)methane. Solution Dynamics and Chemistry of $[Co_2(CO)_4(\mu\text{-dmpm})_2]$ Isomers.

Chapter Five

Syntheses and Structural Characterization of Monomeric Nickel(II) Complexes Stabilized with the Ligand Bis(diphenylphosphino)methane.

Chapter Six

Synthesis, Characterization and Reactivity Studies of Di and Trinuclear Nickel Complexes Bridged by Bis(diphenylphosphino)methane.

Chapter Seven

Synthesis and Characterization of Di- and Trinuclear Nickel Complexes with Bis(dimethylphosphino)methane Bridging Ligands.

List of Figures

List of Tables:

List of Reaction Schemes

List of Appendices

KEY ABBREVIATIONS

Å	=	Angstrom
Anal. calc.	=	analysis calculated
COD	=	cyclooctadiene
Cp	=	cyclopentadiene
dmpm	=	bis(dimethylphosphino)methane
dpam	=	bis(diphenylarsino)methane
dppm	=	bis(diphenylphosphino)methane
FAB	=	fast atom bombardment
Et	=	ethyl
IR	=	infrared
v	=	frequency
L	=	two electron donating ligand
LL	=	bidentate ligand
dppp	=	bis(diphenylphosphino)propane
M	=	metal centre
Me	=	methyl
MS	=	mass spectrum
NMR	=	nuclear magnetic resonance
δ	=	chemical shift
s	=	singlet
d	=	doublet
t	=	triplet
quart.	=	quartet
quint.	=	quintet
br	=	broad
J	=	coupling constant
OAc	=	acetate
Ph	=	phenyl
PP	=	bidentate phosphine
R	=	alkyl or aryl
TBP	=	trigonal bipyramid
THF	=	tetrahydrofuran
X	=	halogen
BM	=	Bohr Magneton
K	=	Kelvin
EDX	=	energy dispersive X-ray

Chapter 1

Introduction

1.1 General Comments:

The chemistry of carbonyl complexes of the transition metals has been, and still remains, one of the most active and productive areas of chemical research. Early work was mainly devoted to the synthesis and the study of binary metal carbonyl compounds, and it is interesting to note that the first metal carbonyl, $Ni(CO)_4$, was made by Mond and coworkers as long ago as 1890.[1-3] Since then, numerous other binary metal carbonyls have been discovered. These compounds possess many interesting properties such as high volatility, high chemical reactivity and the ability to form many derivatives. In addition, carbon monoxide has the very important property of being able to stabilize metals in low positive, zero or even negative oxidation states. This property is generally attributed to synergy in the metal carbonyl bonds. Thus, σ-donation of electron density from the carbonyl to an empty metal **d** orbital of appropriate symmetry is accompanied by back donation of excess electron density from a filled metal **d** orbital to a π^* orbital of the CO group.[1-3] This backbonding effect is considered to be crucial in removing negative charge from the metal atom.

A major consequence of the back donation of electron density from metal **d** orbitals to the π^* orbitals of the CO is the reduction of the CO bond order. Infrared spectroscopy is particularly convenient for detecting this phenomenon. Most transition metal carbonyls obey the effective atomic number rule (EAN) by forming eighteen

electron complexes. Metal-metal bonding is common, particularly with di and polynuclear complexes formed by metals with odd atomic number.

As a ligand, CO is very versatile and can coordinate in several different ways as shown in Fig.1.1. The terminal carbonyl is shown in (a), while (b),(c) and (d) represent CO groups bridging two or three metals respectively. The bridging can be unsymmetrical, as in (b), or symmetrical as in (c) or (d). Structures (e)-(k) show CO groups in which the oxygen of the CO ligand is also involved in bonding to one or two metal centres.[4-6] This mainly occurs in substituted carbonyl derivatives or carbonyl anions. The last three examples, (i),(j) and (k) show essentially end-on arrays and these generally occur when strong oxygen acceptors such as $AlEt_3$ are available.[5,6]

1.2. Fluxionality in Metal Carbonyls:

An important aspect in many polynuclear metal carbonyl complexes is the scrambling of carbon monoxide ligands. This fluxionality has been considered to be similar to the movement of adsorbed CO on metal surfaces. The migration of carbonyl groups in clusters can now be investigated with the help of dynamic ^{13}C NMR spectroscopy. There are four distinct fluxional processes which have now been well documented.[7,8]

1.2.1. Localized Exchange Process:

The fluxional process which involves exchange of carbonyl groups on a single metal atom may be of two types, namely the turnstile rotation and the pairwise

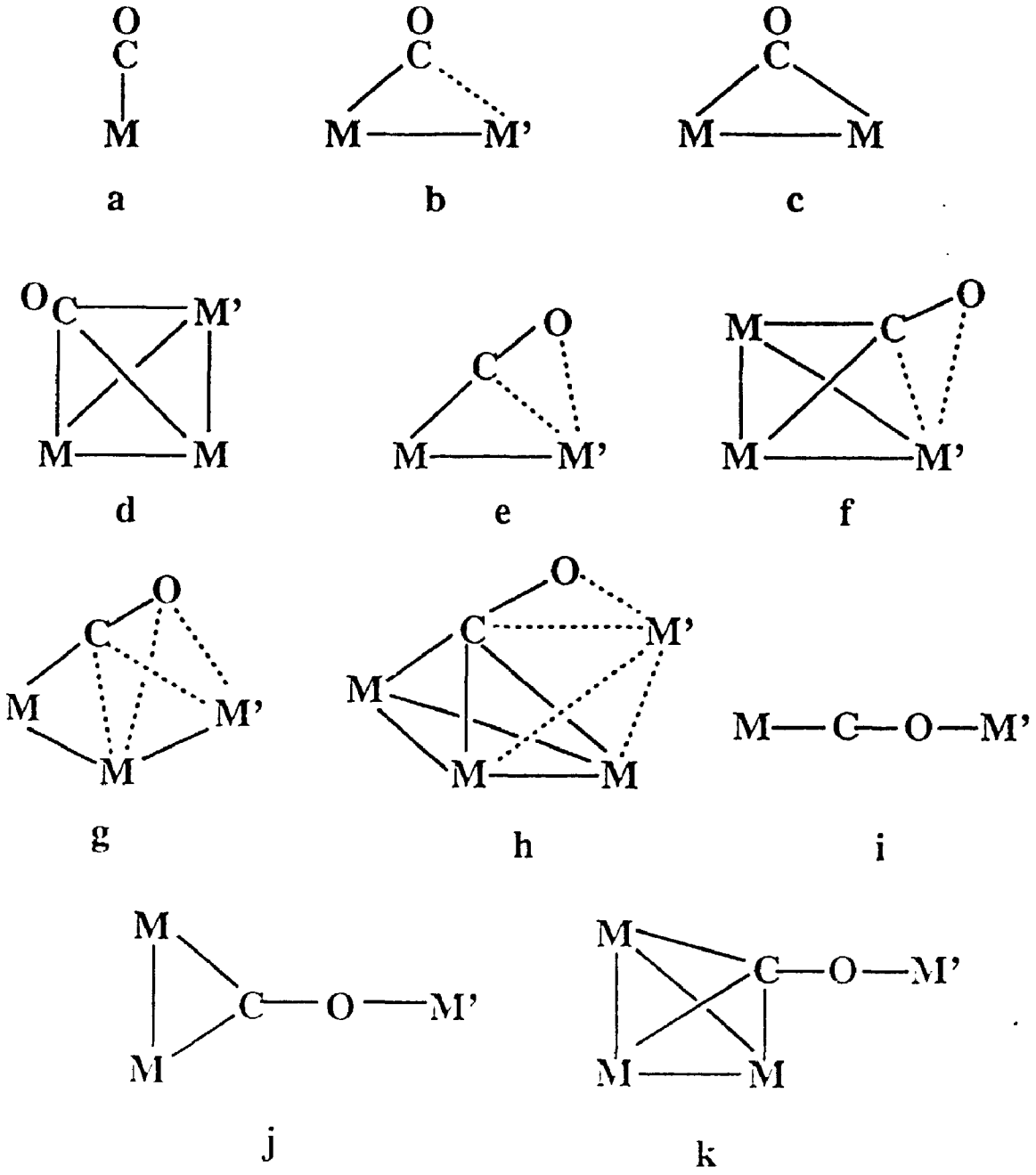

Figure 1.1: Coordination modes of carbon monoxide in metal carbonyls.

exchange. In the complexes $[M_3(\mu\text{-}X)(\mu\text{-}Y)(CO)_{10}]^7$ (M=Os,X=H,Y=H,CR or NO; M=Ru, X=halide, Y=H), turnstile rotation has been observed at $M(CO)_3$ sites and at the two different $M(CO)_3$ sets within the $M(CO)_4$ group. The overall result is exchange of axial/equatorial carbonyl sites. In the pairwise exchange process two carbonyl groups exchange their sites and the configuration is retained. The distinction between pairwise exchange and turnstile rotation is retention of the configuration at the metal in the former process.

1.2.2. Delocalized Exchange:

In contrast to localized exchange involving only one metal atom, a delocalized process occurs between two or more metal atoms. Two mechanisms have been proposed. Johnson has proposed a polytopal rearrangement mechanism for $[Fe_3(CO)_{12}]$.[9,10] The proposal is based on the consideration that the twelve carbonyl groups of $[Fe_3(CO)_{12}]$ can occupy vertices of a distorted icosahedron. The rotation of the Fe_3 triangle inside the polyhedron would lead to equivalence of all carbonyl ligands. The more commonly proposed mechanism involves easy migration of carbonyls between terminal and bridging positions, thus allowing movement across metal-metal bonds.

1.2.3. Oscillation of the Carbonyl.

The unsymmetrically bound carbonyl group of type (e) in Figure 1.1 has been shown to oscillate readily between two metal atoms when this is a degenerate process. The oscillation of an asymmetric bridging ligand therefore, represents a third type of

fluxional process. Thus, in $[Mn_2(\mu\text{-}CO)(CO)_4(\mu\text{-}dppm)_2]$[11], which contain a $\mu\text{-}\eta^2\text{-}CO$ four electron donating ligand, the carbonyl group oscillates between the two metals.

1.2.4. The Rotation of $M(CO)_n$ Unit.

The fourth mechanism involves the rotation of an entire $M(CO)_n$ moiety. Thus, for example, it was observed that the $Pt(CO)(PCy_3)$ moiety rotates above the Os_3 triangle in the complex cation $[Os_3Pt(\mu\text{-}H)_3(CO)_{10}(PCy_3)]^+$.[12] One of four fluxional processes in $[Re_3(CO)_{10}H_3]^{2-}$ involves the rotation of the $ReH(CO)_4$ unit about the axis perpendicular to and bisecting the $[(CO)_3Re(\mu\text{-}H)_2Re(CO)_3]^{2-}$ unit. The dimer anion is isolobal with an acetylene and the proposed motion is reminiscent of acetylene rotation in a side-on η^2-RC≡CR complex.

1.3. Substitution Reactions of Metal Carbonyls:

Substitution reactions of the type shown in equation 1.1 are an important part of metal carbonyl chemistry and may occur (i) simply by mixing together the carbonyl and the appropriate ligand,[13] (ii) by the input of thermal or photochemical energy[14-16] or (iii) by electrochemical activation and related methods.[17]

$$M(CO)x + YL \rightarrow M(CO)_Z L_y + (x\text{-}z)\,CO \quad (1.1).$$

Examples of each method are listed in Table 1.1, which, for the sake of clarity, illustrates mostly phosphines as displacing ligands even though a much wider range of ligands has been used.

Table 1.1 Examples of Substitution Reactions in Metal Carbonyls by Phosphine Ligands.

Reactants			Products	Ref
$Ni(CO)_4 + P(OEt)_3$		→	$Ni(CO)_3(P(OEt)_3)$	13
$Co_2(CO)_8 + 2PPh_3$		→	$Co_2(CO)_6(PPh_3)_2$	13
$Ru_3(CO)_{12}$ +dppm	Δ	→	$Ru_3(CO)_{10}$(dppm)	14
$Cr(CO)_6$ +dppe	Δ	→	$Cr(CO)_4$(dppe)	16
$Cr(CO)_6$ + dmpe	Δ /hν	→	$Cr(CO)_2(dmpe)_2$	16
$Ru_3(CO)_{12} + P(OMe)_3$	hν	→	$Ru_3(CO)_{11}\{P(OMe)_3\}$	15
$Re_2(CO)_{10}$ +dppe	hν	→	$Re_2(CO)_8$(dppe)	15
	Al anode			
$Mo(CO)_6 + PMe_3$		→	$Mo(CO)_5(PMe_3)$	17
	Al anode			
$Mo(CO)_6$ + dmpe		→	$Mo(CO)_4$(dmpe)	17

The characteristics of phosphines as ligands are related to those of CO (and the isocyanides). The phosphorus atom has a pair of electrons which forms a strong σ-bond to the metal. In addition, it has empty 3d orbitals which can accept electron density from the metal[18]. Potentially, therefore, phosphines combine the properties of strong σ donors (as in amines) with those of good π-acceptors (such as CO), although the extent to which the synergic effect and π-bond formation occurs in metal phosphine complexes is a controversial matter.[18-21] The 3d orbitals on phosphorus are much too diffuse and high in energy to interact effectively with the more compact metal nd orbitals. Furthermore, if the metal is in a positive oxidation state then this π-interaction would be further diminished; the higher effective nuclear charge further contracts the metal nd orbitals. Electronegative substituents such as F or OPh on phosphorus increase the effective nuclear charge on phosphorus and contract the 3d orbitals. Such an effect at the same time reduces the basicity of the lone pair on phosphorus. On the other hand, a substituent such as CH_3 on phosphorus would have the opposite effect. It has been shown[19] that the π-acceptor ability of phosphorus donor ligands increases in the following order, $P(^tBu)_3 < PR_3 \sim PPh_3 < P(OR)_3 < PH_3 < P(OPh)_3 < PF_3$ while the σ donor ability is in the approximately reverse order.

For the preparation of binuclear complexes a variety of phosphorus containing ligands have been utilized. Among the most versatile are the diphosphines of the type $R_2P(CH_2)_nPR_2$. These are readily available and are easily handled; several of them are air stable solids.[22,23] In addition, their steric and electronic features can be systematically varied by changing the substituents on the phosphorus atom(s) or by

varying the backbone length between the phosphorus atoms.[24] Details of the steric and electronic effects on transition metal complexes resulting from changing substituents on the phosphorus atom in phosphine ligands have been described elsewhere.[25]

In binuclear complexes these bridging ligands generally adopt trans arrangements at each metal ion. In most cases, this probably occurs for steric reasons, since it places the phosphorus atoms and their bulky substituents as far apart as possible. However, there are now cases known where the phosphine ligand bridges are both cis on each metal and where the phosphine bridges are cis on one metal and trans on another.[26a,b]

The interest in binuclear complexes arises not only due to their novel structures and reactivities but also because of anticipation that they should allow for increased versatility in catalyst design. Complexes with two (or even more) metal atoms can have several advantages over a catalyst containing only a single metal. Small molecules, particularly those like dinitrogen and nitriles which are notoriously difficult to reduce, may be more readily activated by attachment to several metal centres. In catalysts containing two metal centres, one may act to bind the substrate, while the second acts to feed or remove electrons from the first site. Therefore, the presence of two metal atoms may facilitate multi electron redox reactions which could not be handled by only a single metal atom.[26c]

An interesting property of dinuclear complexes bridged by diphosphines is that breaking of metal-metal bonds or the formation or loss of other bridging groups may occur while the actual phosphorus bonds remain intact. Such reactions generally

require that the two metal ions involved are relatively close to one another. As a consequence, bridging phosphine ligands which allow a large distance between metal atoms do not induce particularly interesting chemistry. Conversely, those ligands which force the metals into close association often induce the more interesting new chemistry.[26]

1.4. Metal Cluster Complexes:

Along with the interest in binuclear complexes, there has been considerable development of the chemistry of metal carbonyl clusters. The analogy between metal clusters and metal surfaces as catalytic centres has been drawn.[26,27] A number of clusters have been shown to act as efficient catalysts or catalyst precursors.[28] The precise aim of this activity is to understand, at the molecular level, how catalytic processes occur on metal surfaces by using clusters as models and, possibly, to prepare selective catalysts based on cluster compounds. It has been thought that clusters in which each metal atom is coordinatively unsaturated should be able to mimic the reactions that occur on metal surfaces.[29] Thus, Muetterties had originally observed that many correlations exist between metal surfaces and clusters.[30] Metal core structures of clusters can be viewed as fragments of hexagonal close-packed, or body centred cubic metal bulk structures. The geometries of ligands bound to clusters and to metal surfaces are similar in many instances and the average bond energies for ligand-metal and metal-metal bonds are comparable for specific metals in both the cluster and the transition metal surface. In addition, ligand mobility has been observed for both ligands bound to transition metal clusters and molecules bound to surfaces.

Thus, in the light of the above analogy, the preparation and study of polynuclear complexes can be seen as complementary to the study of surface catalysts. A large variety of metal clusters have therefore been synthesized and their properties investigated. The majority of these cluster complexes are metal carbonyls. An important aspect in cluster catalysis is the integrity of the cluster itself during catalytic processes. Diphosphine substituted metal carbonyl clusters have an added advantage over the binary metal carbonyl clusters since metal carbonyl clusters are held together primarily by metal-metal bonds, whereas phosphine bridged polynuclear complexes have the phosphine bridges, as well as the metal-metal bonds, to maintain the integrity of the polynuclear unit. Thus we find that selective metal-metal bond breaking (as opposed to cluster degradation) is relatively rare for carbonyl clusters.[31] However, metal-metal bond breaking and formation is a fairly common reaction for phosphine-bridged polynuclear complexes. Additionally, with phosphorus ligand-bridged complexes there is an added dimension of synthetic flexibility that occurs because the bridging ligand can now be tailor-made to meet certain requirements. For example, bridging ligands have been constructed with different sites capable of binding different metal ions.

1.5. The Role of $NaBH_4$ and $NaBH_3CN$ in the Synthesis of Metal Carbonyl Complexes:

The extensive use of $NaBH_4$ in synthetic organic chemistry is now well known. However, its use in synthetic inorganic chemistry is fairly limited, although the reduction of metal salts with $NaBH_4$ to produce metal borides of unknown

composition was reported earlier.[32] Several of these borides were found to be catalytically active in the hydrogenation of alkenes.[33] In order to investigate the composition of the catalytically active borides, attempts were made to isolate intermediates by adding tertiary phosphines to the reaction mixtures and hence to obtain a picture of the mechanism of the fast reduction process.[34] This resulted in the isolation of a variety of interesting phosphine complexes of various metals. In addition, several metal-phosphine-borohydride complexes were isolated.

Further insights were obtained when a borohydride in which one of the hydrides in $NaBH_4$ was replaced with an electron withdrawing group was used as reducing agent. This change diminishes the reducing power of the borohydride, and resulted in further slowing down the reduction process. $NaBH_3CN$ was used for reduction of metal halides in the presence of phosphine ligands with interesting results[35]. The CN substituent makes the reagent a versatile ligand as well as a reducing agent, and numerous coordination modes of BH_3CN^- have been identified in products resulting from such reactions.

The introduction of carbon monoxide as an additional stabilizing ligand into the metal halide/phosphine/$NaBH_3Y$ (Y=H,CN) reaction system has provided a rational approach to the synthesis of novel metal-phosphine-carbonyl complexes. Thus, for example, when reaction of $NaBH_4$ or $NaBH_3CN$ with $NiX_2.6H_2O$ and bidentate phosphines were carried out, with a slow stream of CO passed through the solution, a series of Ni(0) complexes were produced.[36,37] It was observed that the complex(es) formed in a particular reaction depends mainly on the nature of the bidentate phosphine and the reducing agent and on the rate of addition of the reducing

agent. Thus, with dppm, $[Ni(CO)_2(\eta^1\text{-dppm})_2]$, $[Ni_2(\mu\text{-CO})(CO)_2(\mu\text{-dppm})_2]$ and $[Ni_2(CO)_4(\mu\text{-dppm})_2]$ were identified. However, with the larger bite phosphines, complexes of the type $[Ni(CO)_2(\eta^2\text{-PP})]$, $[Ni_2(CO)_2(\mu\text{-PP})(\eta^2\text{-PP})_2]$ and $[Ni(CO)(\eta^1\text{-PP})(\eta^2\text{-PP})]$ have been isolated. Similarly, reduction of $PtCl_2/R_2P(CH_2)_nPR_2$ (n = 2, R = Et, Ph, $CHMe_2$; n = 1,3,4, R = Ph) mixtures with $NaBH_4$ under a CO atmosphere provides complexes of the type $[Pt_4(PP)_3(CO)_3]$.[38]

1.6. Aim of the Thesis:

The aim of the research described in this thesis was to synthesize and characterize new diphosphine bridged binuclear and cluster carbonyls of ruthenium, cobalt and nickel. The general synthetic approach was to reduce metal halides with $NaBH_4$ or $NaBH_3CN$ in the presence of the diphosphine and CO in one step. It was anticipated that electron rich carbonyl (diphosphine) metal clusters might be obtained and that these would exhibit high reactivity towards many organometallic reagents.

The thesis is divided into three sections. The first section is concerned with the synthesis and characterization of mononuclear, dinuclear and trinuclear ruthenium complexes with diphosphine ligands. The diphosphine ligands used are dppm and dmpm. The chemistry of the electron rich dinuclear and trinuclear ruthenium complexes has been explored using unsaturated organic and electrophilic inorganic reagents.

The second section deals with the chemistry of cobalt carbonyl complexes with bridging dmpm ligands. The catalytic activity of cobalt carbonyls, particularly in reactions such as hydroformylation, is well known. Moreover, dinuclear and

polynuclear cobalt carbonyls are known to be fluxional and the carbonyl migrations are very fast. It was hoped that diphosphine substituted cobalt carbonyl complexes would give slower carbonyl fluxionality, so that the mechanism could be studied.

The third and the final section is devoted to the chemistry of nickel carbonyl complexes with diphosphine ligands. While palladium and platinum form many useful trinuclear cluster complexes with diphophine ligands, no analogous trinuclear nickel cluster was known prior to this study. It was therefore of interest to prepare new nickel cluster complexes and to compare their chemistry with that of the analogous palladium and platinum clusters. The structural properties of dinuclear nickel complexes were also of interest.

1.7. References:

1. J.C. Hileman; Prep. Inorg. Reactns. *1*, 77 (1964).

2. E.W. Abel; F.G.A. Stone; Quart. Rev. *23*, 325 (1964).

3. J.G. Ameen; H.F. Durfee; J. Chem. Educ. *48*, 372 (1971).

4. F.A.Cotton; G. Wilkinson; Adv. Inorg. Chem, 4th ed. Ch. 25, John Wiley, N.Y. (1980).

5. C.P. Horwitz; D.F. Shriver; Adv. Organomet. Chem. *23*, 219 (1984).

6. I. Haiduc; J.J. Zuckerman; Basic Organomet. Chem., Ch.10, de Gruyter N.Y. (1985).

7. A.J. Deeming; Mech. Inorg. Organomet. React. *4*, 377 (1986).

8. T. Beringhelli; G.D'Alfonso; H. Molionari; D.E. Mann; B.T. Pickup; C.M. Spencer; J.Chem. Soc. Chem. Commun. 796 (1986).

9. B.F.G. Johnson; J. Chem. Soc. Chem. Commun. 703 (1973).

10. (a) H.Dorn; B.E. Hanson; E. Modell; Inorg. Chim. Acta. *54*, L71 (1981).

(b) B.E. Hanson; E.C. Lisic; J.T. Petty; G.A. Iannaconne; Inorg. Chem. *25*, 4062 (1986).

11. J.A. Marsella; K.G. Caulton; Organometallic *1*, 274 (1982).

12. P. Ewing; L.J. Farrugia; D.S. Rycroft; Organometallics *7*, 859 (1988).

13. L.S. Meriwether; M.L. Fiene; J. Am. Chem. Soc. *81*, 4200 (1959).

14. F.A. Cotton; B.E. Hanson; Inorg. Chem. *16*, 3369 (1977).

15. M.F. Desrosiers; D.A. Wink; R. Trautman; A.E. Friedman; P.C. Ford; J. Am. Chem. Soc. *108*, 1917 (1986).

16. J. Chatt; H.R. Watson; J. Chem. Soc. 4980 (1961).

17. D.A. Edwards; Organomet. Chem. *11*, 212 (1983).

18. (a) D.E.C. Corbridge; The Structural Chemistry of Phosphorus, Ch.11, Elsevier Scientific Publishing Co. N.Y. (1974).

(b) D.E.C. Corbridge; Studies in Inorganic Chemistry 2, Ch.10, Elsevier Scientific Publishing Co. N.Y. (1980).

19. A. Pidcock; Transition Metal Complexes Containing P, As, Sb and Bi ligands, Ed. C.A. McAuliffe, McMillan Press, London (1973).

20. E.O. Fischer; E. Louis; R.J.J. Schneider; Angew. Chem. Int. Ed. Engl. *7*, 136 (1968).

21. W. Strohmeir; F.J. Muller; Chem. Ber. *100*, 2812 (1967).

22. J. Chatt; F.A. Hart; J. Chem. Soc. 1378 (1960).

23. W. Hewertson; H.R. Watson; J. Chem. Soc. 1490 (1962).

24.(a) A.R. Sanger; J. Chem. Soc. Chem. Commun. 893 (1975).

(b) ibid, J. Chem. Soc. Dalton Trans. 1971 (1977).

25. C.A. Tolman; Chem. Rev. *77*, 313 (1977).

26. (a) R.J. Puddephatt; Chem. Soc. Rev. 99(1981).

(b) D.G. Holah; A.N. Hughes; V.R. Magnuson; H.A. Mirza; K.O. Parker; Organomet; *7*, 1233 (1988).

(c) A.L. Balch; Homogeneous Catalysis with Metal Phosphine Complexes; ed. L.H. Pignolet, Plenum Press N.Y. (1983).

27. E.L. Muetterties; Bull. Soc. Chem. Belg. *84*, 959 (1975).

28. R. Whyman; Transition Metal Clusters; Ed. B.F.G. Johnson, John Wiley, N.Y. (1980).

29. E.L. Muetterties; Catal. Rev. Sci. Eng. ***23***, 69 (1981).

30.(a) E.L. Muetterties; Angew. Chem. Int. Ed. Engl. ***17***, 545 (1978).

(b) E.L. Muetterties; Science ***196***, 839 (1977).

(c) E.L. Muetterties; J.N. Rhodin; E. Band; C.F. Brucker; W.R. Pretzer; Chem. Rev. ***79***, 91 (1979).

(d) E.Band; E.L. Muetterties; Chem. Rev. ***78***, 639 (1978).

(e) E.L. Muetterties; J. Stein; Chem. Rev. ***79***, 479 (1979).

(f) E.L. Muetterties; J. Organomet. Chem. ***200***, 177 (1980).

(g) E.L. Muetterties; Isr. J. Chem. ***20***, 84 (1980).

31. D.H. Farrar; P.G. Jackson; B.F.G. Johnson; J. Lewis; W.J.H. Nelson; M.D. Vargas; M. McPartlin; J. Chem. Soc. Chem. Commun. 1009 (1981).

32. K. Wade; D.G. Holah; A.N. Hughes; B.C. Hui; Cat. Rev. Sci. Eng. ***14***, 211 (1976).

33. D.G. Holah; I.M. Hoodless; A.N. Hughes; L. Sedor; J. Catal. ***60***, 148 (1979).

34. D.G. Holah; A.N. Hughes; B.C. Hui; S. Khan; Can. J. Chem. ***56***, 2552 (1978).

35. D.G. Holah; A.N. Hughes; N.I. Khan; Can. J. Chem. ***62***, 1016 (1984).

36. D.G. Holah; A.N. Hughes; H. A. Mirza; J.D. Thompson; Inorg. Chim. Acta. ***126***, L7 (1987).

37. D.G. Holah; A.N. Hughes; V.R. Magnuson; H.A. Mirza; K.O. Parker; Organometallics ***1***, 1233 (1988).

38. G. Li; Q. Jiang; L. Zhang; Z. Zhou; S. Wang; Huxaxue Xuebao ***47***, 449 (1989).

Chapter 2

The Reactions of Ru(III) Salts with $NaBH_4$ and $NaBH_3CN$ in the Presence of Diphosphines and CO. The Synthesis, Crystal Structure and Chemistry of $[Ru_2(CO)_4(\mu\text{-}CO)(\mu\text{-}dppm)_2]$.

2.1. Introduction

Although dppm chemistry of other group VIII transition metals has been studied quite extensively, the related chemistry of ruthenium has been rarely studied,[1] perhaps due to the lack of an easily available starting material. Ru-dppm chemistry is mainly limited to mononuclear derivatives, although some binuclear and trinuclear complexes have also been studied in recent years.[2-4] Unlike $[Fe_2(CO)_9]$ which is stable and commercially available, $[Ru_2(CO)_9]$ is extremely unstable and is observed, for example in the formation of $[Ru_3(CO)_{12}]$, as a short lived intermediate.[5] The lack of a simple binuclear carbonyl precursor has made investigations of low valent dinuclear ruthenium complexes difficult. However, some diphosphine derivatives of the unstable binuclear ruthenium carbonyl, $[Ru_2(CO)_9]$,[6] have been prepared and shown to have fascinating properties. Thus for example, the complex $[Ru_2(\mu\text{-}CO)(CO)_4(\mu\text{-}dmpm)_2]$, dmpm = $Me_2PCH_2PMe_2$, has recently been prepared from $[Ru_3(CO)_{12}]$ and dmpm and has been shown to exhibit a very interesting chemistry with unsaturated reagents.[7] The other related complexes $[Ru_2(CO)_4(\mu\text{-}CO)\{\mu\text{-}R_2PN(Et)PR_2\}_2]$, R = OMe or o-i-Pr, are known and displayed unusual chemistry with electrophiles and in redox reactions, forming new carbon dioxide, $Ru_2(\mu\text{-}CO_2)$, complexes for example.[8] However, $[Ru_2(CO)_4(\mu\text{-}CO)(\mu\text{-}dppm)_2]$, 2.1, can only be

prepared by photolysis of $[Ru_3(CO)_{12}]$ with dppm, and the recent synthesis of $[Ru_2(CO)_6(\mu\text{-}CO)(\mu\text{-}dppm)]$ also involves a photochemical step.[8,9] The thermal reaction of $[Ru_3(CO)_{12}]$ with dppm may give $[Ru_3(CO)_{12-2x}(\mu\text{-}dppm)_x]$, x = 1-3, or products arising from metallation of the dppm ligands, but fragmentation to Ru_2 complexes does not occur.[9] This chapter describes the simple one pot, non-photochemical high yield synthesis of 2.1 directly from easily available Ru(III) salts and dppm under carbon monoxide atmosphere using $NaBH_4$ as reducing agent, which makes this complex readily available for studies of its reactivity. In addition, some mononuclear and trinuclear ruthenium complexes were also isolated under these reaction conditions. The chemistry of $[Ru_2(\mu\text{-}CO)(CO)_4(\mu\text{-}dppm)_2]$ 2.1 with unsaturated organic ligands is also explored. Details are discussed in the proceeding pages.

2.2. Ru(III) / dppm / CO / $NaBH_4$ Reaction System:

The reduction of metal halides by sodium borohydride in the presence of carbon monoxide and dppm, has proved to be a useful method for the synthesis of binuclear dppm-bridged metal carbonyl derivatives.[10-13] This method was tested as a possible route to $[Ru_2(CO)_4(\mu\text{-}CO)(\mu\text{-}dppm)_2]$, 2.1. Reduction of $RuCl_3.3H_2O$ under these conditions always gave trans-$[RuCl_2(dppm)_2]$[14] as a major product (scheme 2.1) although, in some syntheses, the desired complex 2.1 was also formed in low yields. It seemed likely that the strong Ru-Cl bonds in $[RuCl_2(dppm)_2]$ were responsible for the difficulty of reduction to the Ru(0) level, and so experiments were carried out in which three equivalents of silver acetate were added to the ruthenium(III) chloride

Scheme 2.1: Reduction of Ru(III) with $NaBH_4$ prior to the addition of ($AgCH_3CO_2$).

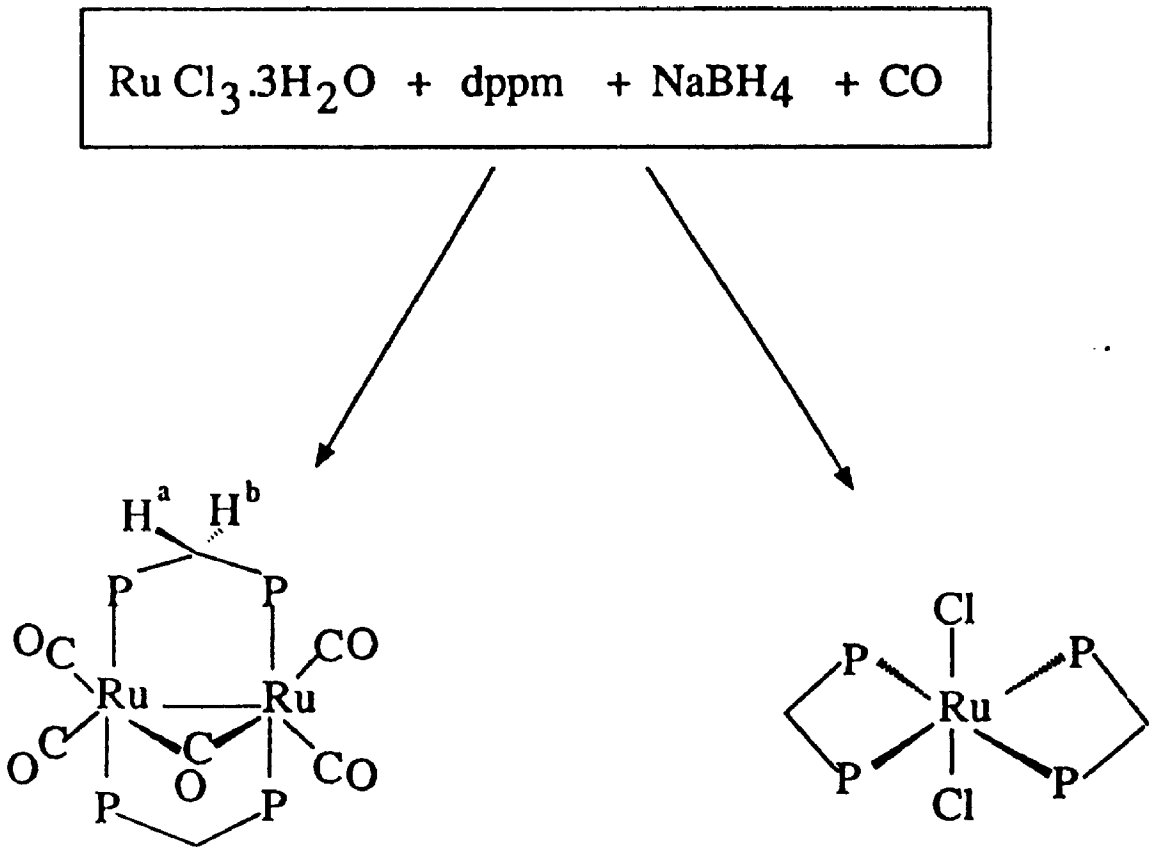

solution to generate in-situ a solution of ruthenium(III) acetate, which was then reduced in the usual way by borohydride in the presence of CO and dppm. This synthesis routinely gave the desired product 2.1 in >60% yield in a single step from ruthenium(III) chloride and so gives a cheaper and more convenient synthesis than the previous methods.[8] This synthesis also gives some trans-$[RuH(CO)(dppm)_2]^+$ ion (scheme 2.2), conveniently isolated as the BPh_4^- salt, which is easily separated from 2.1.[15] In addition, the cluster complex $[Ru_3(CO)_6(\mu\text{-dppm})_3]$, which is more conveniently prepared by reaction of dppm with $[Ru_3(CO)_{12}]$,[9a] can be isolated in low yield from this reaction (scheme 2.2).

2.2.1. The Synthesis of $[Ru_2(CO)_4(\mu\text{-CO})(\mu\text{-dppm})_2]$ 2.1.

The complex 2.1 was synthesized in high yield when Ru(III) acetate, prepared in-situ, was treated with $NaBH_4$ in the presence of dppm under an atmosphere of carbon monoxide. The complex may have been formed according to the following equation.

$$2Ru(III) + 2dppm + 6BH_4^- + 5CO \rightarrow [Ru_2(CO)_5(\mu\text{-dppm})_2] + 3B_2H_6 + 3H_2 \qquad (2.1)$$

The structure of 2.1 was deduced from the spectroscopic data and has also been confirmed by X-ray structure analysis of its solvate $[Ru_2(\mu\text{-CO})(CO)_4(\mu\text{-dppm})_2].C_2H_4Cl_2$, details of which are given below.

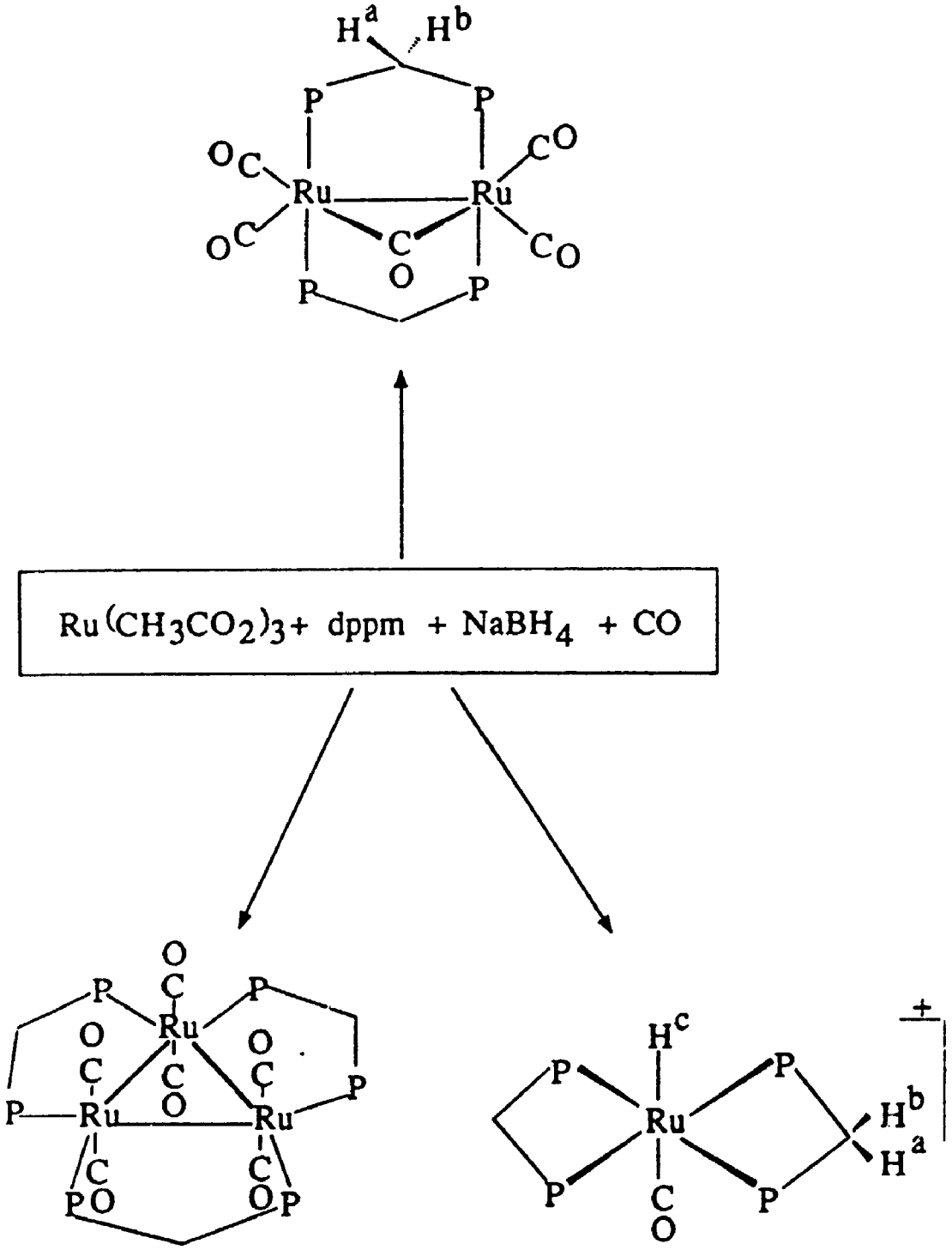

Scheme 2.2: Reduction of Ru(III) with $NaBH_4$ after the addition of $Ag(MeCO_2)$.

2.2.1.1. The X-ray Crystal Structure of $[Ru_2(CO)_4(\mu\text{-}CO)(\mu\text{-}dppm)_2].C_2H_4Cl_2$

A single crystal obtained by slow diffusion of n-pentane to a $C_2H_4Cl_2$ solution of 2.1 was found to be suitable for X-ray diffraction analysis which was carried out by Dr. N.J. Taylor at the University of Waterloo. The structure of $[Ru_2(CO)_4(\mu\text{-}CO)(\mu\text{-}dppm)_2].C_2H_4Cl_2$ consists of well separated units of complex 2.1 and solvent molecules. The ORTEP diagram of the molecular structure is illustrated in Figure 2.1 while bond distances and angles data are listed in Table 2.1. This shows that two ruthenium atoms, which are separated by a distance of 2.903(2)Å, corresponding to a formal ruthenium-ruthenium bond, are bridged by two dppm ligands and a carbonyl group. Each ruthenium metal is further coordinated by two terminal carbonyl groups to achieve 18 electron counts. In addition each Ru_2P_2C ring adopts an envelope conformation with the "flap" directed away from the μ-CO ligand. This leads to axial phenyl substituents surrounding the μ-CO ligand, while the phenyl substituents on the other side of the 5-membered ring are equatorial, thus making room for the carbonyls C(2)-O(2) and C(4)-O(4) (Figure 2.1). The geometric ligand arrangement surrounding each metal can best be described as either approximately trigonal bipyramidal or distorted octahedral with the metal-metal bond occupying the sixth site. For a TBP complex these positions are assigned to two phosphorus atoms of dppm ligands occupying axial sites on each metal and two terminal and a bridging carbonyl group form the equatorial positions. It is apparent from the Table 2.1 that two of the terminal carbonyl groups are essentially orthogonal to the ruthenium-ruthenium vector [Ru(1)-Ru(2)-C(4) 100.0(5)°; Ru(2)-Ru(1)-C(2) 86.9(6)°] while the other two are roughly collinear with it [Ru(1)-Ru(2)-C(3) 148.6(6)°; Ru(2)-Ru(1)-C(1) 155.3(6)°].

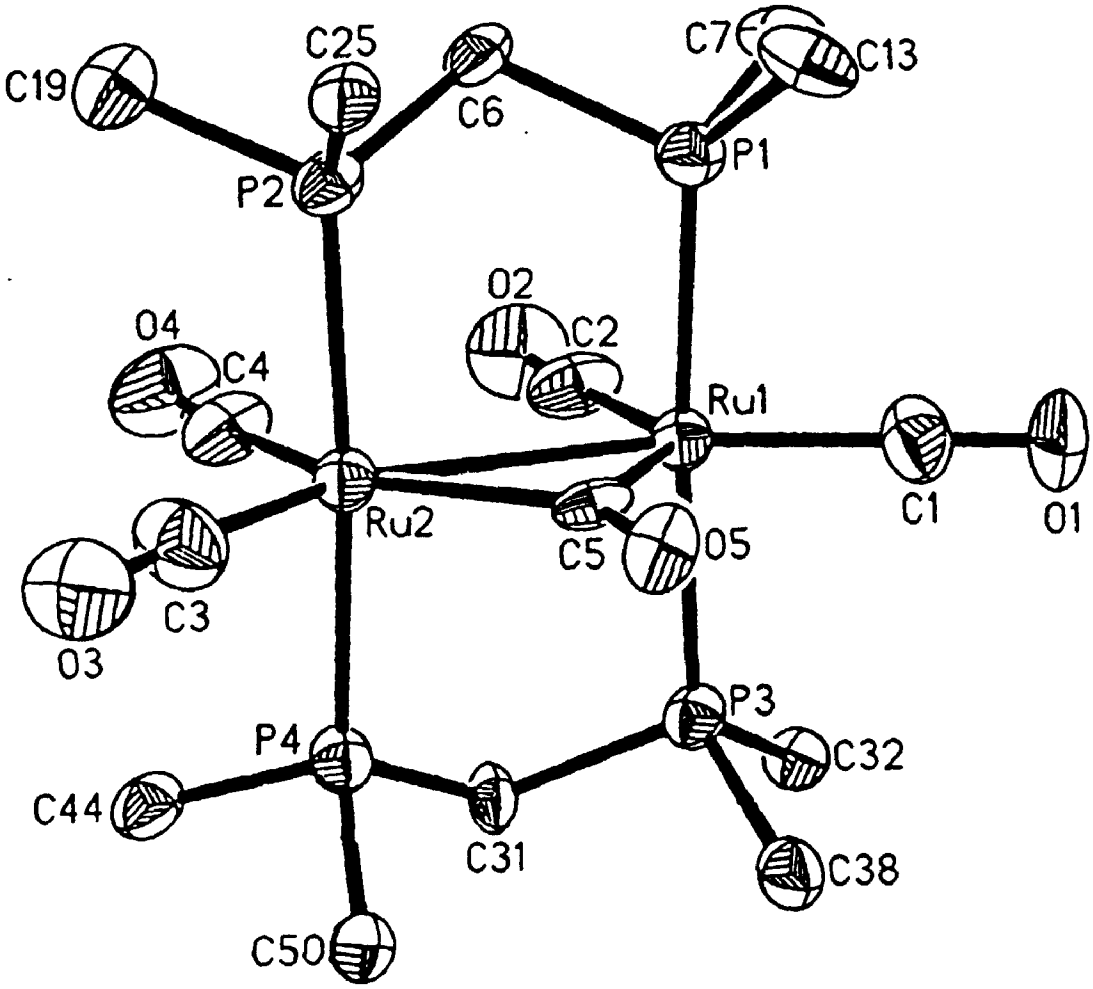

Figure 2.1: The ORTEP diagram of $[Ru_2(CO)_4(\mu\text{-}CO)(\mu\text{-}dppm)_2]$, 2.1.

Table 2.1: Bond Lengths (Å) and Bond Angles (°) for $[Ru_2(\mu\text{-}CO)(CO)_4(\mu\text{-}dppm)_2]$

Ru(1)-Ru(2)	2.903 (2)	Ru(1)-P(1)	2.333 (4)
Ru(1)-P(3)	2.343 (4)	Ru(1)-C(1)	1.869 (18)
Ru(1)-C(2)	1.962 (20)	Ru(1)-C(5)	2.130 (13)
Ru(2)-P(2)	2.340 (4)	Ru(2)-P(4)	2.335 (4)
Ru(2)-C(3)	1.878 (19)	Ru(2)-C(4)	1.917 (17)
Ru(2)-C(5)	2.124 (14)	P(1)-C(6)	1.859 (16)
P(1) -C(7)	1.854 (17)	P(1)-C(13)	1.830 (19)
P(2) -C(6)	1.851 (16)	P(2)-C(19)	1.830 (17)
P(2) -C(25)	1.826 (14)	P(3)-C(31)	1.880 (14)
P(3) -C(32)	1.838 (14)	P(3)-C(38)	1.830 (16)
P(4) -C(31)	1.840 (15)	P(4)-C(44)	1.818 (16)
P(4) -C(50)	1.825 (17)	O(1)-C(1)	1.134 (22)
O(2) -C(2)	1.155 (25)	O(3)-C(3)	1.126 (23)
O(4) -C(4)	1.142 (23)	O(5)-C(5)	1.155 (17)

Bond angles (°)

Ru(2)-Ru(1)-P(1)	91.8(1)	Ru(2)-Ru(1)-P(3)	91.0(1)
P(1)-Ru(1)-P(3)	175.3(1)	Ru(2)-Ru(1)-C(1)	155.3(6)
P(1)-Ru(1)-C(1)	87.8(6)	P(3)-Ru(1)-C(1)	88.0(6)
Ru(2)-Ru(1)-C(2)	86.9(6)	P(1)-Ru(1)-C(2)	89.3(5)
P(3)-Ru(1)-C(2)	94.7(5)	C(1)-Ru(1)-C(2)	117.8(8)
Ru(2)-Ru(1)-C(5)	46.9(4)	P(1)-Ru(1)-C(5)	90.5(4)
P(3)-Ru(1)-C(5)	88.6(3)	C(1)-Ru(1)-C(5)	108.4(7)
C(2)-Ru(1)-C(5)	133.8(7)	Ru(1)-Ru(2)-P(2)	91.5(1)
Ru(1)-Ru(2)-P(4)	91.9(1)	P(2)-Ru(2)-P(4)	175.1(1)
Ru(1)-Ru(2)-C(3)	148.6(6)	P(2)-Ru(2)-C(3)	91.9(6)
P(4)-Ru(2)-C(3)	87.0(6)	Ru(1)-Ru(2)-C(4)	100.0(5)
P(2)-Ru(2)-C(4)	88.3(5)	P(4)-Ru(2)-C(4)	87.7(5)

C(3)-Ru(2)-C(4)	111.3(8)	Ru(1)-Ru(2)-C(5)	47.1(4)
P(2)-Ru(2)-C(5)	91.4(4)	P(4)-Ru(2)-C(5)	93.4(4)
C(3)-Ru(2)-C(5)	101.7(7)	C(4)-Ru(2)-C(5)	147.0(6)
Ru(1)-P(1)-C(6)	113.0(5)	Ru(1)-P(1)-C(7)	114.2(5)
C(6)-P(1)-C(7)	100.7(8)	Ru(1)-P-(1)-C(13)	121.2(6)
C(6)-P(1)-C(13)	103.6(8)	C(7)-P(1)-C(13)	101.3(9)
Ru(2)-P(2)-C(6)	113.8(5)	Ru(2)-P(2)-C(19)	114.5(6)
C(6)-P(2)-C(19)	101.1(7)	Ru(2)-P(2)-C(25)	118.7(5)
C(6)-P(2)-C(25)	106.8(7)	C(19)-P(2)-C(25)	99.9(7)
Ru(1)-P(3)-C(31)	111.3(5)	Ru(1)-P(3)-C(32)	117.0(5)
C(31)-P(3)-C(32)	100.0(7)	Ru(1)-P(3)-C(38)	118.8(5)
C(31)-P(3)-C(38)	105.6(7)	C(32)-P(3)-C(38)	101.9(7)
Ru(2)-P(4)-C(31)	113.8(5)	Ru(2)-P(4)-C(44)	112.3(5)
C(31)-P(4)-C(44)	102.4(7)	Ru(2)-P(4)-C(50)	120.7(6)
C(31)-P(4)-C(50)	103.6(7)	C(44)-P(4)-C(50)	101.8(8)
Ru(1)-C(1)-O(1)	173.9(17)	Ru(1)-C(2)-O(2)	177.5(16)
Ru(2)-C(3)-O(3)	178.3(20)	Ru(2)-C(4)-O(4)	175.1(15)
Ru(1)-C(5)-Ru(2)	86.0(5)	Ru(1)-C(5)-O(5)	135.1(11)
Ru(2)-C(5)-O(5)	138.7(11)	P(1)-C(6)-P(2)	109.8(7)
P(1)-C(7)-C(8)	118.5(18)	P(1)-C(7)-C(8A)	117.7(25)
P(1)-C(7)-C(12)	117.5(22)	P(1)-C(7)-C(12A)	117.2(29)
P(1)-C(13)-C(14)	121.5(17)	P(1)-C(13)-C(18)	115.7(16)
P(2)-C(19)-C(20)	117.8(14)	P(2)-C(19)-C(24)	121.7(14)
P(2)-C(25)-C(26)	120.4(11)	P(2)-C(25)-C(30)	118.7(11)
P(3)-C(31)-P(4)	109.1(7)	P(3)-C(32)-C(33)	118.2(12)
P(3)-C(32)-C(37)	124.2(13)	P(3)-C(38)-C(39)	122.4(12)
P(3)-C(38)-C(43)	118.4(12)	P(4)-C(44)-C(45)	123.1(13)
P(4)-C(44)-C(49)	117.9(13)	P(4)-C(50)-C(51)	117.0(13)
P(4)-C(50)-C(55)	122.7(13)		

The data from Table 2.1 also indicate that all five carbonyl groups, as well as the ruthenium atoms, are approximately coplanar, and that the ruthenium-phosphorus bonds are essentially orthogonal to this plane. Similar structural features were earlier observed in the analogous complexes $[Ru_2(CO)_4(\mu\text{-}CO)(\mu\text{-}dmpm)_2]$ and $[Ru_2(CO)_4(\mu\text{-}CO)\{\mu\text{-}(MeO)_2PN(Et)P(OMe)_2\}_2]$.[7a,8a] Nevertheless the molecule 2.1 is considerably more sterically hindered than the corresponding complexes with dmpm or dmopn ligands. The two dppm ligands are coordinated with ruthenium atoms in approximately trans geometry with an average P-Ru-P of 175.2°. To illustrate similarities and differences between the structures of complex 2.1 with analogous dmpm and dmopn complexes, a comparison of selected molecular dimensions is also given in Table 2.2. The most distinct feature to be noted in Table 2.2 is the ruthenium-ligand bond distances, which follows the series LL = dmopn < dmpm < dppm. The shorter distances for dmopn are probably due to the π-acceptor property of the phosphite ligand which leads to contraction of the orbitals on ruthenium.

2.2.1.2. Spectroscopic Properties of $[Ru_2(CO)_4(\mu\text{-}CO)(\mu\text{-}dppm)_2]$

The infrared spectrum of complex 2.1 is shown in Figure 2.2 and exhibits carbonyl frequencies for both terminal and bridging carbonyl groups at υ(CO) = 1966(s), 1923(vs), 1898(vs), 1883(s) and 1701(s). The lowest energy band is attributed to the carbonyl group coordinated in a bridging fashion, while the remaining bands are assigned to the terminal carbonyl groups. The trend in carbonyl stretching frequencies for 2.1 and analogous dmpm and dmopn complexes is dmopn > dppm > dmpm, indicating that the π-acceptor property of diphosphine ligands

Table 2.2. A Comparison of Molecular Dimensions in $[Ru_2(\mu\text{-}CO)(CO)_4(\mu\text{-}LL)_2]$[a]

	dppm	dmpm	dmopn
Distances (Å)			
Ru-Ru	2.903(2)	2.8928(8)	2.801(2)
Ru-P	2.333(4)-2.343(4)	2.319(1)-2.335(1)	2.290(4)-2.302(4)
Ru-μCO	2.124(15),2.130(15)	2.090(4),2.114(3)	2.06(2),2.08(2)
Ru-C1	1.87(2),1.88(2)	1.859(4),1.865(5)	1.83(2),1.85(2)
Ru-C2	1.92(2),1.96(2)	1.936(3),1.939(3)	1.89(2),1.89(2)
Angles(°)			
Ru-Ru-P	91.0(1)-91.9(1)	90.76(3)-92.53(3)	91.2(1)-91.5(1)
P-Ru-P	175.1(1),175.3(2)	173.1(1),175.9(1)	177.1(2),177.2(2)
Ru-μC-O	135(1),139(1)	136.1(3),136.5(3)	136(1),138(1)
C1-Ru-μC	101.7(8),108.4(7)	101.0(2),103.1(2)	106.3(6),106.6(7)
C2-Ru-μC	133.8(7),147.0(6)	139.4(2),143.1(2)	141.2(5),141.5(6)
C1-Ru-C2	111.3(8),117.8(8)	115.4(2),117.4(2)	112.2(7),112.3(8)
Ru-Ru-μC	46.9(4),47.1(4)	46.2(1),46.9(1)	47.2(4),47.7(4)
Ru-Ru-C1	148.6(6),155.3(6)	147.2(1),149.9(1)	153.9(6),153.8(6)
Ru-Ru-C2	86.9(6),100.0(5)	92.6(1),97.4(1)	93.8(5),94.0(5)

[a]dmpm = $Me_2PCH_2PMe_2$, ref 7a; dmopn = $(MeO)_2PN(Et)P(OMe)_2$, ref 8a

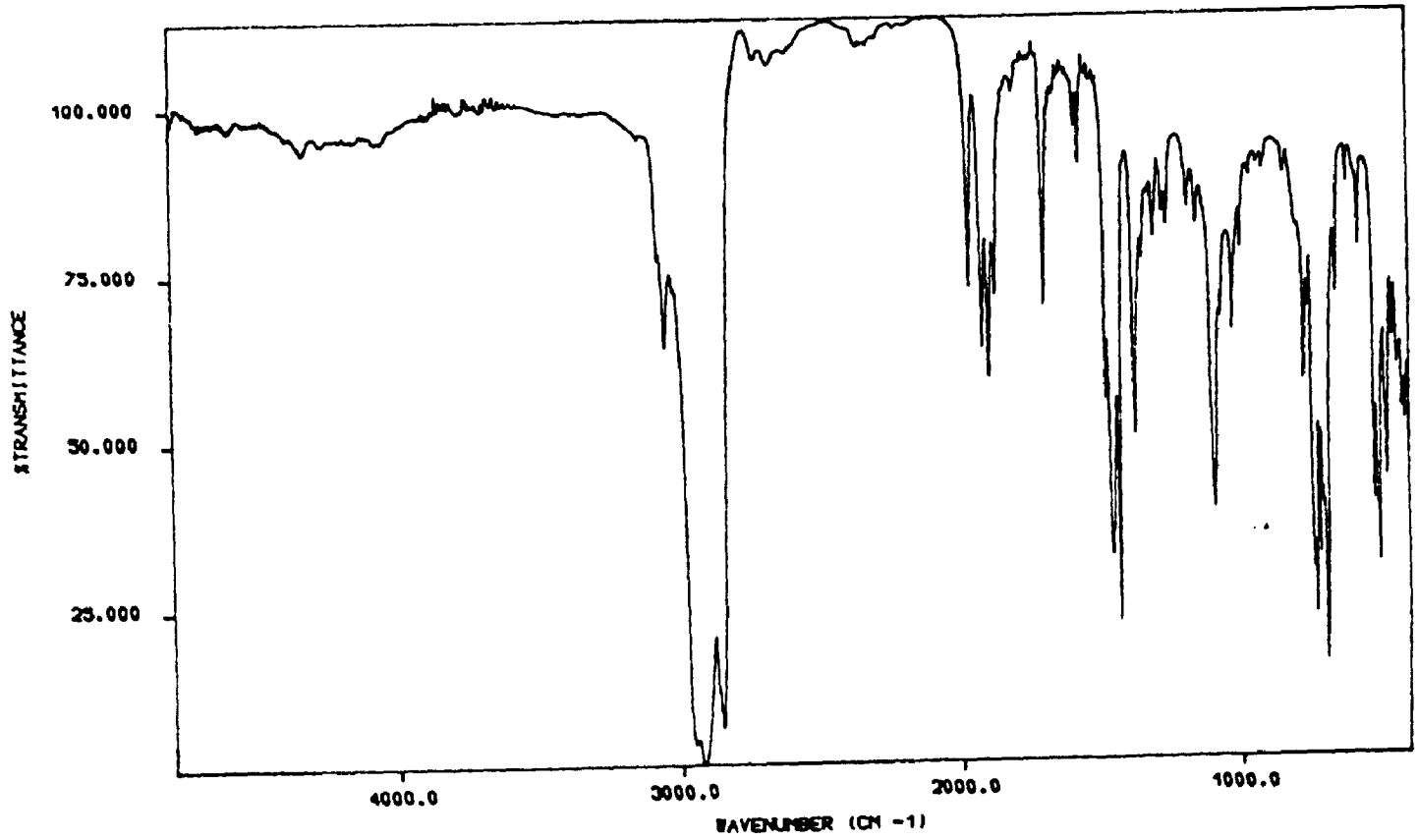

Figure 2.2: The IR spectrum (Nujol) of $[Ru_2(CO)_4(\mu\text{-}CO)(\mu\text{-}dppm)_2]$, 2.1.

follows the same series as that of metal-ligand distances discussed earlier. Thus the ranges for terminal carbonyls are 1913-1999, 1883-1966 and 1874-1954 cm^{-1} and for bridging carbonyls the frequencies are 1703, 1701 and 1694 cm^{-1} for LL = dmopn, dppm and dmpm respectively.[7,8] The longer ruthenium ligand bonds for LL = dppm over dmpm as discussed above are therefore not expected in terms of π-bonding and are attributable to the greater steric hindrance when LL = dppm. The greater steric hindrance is probably also responsible for the greater ranges of apparently equivalent bond distances and angles around the ruthenium centres for LL = dppm, a trend which can be clearly seen from the data in Table 2.2.

The ^{31}P NMR spectrum in CD_2Cl_2 shows, as expected, a single resonance for the two dppm ligands at $\delta = 34.3$ ppm. This suggests that all phosphorus atoms are equivalent and that the dppm is coordinated in a bridging mode to the ruthenium atoms. The ^{1}H NMR spectrum contains only a single resonance for the CH_2 protons of the dppm ligands at $\delta = 3.62$ ppm which splits into a quintet due to coupling with the four phosphorus atoms of the bridging dppm ligands with $J(PH)_{obs} = 4.7$ Hz. Since there is no plane of symmetry containing the Ru_2P_2C rings, due to the presence of the μ-CO ligand on one side only, the $CH^aH^bP_2$ protons of each dppm ligand are expected to be non-equivalent. The apparent equivalence is thus attributed to fluxionality of the carbonyl ligands.[7] Thus, all of the above data is consistent with the structure determined by X-ray crystallographic methods and shown in Figure 2.1.

2.2.2. Characterization of Other Products:

As mentioned earlier and shown in the reaction schemes 2.1 and 2.2, at least

three other products besides 2.1 were also isolated from these reactions. Thus, when reactions were carried out without abstracting chlorides, a yellow crystalline complex could be isolated from the reaction solutions as the major product. The ^{31}P NMR spectrum of this complex in CD_2Cl_2 solution exhibits a single resonance at δ = -12.5 ppm, suggesting that all the phosphorus atoms are equivalent and that the dppm ligand is coordinated in the chelating mode. The ^{1}H NMR spectrum shows a multiplet resonance for the CH_2P_2 protons of the dppm ligand at δ = 5.0 ppm. The IR spectrum does not exhibit any carbonyl band and the elemental analysis suggests a formulation of $[RuCl_2(dppm)_2]$. This was further supported by the FAB-mass spectrum which shows mass ion peak at m/e 940 for $RuCl_2(dppm)_2^+$, in addition it shows peaks at 905 and 869 amu assigned to the $RuCl(dppm)_2^+$ and $Ru(dppm)_2^+$ respectively. Thus, on the basis of all the above information, the compound is characterized as the known octahedral complex trans-$[RuCl_2(dppm)_2]$ 2.2,[14] with both dppm ligands coordinated in a chelating mode.

In contrast, when reduction of $RuCl_3$ with $NaBH_4$ was carried out after abstracting the chlorides with silver acetate, which gives in-situ ruthenium(III) acetate, in addition to the major product 2.1, two additional products, a pale yellow complex 2.3 and a red crystalline complex 3.1 were also isolated from the reaction mixture. The complex 3.1 which was characterized by X-ray diffraction studies will be discussed in chapter 3. The pale yellow complex 2.3 which could be isolated from the mother liquor in about 10% yield by adding $NaBPh_4$ was fully characterized by using the spectroscopic and analytical techniques discussed below.

The ^{31}P NMR spectrum of 2.3 in CD_2Cl_2 solution shows a single resonance at

δ = -6.2 ppm suggesting that the dppm ligand is acting as a chelating ligand and that all the phosphorus atoms are equivalent. The ^1H NMR spectrum of 2.3 is depicted in Figure 2.3 and it shows a high field resonance at δ = -3.6 ppm attributed to a hydride ligand bound to ruthenium, which is split into a quintet with $^2J(PH)$ = 20.5 Hz. due to coupling with four equivalent phosphorus atoms of the two chelating dppm ligand and each line is further split into a triplet with J(HH) = 3.2 Hz., due to coupling with two equivalent methylene protons of the dppm ligands. The methylene protons of the dppm ligand appear as two multiplet resonances centred at δ = 4.97 and 5.30 ppm.

The infrared spectrum shows a strong band at 1983 cm^{-1} with a shoulder at 1999 cm^{-1} arising due to the terminal carbonyl group. Thus, all the above data suggests that the six coordinate complex is monomeric with ruthenium atom chelated by two dppm ligands, and that the CO group and hydride ligand occupy axial positions trans to each other. The crystal structure of the cation has recently been reported by Poilblanc and coworkers[15] who have independently prepared this complex as $[RuH(CO)(dppm)_2][Mn(CO)_5]^-$, IR, ν(CO) = 1990, 1880, 1865, 1830 cm^{-1}; ^{31}P δ = 0 ppm; ^1H, δ = -3.64 J(PH) = 19Hz., [RuH]; 4.9 and 4.7 $[CH_2P_2]$.

2.3. The Ru(III) / dmpm / CO / $NaBH_4$ or $NaBH_3CN$ Reaction System:

While the above reactions, which are abbreviated as the Ru(III) / dppm system, yielded several isolable products, the substitution of the highly basic dmpm ligand for dppm was less successful and produced only one isolable product. This product was characterized by analytical and spectroscopic data. The chemical analysis

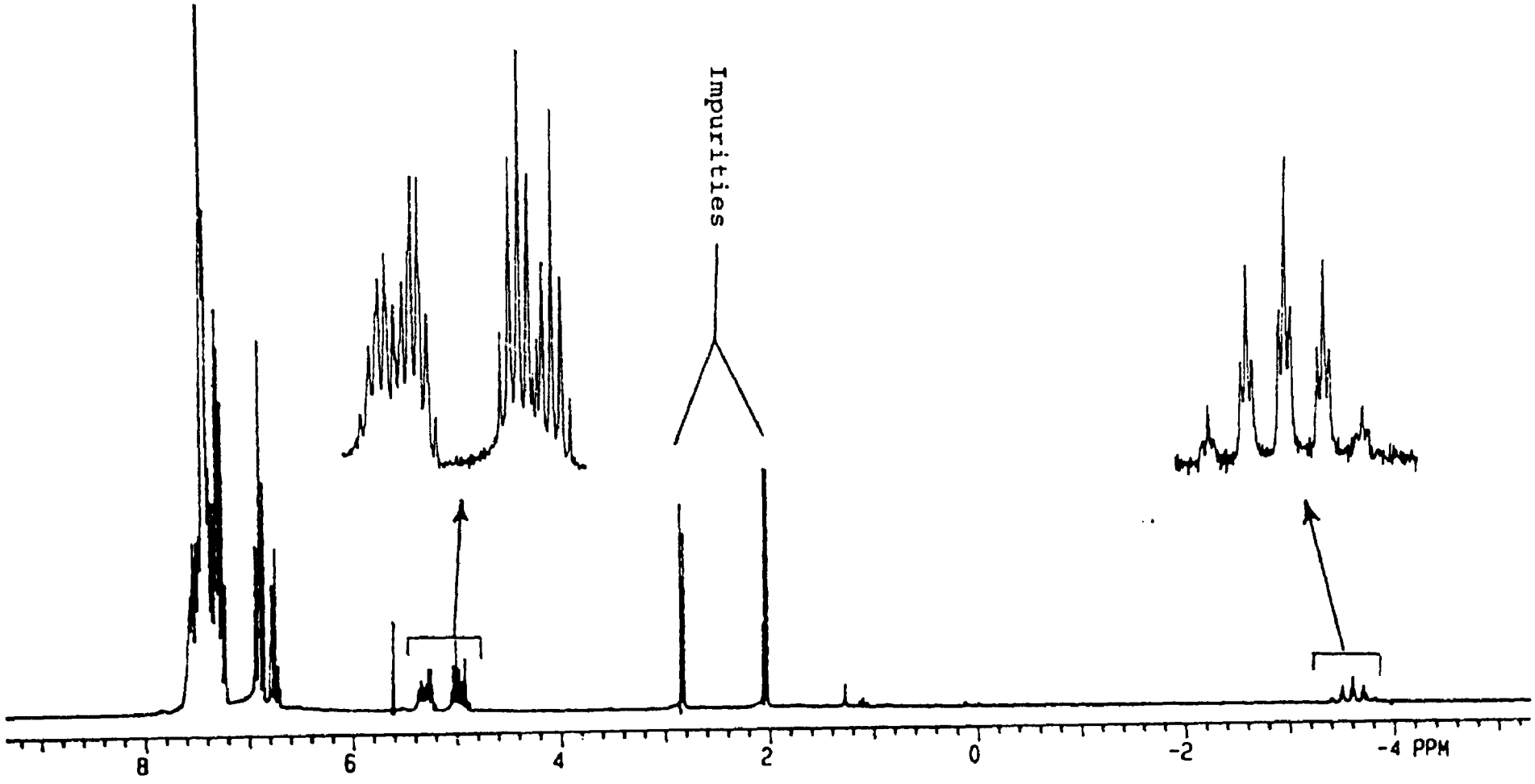

Figure 2.3: The ^{1}H NMR spectrum of $[Ru(H)(CO)(dppm)_2]BPh_4$, 2.3.

suggests a formulation $[Ru(BH_3CN)_2(dmpm)_2]$, 2.4. The infrared spectrum shows bands at 2323 and 2275 cm^{-1} for ν(BH) and two bands at 2218 and 2170 cm^{-1} for ν(C≡N). These bands were assigned to BH_3CN moieties coordinated to ruthenium. Similar bands have been observed for other complexes in which BH_3CN^- acts as a ligand.[16] The ^{31}P NMR spectrum in CD_2Cl_2 solutions shows a sharp singlet resonance at δ = -39.0 ppm consistent with a chelate dmpm ligand and with all the phosphorus atoms equivalent. The ^1H NMR spectrum exhibits a quintet resonance at δ = 3.9 ppm with $J(PH)_{obs}$ = 2.5 Hz., for the CH_2P_2 protons of the dmpm ligand, and a broad multiplet resonance centred at δ = 1.7 ppm which can be attributed to the BH protons of the coordinated BH_3CN^- ligand. Moreover, it shows a doublet resonance at δ = 1.9 ppm assigned to the MeP protons of the dmpm ligand. These protons couple with phosphorus and appear as a doublet with J(PH) = 14 Hz. Thus, on the basis of all the above data, the complex is characterized as octahedral trans-$[Ru(BH_3CN)_2(dmpm)_2]$ where both dmpm ligands are in the chelating mode.

2.4. The Reaction Chemistry of $[Ru_2(CO)_4(\mu\text{-}CO)(\mu\text{-}dppm)_2]$ 2.1.

The organic chemistry of mononuclear metal complexes is fairly well established now, and more attention is being paid to dinuclear metal centres. In seeking to understand the catalysis of organic reactions by metal surfaces or by metal clusters, it is clearly important to consider the simpler dinuclear metal centres as models, particularly with respect to the nature of bonding and reactivity of organic species coordinated at the centre. The premise that the study of polynuclear metal compounds may shed light on metal surface phenomena has been discussed by

Muetterties earlier.[17] The interactions of transition metal complexes with alkynes have been studied in depth. Much of the chemistry remains obscure mechanistically, but there has been speculation that metallacycles are involved with monometal complexes and dimetallacycles with dimetal complexes as reaction intermediates. Moreover, it has also been shown that, in certain metal carbonyl complexes, insertion of an alkyne into a metal-carbon bond can also take place.[18-22] When we started our investigation, diphosphine stabilized dinuclear complexes of ruthenium had not been investigated for their reactivity in this regard. However, Gladfelter and his coworkers have recently reported some reactions of alkynes with the complex $[Ru_2(\mu\text{-}CO)(CO)_4(\mu\text{-dmpm})_2]$ (scheme 2.3).[7] It was considered of interest to investigate the chemistry of electron rich $[Ru_2(\mu\text{-}CO)(CO)_4(\mu\text{-dppm})_2]$ 2.1 with alkynes. The details of these investigations are described in the following pages.

2.4.1. Reaction of 2.1 with PhC≡CPh.

When equimolar amounts of PhC≡CPh and 2.1 were stirred in solution at room temperature no reaction was observed. However, when a solution in $C_2H_4Cl_2$ was heated under reflux for six hours a reddish-yellow solution was formed which, on adding n-pentane, yielded a deep yellow microcrystalline product. This was characterized on the basis of analytical and spectroscopic data. The elemental analysis of this complex suggests a chemical formulation $[Ru_2(CO)_5(PhC{\equiv}CPh)(dppm)_2]$. The IR spectrum of this complex is shown in Figure 2.4 and it exhibits ν(CO) bands at 1972(vs), 1908(vs) and 1690(vs). The energy of the lowest energy band is typical for a ketonic carbonyl but is 10 cm^{-1} lower in energy than the μ-CO ligand in the parent

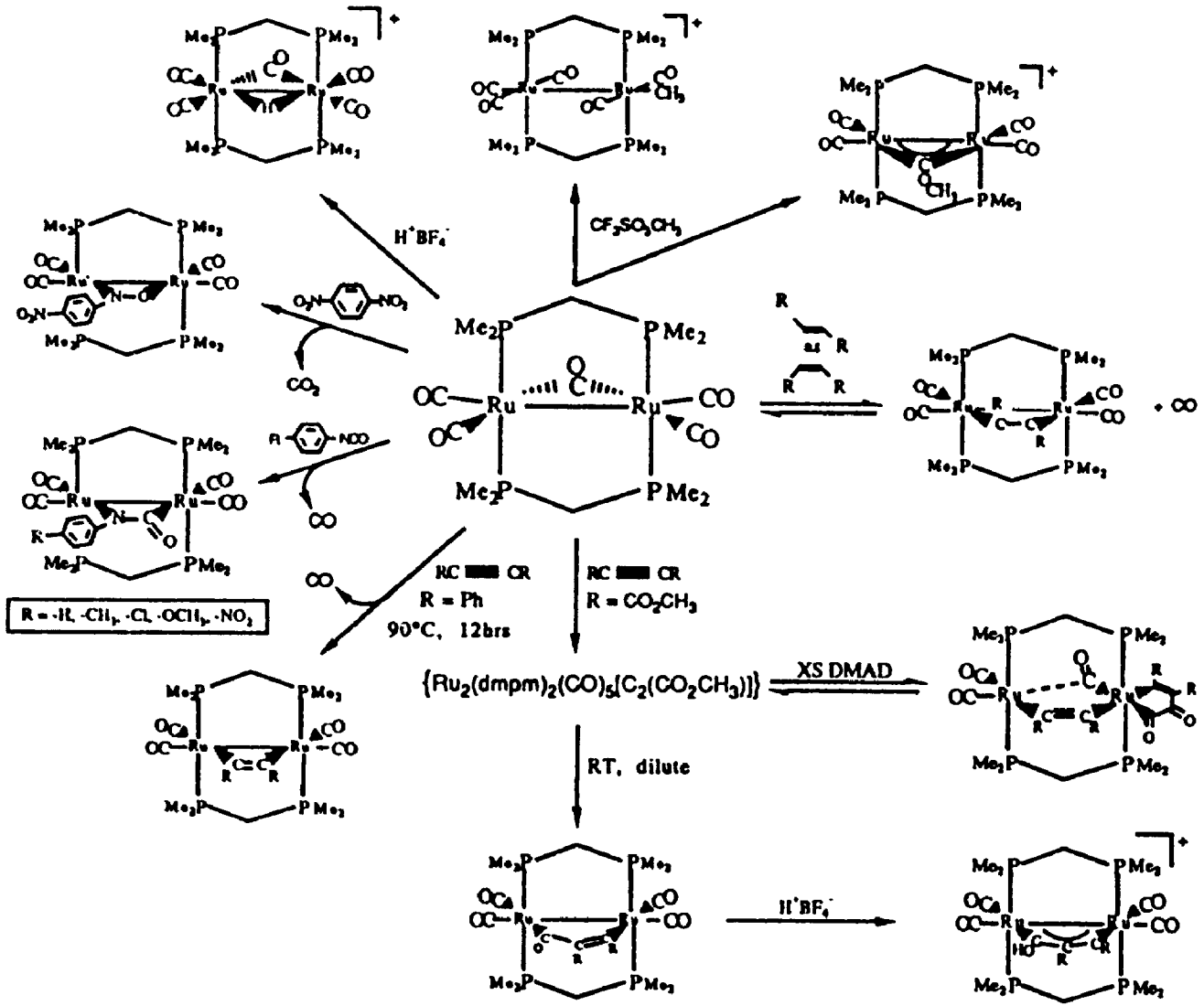

Scheme 2.3: Reactions of $[Ru_2(\mu\text{-CO})(CO)_4(\mu\text{-dmpm})_2]$ with Organic and Inorganic reagents.

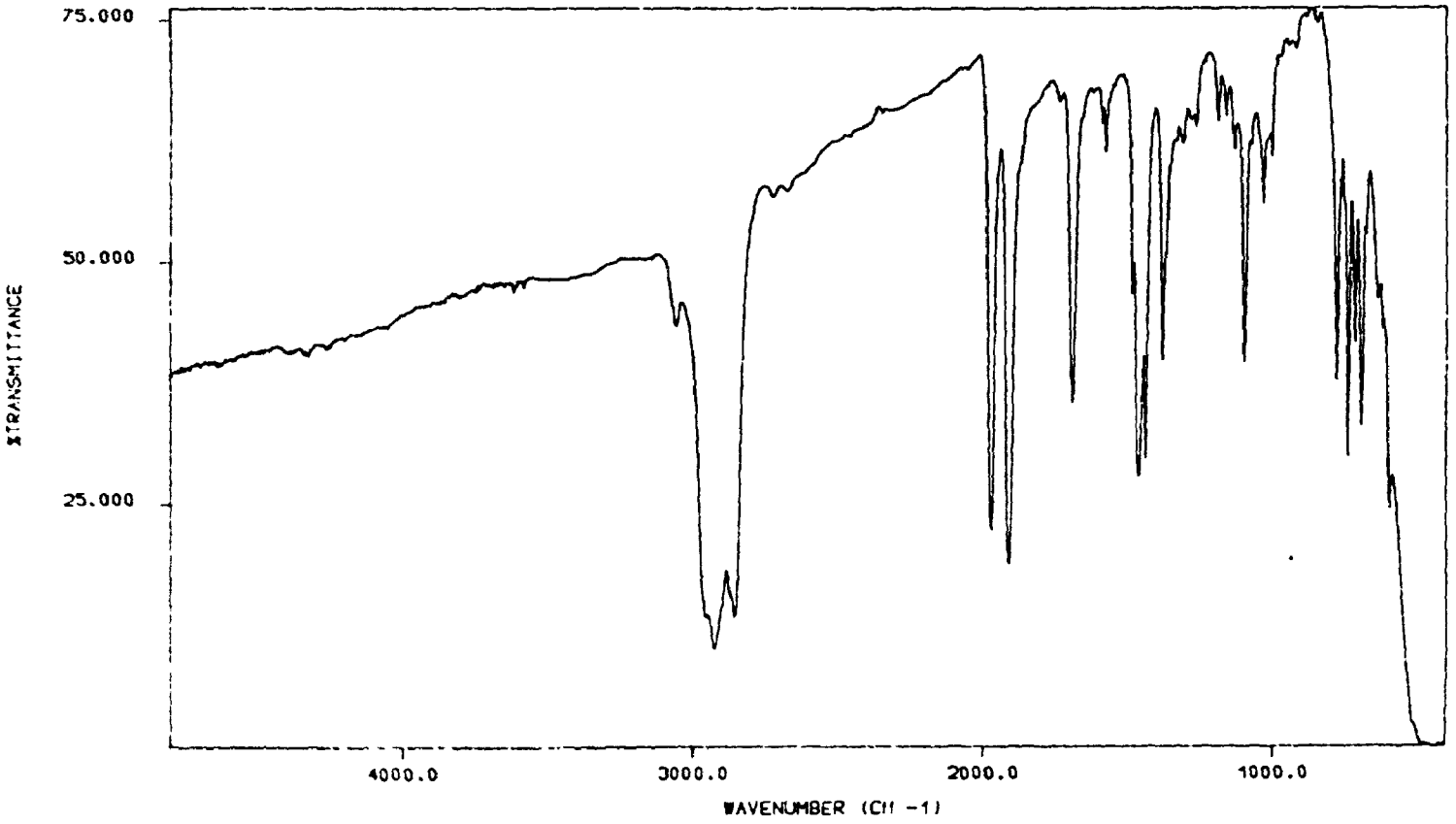

Figure 2.4: The IR spectrum (Nujol) of $[Ru_2(CO)_6\{\mu\text{-}(CO)PhC_2Ph\}(\mu\text{-dppm})_2]$, 2.5.

complex 2.1. The insertion of acetylenes into metal-carbon bonds is well known for both mononuclear and dinuclear metal complexes.[18-21] Thus, for example $M_2(CO)_4(\eta\text{-}C_5H_5)_2$ (M = Fe, Ru) react with RC≡CR to produce complexes in which acetylenes are inserted into metal-carbonyl bond, forming either metallacyclic or dimetallacyclic complexes.[18] Thus, it is possible that PhC≡CPh might have been inserted into a metal carbonyl bond in the above reaction.

The ^{31}P NMR spectrum of the product in CD_2Cl_2 solution is depicted in Figure 2.5. This exhibits an AA'BB' pattern with two apparent triplet resonances centred at δ = 24.0 and 16.8 ppm and with $J(P^aP^b)_{obs}$ = 31.0 Hz. This clearly indicates that the dppm ligands are coordinated in a bridging mode but the two phosphorus atoms of each dppm ligand are inequivalent. The ^1H NMR spectrum of this complex is shown in Figure 2.6. Two multiplet resonances at δ = 3.25 and 4.0 ppm were exhibited in the ^1H NMR, which were attributed to the CH_2P_2 protons of the dppm ligand. Hence there is no plane of symmetry containing the Ru_2dppm_2 skeleton. The presence of the methylene proton signals as doublet of quintets, which appears as an eight line spectrum due to overlap of two lines, confirms that the two dppm ligands were also inequivalent, the quintets being derived from proton-proton coupling along with two different phosphorus-proton couplings. In addition, the ^1H NMR spectrum shows multiplet resonances spanning the region of δ = 6.9-7.6 ppm, which were assignable to phenyl protons of the dppm and alkyne ligands. The evidence suggests that the alkyne is unsymmetrically bound to the ruthenium atoms and this lack of symmetry may arise by insertion of the alkyne into a metal-carbonyl bond as shown in Figure 2.7, structure *a*. The analogous dmpm complex, prepared

Figure 2.5: The ^{31}P NMR spectrum of $[Ru_2(CO)_4\{\mu\text{-}(CO)PhC_2Ph\}(\mu\text{-dppm})_2]$ in CD_2Cl_2.

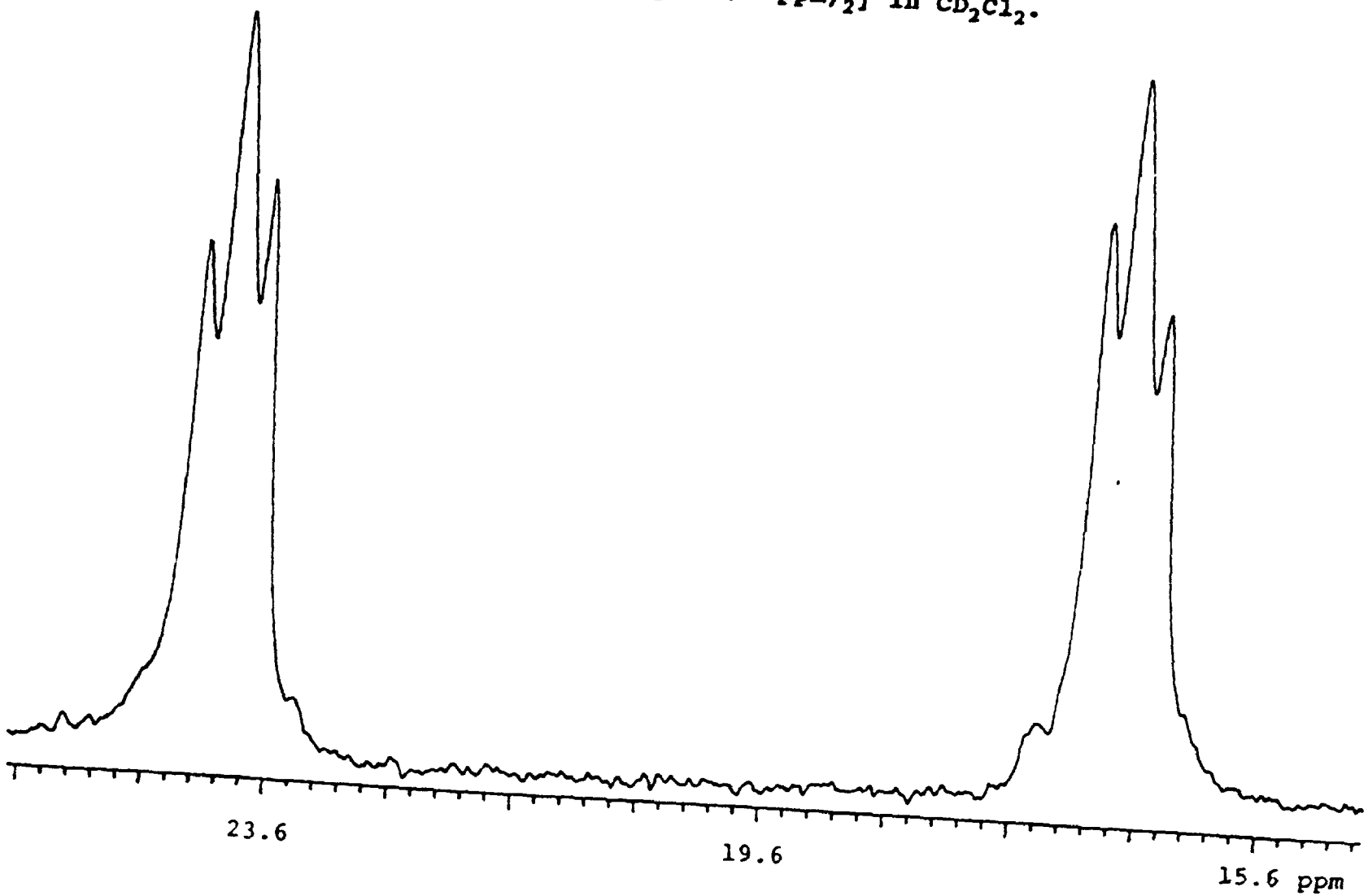

Figure 2.6: The ^{1}H NMR spectrum of $[Ru_2(CO)_4\{\mu\text{-}(CO)PhC_2Ph\}(\mu\text{-dppm})_2]$ in CD_2Cl_2.

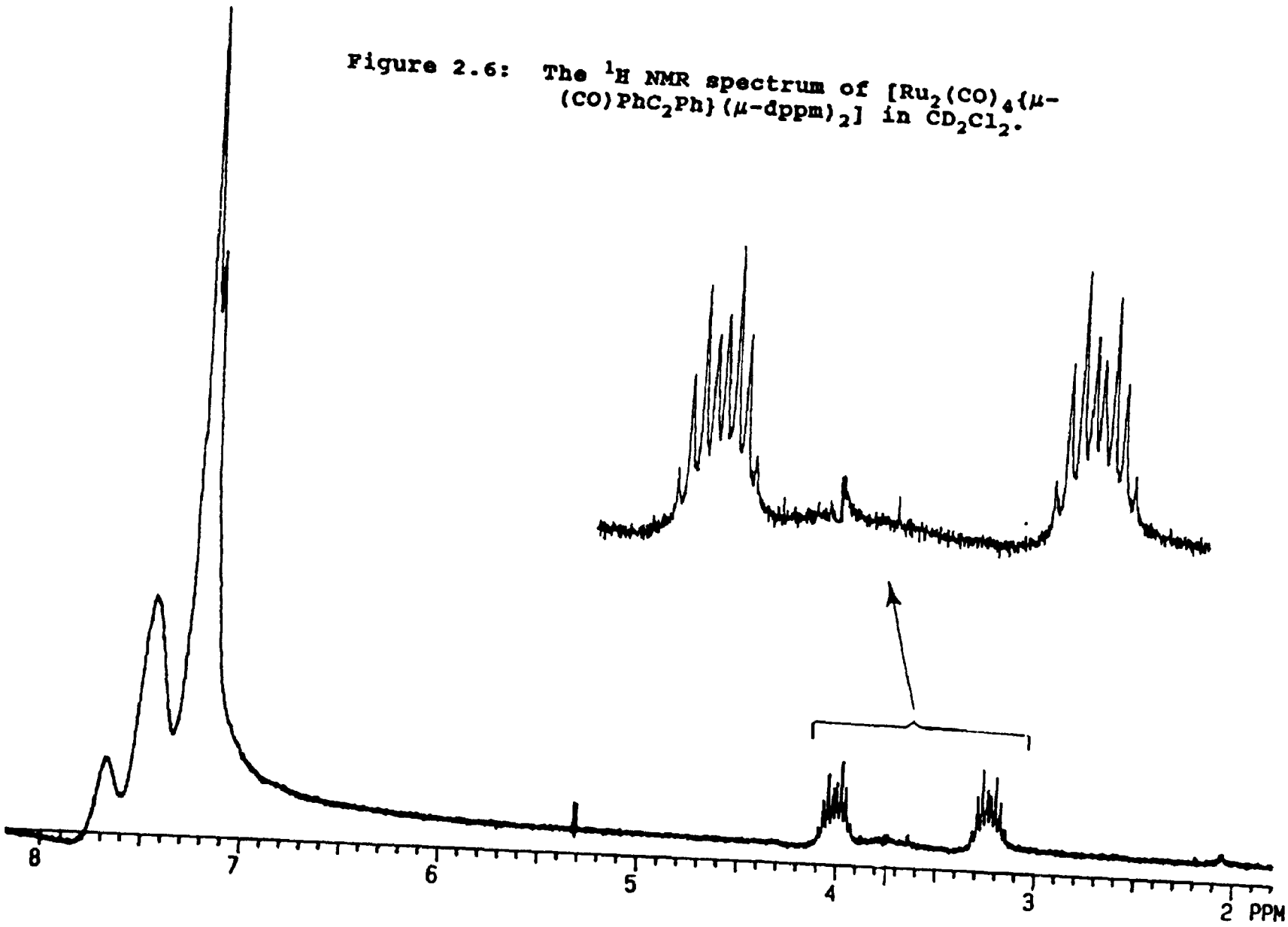

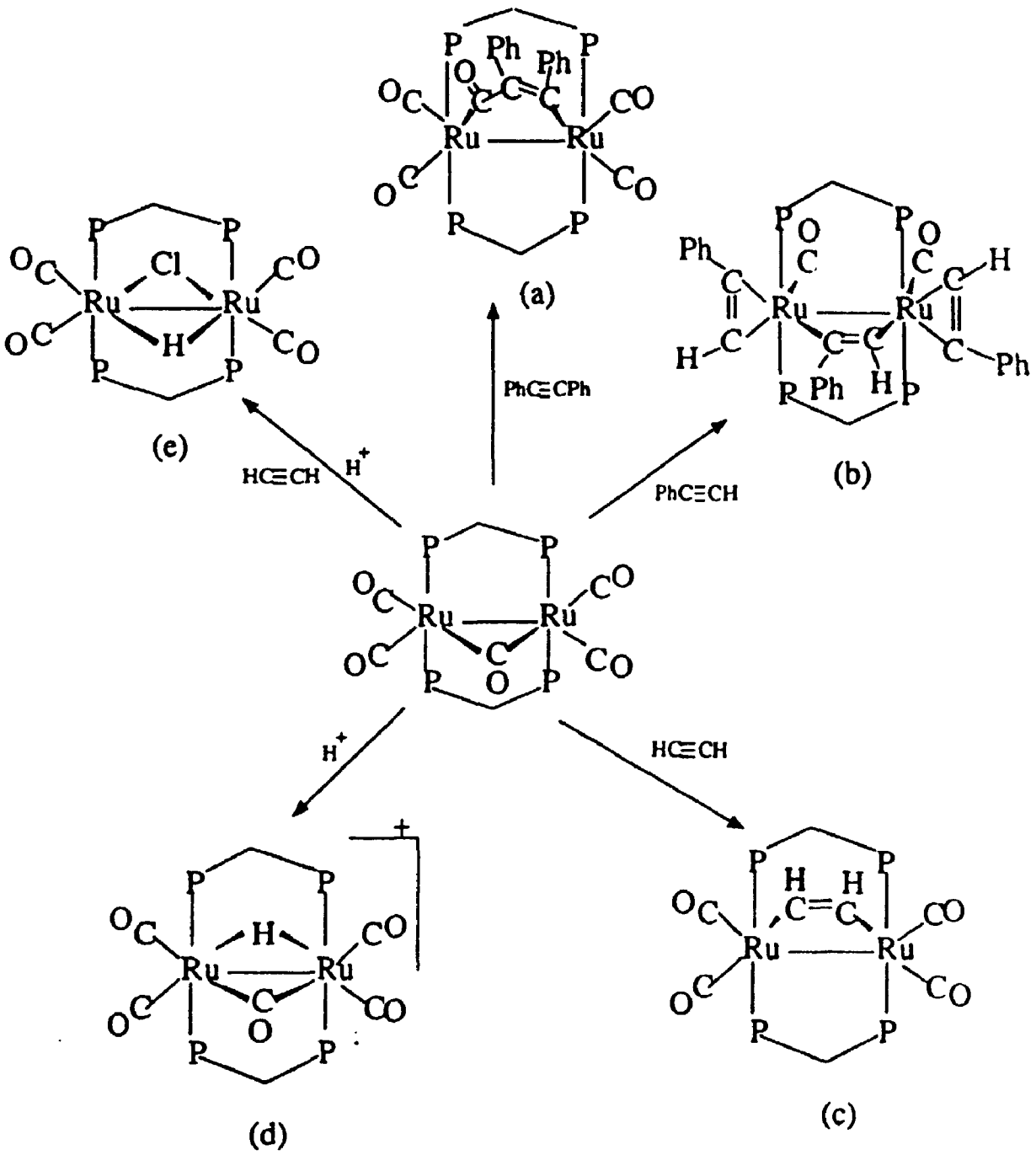

Figure 2.7: The chemistry of $[Ru_2(CO)_4(\mu\text{-}CO)(\mu\text{-}dppm)_2]$, **2.1.**

by Gladfelter and coworkers, reacts with PhC≡CPh at 90°C to produce [$Ru_2(\mu$-PhC=CPh)$(CO)_4(\mu$-dmpm$)_2$] where the alkyne is symmetrically bridged across the Ru-Ru bond.[7a]

2.4.2. Reactions of 2.1 with PhC≡CH.

In contrast to reaction of 2.1 with PhC≡CPh which requires heating for the reaction to proceed, the reaction with the less bulky alkyne PhC≡CH goes to completion within two hours at room temperature. The completion of the reaction is marked by a change in the colour of the solution from yellow to clear reddish-orange. On adding a layer of EtOH to the reaction solution, a transparent reddish-orange crystalline product was formed. These crystals rapidly turned opaque when solvent was removed, probably due to the loss of solvent from the crystal lattice. The complex is readily soluble in most organic solvents and it is characterized on the basis of analytical and spectroscopic data.

The IR spectrum of the complex is shown in Figure 2.8. This exhibits ν(CO) bands at 1970(s), 1946(vs), 1919(sh), 1887(vs) and 1842(sh) cm^{-1}, indicating that all the carbonyl groups are terminally bound to the ruthenium atoms. In addition it shows a strong band at 1539 cm^{-1} and a weak band at 1590 cm^{-1} which may be assigned to ν(C=C).

The ^{31}P NMR spectrum in CD_2Cl_2 solution at room temperature shows two multiplet resonances centred at δ = 19.3 and 15.3, typical of an AA'BB' system, as shown in Figure 2.9. There is also some indication of the presence of a second isomer in solution. This was apparent when the spectrum was recorded at -90°C, when four

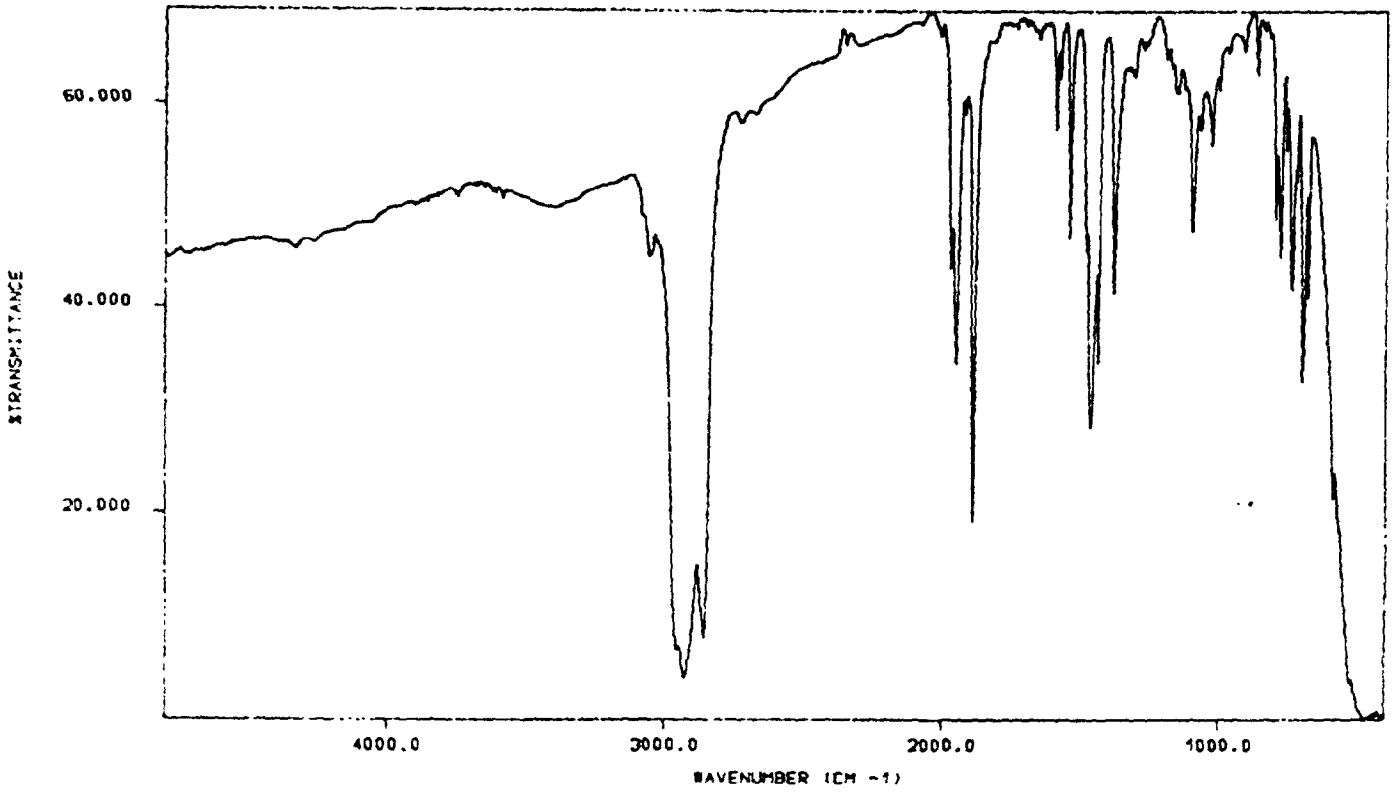

Figure 2.8: The IR spectrum of $[Ru_2(CO)_2(\mu\text{-}PhC_2H)(PhC_2H)_2(\mu\text{-dppm})_2]$, 2.6.

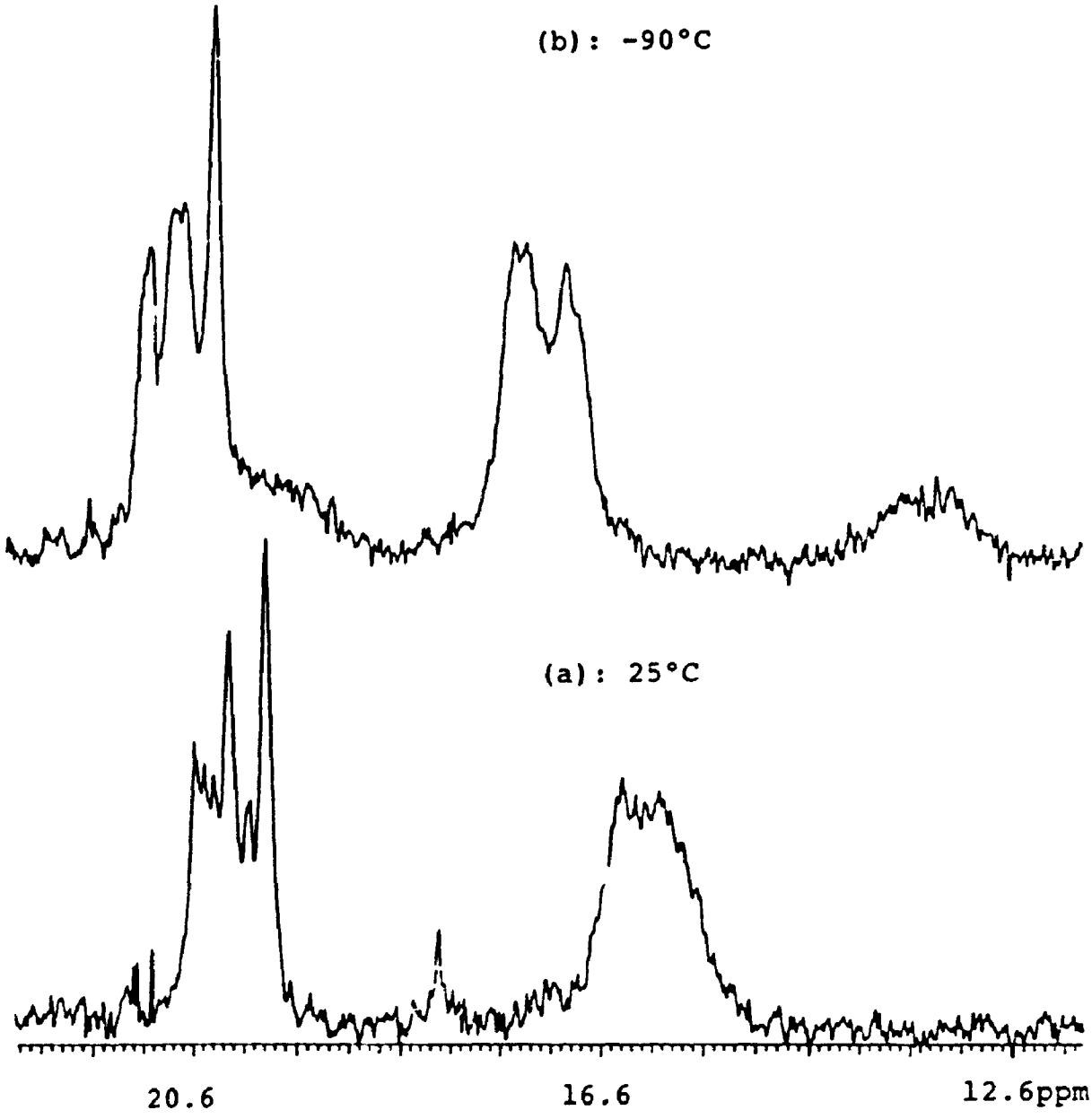

Figure 2.9: The ^{31}P NMR spectra of $[Ru_2(CO)_2(\mu\text{-}PhC_2H)(PhC_2H)_2(\mu\text{-dppm})_2]$, 2.6.

resonances were observed. Two stronger intensity resonances were at δ = 16.1 and 19.6 ppm and two weaker resonances were at δ = 12.3 and 19.0 ppm. This suggests that two isomeric forms, with an intensity ratio of 3.5:1, are present in the solution and that they interconvert rapidly at room temperature.

The ^1H NMR spectrum of the complex (Figure 2.10) shows two partially resolved multiplet resonances centred at δ = 3.45 and 3.70 ppm with $J(PH)_{obs}$ = 5.2 Hz for the CH_2P_2 protons of the dppm ligand. In addition it shows a doublet resonance at δ = 5.34 ppm with $J(HH)_{obs}$ = 3 Hz., and a broad resonance at δ = 5.9 ppm. Moreover, it shows multiplet resonances spanning the region δ = 6.5-7.6 ppm attributable to phenyl protons of both dppm and alkyne ligands. At -90°C the entire spectrum was broadened. The elemental analysis of the complex suggests a chemical formula of $[Ru_2(CO)_2(PhC{\equiv}CH)_3(dppm)_2]$. This is also supported by the mass spectral analysis of the crystalline sample which shows mass ion peak for $Ru_2(CO)_2(PhC{\equiv}CH)_3(dppm)_2^+$ at m/e 1334. In addition it shows peaks at 1204 and 999 which can be assigned to the fragment ions $Ru_2(CO)(PhC{\equiv}CH)_2(dppm)_2^+$ and $Ru_2(CO)(dppm)_2^+$ respectively. It is suggested that two units of alkynes are chelated on each metal atom, while the third alkyne unit is coordinated in a bridging fashion to the dimeric complex, a possible structure of which is shown in Figure 2.7 as *b*, but it is also possible that alkyne coupling has occurred.

2.4.3. Reaction of 2.1 with HC≡CH

This is one of the most interesting but complex reactions of an alkyne with $[Ru_2(CO)_4(\mu\text{-}CO)(\mu\text{-}dppm)_2]$, 2.1. The spectroscopic evidence indicates that HC≡CH

Figure 2.10: The ^{1}H NMR spectrum of $[Ru_2(CO)_2(\mu\text{-}PhC_2H)(PhC_2H)_2(\mu\text{-dppm})_2]$, 2.6.

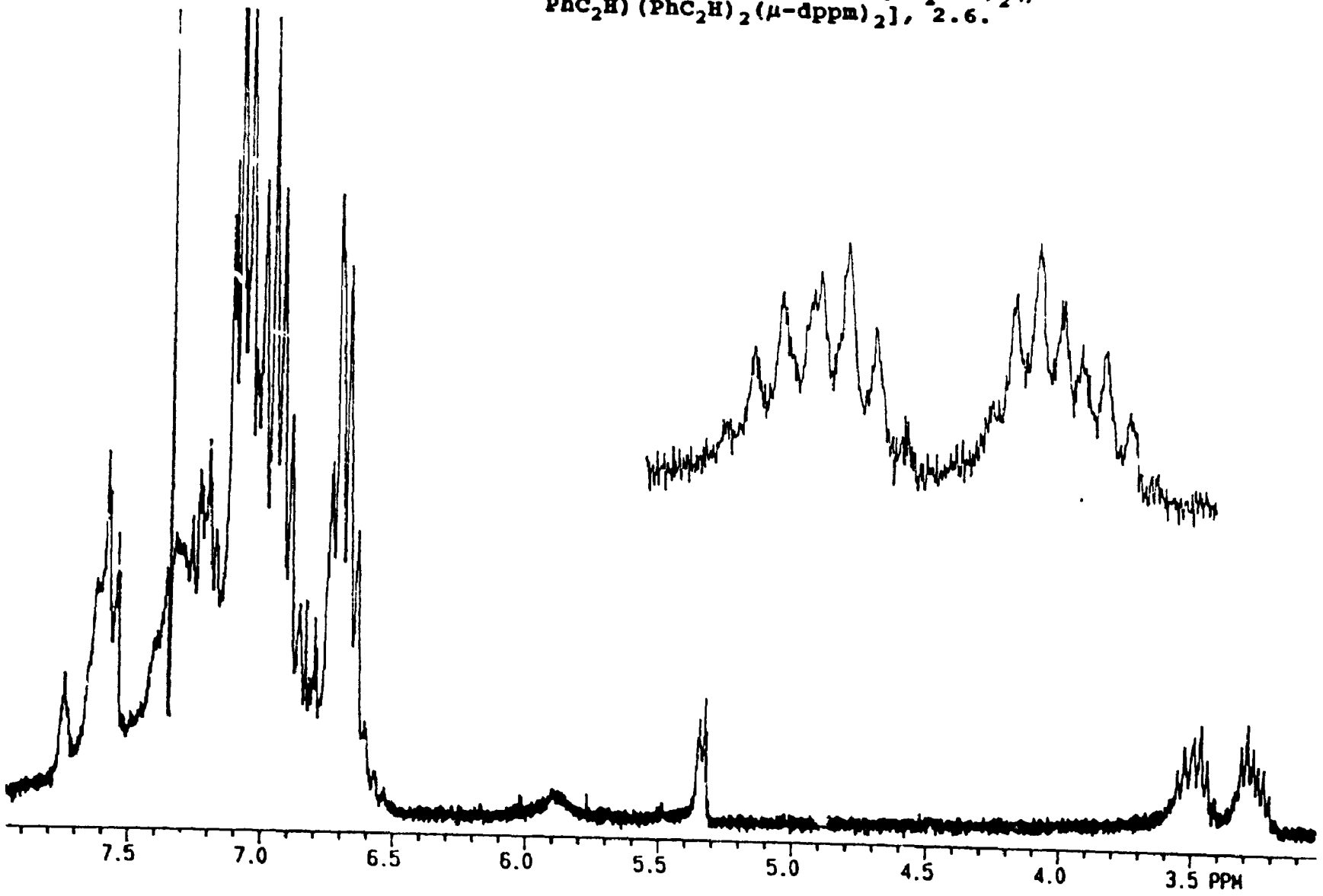

reacts with 2.1 in three different stages, thus forming three different products. However, only one product has been isolated and characterized on the basis of spectroscopic and analytical data. This complex is formed when HC≡CH is briefly bubbled through a solution of complex 2.1 in benzene over a period of 4-5 minutes and the solvent is then removed from the mother liquor via vacuum within 0.5 hour after bubbling HC≡CH.

The infrared spectrum of this complex as shown in Figure 2.11 exhibits four ν(CO) bands at 1995(s), 1943(vs), 1925(vs) and 1879(s), consistent with the carbonyl groups being coordinated terminally to the ruthenium atoms.

The ^{31}P NMR spectrum of this complex in CD_2Cl_2 solution shows only a sharp singlet resonance at δ = 24.1 ppm which remains unchanged at lower temperatures. This suggests that all the phosphorus atoms are occupying equivalent positions and that the dppm is coordinated in the bridging mode. The ^1H NMR spectrum shows two multiplet resonances at δ = 3.5 and 4.7 ppm with $J(PH)_{obs}$ = 9Hz., assigned to the CH_2P_2 protons of the dppm ligand. In addition, it shows a well resolved quintet resonance at 7.8 ppm with $J(PH)_{obs}$ = 1 Hz., which is attributed to the HC≡CH protons. The FAB-mass spectrum of this complex shows a mass ion peak for the $Ru_2(CO)_4(HC{\equiv}CH)(dppm)_2^+$ at 1110 amu. In addition, it shows peaks at 1082, 1054, 1026 and 998 amu attributed to $Ru_2(CO)_3(HC{\equiv}CH)(dppm)_2^+$, $Ru_2(CO)_2(HC{\equiv}CH)(dppm)_2^+$, $Ru_2(CO)(HC{\equiv}CH)(dppm)_2^+$ and $Ru_2(HC{\equiv}CH)(dppm)_2^+$, due to the loss of one, two, three and four CO groups. Therefore, based on the above information, a reasonable structure is shown in Figure 2.7 as structure *c*.

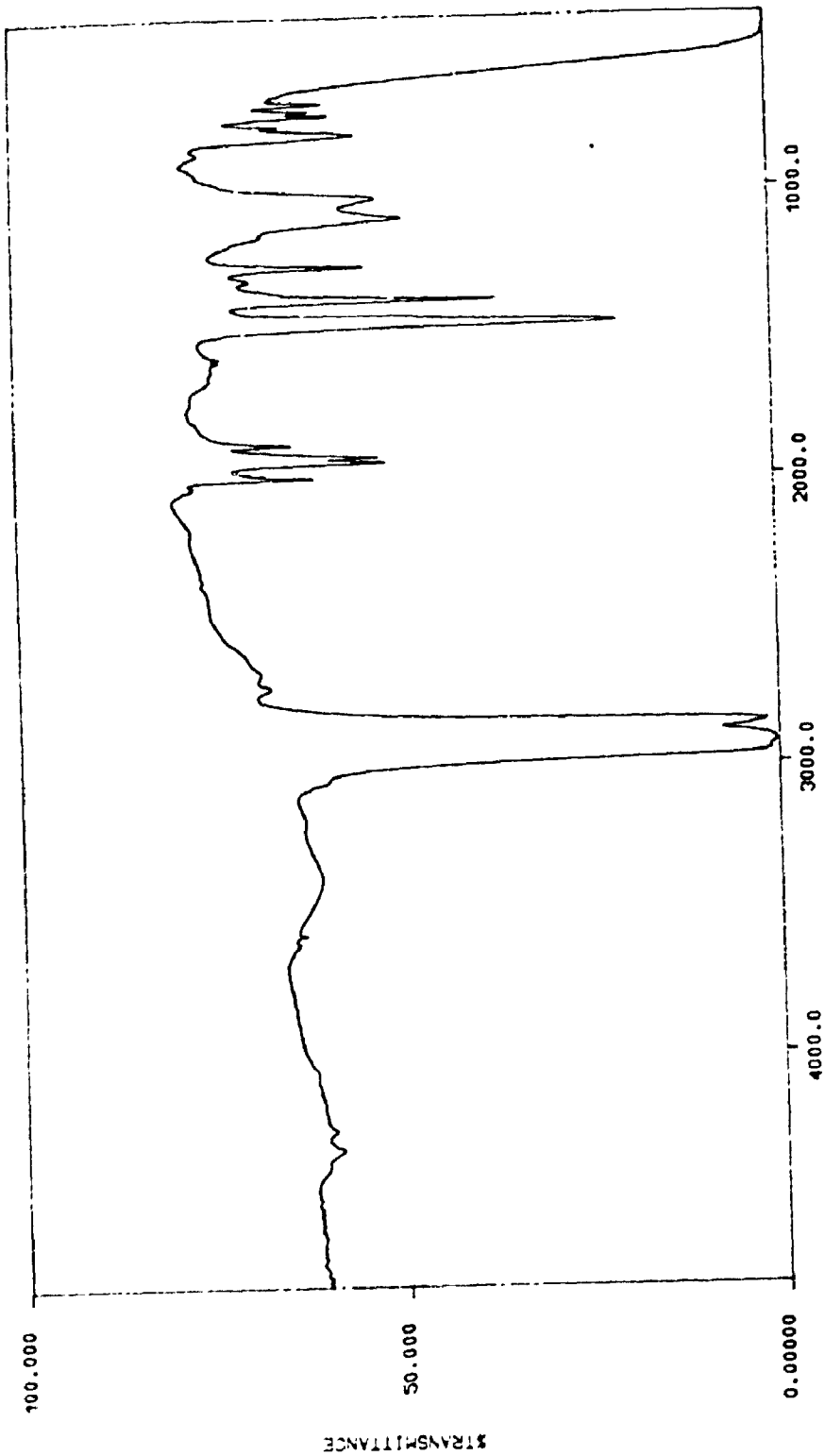

Figure 2.11: The IR spectrum (Nujol) of $[Ru_2(CO)_4(\mu\text{-}C_2H_2)(\mu\text{-dppm})_2]$, 2.7.

However, when the reaction of 2.1 with acetylene is allowed to occur over a period of 8-10 hours, in the presence of excess of HC≡CH, the NMR evidence indicates that further reaction occurs. The product is an unsymmetrical species which exhibits a second order pattern, typical of AA'BB' spin system, in the ^{31}P NMR spectrum (Figure 2.12). The ^{1}H NMR of this species gives resonances due to CH_2P_2 groups at δ = 4.20 and 4.75 ppm and multiplets at 8.0 ppm which are attributed to the HC≡CH groups. This species reacts further with HC≡CH and forms yet another complex which is also unsymmetrical in nature. The ^{31}P NMR spectrum as shown in Figure 2.13 exhibits three sets of multiplet resonances, indicating the formation of at least three different species in solution, all of them unsymmetrical, with an intensity ratio of 13:2:1. In the ^{1}H NMR spectrum resonances typical for vinyl groups were observed. However, all attempts to isolate these complexes in pure form were unsuccessful, as were attempts to grow suitable single crystals. The precise structures of these unusual species therefore remains to be determined.

2.4.4. Reaction of 2.1 with HX, $X^- = F^-$, BF_4^- and PF_6^-.

In attempts to protonate the Ru-Ru bond in the electron rich [$Ru_2(\mu$-CO)$(CO)_4(\mu$-dppm$)_2$], 2.1, several reactions were carried out with aqueous acids. In most of the reactions, addition of excess acid produced several species in solution, none of which could be isolated in pure form. However, when reactions of HPF_6 and HBF_4 were attempted at low temperatures and the reaction solutions were monitored by ^{31}P NMR spectroscopy, the formation of two products, typically with an intensity ratio of 5:1, was demonstrated. The minor product shows a single resonance in the

Figure 2.12: The ^{31}P NMR spectrum of reaction of 2.1 with HC≡CH at the second stage.

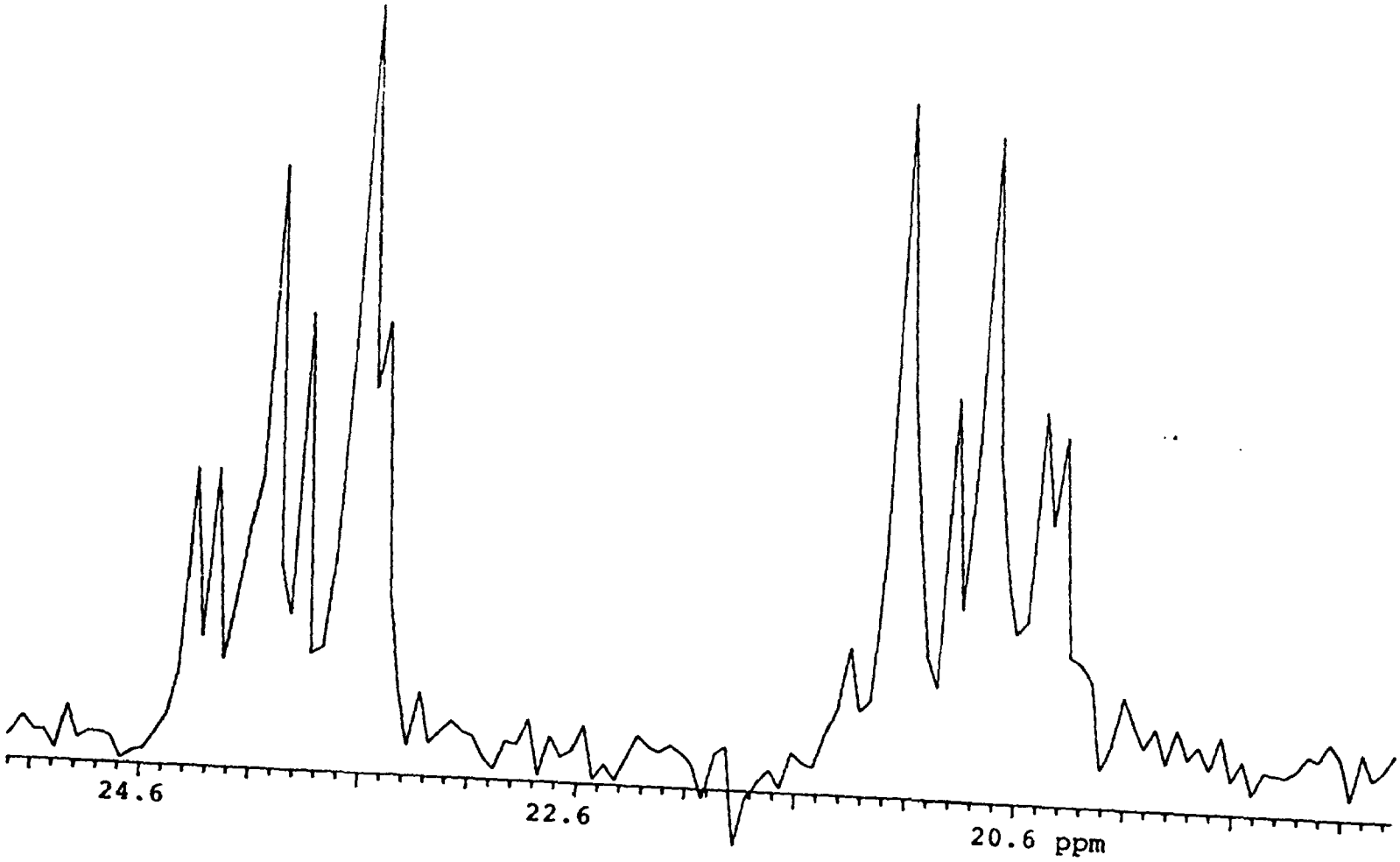

Figure 2.13: The ^{31}P NMR spectrum of reaction of 2.1 with HC≡CH at the final stage.

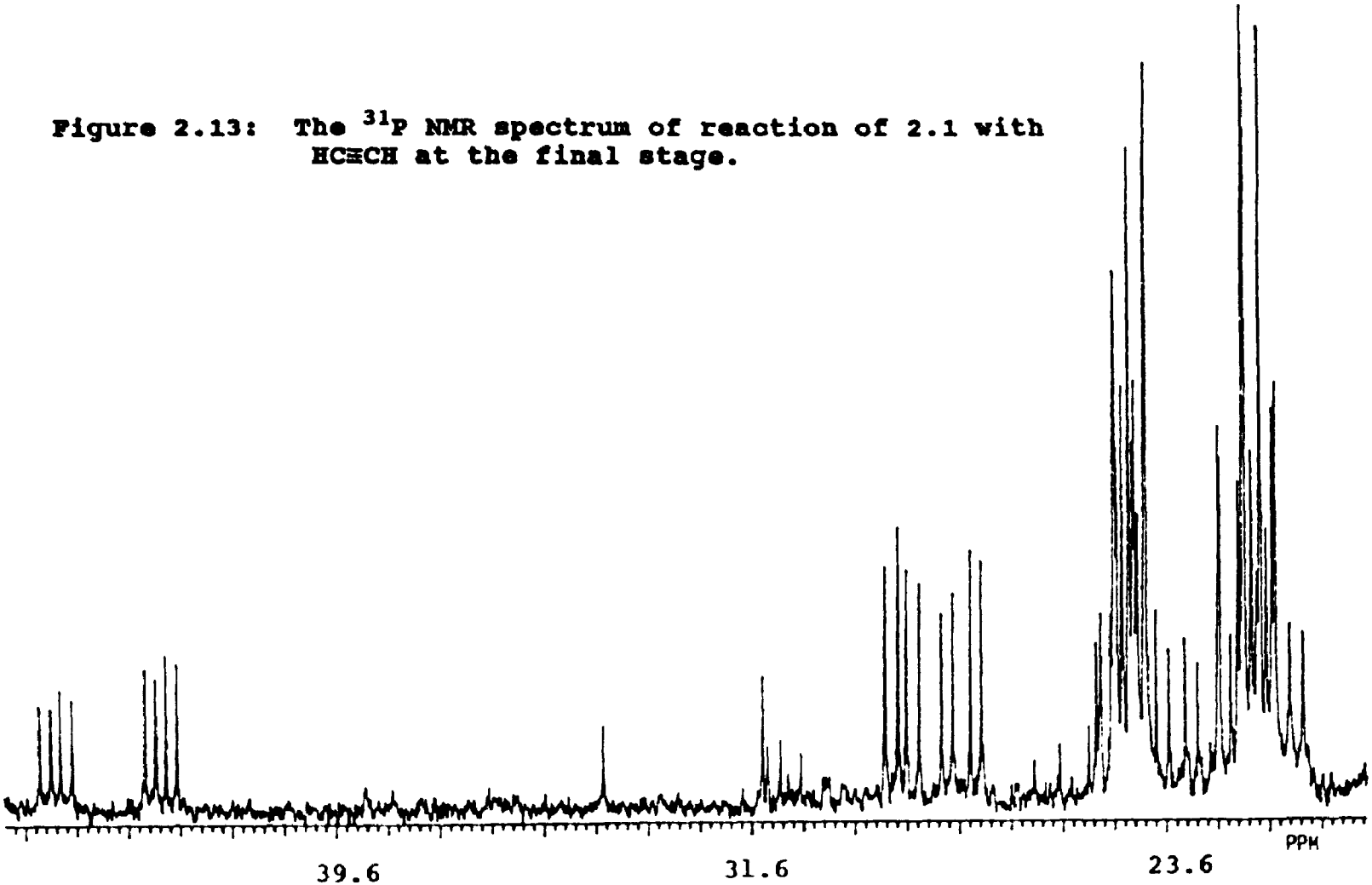

^{31}P NMR spectrum at δ = 20.3 ppm, showing that all the phosphorus atoms of the dppm ligands are equivalent. The ^{1}H NMR spectrum of this species shows, in addition to the CH_2P_2 resonances of the dppm ligand at δ = 3.44 and 3.60 ppm, an unresolved upfield quintet resonance at δ = -9.35 ppm, which could be attributed to the hydride ligand symmetrically bridging the Ru-Ru bond. Very recently Haines and coworkers have also prepared this complex.[8b] Thus, on the basis of the above information, together with comparison with the data reported by Haines et.al.,[8b] the complex cation is characterized as $[Ru_2(\mu\text{-H})(\mu\text{-CO})(CO)_4(\mu\text{-dppm})_2]^+$ and shown in Figure 2.7, structure ***d***.

The major product in the above reaction was isolated in pure form when, after protonation of 2.1 with HPF_6, HC≡CH was bubbled through the solution. The reaction mixture yielded a pale-yellow powder. The IR spectrum of this complex shows three ν(CO) bands at 2087(vs), 2037(vs) and 1995(m) cm^{-1} which are assigned to carbonyl groups coordinated terminally to the ruthenium atoms.

The ^{31}P NMR spectrum in CD_2Cl_2 solution shows only a single resonance at δ = 10.9 ppm, consistent with dppm being coordinated in bridging fashion. The ^{1}H NMR spectrum of this complex in CD_2Cl_2 solution shows, in addition to two multiplet resonances centred at δ = 4.05 and 4.35 ppm for the CH_2P_2 protons of the dppm ligands, a high field resonance centred at δ = -12.63 ppm (Figure 2.14), which appears as a quintet of triplets. The coupling of the hydride with four equivalent phosphorus atoms gives a quintet, each line further split into a triplet due to coupling with two equivalent methylene protons of the dppm ligands. In the mass spectral analysis two envelopes of peaks at 1062 and 1007 amu were observed which could be

Figure 2.14: The ^{1}H NMR spectrum of $[Ru_2(CO)_4(\mu\text{-}H)(\mu\text{-}Cl)(\mu\text{-}dppm)_2]$.

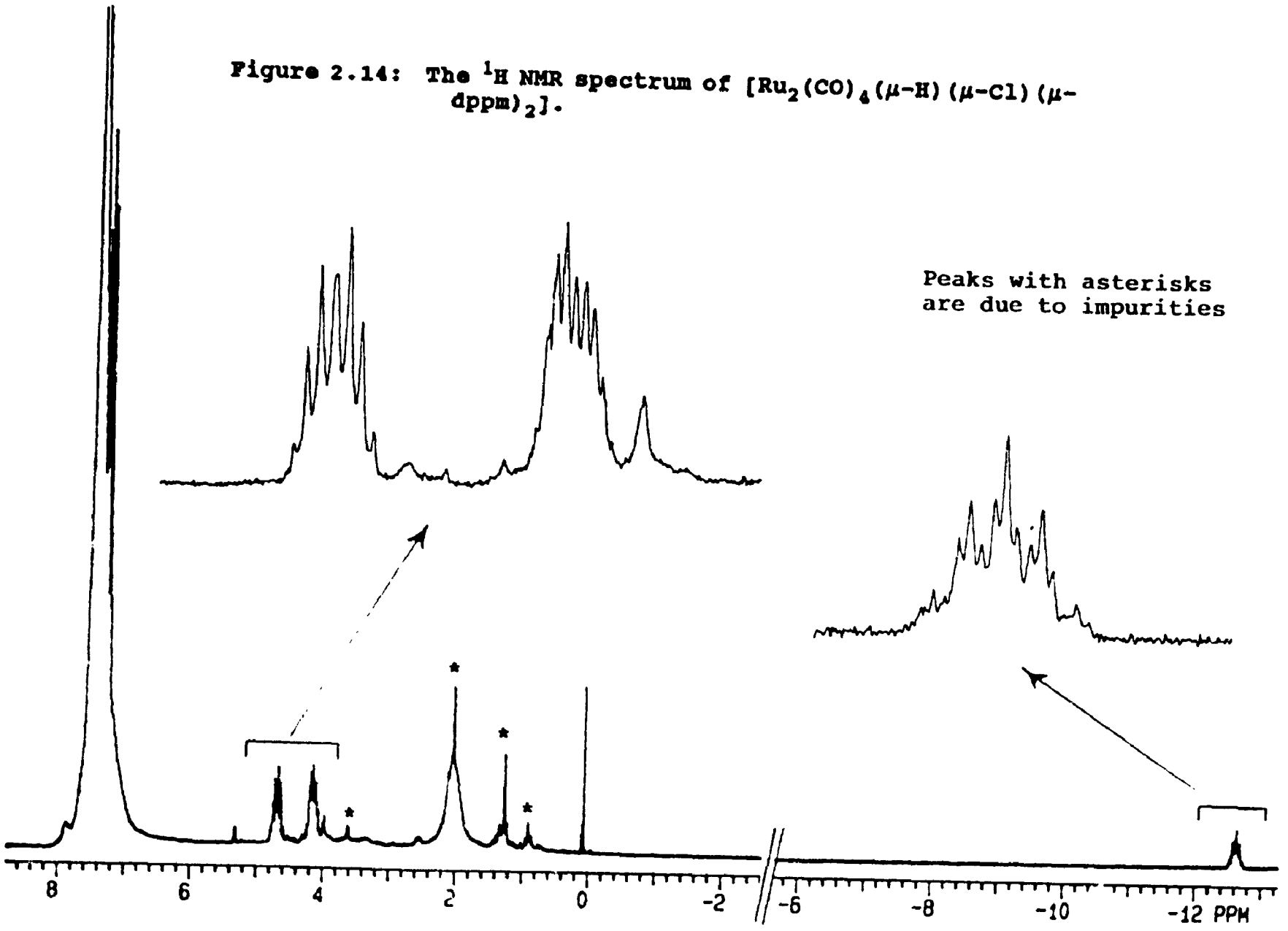

assigned to the fragment ions $Ru_2(CO)_2Cl(dppm)_2^+$ and $Ru_2Cl(dppm)_2^+$ respectively. This arises due to the loss of two CO's and four CO's and a hydride respectively from the $Ru_2H(CO)_4Cl(dppm)_2^+$ mass ion. EDX analysis confirmed the presence of chloride in the solid sample. The chloride ion in the complex may have come from the solvent CH_2Cl_2, which was used to dissolve the parent complex. Thus on the basis of the limited information on hand, the complex is characterized as double A-frame $[Ru_2(\mu\text{-}H)(\mu\text{-}Cl)(CO)_4(\mu\text{-}dppm)_2]$ structure *e* in Figure 2.7.

2.5. Conclusions:

The mechanism of reduction of metal halides by sodium borohydride is difficult to determine, and the success or failure of the method in any particular case is difficult to predict.[13] This work shows that easy reduction of ruthenium(III) to ruthenium(0) can occur, in the presence of CO and dppm, if good leaving groups are present on ruthenium(III) but not if chloride ligands are present. The easier reduction of metal carboxylates than metal halides should be a general effect for soft metal ions, but its success is still difficult to predict. For example, the attempted reduction of ruthenium(III) in the presence of CO and bis(dimethylphosphino)methane, dmpm, gave $[Ru(dmpm)_2(BH_3CN)_2]$ but failed to give any ruthenium(0) carbonyl even though both $[Ru_2(CO)_5(\mu\text{-}dmpm)_2]$ and $[Ru_3(CO)_{12-2n}(\mu\text{-}dmpm)_n]$ (n = 1, 2) are stable complexes,[7,8] and attempted reduction of osmium(III) chloride in the presence of silver acetate, dppm and CO failed to give any osmium(0) carbonyls. This unpredictability is certainly a major problem in further extension of the synthetic method. Nevertheless, the one step synthesis of electron-rich binuclear carbonyls from

metal halides is very attractive and the synthesis of 2.1 by this method is reproducible and convenient.

The electron rich $[Ru_2(\mu\text{-}CO)(CO)_4(\mu\text{-}dppm)_2]$ 2.1 shows remarkable reactivity towards sterically less demanding unsaturated organic reagents and forms several interesting new products. Although work described in the last section is only preliminary, the evidence indicates that simple alkynes react with 2.1 in steps to form several new species. Further work is needed to isolate all these products in pure form and to complete the structural characterization.

Table 2.3: Spectroscopic data of ruthenium complexes.

COMPLEX	IR	^{31}P	^{1}H
$[Ru_2(CO)_5(dppm)_2]$ 2.1	1966(s), 1923(vs) 1898(vs),1883(s),1701	34.3(s)	3.62(q)
$[RuCl_2(dppm)_2]$ 2.2		-12.5	5.0(m)
$[RuH(CO)(dppm)_2]^+$ 2.3	1983(vs),1999(sh)	-6.2(s)	-3.6(q,t); 4.97(m); 5.30(m)
$[Ru(BH_3CN)_2(dmpm)_2]$ 2.4	2323,2275,2218,2170	-39(s)	3.9(q)1.9(d) 1.7(m)
$[Ru_2(CO)_4\{\mu$-(CO)PhC CPh$\}(dppm_2]$ 2.5	1972(vs),1908(vs) 1690(vs).	AA'BB' 24,16.8	3.25(m), 4.0(m)
$[Ru_2(CO)_2(PhC_2H)_2$ $(\mu$-$PhC_2H)(dppm)_2$ 2.6	1970(s),1946(vs),1919(sh) 1887(vs),1842(sh).	19.3(m) 15.3(m)	3.45(m) 3.70(m) 5.34(d)
$[Ru_2(CO)_4(HC\equiv CH)$ $(dppm)_2]$ 2.7	1995(s),1943(vs) 1925(vs),1879(s)	24.1(s)	4.85(m), 5.05(m)
$[Ru_2(H)(Cl)(CO)_4$ $(dppm)_2]$ 2.8	2087(vs,2037(vs), 1995(m)	10.9(s)	-12.63(q,t) 4.05(m) 4.35(m)

2.6. Experimental

2.6.1. $[Ru_2(CO)_4(\mu\text{-}CO)(\mu\text{-}dppm)_2]$.

Silver acetate (2.2 g; 13.18 mmol) was added to a stirred solution of $RuCl_3.3H_2O$ (1.0 g; 3.83 mmol) in EtOH (30 mL). The mixture was stirred for 10 min., allowed to stand overnight and then filtered to remove AgCl. To the filtrate was added dppm (1.6 g; 4.16 mmol) in toluene (30 mL) and the solution was saturated with CO. To this solution was added dropwise a suspension of $NaBH_4$ (1.0 g; 26.43 mmol) in EtOH (25 mL), with rapid bubbling of CO through the solution. The mixture was stirred for a further 4h., and then the orange precipitate of the product $[Ru_2(CO)_4(\mu\text{-}CO)(\mu\text{-}dppm)_2]$ was separated by filtration.

Yield 62%. M.P. 238-240°C.

IR (Nujol): ν(CO) = 1966 (s), 1923 (vs), 1898 (vs), 1883 (s), 1701 (s). NMR in CD_2Cl_2: ^1H; δ = 3.62 [quintet, $J_{obs}(PH)$ = 4.7 Hz]; ^{31}P; δ = 34.4 [s].

2.6.2. trans-$[RuH(CO)(dppm)_2]BPh_4$

The solvent was evaporated from the mother liquor from the above synthesis. The residue was dissolved in EtOH (60 mL) and $NaBPh_4$ (0.3 g; 0.88mmol) was added to precipitate the product, which was recrystallized from CH_2Cl_2 / ether.

Yield 9%. M.P. 247-250°C.

Anal. Calc. for $C_{75}H_{65}BORu.0.5CH_2Cl_2$: C, 72.8%; H, 5.3% Found: C, 72.7%; H, 5.6%.

IR (Nujol): ν(CO) = 1999 (sh) , 1983 (s) cm^{-1}.

NMR in CD_2Cl_2: ^1H; δ = -3.6 [triplet of quintets, $^2J(PH)$ = 20.5, J(HH) =3.2 Hz];

4.97 [m, $^2J(PH) + {}^4J(PH) = 9$, $^2J(H^aH^b) = 16$ Hz, CH^a]; 5.30 [m, $^2J(PH) + {}^4J(PH) = 9$, $^2J(H^aH^b) = 16$, $J(H^aRu) = 3.2$, H^b]; ^{31}P; $\delta = -6.2$ [s].

Lit.[15] for $[RuH(CO)(dppm)_2][Mn(CO)_5]$: IR, ν(CO) 1990, 1880, 1865, 1830 cm^{-1}; NMR: ^1H, δ -3.64[RuH, J(PH) = 19 Hz.]; 4.7[m, CH_2P_2]; 4.9[m, CH_2P_2]; ^{31}P, δ -0.6 (s).

2.6.3. $[RuCl_2(dppm)_2]$.

A solution of $RuCl_3.3H_2O$ (0.5 g; 1.91 mmol) and dppm (1.6 g; 4.16 mmol) in toluene/ethanol (1:1, 60 mL) was saturated with CO. To this solution was added dropwise $NaBH_4$ (0.8 g; 21.14 mmol) in EtOH (15 mL) and the mixture was stirred for 2.5 h. The yellow precipitate of the product was separated by filtration and recrystallized from CH_2Cl_2/EtOH.

Yield 15%.

NMR in CD_2Cl_2: ^1H; $\delta = 5.0$ [m,CH_2]; ^{31}P; $\delta = -12.5$ [s]. FAB-MS: m/e 940, $RuCl_2(dppm)_2^+$; 905, $RuCl(dppm)_2^+$; 869, $Ru(dppm)_2^+$.

2.6.4. $[Ru(BH_3CN)_2(dmpm)_2]$

To a solution of $RuCl_3.3H_2O$ (0.3 g; 1.15 mmol) in ethanol (30 mL) was added dmpm (1.0 mL; 8.69 mmol) and the mixture was stirred for 5 min., then $NaBH_3CN$ (0.45 g; 7.14 mmol) in ethanol (10 mL) was added dropwise. The mixture was stirred for 16 h, then filtered and the filtrate was allowed to stand for 2 weeks. The pale yellow crystalline product precipitated and was isolated by filtration, then washed with ethanol.

Yield 0.15 g. MP 266-269°C.

Anal. Calc. for $C_{12}H_{34}B_2N_2P_4Ru$: C, 31.8; H, 7.5; N, 6.2.

Found: C, 30.2; H, 7.2; N, 5.1%

IR (Nujol): 2323, 2275 [ν(BH)], 2218, 2170 [ν(C≡N)] cm^1.

NMR in CD_2Cl_2; (^1H), δ = 3.9 [quin., 4H, $J(PH)_{obs}$ = 2.5, CH_2P_2]; 1.7 [m,BH]; 1.9 [d, 24H, J(PH) = 14, MeP]; (^{31}P), δ = -39.0 [s, dmpm].

2.6.5. Reaction of 2.1 with PhC≡CPh

To a stirring solution of $Ru_2(CO)_4(\mu\text{-}CO)(\mu\text{-}dppm)_2$ (0.25g; 0.23 mmol) in $C_2H_4Cl_2$ (10 mL) was added PhC≡CPh (0.05g; 0.25 mmol). The yellow solution was then heated to reflux. The colour of the solution changed from yellow to reddish-orange within 15 minutes. The solution was refluxed for a further 4-6 hours. No further change in the colour was observed. The solution was then brought to room temperature and a layer of n-pentane (25 mL) was carefully added to it. This was then allowed to stand over a period of two weeks during which time a dark yellowish-orange microcrystalline solid formed. This product was filtered off and washed with EtOH (5 mL), n-heptane (10 mL) and dried under rec . pressure.

Yield: 55%

Anal. Calc. for $C_{69}H_{76}O_5P_4Ru_2$: C, 64.2%; H, 4.2%; Found: C, 64.3%; H. 3.8%.

IR(Nujol): ν(CO) 1972(vs) 1908(vs) and 1690(vs) cm^{-1}

NMR(CD_2Cl_2): ^1H, δ = 3.25[m, $CH^aH^bP_2$, CH^a], 4.0[m, $CH^aH^bP_2$, CH^b], 6.9-7.6[m, Ph]; ^{31}P: δ = 24.0 (m), 16.8 (m).

2.6.6. Reaction of 2.1 with PhC≡CH.

$Ru_2(CO)_4(\mu\text{-}CO)(\mu\text{-}dppm)_2$ (0.1g, 0.09 mmol) was dissolved in C_6H_6 (10 mL) and stirred under N_2 gas. To this was then added excess PhC≡CH (0.04 mL; 0.36 mmol). The colour of the solution immediately changed to dark yellow. The mixture was stirred for a further 5h during which time a clear reddish-orange solution was formed. Solvent was then removed under vacuum to approximately 50%. To the solution was then added carefully a layer of EtOH (15 mL) and this was than allowed to stand over a period of six weeks. The red crystalline product so formed was filtered off, washed with two portions of EtOH (5 mL each) and the crystals were dried under reduced pressure.

Yield: 15%

Anal. Calc. for $C_{78}H_{62}O_4P_4Ru_2$: C, 68.4%; H, 4.7%; Found: C, 68.1%, H, 5.0%

IR(Nujol): ν(CO) = 1970(s), 1946(vs), 1919(sh), 1887(vs) and 1842(sh) cm^{-1}.

NMR (CD_2Cl_2): ^1H, δ = 3.45 [m, CH^aH^bP, CH^a], 3.70[m, CH^aH^bP, CH^b], 5 52 [d, C=CH]; ^{31}P, δ = 19.3 (m), 15.3 (m) ppm

FAB-MS: m/e 1334, 1204, 999 amu.

2.6.7. Reaction of 2.1 with HC≡CH.

$Ru_2(CO)_4(\mu\text{-}CO)(\mu\text{-}dppm)_2$ (0.07g; 0.06 mmol) was dissolved in C_6H_6 (20 mL). A slow stream of HC≡CH was then passed through this solution for about 4-5 minutes. The greenish-yellow solution immediately turned bright yellow. The flask was sealed and the solution was stirred for about 0.5h in an atmosphere of HC≡CH. Solvent was then removed to dryness under vacuum. The yellow solid so formed was

washed with EtOH (5 mL) and dried under reduced pressure.

Yield: 85%

Anal. Calc. for $C_{56}H_{46}O_4P_4Ru_2.4CH_2Cl_2$: C, 49.7; H, 3.7%; Found: C, 49.4; H, 4.5%.

IR(Nujol): ν(CO) = 1995(s), 1943(vs), 1925(vs) and 1879(s) cm^{-1}; NMR(CD_2Cl_2): ; ^1H, δ = 4.85[m, $J(PH)_{obs}$ = 8Hz, CH_2P_2,1H], 5.05[m,br, CH_2P_2, 1H], 6.8-7.7[m, Ph, 40H]; ^{31}P, δ = 24.1(s) ppm. FAB-MS: m/e 1110, 1082, 1054, 1026 and 998 amu.

2.6.8. Reaction of 2.1 with HPF_6 and HC≡CH.

$Ru_2(CO)_4(\mu\text{-}CO)(\mu\text{-}dppm)_2$ (0.20g; 0.18 mmol) was dissolved in CH_2Cl_2 (10 mL). The solution was cooled on a dry ice bath. To this was than added HPF_6 (0.04 mL) and the mixture was stirred for about 5 min. A slow stream of HC≡CH gas was then passed through this solution over a period of 0.5 h. The solution was than brought to room temperature and HC≡CH gas was bubbled for another 0.5 h. The flask was than left aside over two days under N_2. Excess of n-pentane (20 mL) was added, forming a pale yellow precipitate. This was filtered off, washed with n-pentane (10 mL) and dried under reduced pressure.

Yield: 30% M.P. 213°C (dec).

NMR (CD_2Cl_2):^1H, δ = -12.6[q,t, $^2J(PH)$ = 9.3 Hz.,$^4J(HH)$ = 2.9 Hz., RuH]; 4.17[m, $CH^aH^bP_2$, H^a]; 4.7[m,$CH^aH^bP_2$, H^b]; 7-8[m, Ph, 40H]. ^{31}P, δ = 10.9(s) ppm. FAB-MS: m/e = 1062, 1007 for $Ru_2(CO)_2Cl(dppm)_2^+$ and $Ru_2Cl(dppm)_2^+$ respectively.

2.7. References:

1. B. Chaudret; B. Delavaux and R. Poilblanc; Coord. Chem. Rev. ***86***, 91 (1988).

2. M.I. Bruce; D.C. Kehoe; J.G. Matisons; B.K. Nicholson; P.H. Rieger and M.L. Williams; J. Chem. Soc. Chem. Commun. 442 (1982).

3. D.W. Engel; K.G. Moodley; L. Subramony and R.J. Haines; J. Organomet. Chem. ***349***, 393 (1988).

4.(a) M.I. Bruce; P.A. Humphrey; B.W. Skelton; A.H. White and M.L. Williams; Aust. J. Chem. ***38***, 1301 (1985).

(b) C. Bergounhou; J. Bonnet; P. Fompeyrine; G. Lavigne; N. Lugan and F. Mansilla; Organometallics *5*, 60 (1986).

5. E.A. Seddon; K.R. Seddon; The Chemistry of Ruthenium, Elsevier, Amsterdam, (1984).

6. M.I. Bruce; Comprehensive Organometallic Chemistry, Edit. by G. Wilkinson; F.G.A. Stone; E.W. Abel; Pergamon, Oxford, Vol. 4, ch. 32.2. (1982).

7.(a) K.A. Johnson; W.L. Gladfelter; Organometallics *8*, 2866 (1989).

(b) K.A. Johnson; W.L. Gladfelter; Organometallics ***9***, 2101 (1990).

(c) K.A. Johnson; W.L. Gladfelter; J. Am. Chem. Soc. ***113***, 5097 (1991).

(d) K.A. Johnson; W.L. Gladfelter; Organometallics ***10***, 375 (1991).

8.(a) G. De Leeuw; J.S. Field; R.J. Haines; D. McCulloch; E. Meintjies; C. Monberg; G.M. Oliver; P. Ramdial; C.N. Sampson; B. Sigwarth; N.D. Steen; K.G. Moodley; J. Organomet. Chem. ***275***, 99 (1984).

(b) J.S. Field; R.J. Haines; C.N. Sampson; J. Sundermeyer; K.G. Moodley; J. Organomet. Chem. ***322***, C7 (1987).

(c) D.W. Engel; K.G. Moodley; L. Subramony; R.J. Haines; J. Organomet. Chem. ***149***, 393 (1988).

(d) J.S. Field; A.M.A. Francis; R.J. Haines; S.F. Woollam; J. Organomet. Chem. ***412***, 383 (1991).

(e) J.S. Field; R.J. Haines; J. Sundermeyer; S.F. Woollam; J. Chem. Soc. Chem. Commun. 985 (1990).

(f) G.Y. Kiel; J. Takat; Organometallics *8*, 839 (1989).

9.(a) S. Cartwright; J.A. Clucas; R.H. Dawson; D.F. Foster; M.M. Harding; A.K. Smith; J. Organomet. Chem. ***302***, 403 (1986). (b) N. Lugan; J.J. Bonnet; J.A. Ibers; J. Am. Chem. Soc. ***107***, 4484 (1985).

(c) M.I. Bruce; O.B. Shawkataly; M.L. Williams; J. Organomet. Chem. ***287***, 127 (1985).

(d) Lj. Manojlovic-Muir; D.A. Brandes; R.J. Puddephatt; J. Organomet. Chem. ***332***, 201 (1987).

10. D.G. Holah; A.N. Hughes; H.A. Mirza and J.D. Thompson; Inorg. Chim. Acta. ***126***, L7 (1987).

11. D.G. Holah; A.N. Hughes; V.R. Magnuson; H.A. Mirza and K.O. Parker; Organometallics *7*, 1233 (1988).

12. H.A. Mirza; M.Sc. Thesis, Lakehead University (1988).

13. D.J. Elliot; G. Ferguson; D.G. Holah; A.N. Hughes; M.C. Jennings; V.R. Magnuson; D. Potter; R.J. Puddephatt; Organometallics *9*, 1336 (1990) and refs. therein.

14.(a) R. Mason; D.W. Meek; G.R. Scollary; Inorg. Chim. Acta. ***16***, L11 (1976).

(b) C.W. Jung; P.E. Garrou; P.R. Hoffman; K.G. Caulton; Inorg. Chem. *23*, 726 (1984).

15. H. BenLaarab; B. Chaudret; F. Dahan; J. Devillers; R. Poilblanc; S. Sabo-Etienne; New J. Chem. *14*, 321 (1990).

16. D.J. Elliot; S. Haukilahti; D.G. Holah; A.N. Hughes; S. Maciaszek; R.J. Barton; Y. Luo and B.E. Robertson: Can. J. Chem. *66*, 1770 (1988).

17. E.L. Muetterties; R.N. Rhodin; E. Band; C.F. Brucker and W.R. Pretzer; Chem. Rev. *79*, 91 (1979).

18. A.F. Dyke; S.A.R. Knox; P.J. Naish and G.E. Taylor; J. Chem. Soc. Dalton Trans. 1297 (1982).

19. S.A.R. Knox; J. Organomet. Chem. *400*, 255 (1990).

20. S.G. Davies; J.P. McNally and A.J. Smallridge; Adv. Organomet. Chem. *30*, 1 (1990).

21. G.S. Lewandos; S.A.R. Knox and A.G. Orpen; J. Chem. Soc. Dalton Trans. 2703 (1987).

22. C.M. Lukehart; Fundamental Transition Metal Organometallic Chemistry, Ch. 5, Brooks/Cole Publishing Co. California (1985).

Chapter 3

The Synthesis, Structural Characterization and Reactivity of a 48 Electron Cluster, $[Ru_3(CO)_6(\mu\text{-dppm})_3]$.

3.1. Introduction

The current interest in transition metal clusters arises in part from their possible utility in homogeneous catalysis. An attractive feature of metal clusters is their ability to transform various organic substrates through pathways that are not accessible to mononuclear species, as a result of cooperative interactions among adjacent metal centres.[1] However, the application of transition metal clusters in catalysis is somewhat restricted by the lack of stability of the metal atom framework under the conditions required for many catalytic reactions to take place. Many clusters fragment to mononuclear species, for example under high carbon monoxide pressure,[2] and although there is a large and increasing number of reports of reactions catalysed by clusters,[3] there is in most cases no evidence that the nuclearity of the cluster is maintained throughout the reaction cycle.[2b] Catalytic as well as stoichiometric reactivity of clusters requires coordinative unsaturation, which can be produced by loss of a ligand or by metal-metal bond scission.[4] For an effective catalytic process, a compromise between the stability of the cluster framework and reactivity of the complex must be reached. One such approach is to use bridging ligands to maintain the integ ity of the polymetallic core and to ensure that possible metal-metal bond cleavage be reversible.[5] Some of the most important and widely used ligands in this regard are the bidentate tertiary phosphines $R_2P(CH_2)_nPR_2$. These ligands often form

very strong metal-phosphorus bonds, and are also used to stabilize metal complexes in low oxidation states.[6] With the exception of the ligand with n=2, which prefers to form a strain free five membered chelating ring, all other ligands in the series have some tendency to form metal complexes in which the ligand is coordinated in a bridging mode.[7,8] Ligands with n=1 are particularly known to form bi and polynuclear complexes by bridging two or more metal atoms.[6,9,10] The first organometallic compound containing ruthenium was reported in 1910 by Mond, who isolated an unidentified volatile rose-orange solid from the reaction between ruthenium black and carbon monoxide at 300°C and 400 atmospheres.[11] This compound, on thermal or photochemical decomposition, yielded orange $[Ru_3(CO)_{12}]$. The precise nature of this orange solid remained unknown until X-ray studies several decades later.[12] The subsequent development of the organometallic chemistry of ruthenium has centered on two major areas. The first is that of the Ru-H bond in a variety of hydridoruthenium complexes containing tertiary phosphine ligands.[12] In addition their reactions have spawned a great variety of novel complexes of interest in their own right. The study of the chemistry of the cluster carbonyl $[Ru_3(CO)_{12}]$, as one of the first readily accessible polynuclear carbonyl derivative, helped spark off the current interest in these complexes, and this compound is the source of a wide range of unusual compounds containing three or more metal atoms.[12,13]

The more robust nature of the Ru_3 cluster in $[Ru_3(CO)_{12}]$, when compared with Fe_3 cluster in $[Fe_3(CO)_{12}]$, is amply demonstrated by its reactions. Even in simple substitution reactions, for example with tertiary phosphines, the Fe_3 cluster fragments to give mononuclear complexes.[14,15] In contrast, substitution of CO groups

generally occurs in the reactions of $[Ru_3(CO)_{12}]$ with tertiary phosphines.[16] Spectroscopic studies have shown that the reaction of dppm with $[Ru_3(CO)_{12}]$ proceeds via the complexes $[Ru_3(CO)_{10}(\mu\text{-dppm})]$ and $[Ru_3(CO)_9(\mu\text{-dppm})(\eta^1\text{-dppm})]$ to form the very stable $[Ru_3(CO)_8(\mu\text{-dppm})_2]$.[16] Recent kinetic studies on the formation of $[Ru_3(CO)_{10}(\mu\text{-dppm})]$ and $[Ru_3(CO)_8(\mu\text{-dppm})_2]$ indicate that the substitution of the first carbonyl group is mainly ligand dependent (i.e. [dppm]) and the coordination of dppm occurs via stepwise loss of CO.[17] For the formation of $[Ru_3(CO)_8(\mu\text{-dppm})_2]$ from $[Ru_3(CO)_{10}(\mu\text{-dppm})]$, it was clearly shown that the major part of the reaction occurs via reversible dissociation of a CO from the $Ru(CO)_4$ moiety. The coordinatively unsaturated $Ru(CO)_3$ moiety is then competitively attacked either by CO or by dppm to form $[Ru_3(CO)_9(\mu\text{-dppm})(\eta^1\text{-dppm})]$. The dissociation of an equatorial CO from a Ru atom that is already bridged by a dppm ligand then creates a vacant coordination site where the free end of the monodentate dppm enters to form the thermodynamically favoured product. Further substitution of carbonyl groups with dppm is expected to proceed similarly.

3.2. Synthesis of $[Ru_3(CO)_6(\mu\text{-dppm})_3]$ (3.1) by the Reduction of Ruthenium (III) Salts.

As mentioned in chapter 2, crystals of the cluster complex $[Ru_3(CO)_6(\mu\text{-dppm})_3]$, form in low yield in the reaction of Ru(III) with $NaBH_4$ in the presence of dppm under CO atmosphere. The reaction may have proceeded according to the following equation.

$$3Ru(III) + 3dppm + 6CO + 9BH_4^- \rightarrow [Ru_3(CO)_6(dppm)_3] + 4.5B_2H_6 + 4.5H_2 \quad (3.1)$$

The red crystalline complex precipitated out from the mother liquor over a period of 2-3 weeks. However, the cluster complex can more conveniently be prepared by the reaction of dppm with $[Ru_3(CO)_{12}]$ in refluxing benzene.[14] The crude product obtained can then be recrystallized from CH_2Cl_2 and n-heptane.

3.2.1. The Crystal Structure of $[Ru_3(CO)_6(\mu\text{-dppm})_3]$ (3.1).

A crystal obtained from the mother liquor of the above mentioned reduction reaction was found to be suitable for X-ray analysis which was carried out by Dr. Vittal at the X-ray diffraction facilities of the University of Western Ontario. The molecular structure of the cluster 3.1 is shown by the ORTEP diagram depicted in Figure 3.1 and bond distances, angles and deviations from the Ru_3 plane are listed in Table 3.1. The structure contains a triangle of ruthenium atoms with equatorial μ-dppm ligands bridging each edge of the triangle. There are six axial carbonyl ligands, all of which are terminally bonded to ruthenium atoms. All Ru-Ru distances are within the expected range for a single Ru-Ru bond and with an average bond length of 2.8551 Å.[12b,18,19] However, the Ru(1)-Ru(2) distance at 2.8625(13) Å is slightly longer (0.011 Å) than the other two metal-metal distances. The data from Table 3.1 also reveals that the carbonyl groups are not linearly disposed around the metal atoms. Thus, the average of the Ru-C-O bond angles at 172.5° shows a deviation of 8° from the ideal 180°, indicating that the carbonyl groups are bent away from each

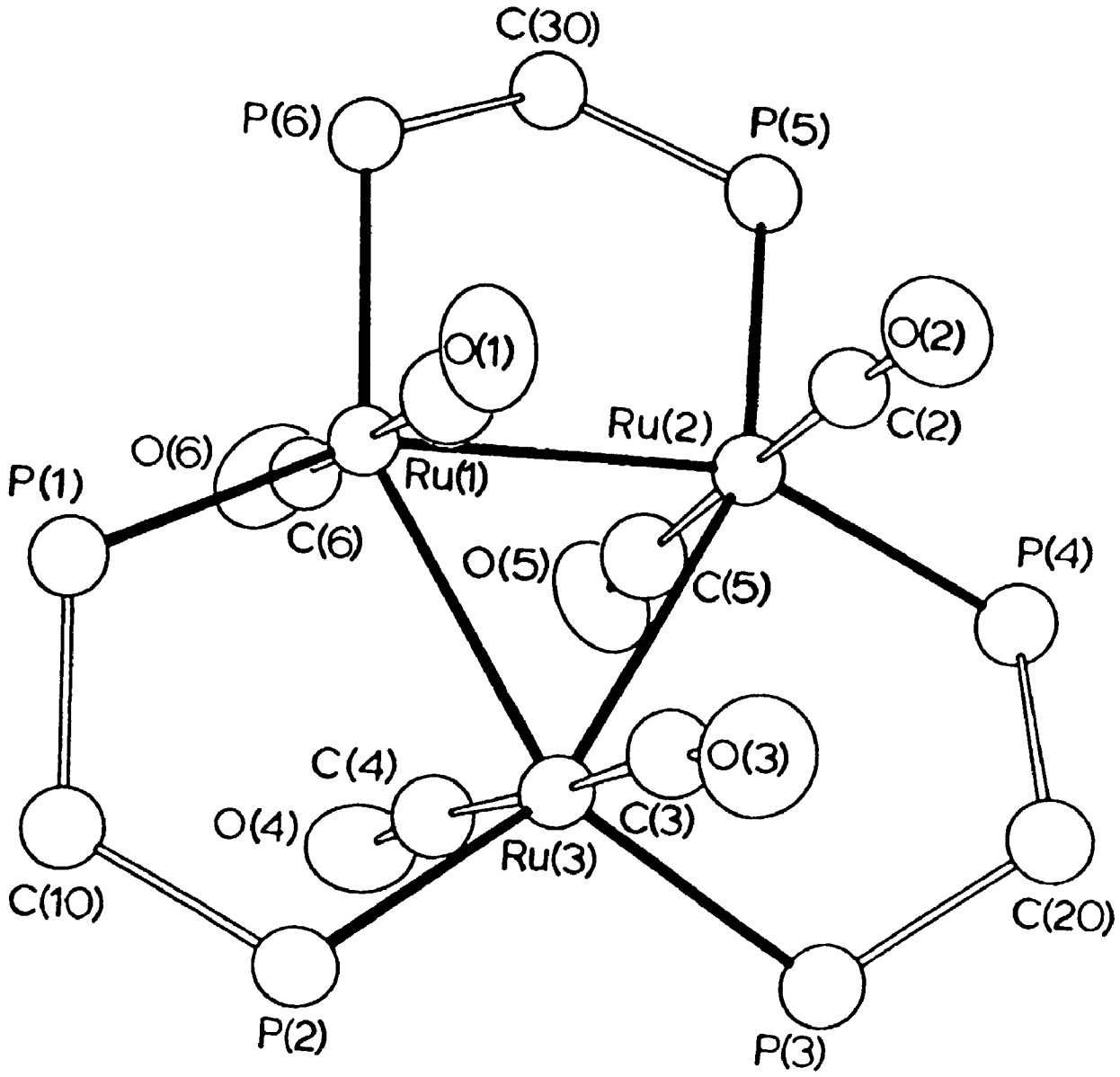

Figure 3.1: The ORTEP diagram of $[Ru_3(CO)_6(\mu\text{-dppm})_3]$, 3.1.

Table 3.1: Selected Bond Distances (Å) and Angles (°) for $[Ru_3(CO)_6(\mu\text{-dppm})_3]$.

Ru(1)-Ru(2)	2.8625(13)	Ru(1)-Ru(3)	2.8515(13)
Ru(2)-Ru(3)	2.8513(14)	Ru(1)-P(1)	2.329(3)
Ru(1)-P(6)	2.300(3)	Ru(1)-C(1)	1.906(14)
Ru(1)-C(6)	1.930(13)	Ru(2)-P(4)	2.302(3)
Ru(2)-P(5)	2.307(3)	Ru(2)-C(2)	1.898(13)
Ru(2)-C(5)	1.910(14)	Ru(3)-P(2)	2.286(3)
Ru(3)-P(3)	2.317(3)	Ru(3)-C(3)	1.898(13)
Ru(3)-C(4)	1.900(14)	P(1)-C(10)	1.854(10)
P(1)-C(111)	1.835(8)	P(1)-C(121)	1.841(7)
P(2)-C(10)	1.867(10)	P(2)-C(211)	1.861(8)
P(2)-C(221)	1.828(8)	P(3)-C(20)	1.882(11)
P(3)-C(311)	1.856(8)	P(3)-C(321)	1.838(9)
P(4)-C(20)	1.852(11)	P(4)-C(411)	1.846(7)
P(4)-C(421)	1.832(8)	P(5)-C(30)	1.845(10)
P(5)-C(511)	1.851(7)	P(5)-C(521)	1.855(8)
P(6)-C(30)	1.872(10)	P(6)-C(611)	1.848(7)
P(6)-C(621)	1.835(7)	O(1)-C(1)	1.159(16)
O(2)-C(2)	1.165(15)	O(3)-C(3)	1.157(16)
O(4)-C(4)	1.162(16)	O(5)-C(5)	1.169(17)
O(6)-C(6)	1.144(16)		

Bond Angles (°)

Ru(2)-Ru(1)-Ru(3)	59.87(3)	Ru(2)-Ru(1)-P(1)	152.89(8)
Ru(2)-Ru(1)-P(6)	91.62(8)	Ru(2)-Ru(1)-C(1)	81.7(4)
Ru(2)-Ru(1)-C(6)	95.4(3)	Ru(3)-Ru(1)-P(1)	93.41(8)
Ru(3)-Ru(1)-P(6)	151.13(8)	Ru(3)-Ru(1)-C(1)	79.5(4)
Ru(3)-Ru(1)-C(6)	100.2(4)	Ru(1)-Ru(2)-Ru(3)	59.87(3)
Ru(1)-Ru(2)-P(4)	153.64(9)	Ru(1)-Ru(2)-P(5)	95.50(8)
Ru(1)-Ru(2)-C(2)	94.2(3)	Ru(1)-Ru(2)-C(5)	80.5(4)

Ru(3)-Ru(2)-P(4)	93.93(8)	Ru(3)-Ru(2)-P(5)	154.82(9)
Ru(3)-Ru(2)-C(2)	92.9(4)	Ru(3)-Ru(2)-C(5)	79.9(4)
Ru(1)-Ru(3)-Ru(2)	60.26(3)	Ru(1)-Ru(3)-P(2)	95.41(8)
Ru(1)-Ru(3)-P(3)	152.81(8)	Ru(1)-Ru(3)-C(3)	96.5(4)
Ru(1)-Ru(3)-C(4)	79.2(4)	Ru(2)-Ru(3)-P(2)	154.64(9)
Ru(2)-Ru(3)-P(3)	92.69(8)	Ru(2)-Ru(3)-C(3)	86.4(4)
Ru(2)-Ru(3)-C(4)	96.0(4)	P(1)-Ru(1)-P(6)	114.5(1)
P(1)-Ru(1)-C(1)	89.3(4)	P(1)-Ru(1)-C(6)	93.7(3)
P(6)-Ru(1)-C(1)	92.8(4)	P(6)-Ru(1)-C(6)	86.1(4)
C(1)-Ru(1)-C(6)	176.9(5)	P(4)-Ru(2)-P(5)	110.2(1)
P(4)-Ru(2)-C(2)	89.8(4)	P(4)-Ru(2) C(5)	92.7(4)
P(5)-Ru(2)-C(2)	94.2(4)	P(5)-Ru(2)-C(5)	91.6(4)
C(2)-Ru(2)-C(5)	127.5(5)	P(2)-Ru(3)-P(3)	111.8(1)
P(2)-Ru(3)-C(3)	89.8(4)	P(2)-Ru(3)-C(4)	85.3(4)
P(3)-Ru(3)-C(3)	83.4(4)	P(3)-Ru(3)-C(4)	102.9(4)
C(3)-Ru(3)-C(4)	173.2(5)	Ru(1)-P(1)-C(10)	112.7(3)
Ru(1)-P(1)-C(111)	119.2(3)	Ru(1)-P(1)-C(121)	120.0(3)
C(10)-P(1)-C(111)	97.2(4)	C(10)-P(1)-C(121)	104.0(4)
C(111)-P(1)-C(121)	100.3(3)	Ru(3)-P(2)-C(10)	111.6(3)
Ru(3)-P(2)-C(211)	121.1(3)	Ru(3)-P(2)-C(221)	117.3(3)
C(10)-P(2)-C(211)	97.1(4)	C(10)-P(2)-C(221)	105.5(4)
C(211)-P(2)-C(221)	101.3(4)	Ru(3)-P(3)-C(20)	110.3(4)
Ru(3)-P(3)-C(311)	116.8(3)	Ru(3)-P(3)-C(321)	123.6(3)
C(20)-P(3)-C(311)	99.0(4)	C(20)-P(3)-C(321)	102.2(4)
C(311)-P(3)-C(321)	101.3(4)	Ru(2)-P(4)-C(20)	110.1(3)
Ru(2)-P(4)-C(411)	119.9(3)	Ru(2)-P(4)-C(421)	121.4(3)
C(20)-P(4)-C(411)	98.1(4)	C(20)-P(4)-C(421)	104.4(4)
C(411)-P(4)-C(421)	99.6(3)	Ru(2)-P(5)-C(30)	111.9(3)
Ru(2)-P(5)-C(511)	115.8(3)	Ru(2)-P(5)-C(521)	123.9(3)
C(30)-P(5)-C(511)	101.2(4)	C(30)-P(5)-C(521)	102.5(4)
C(511)-P(5)-C(521)	98.4(3)	Ru(1)-P(6)-C(30)	112.3(3)

Ru(1)-P(6)-C(611)	121.6(3)	Ru(1)-P(6)-C(621)	116.3(3)
C(30)-P(6)-C(611)	98.3(4)	C(30)-P(6)-C(621)	105.5(5)
C(611)-P(6)-C(621)	100.4(4)	Ru(1)-C(1)-O(1)	172.0(10)
Ru(2)-C(2)-O(2)	173.7(10)	Ru(3)-C(3)-O(3)	171.2(10)
Ru(3)-C(4)-O(4)	171.9(10)	Ru(2)-C(5)-O(5)	172.9(11)
Ru(1)-C(6)-O(6)	173.1(10)	P(1)-C(10)-P(2)	119.1(5)
P(3)-C(20)-P(4)	113.2(6)	P(5)-C(30)-P(6)	117.4(6)
P(1)-C(111)-C(112)	118.7(5)	P(1)-C(111)-C(11[illegible]	121.2(5)
P(1)-C(121)-C(122)	118.3(5)	P(1)-C(121)-C(126)	121.6(5)
P(2)-C(211)-C(212)	120.7(5)	P(2)-C(221)-C(222)	119.7(6)
P(2)-C(221)-C(226)	120.3(6)	P(3)-C(311)-C(312)	118.0(6)
P(3)-C(311)-C(316)	121.8(5)	P(3)-C(321)-C(322)	121.0(6)
P(3)-C(321)-C(326)	118.9(6)	P(4)-C(411)-C(412)	120.4(5)
P(4)-C(411)-C(416)	119.5(5)	P(4)-C(421)-C(422)	119.3(6)
P(4)-C(421)-C(426)	120.7(6)	P(5)-C(511)-C(512)	118.6(5)
P(5)-C(511)-C(516)	121.2(5)	P(5)-C(521)-C(522)	119.8(6)
P(5)-C(521)-C(526)	120.1(6)	P(6)-C(611)-C(612)	121.1(5)
P(6)-C(611)-C(616)	118.9(5)	P(6)-C(621)-C(622)	119.9(6)
P(6)-C(621)-C(626)	119.3(6		

other owing to repulsion between adjacent oxygen atoms. Similar bonding effects were earlier observed in the parent $[Ru_3(CO)_{12}]$ and other related clusters.[1c,12b,20]

3.2.2. Spectroscopic Characterization.

The infrared spectrum of the complex 3.1, depicted in Figure 3.2, shows carbonyl stretches at 1937(vs), 1925(vs), 1914(vs) and 1875(w) cm^{-1} for terminally bound carbonyl groups. These frequencies are shifted significantly to low energy compared to the parent $[Ru_3(CO)_{12}]$ cluster, which exhibits carbonyl stretches at 2066, 2026 and 2004 cm^{-1}.[16b,21] This low energy shift may be attributed to increase in back donation of electronic charge from metal to CO π^* orbitals as a result of substitution of carbonyl groups with phosphine ligands. Substitution of electron withdrawing CO groups with electron donating phosphine ligands causes high electronic charge on the metal atoms. Similar effects have been observed in other binary carbonyl complexes when substituted with donor ligands such as phosphines.[7,22]

The red crystalline complex is readily soluble in most chlorinated solvents. Thus, characterization by NMR spectroscopic methods was possible. The ^{31}P NMR spectrum of 3.1 exhibited, as expected, a single resonance at $\delta = 17.7$ ppm, consistent with all phosphorus atoms being in equivalent sites and dppm being coordinated in bridging fashion.

It is apparent from the solid state structure that all the methylene protons of the dppm ligands are equivalent. Therefore, a single resonance for these protons is expected. The ^1H NMR in CD_2Cl_2 solution indeed shows a single resonance at $\delta =$

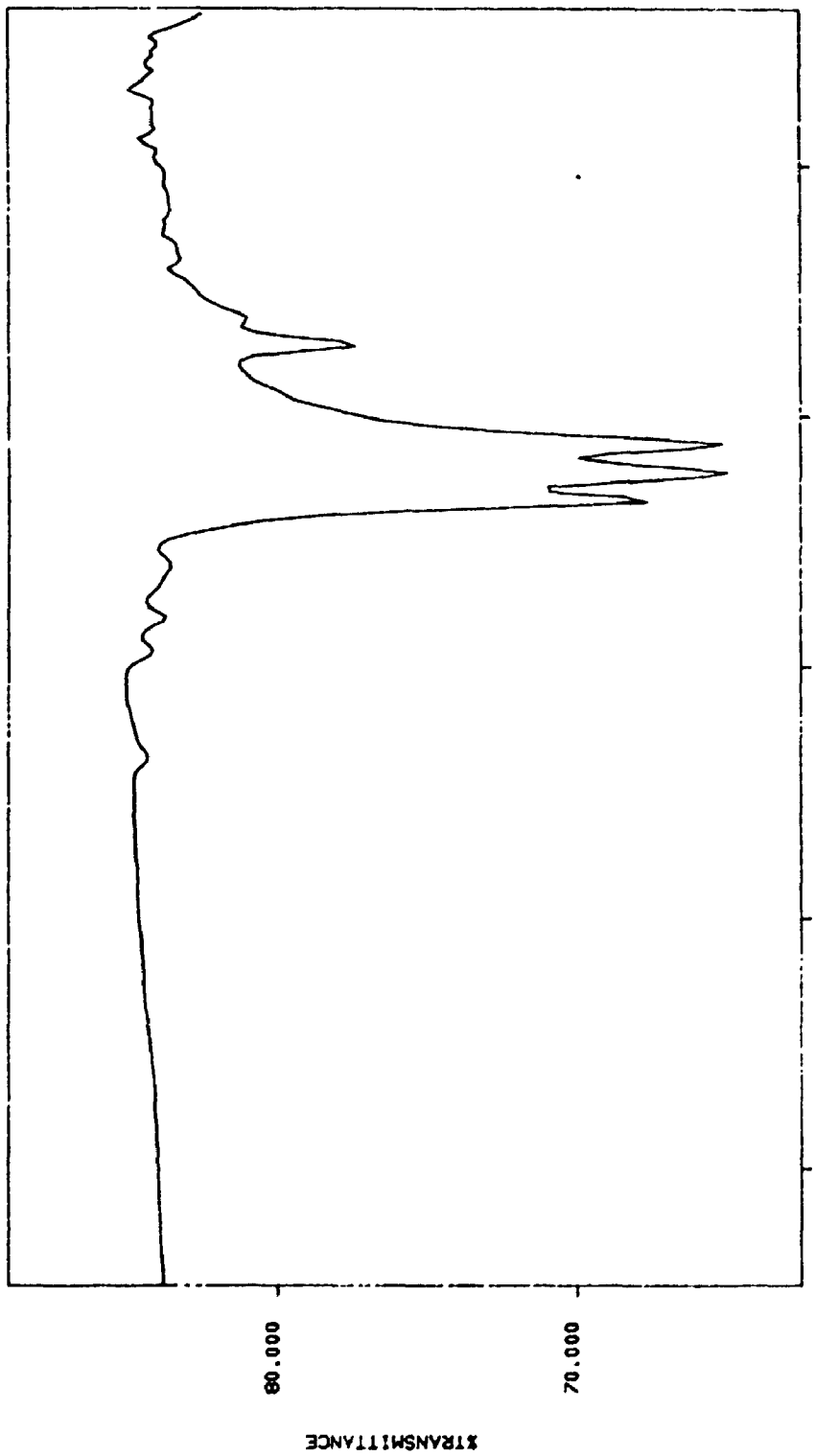

Figure 3.2: The IR spectrum of $[Ru_3(CO)_6(\mu\text{-dppm})_3]$, 3.1.

3.9 ppm for the CH_2P_2 protons of the dppm, which occurs as a triplet due to the coupling to two adjacent phosphorus atoms with $^2J(PH) = 8.9$ Hz. In addition it shows a set of multiplet resonances in the region δ = 7-7.3 ppm for the phenyl protons of the dppm ligand. All these data are, therefore, consistent with the X-ray crystallographic structure shown in Figure 3.1.

3.2.3. Protonation of $[Ru_3(CO)_6(\mu\text{-dppm})_3]$ with Acids

One of the objectives of metal cluster chemistry is to investigate the reactivity of clusters and thus their utility in catalytic reactions. Ruthenium clusters are known to possess unusual properties and are considered as potential candidates for various catalytic transformations. Thus, for example $[Ru_3(CO)_{11}H]^-$ is well known for its reactivity towards hydrogenation of ethylene and propylene.[23] This cluster is also reported to catalyze hydroformylation of ethylene and propylene at higher temperature in the presence of CO.[24] Similarly $[Ru_3(CO)_{12}]$ has been shown to catalyze the hydrogenation of CO,[25] and $[Ru_3(\mu\text{-NCO})(CO)_{10}]^-$ has been shown to catalyze olefin hydrogenation.[26]

The highly electron rich cluster $[Ru_3(CO)_6(\mu\text{-dppm})_3]$, formed during this study, was therefore subjected to various reactions to determine its reactivity pattern. Although in most cases the cluster 3.1 exhibited unusual stability, a facile reaction was observed with acids. Thus, when 3.1 was treated with HBF_4, a proton adduct was formed. This was characterized using analytical and spectroscopic techniques and the structure of this protonated cluster derivative was established by X-ray diffraction studies. Details of these are given below.

3.3. Reaction of 3.1 with HX, the Formation of $[Ru_3(CO)_6(\mu\text{-}H)(\mu\text{-}dppm)_3]X$ (3.2), [X=BF_4 and PF_6].

The NMR spectra in chlorinated solvents of the product $[Ru_3(CO)_6(\mu\text{-}dppm)_3]$, 3.1, often contained a second set of resonances which were finally attributed to the protonated derivative $[Ru_3(H)(CO)_6(\mu\text{-}dppm)_3]^+$, 3.2. This hydridotriruthenium cation is easily formed by protonation of 3.1 and impurities of HCl in chlorinated solvents are sufficient for the purpose. However, complex 3.2 was prepared in high yield when CH_2Cl_2 solutions of 3.1 were treated with either HBF_4 or HPF_6.

3.3.1. The X-ray Structure of $[Ru_3(\mu\text{-}H)(CO)_6(\mu\text{-}dppm)_3]BF_4$ (3.2)

The structure of the cluster cation 3.2 is shown in Figure 3.3 and selected distances, angles and deviations from the Ru_3 plane are in Table 3.2. The structure contains a triangle of ruthenium atoms with equatorial μ-dppm ligands bridging each edge and with six axial carbonyl ligands, all of which are terminally bonded. The hydride ligand in 3.2 was successfully located and refined and bridges the Ru(1)-Ru(3) bond as shown in Figure 3.3. The hydride is not in the Ru_3 plane but lies above the plane and the associated μ-dppm ligand is displaced below, presumably because steric effects are unfavourable with the hydride and μ-dppm ligands co-planar. The Ru-H distances found, while not accurately determined, are similar to those for other $Ru_2(\mu\text{-}H)$ complexes.[1c,14,20,27,28] For example, $[Ru_3(\mu\text{-}H)(CO)_9(\mu_3\text{-}\eta^3\text{-}Me_2PCHPMe_2)]$ has Ru-H distances of 1.66(5) and 1.75Å.[20] Further evidence that the hydride location is correct was obtained from a comparison of differences in bond distances and angles between the structures of 3.1 and 3.2. The essential details of

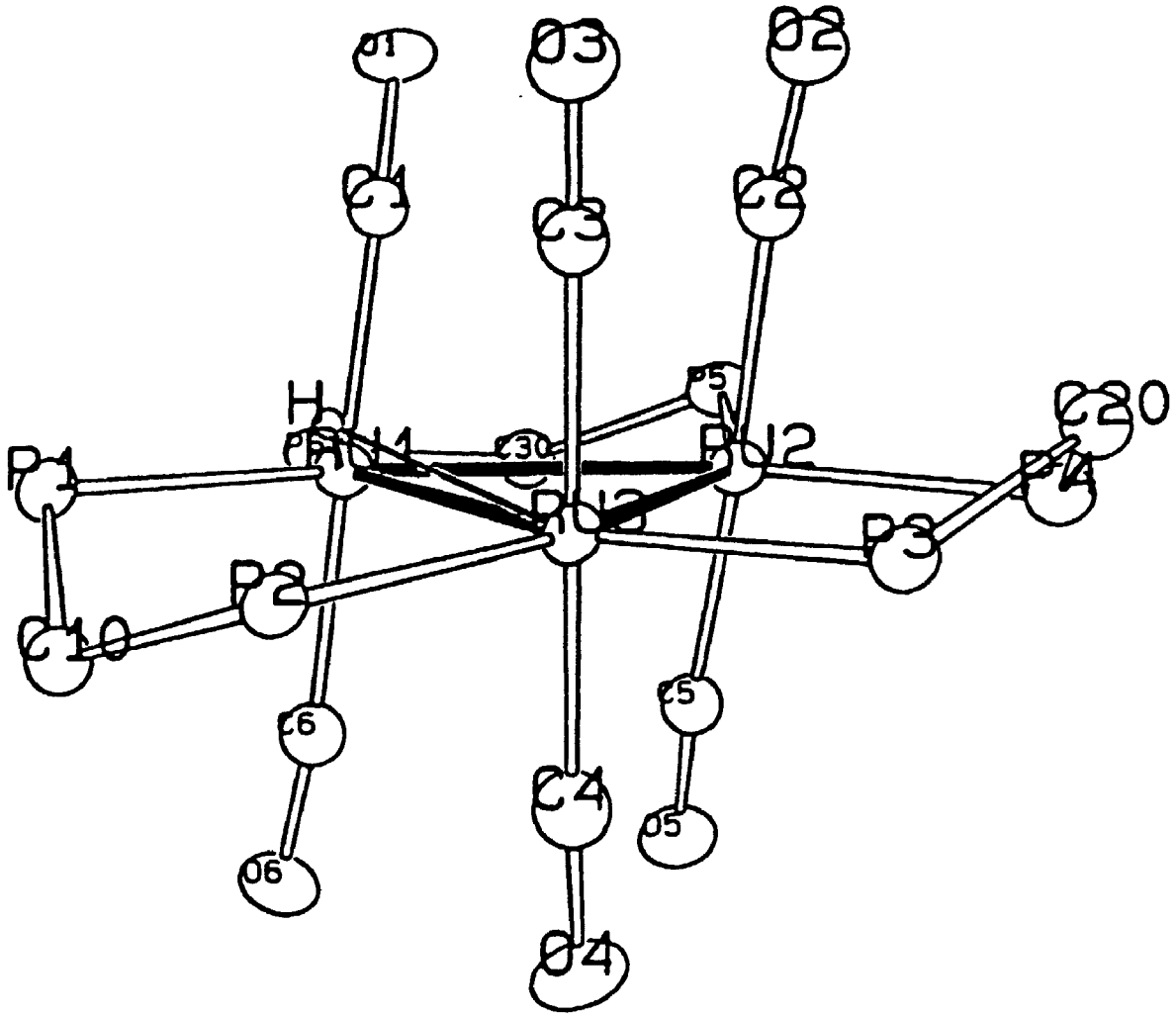

Figure 3.3: The X-ray structure of the cation $[Ru_3(\mu\text{-}H)(CO)_6(\mu\text{-}dppm)_3]^+$, 3.2.

Table 3.2: A Comparison of Selected Bond Distances (Å) and Angles (°) for 3.1 and 3.2.

Distances (Å)	Complexes 3.1	Complex 3.2
Ru(1) - Ru(2)	2.8625(13)	2.8516(18)
Ru(1) - Ru(3)	2.8515(13)	2.9402(18)
Ru(2) - Ru(3)	2.8513(14)	2.8764(18)
Ru(1) - P(1)	2.329(3)	2.349(4)
Ru(1) - P(6)	2.300(3)	2.325(5)
Ru(2) - P(4)	2.302(3)	2.339(5)
Ru(2) - P(5)	2.307(3)	2.306(5)
Ru(3) - P(2)	2.286(3)	2.343(4)
Ru(3) - P(3)	2.317(3)	2.329(4)
Ru(1) - C(1)	1.906(14)	1.930(17)
Ru(1) - C(6)	1.930(13)	1.942(18)
Ru(2) - C(2)	1.898(13)	1.917(17)
Ru(2) - C(5)	1.910(14)	1.875(17)
Ru(3) - C(3)	1.898(13)	1.918(17)
Ru(3) - C(4)	1.900(14)	1.907(20)
Ru(1) - H		1.69(18)
Ru(3) - H		1.95(17)
P - CH_2	1.85(1)-1.88(1)	1.82(2)-1.91(2)
P - C(Ph)	1.828(8)-1.861(8)	1.82(2)-1.86(1)
C - O	1.14(2)-1.17(2)	1.12(2)-1.18(2)

Bond angles(°)

Ru(3) - Ru(1) - Ru(2)	59.87(3)	59.53(4)
Ru(3) - Ru(1) - Ru(1)	59.87(3)	61.77(4)
Ru(2) - Ru(3) - Ru(1)	60.26(3)	58.70(4)
C(6) - Ru(1) - C(1)	176.9(5)	174.5(7)
C(5) - Ru(3) - C(2)	172.5(5)	173.3(7)
C(4) - Ru(3) - C(3)	173.2(5)	174.5(8)
C(1) - Ru(1) - P(1)	89.3(4)	99.7(5)
C(6) - Ru(1) - P(1)	93.7(3)	83.8(5)
C(3) - Ru(3) - P(2)	89.8(4)	94.5(5)
C(4) - Ru(3) - P(2)	85.3(4)	89.1(6)
C(1) - Ru(1) - P(6)	92.8(4)	87.8(5)
C(6) - Ru(1) - P(6)	86.1(4)	86.9(5)
C(3) - Ru(3) - P(3)	83.4(4)	88.8(5)
C(4) - Ru(3) - P(3)	102.9(4)	93.6(6)
C(2) - Ru(2) - P(4)	89.8(4)	83.9(5)
C(2) - Ru(2) - P(5)	94.2(4)	88.0(5)
C(5) - Ru(2) - P(4)	92.7(4)	101.3(5)
C(5) - Ru(2) - P(5)	91.6(4)	86.1(5)
P - Ru - P	110.2(1)-114.5(1)	112.3(2)-114.7(2)
Ru - C - O	171(1)-174(1)	171.3(2)-178(2)
Ru - Ru - C	91.62(8)-95.50(8)	91.1(1)-94.7(1)
Ru - Ru - C	79.2(4)-100.2(4)	82.4(5)-96.7(5)

Ru(1) - H - Ru(3)	107.7(9)
C(1) - Ru(1) - H	79.8(6)
C(6) - Ru(1) - H	105.7(6)
C(3) - Ru(3) - H	71.9(5)
C(4) - Ru(3) - H	105.8(5)
P(1) - Ru(1) - H	58.6(6)
P(2) - Ru(3) - H	68.5(5)

Deviations (Å) of Selected Atoms from the Ru_3 Plane

Complex	**3.1**	**3.2**
P(1)	0.196(4)	0.067(4)
P(2)	0.299(4)	-0.174(4)
P(3)	-0.115(4)	0.069(5)
P(4)	-0.127(4)	-0.033(5)
P(5)	-0.223(4)	0.234(5)
P(6)	0.192(4)	-0.272(5)
H		0.6(2)

analogies and differences between the structures of 3.1 and 3.2 is therefore, discussed in this section.

The complexes containing the $M_3(\mu\text{-dppm})_3$ core do not have regular planar structures as a result of two different effects.[5d] Firstly, the $M_2(\mu\text{-dppm})$ units adopt envelope conformations with the CH_2 group at the "flap". If the flap is up (i.e. CH_2 above the M_3P_6 plane), the phenyl groups above the plane are equatorial and so cause less steric congestion than those below the plane which are axial. This effect alone leads to six possible orientations of the $Ru_3(\mu\text{-dppm})_3$ unit. Since this is the major effect in determining overall steric hindrance, the numbering system for the structure of 3.2 has been chosen to be the same as that for the structure of 3.1 so that the conformations of the dppm ligands within the $Ru_3(\mu\text{-dppm})_3$ units are the same in each case. Thus, each structure has the flap atoms C(10) and C(30) below and C(20) above the Ru_3 plane. The second type of distortion which occurs to minimize steric effects is a twisting of the dppm ligands such that the phosphorus atoms are displaced from the Ru_3 plane. Thus, in $[Ru_3(CO)_{12}]$ the equatorial carbonyls are displaced from the Ru_3 plane by a maximum of only 0.041 Å[12b] but in 3.1 and 3.2 the analogous maximum displacements of phosphorus atoms are 0.299 and 0.272 Å respectively. While the direction of the dppm twist in the structures of 3.1 and 3.2 is the same for P(3)C(20)P(4), it is opposite for P(1)C(10)P(2) and P(5)C(30)P(6). The greatest difference is for the dppm ligand P(5)C(30)P(6); thus in complex 3.1, P(5) is 0.223 Å below and P(6) is 0.192 Å above the Ru_3 plane whereas, in 3.2, P(5) is 0.234 Å above and P(6) is 0.272 Å below the Ru_3 plane. These distortions define the octahedral coordination axes for each ruthenium centre[19] and so the orientations of

the carbonyl ligands are also different in the structures of 3.1 and 3.2. In $[Ru_3(CO)_{12}]$ the range of Ru-Ru-C(axial) angles is only 87.7- 90.5°,[12b] but in 3.1 and 3.2 the ranges are much greater at 79.2-100.2 and 82.4-96.7° respectively and the pattern of distortions from 90° is different in each case. Because the dppm ligands are the major source of steric effects, the differences in orientations of these ligands in 3.1 and 3.2 will cause significant differences in other bond parameters thereby complicating the interpretation of structural differences due to the hydride in 3.2. This should be borne in mind in the following discussion.

Considering trends in bond distances, both the average Ru-P and Ru-C distances are slightly greater in 3.2 than in 3.1, and this could be due either to greater steric effects or to reduced backbonding in the hydrido cation. The greatest difference is in the Ru(1)-Ru(3) distance which is 0.089(2)Å longer in 3.2 than in 3.1, consistent with this bond being the site of protonation.

As discussed above, differences in angles must be interpreted with caution. Thus, it is noted that the angles C(1)-Ru(1)-P(1) and C(3)-Ru(3)-P(2) increase by 10.4 and 4.7° respectively from 3.1 to 3.2 as expected if the hydride is present above the Ru(1)-Ru(3) edge, but there are marked differences between many other C-Ru-P angles (Table 3.2). More convincing evidence that the hydride is correctly located comes from a consideration of the displacements of phosphorus atoms from the Ru_3 plane. If we define this displacement for P(n) as δ[P(n)], then the values of $\Sigma\delta$[P(n)] for 3.1 and 3.2 are 0.222 and -0.109Å respectively. That is, the net displacement of all P atoms is 0.222Å above the plane in 3.1 but 0.109 Å below the plane in 3.2. This is consistent with an overall repulsion by the hydride in 3.2 which lies above the

plane. The difference in net P displacement between the two structures is 0.331 Å which can be factored as 0.602 [P(1) + P(2)] + 0.280 [P(3) + P(6)] - 0.551 [P(4) + P(5)] Å. Thus, the hydride repels the closest phosphorus atoms P(1) and P(2) most, while P(3) and P(6) are more weakly repelled. Since these displacements affect steric effects below the plane, therefore, P(4) and P(5), which are not directly affected by the hydride, are displaced above the plane in response. The overall differences in geometry of the dppm ligands between 3.1 and 3.2 thus follow naturally from the position of the hydride ligand and, in turn, provide strong evidence that the hydride ligand is located correctly by the X-ray structure determination.

3.3.2. Spectroscopic Characterization

The IR spectrum of 3.2 is depicted in Figure 3.4 and shows carbonyl stretches at 1995(w), 1966(vs), 1952(vs), 1930(sh), 1907(sh) and 1885(w) cm^{-1}. The high energy shift of these bands compared to the parent $[Ru_3(CO)_6(\mu\text{-dppm})_3]$ (3.1) are consistent with the expected decrease in Ru-CO backbonding in the cation 3.2.

In the ^1H NMR spectrum, cation 3.2 gives a broad singlet attributed to a ruthenium hydride proton at δ = -18.68 ppm, and a single resonance due to the CH_2P_2 protons of the dppm ligands at δ = 3.87 ppm, while the ^{31}P NMR spectrum contains a sharp singlet due to the phosphorus atoms of dppm. The spectra were unchanged at -80°C. These data show that the cation has effective D_{3h} symmetry on the NMR time scale. Thus, three fold symmetry is necessary for equivalence of the six phosphorus atoms and a plane of symmetry containing the $Ru_3(\mu\text{-dppm})_3$ unit is necessary for equivalence of the $CH^aH^bP_2$ protons of each dppm ligand. For a non-

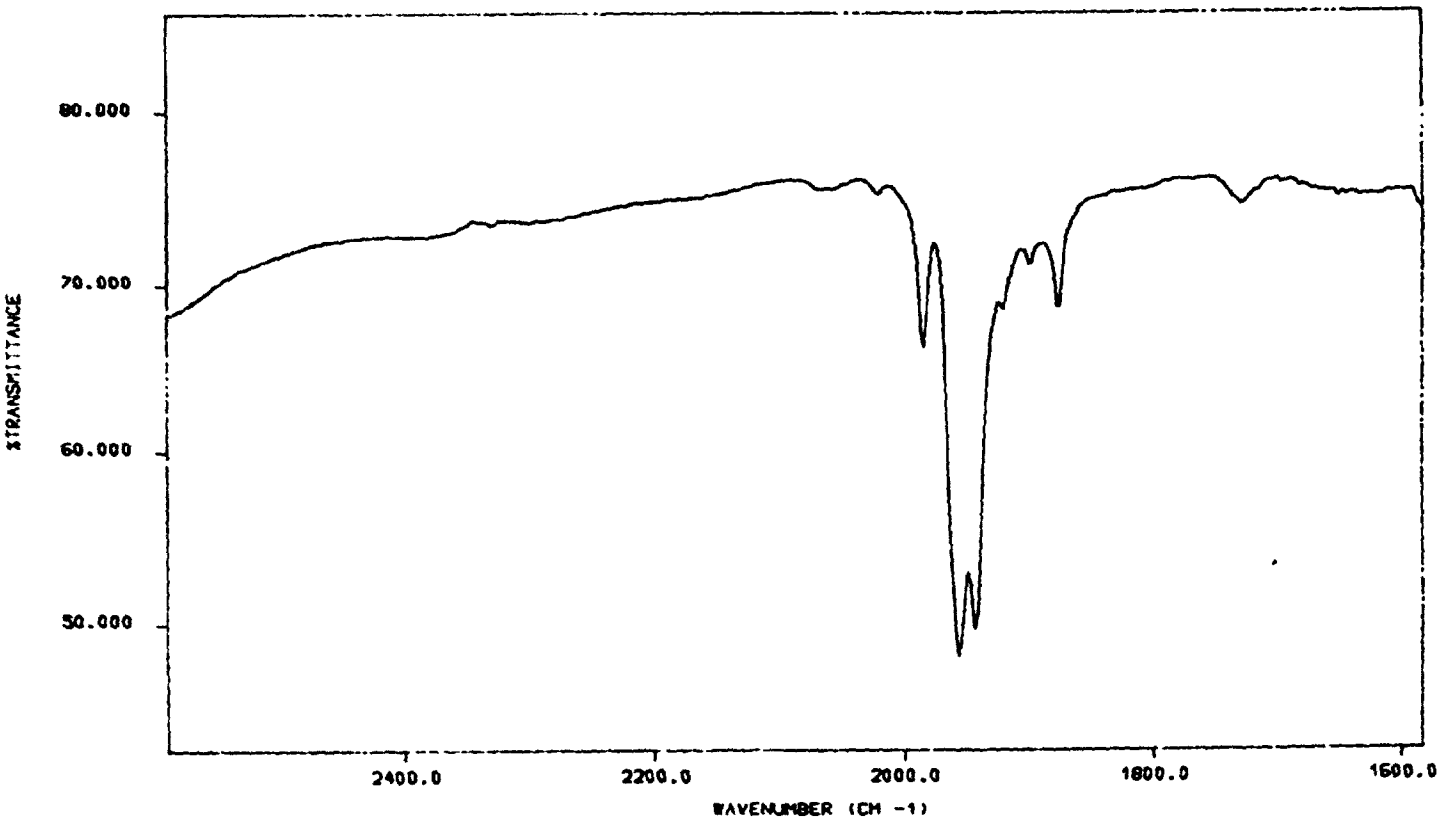

Figure 3.4: The IR spectrum of $[Ru_3(\mu\text{-}H)(CO)_6(\mu\text{-}dppm)_3]BF_4$, 3.2.

fluxional structure, this would indicate that an unprecedented planar $Ru_3(\mu_3\text{-}H)$ group is present. The alternative is a fluxional cluster containing either a non-planar $Ru_3(\mu_3\text{-}H)$ group or a $Ru_2(\mu\text{-}H)$ group, the latter requiring a greater degree of fluxionality. The precedents are all for addition of electrophiles to an edge of Ru_3 clusters. For example, H^+ adds to an unbridged edge in both $[Ru_3(CO)_{12}]$ and in $[Ru_3(CO)_8(\mu\text{-dppm})_2]$.[29] Since complex 3.1 has all edges bridged by μ-dppm ligands, edge protonation must lead to increased steric hindrance between the hydride and μ-dppm. It thus seemed possible that face bridging of the hydride might be preferred, although this is unprecedented in $[Ru_3(CO)_{12}]$ or its phosphine-substituted derivatives.[13,28]

3.3.4. Fluxional Process in $[Ru_3(\mu\text{-}H)(CO)_6(\mu\text{-dppm})_3]^+$ (3.2).

The new hydride cluster cation 3.2 has interesting structural and fluxional properties. The X-ray structure determination, as discussed earlier, shows convincingly that the cation in the solid state should be formulated as $[Ru_3(\mu\text{-}H)(CO)_6(\mu\text{-dppm})_3]^+$. However, the NMR spectra, even at -80°C, indicate three fold symmetry and so, assuming the preferred structures are the same in the solid and solution states, the compound is fluxional. The migration of hydride from edge to edge of the cluster must be particularly easy in 3.2 and this is likely to occur by way of a $Ru_3(\mu_3\text{-}H)$ intermediate as shown in Scheme 3.1.

In addition the hydride must be able to migrate easily from one side of the Ru_3 triangle to the other. This could occur either on the outside of the triangle, through a transition state in which the μ-H and μ-dppm ligands are coplanar, or by tunnelling through the centre of the Ru_3 triangle (scheme 3.2) as has been suggested to occur for

Scheme 3.1: Edge to edge migration of the hydride ligand.

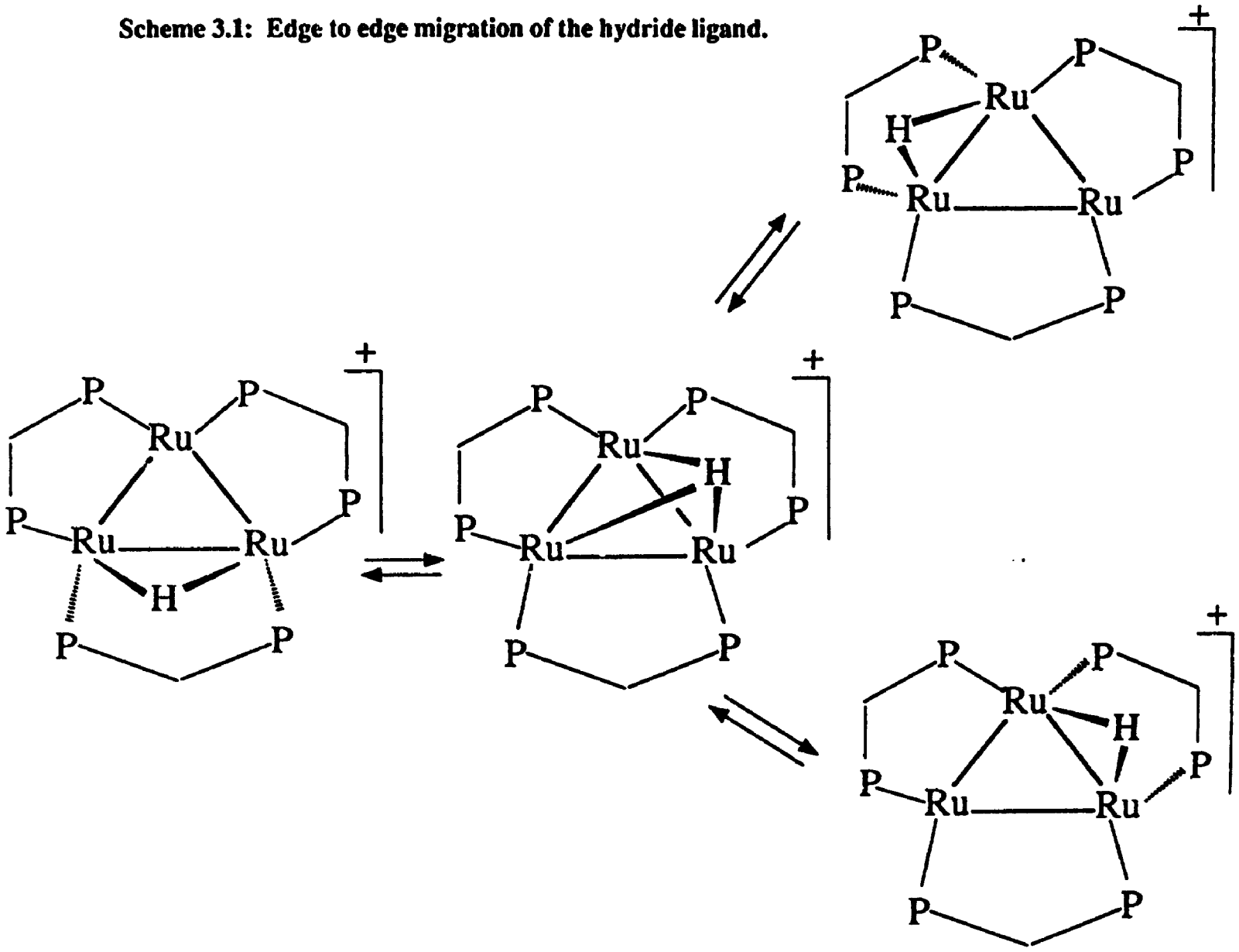

Scheme 3.2: Face to face migration of the hydride ligand.

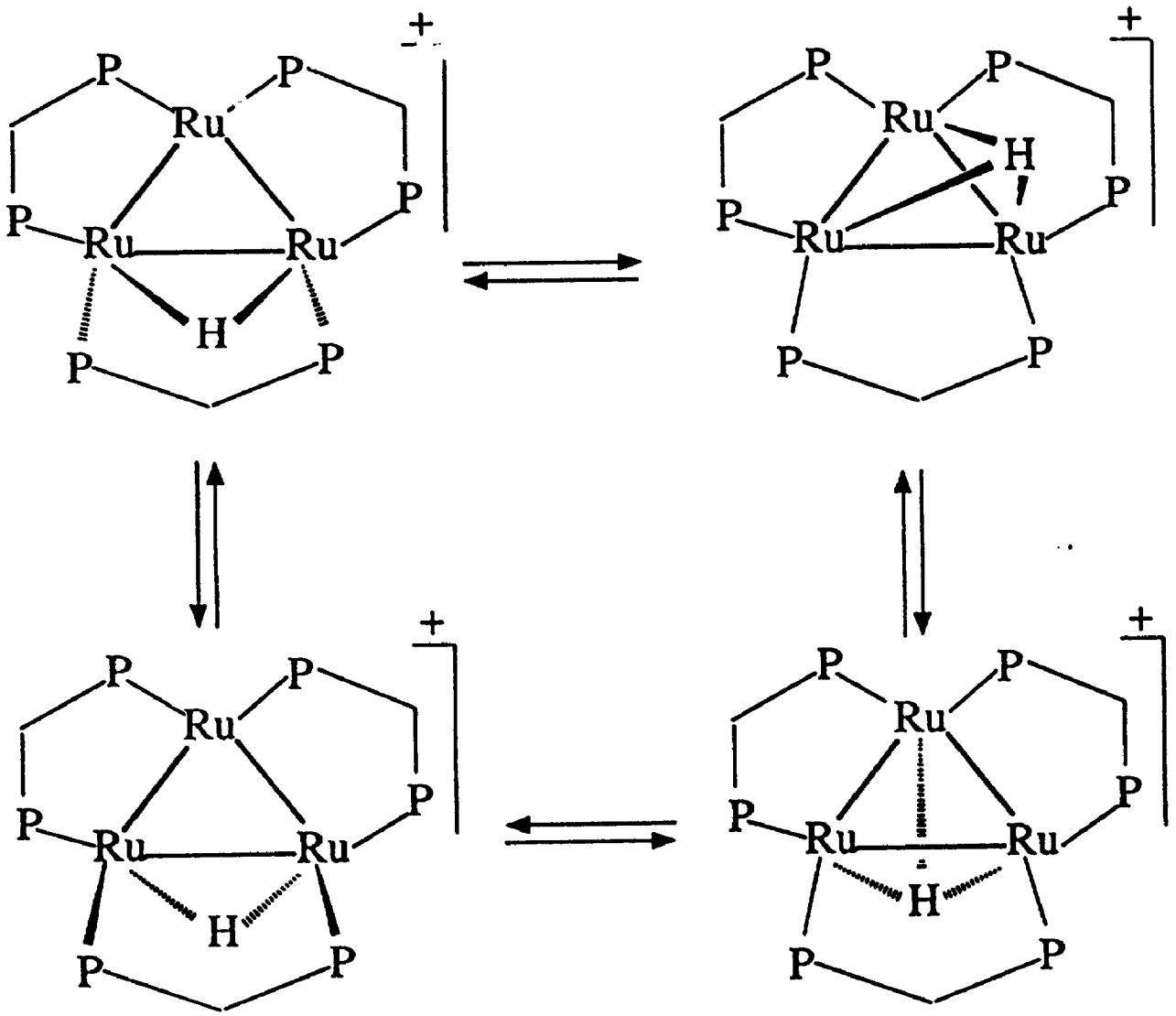

$[Pt_3](\mu_3\text{-H})(\mu\text{-dppm})_3]^+$.[30] However, the above data cannot distinguish between the two mechanisms.

The protonation of $[Ru_3(CO)_6(\mu\text{-dppm})_3]$ occurs much more easily than for either $[Ru_3(CO)_{12}]$ or $[Ru_3(CO)_8(\mu\text{-dppm})_2]$.[29] This is of course expected in terms of electronic effects since substitution of dppm for carbonyls increases the electron density at ruthenium, but is opposed by steric effects. For the proton, electronic effects are dominant but attempts to add bulkier electrophiles such as Ag^+ or Ph_3PAu^+ to 3.1 have been unsuccessful, presumably due to unfavourable steric effects. The increase in electron density at the Ru_3 triangle is also indicated by the decrease in values of ν(CO) as more dppm ligands are introduced. The strong ν(CO)/cm^{-1} bands are as follows: $[Ru_3(CO)_{12}]$, 2066, 2026, 2004; $[Ru_3(CO)_{10}(\mu\text{-dppm})]$, 2013, 2003, 1966; $[Ru_3(CO)_8(\mu\text{-dppm})_2]$, 2023, 1981, 1970; $[Ru_3(CO)_6(\mu\text{-dppm})_3]$, 1937, 1925, 1914.[16b]

3.4 Conclusions:

This chapter describes the synthesis of a highly substituted ruthenium carbonyl cluster $[Ru_3(CO)_6(\mu\text{-dppm})_3]$, 3.1, from the in-situ reduction of Ru(III) salts with $NaBH_4$ in the presence of dppm under an atmosphere of CO. The structure of electronically saturated cluster 3.1, is established by single crystal X-ray diffraction studies. It is also shown that this electron rich cluster complex is very reactive towards small molecules. Thus, protonation with, for example, HBF_4 yields the adduct $[Ru_3(\mu\text{-H})(CO)_6(\mu\text{-dppm})_3]^+$, 3.2, whose structure is also established from X-ray crystallography. The presence of hydride is confirmed by spectroscopic means

and is also correctly located from the difference Fourier map in the X-ray structure determination. Spectroscopic data also indicate that the hydride is fluxional and the mechanism of the fluxional process is proposed.

3.5. Experimental:

3.5.1. Synthesis of $[Ru_3(CO)_6(\mu\text{-dppm})_3]$ (3.1).

Silver acetate (2.2 g) was added to a stirred solution of $RuCl_3.3H_2O$ (1.0 g) in EtOH (30 mL). The mixture was stirred for 10 min., allowed to stand overnight and then filtered to remove AgCl. To the filtrate was added dppm (1.6 g) in toluene (30 mL) and the solution was saturated with CO. To this solution was added dropwise a suspension of $NaBH_4$ (1.2 g) in EtOH (25 mL), with rapid bubbling of CO through the solution. The mixture was stirred for a further 4h., and then the orange precipitate of the product $[Ru_2(CO)_4(\mu\text{-CO})(\mu\text{-dppm})_2]$ was separated by filtration. The mother liquor was allowed to stand for 3 weeks at room temperature, whereupon red crystals of the product slowly formed.

Yield 5%.

IR (Nujol); ν(CO): 1937 (vs), 1925 (vs), 1914 (vs), 1875 (w).

NMR CD_2Cl_2 ^1H: δ =3.9 [t, $^2J(PH)$ = 8.9, CH_2P_2]; ^{31}P: δ = 17.7 [s].

3.5.2. $[Ru_3(\mu\text{-H})(CO)_6(\mu\text{-dppm})_3][PF_6]$ (3.2).

To a solution of $Ru_3(CO)_6(\mu\text{-dppm})_3]$ (0.1 g) in CH_2Cl_2 (10 mL) was added aqueous HPF_6 (1 mL). Monitoring by ^{31}P NMR showed that conversion to the product was essentially quantitative. The solvent was evaporated to dryness and the product was washed with ether. The crude product was then recrystallized with $C_2H_4Cl_2$ and n-heptane (1:2, 15 mL).

Yield: 95%

NMR in CD_2Cl_2: $\delta(^1H)$ = 3.87 [t, 6H, $J(PH)_{obs}$ = 10, CH_2P_2]; -18.68 [s,1H,

RuH]; $\delta(^{31}P)$ = 15.3 [s, dppm]. IR: ν(CO) =1995(w), 1966(vs), 1952(vs), 1930(sh), 1907(sh), 1885(w). The BF_4^- salt was prepared similarly and the cation had identical spectroscopic properties.

3.6. References:

1. (a) E.L. Muetterties; Science ***196***, 839 (1977).

(b) E.L. Muetterties and M.J. Krause; Angew. Chem. Int. Ed. Engl. ***22***, 135 (1983).

(c) N. Lugan; J.J. Bonnet and J.A. Ibers; J. Am. Chem. Soc. ***107***, 4484 (1985).

2. (a) R. Whyman; J. Chem. Soc. Dalton Trans. 1375 (1972).

(b) J.A. Clucas; M.M. Harding; B.S. Nicholls and A.K. Smith; J. Chem. Soc. Dalton Trans. 1835 (1985).

3. S.D. Jackson; P.B. Wells; R. Whyman and P. Worthington; Catalysis, Ed. C. Kemball and D.A. Dowden, Royal Soc. Chem. ***4***, 75 (1981).

4. C.U. Pittman Jr.; G.M. Wilemon; W.D. Wilson; R.C. Rayan; Angew. Chem. Int. Ed. Engl. ***19***, 478 (1980).

5. (a) G. Huttner; J. Schneider; H.D. Müller; G. Mohr; J. vonSeyerl and L. Wohlfahrt; Angew. Chem. Int. Ed. Engl. ***18***, 76 (1979).

(b) A.J. Carty; S.A. Maclaughlin and N.J. Taylor; J. Organomet. Chem. ***204***, C27 (1981).

(c) S.A. Maclaughlin; N.J. Taylor and A. J. Carty; Organomet. ***2***, 1194 (1983).

(d) R.J. Puddephatt; Lj. Manojlovic-Muir and K.W. Muir; Polyhedron ***23***, 2767 (1990) and refs. therein.

6. R.J. Puddephatt; Chem. Soc. Rev. 99 (1983).

7. H. A. Mirza; M.Sc. Thesis, Lakehead University (1988).

8. (a) A.R. Sanger; J. Chem. Soc. Chem. Commun. 893 (1975).

(b) A.R. Sanger; J. Chem. Soc. Dalton Trans. 120 (1977).

9. G. Ferguson; M.C. Jennings; H.A. Mirza and R.J. Puddephatt; Organomet. *9*, 1576 (1990).

10. (a) H.A. Mirza; J.J. Vittal and R.J. Puddephatt; J. Chem. Soc. Chem. Commun. 309 (1991).

(b) D.J. Elliot; H.A. Mirza; R.J. Puddephatt; D.G. Holah, A.N. Hughes; R.H. Hill and W. Xia; Inorg. Chem. *28*, 3282 (1989).

(c) D.G. Holah; A.N. Hughes; H.A. Mirza and J.D. Thompson; Inorg. Chim. Acta. *126*, L7 (1987).

11. (a) L. Mond; H. Hirtz and M.D. Cowap; Proc. Chem. Soc. *26*, 67 (1910).

(b) L. Mond and A.E. Wallis; J. Chem. Soc. *121*, 29 (1922).

12. (a) M.I. Bruce; "Comprehensive Organometallic Chemistry", G. Wilkinson, F.G.A. Stone and E.W. Abel eds., Pergamon, Oxford, (1982), Vol. *4*, ch. 32.1.

(b) M.R. Churchill; F.J. Hollander; J.P. Hutchinson; Inorg. Chem. *16*, 2655 (1977).

13. E.A. Seddon and K.R. Seddon; "The Chemistry of Ruthenium", Elsevier, Amsterdam, (1984).

14. S. Cartwright; J.A. Clucas; R.H. Dawson; D.F. Foster; M.M. Harding; A.K. Smith; J. Organomet. Chem. *302*, 403 (1986).

15. M.I. Bruce; "Comprehensive Organometallic Chemistry", G. Wilkinson, F.G.A. Stone and E.W. Abel eds., Pergamon, Oxford, (1982), Vol. *4*, ch. 32.5.

16. (a) W. Radecka-Paryzek and R.J. Puddephatt; Inorg. Chim. Acta. *147*, 207 (1988).

(b) M.I. Bruce; J.G. Matisons; B.K. Nicholson; J. Organomet. Chem. *247*, 321 (1983).

17. (a) B. Ambwani; S. Chawla and A. Poë; Inorg. Chem. *24*, 2635 (1985).

(b) B. Ambwani; S.K. Chawla and A. Poë; Inorg. Chim. Acta. *133*, 93 (1987).

18. D.W. Engel; K.G. Moodely; L. Subramony; R.J. Haines; J. Organomet. Chem. *149*, 393 (1988).

19. G. Lavigne; N. Lugan; J. Bonnet; Acta. Cryst. B, *B38*, 1911 (1982).

20. Lj. Manojlovic-Muir; D.A. Brandes; R.J. Puddephatt; J. Organomet. Chem. *332*, 201 (1987).

21. J.A. Ladd; H. Hope and A.L. Balch; Organomet. *3*, 1838 (1984).

22. (a) K.S. Raghuveer and R.B. King; Inorg. Chem. *23*, 2482 (1984).

(b) R.B. King and J. Gimeno; Inorg. Chem. *17*, 2390 (1978).

(c) K.S. Raghuveer; Ph.D. Thesis, University of Georgia (1983).

23. (a) G. Süss-Fink; J. Organomet. Chem. *193*, C20 (1980).

(b) G. Süss-Fink and R. Reiner; J. Mol. Catal. *16*, 231 (1982).

24. W.L. Gladfelter and K.J. Roesselet; "The Chemistry of metal cluster complexes", ed. D.F. Shriver, H.D. Kaesz and R.D. Adams, VCH publishing Inc. N.Y. (1990).

25. (a) J.F. Knifton; J. Am. Chem. Soc. *103*, 3959 (1981).

(b) B.D. Dombek; J. Am. Chem. Soc. *103*, 6508 (1981).

(c) B.K. Warren and B.D. Dombek; J. Mol. Catal. *79*, 334 (1983).

26. J.L. Zuffa; M.L. Blohm and W.L. Gladfelter; J. Am. Chem. Soc. *108*, 552 (1986).

27. M.I. Bruce, O.B. Shawkataly, M.L. Williams; J. Organomet. Chem. *287*, 127 (1985).

28. T. Yoshida; T. Adachi; T. Tanaka; F. Goto; J. Organomet. Chem. *428*, C12

(1992).

29. (a) J. Knight; M.J. Mays; J. Chem. Soc. A, 711 (1970).

(b) G. Lavigne; N. Lugan; J. Bonnet; J. Organomet. *1*, 1040 (1982).

(c) J.A. Ladd; H. Hope and A.L. Balch; Organomet. *3*, 1838 (1984).

30. B.R. Lloyd and R.J. Puddephatt; J. Am. Chem. Soc. *107*, 7785 (1985).

Chapter 4

Synthesis of Di and Tetranuclear Cobalt Complexes Stabilized with Bis(dimethylphosphino)methane. Solution Dynamics and Chemistry of $[Co_2(CO)_4(\mu\text{-dmpm})_2]$ Isomers.

4.1. Introduction

One of the historically important organometallic species is $[Co_2(CO)_8]$ since it was among the first binary metal carbonyl complexes to be discovered in the early 1900's.[1] Dicobalt octacarbonyl is of considerable interest because it is an important catalyst precursor. Thus, the catalyst $[HCo(CO)_4]$ can be readily formed by the reaction of H_2 as illustrated by equation 4.1[2]

$$[Co_2(CO)_8] + H_2 = 2[HCo(CO)_4] \qquad (4.1)$$

Dicobalt octacarbonyl $[Co_2(CO)_8]$ is also of interest because it exhibits unusually complex structural characteristics. Thus, in the solid state, the structure is of C_{2v} symmetry involving a pair of bridging CO groups.[3] However, in solution, IR studies have suggested that in addition to the C_{2v} structure, there exist two non bridged forms with D_{3d} and D_{2d} symmetry.[4] Stereochemical nonrigidity and the interconversions of these isomers, as shown in equation 4.2, have been the subject of detailed investigations. However, the interconversions are too rapid even at -150°C to allow a study of the dynamics by ^{13}C NMR spectroscopy. A similar situation is observed in those phosphine substituted derivatives that have been studied so far, including

$[Co_2(CO)_4(\mu\text{-}CO)_2(\mu\text{-dppm})]$.[5]

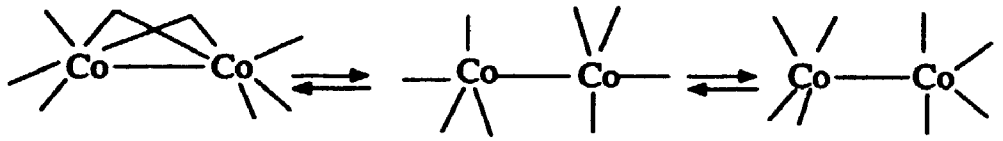

A B C (4.2)

In solution $[Co_2(CO)_8]$ reacts rapidly with nucleophiles, such as phosphines to give a variety of products. In general, disproportionation occurs in polar solvents with monodentate phosphines to give ionic complexes of the type $[Co(CO)_3L_2]^+[Co(CO)_4]^-$ while, in nonpolar solvents, neutral complexes of the type $[Co_2(CO)_6L_2]$ have been isolated.[6] The monosubstituted compounds such as $[Co_2(CO)_7L]$ can also be prepared by direct reaction in Nujol solutions.[7] Direct substitution of more than two CO molecules does not occur readily. More highly substituted products, however, can be prepared by other indirect methods. Substitution with potentially bridging phosphine ligands has led to complexes of the type $[Co_2(CO)_4(\eta^2\text{-PP})_2(\mu\text{-PP})]^{2+}$, $[Co(CO)_3(PP)]^+[Co(CO)_4]^-$ or $[Co_2(CO)_{8-2n}(PP)_n]$ depending on the reaction conditions. Of the latter complexes, species with n=1 are known for dmpm and related phosphines.[8] The ligand is found in a bridging mode in a doubly CO bridged structure resembling the solid state structure of $[Co_2(CO)_8]$, that is as $[Co_2(CO)_4(\mu\text{-}CO)_2(\mu\text{-dmpm})]$. A second substitution to provide $[Co_2(\mu\text{-}PP)_2(CO)_4]$ complexes is generally observed only for ligands containing strong electron withdrawing substituents on the phosphorus donor such as $(RO)_2PN(R')P(OR)_2$ (R=CH_2,Me or Pr^i [9], R=R'=Me[10]). Substitution in $[Co_2(\mu\text{-}$

$CO)_2(CO)_2$(norbornadiene)$_2$] by the tetradentate ligand $(Et_2PCH_2CH_2)(Ph)PCH_2P(Ph)(CH_2CH_2PEt_2)$[11] provides the complex meso-[$Co_2(\mu$-$CO)_2(CO)_2$(eLTTP)]. With the bidentate ligand $CH_3N(PF_2)_2$ substitution of six or even eight carbonyls can be achieved to provide [$Co_2(\mu$-PP)$_3(CO)_2$] and carbonyl free [$Co_2(\mu$-PP)$_3(\eta^1$-PP)$_2$] complexes respectively.[12] [$Co_2(CO)_4(PP)_2$] type complexes are also known in which the phosphine adopts a chelating mode of coordination.[13]

In the absence of a nucleophile, [$Co_2(CO)_8$] decomposes on heating in solution to form the tetranuclear species [$Co_4(CO)_{12}$].[14] Crystal disorder has rendered difficulty in accurate structure determination, but it has been shown that it contains a tetrahedron of cobalt atoms with both terminal and bridging carbonyl groups and having approximate C_{3v} symmetry shown in Figure 4.1a.[15] The structure of [$Co_4(CO)_{12}$] in solution has been the subject of much controversy. The presence of a D_{2d} structure (Figure 4.1b) in solution was suggested earlier on the basis of IR evidence.[16] However, later work using concentrated solutions and ^{13}C labelling favours the solid state C_{3v} structure. In solution the molecule is fluxional, and it has been proposed that rapid carbonyl exchange occurs via an unbridged intermediate of Td symmetry.[17]

Unlike the case with [$Co_2(CO)_8$] the substitution reactions of [$Co_4(CO)_{12}$] have not been studied in detail. It has been shown that up to four CO groups in [$Co_4(CO)_{12}$] can be substituted with monodentate phosphines to prepare complexes of the type [$Co_4(CO)_{12-n}L_n$] without the break-up of the cluster.[7,18] However, with bidentate phosphine ligands, complexes of the type [$Co_4(CO)_{12-2n}(PP)_n$] have been isolated for n=1 and 2.[5,7] The highly substituted complexes with n=1-5 have only

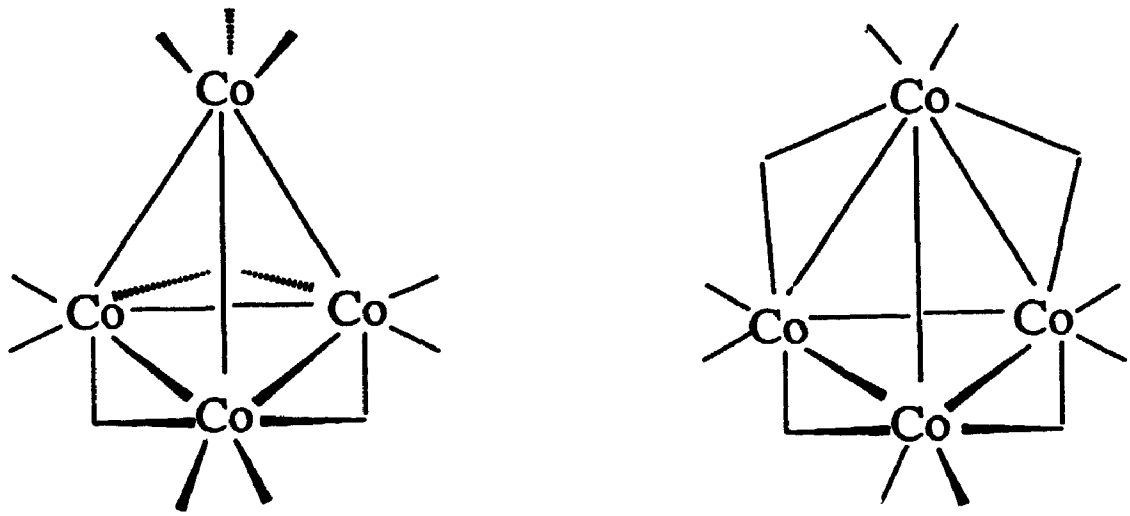

C_{3v} D_{2d}

Figure 4.1: The structures of $[Co_4(CO)_{12}]$

been prepared with PP= $MeN(PF_2)_2$, where the ligand bridges up to five of the six tetrahedral edges without degradation of the cluster.[19]

This chapter describes the syntheses of di and tetranuclear cobalt complexes from cobalt(II) halide salts. This one pot synthetic route is very convenient since a variety of electron rich products can be obtained simply by tuning the reaction conditions. The dynamics, thermodynamics and chemical reactivity of $[Co_2(CO)_4(dmpm)_2]$ are also investigated, and results of these studies are discussed.

4.2. Synthesis of $[Co_2(CO)_4(\mu\text{-dmpm})_2]$ (4.1)

The dppm chemistry of cobalt has been extensively studied.[7] In contrast there has only been very limited work done with dmpm.[5] It was therefore of interest to prepare new Co-dmpm complexes and to examine their reactivity pattern when compared to those of dppm and other related phosphines. Thus, when an ethanolic suspension of $NaBH_4$ was slowly added to a 1:2.5-3 Co(II)/dmpm mixture under an atmosphere of CO, a yellowish-orange product 4.1 with a chemical composition of $[Co_2(CO)_4(dmpm)_2]$ was formed according to the following equation.

$$2Co(II) + 2dmpm + 4BH_4^- + 4CO \rightarrow Co_2(CO)_4(dmpm)_2 + 2B_2H_6 + 2H_2 \qquad (4.3)$$

4.2.1. Spectroscopic Characterization of 4.1

The solid state IR spectrum of this yellowish-orange complex, as shown in Figure 4.2 suggests that it has both terminal and bridging carbonyl groups. In

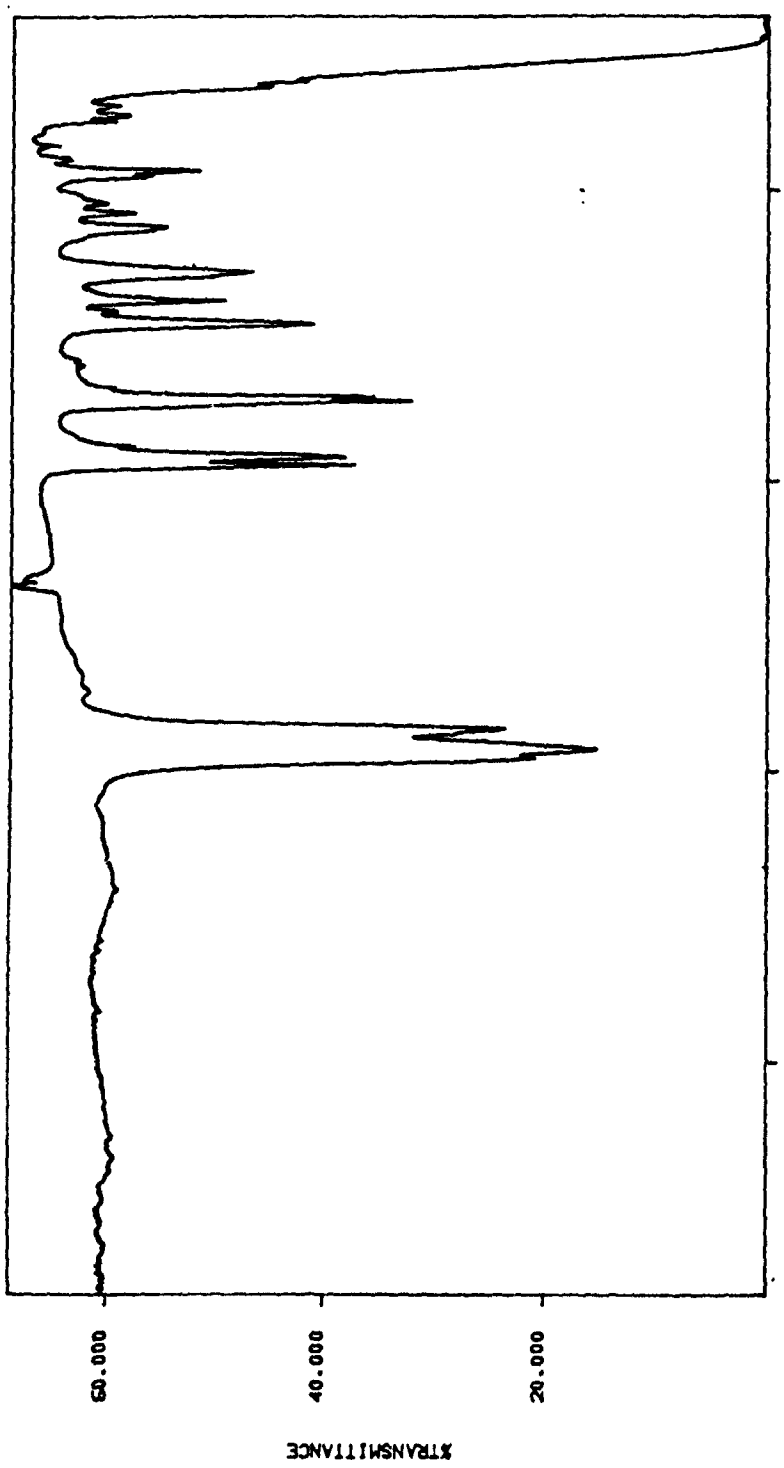

Figure 4.2: The IR spectrum (Nujol) of $[Co_2(\mu\text{-}CO)_2(CO)_2(\mu\text{-}dmpm)_2]$, 4.1a.

solution, the IR spectrum shows bands due only to the terminal carbonyl groups. This clearly indicates that the molecule has two forms, one with terminal CO groups and one with both terminal and bridging CO groups. This was further supported by the solution IR spectrum at -90°C which shows both bridging and terminal CO groups as observed in the solid state IR spectrum.

The ^{31}P NMR spectrum of 4.1 at -90°C shows a singlet resonance centred at 33.2 ppm, suggesting that all phosphorus atoms are equivalent and that the dmpm is coordinated in a bridging mode. At room temperature this resonance was significantly broadened and shifted to $\delta = 14.4$ ppm. The room temperature ^{1}H NMR spectrum shows a broad resonance at $\delta = 2.35$ ppm for the CH_2P_2 protons of the dmpm ligand and another resonance at $\delta = 1.5$ ppm for the PMe protons. At -90°C resonances due to $CH^aH^bP_2$ protons were still broad but appeared as an AB pattern at $\delta = 3.01$ and $\delta = 3.36$ ppm. In addition it shows a broad, partially resolved resonance due to the PMe protons of the ligand centred at $\delta = 1.4$ ppm. In addition, the FAB mass spectrum of 4.1 shows a parent ion peak for $[Co_2(CO)_4(dmpm)_2]^+$ at m/e= 502 amu and peaks arising from the loss of one, two, three and four CO groups at 474, 446, 418 and 390 amu respectively. On the basis of these pieces of evidence it was deduced that there are two isomers of this complex, one dominating in solution at room temperature while the other is predominant at lower temperatures and in the solid state. Both isomers have the chemical composition $[Co_2(CO)_4(dmpm)_2]$.

Analogous complexes with dppm have recently been prepared.[20] They exhibit very similar solution properties as those of the dmpm complexes. It was, however,

possible with dppm to isolate both species in the solid state and to study their structures by X-ray diffraction analysis, which shows that there are indeed two isomers of formula $[Co_2(CO)_4(\mu\text{-dppm})_2]$. The red isomer contains two bridging and two terminal CO groups while the black isomer contains four terminal CO groups. Thus, on the basis of the above data and by comparing with the known dppm analogues, it is suggested that the dmpm species formed at room temperature in solution is the isomer with all CO groups terminally bound to cobalt, $[Co_2(CO)_4(\mu\text{-dmpm})_2]$ 4.1b, while, in the solid state and at low temperature in solution, the predominant species is the bridging carbonyl complex, $[Co_2(\mu\text{-CO})_2(CO)_2(\mu\text{-dmpm})_2]$, 4.1a (Figure 4.3). In solution both forms readily interconvert. A detailed investigation was therefore carried out to investigate the mechanism of fluxionality and the thermodynamics of the equilibrium between the bridged and non-bridged forms, and this study is discussed below.

4.2.2. Dynamics and Thermodynamics of Equilibrium between Bridged and Non-bridged Isomers of $[Co_2(CO)_4(\mu\text{-dmpm})_2]$

The complex $[Co_2(\mu\text{-CO})_2(\mu\text{-dmpm})_2(CO)_2]$, **4.1a**, is readily soluble in most organic solvents and gives an equilibrium mixture of 4.1a and 4.1b and thus characterization by NMR and solution FTIR techniques was possible. These techniques were employed to study the dynamics and thermodynamics of the equilibrium between the carbonyl bridged isomer **4.1a** and the nonbridged isomer **4.1b** (Equation 4.4) and the analogous dppm complexes.[21]

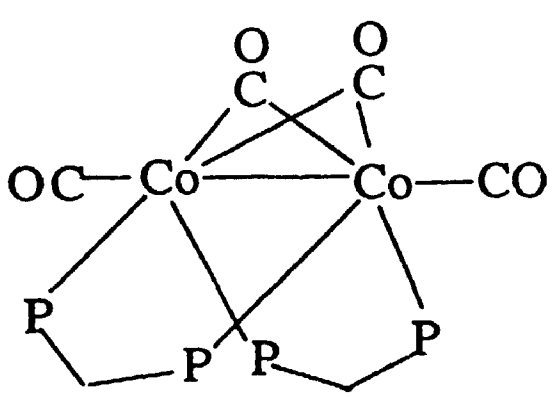

4.1a

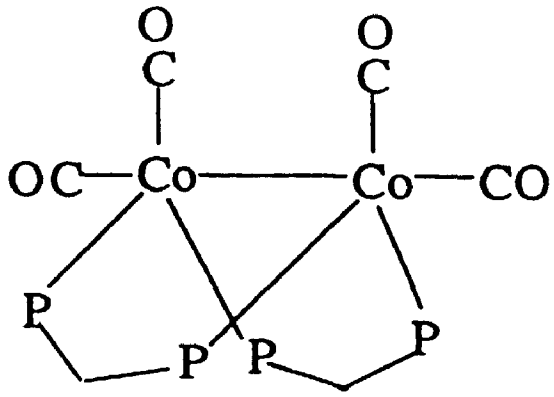

4.1b

Figure 4.3: Structures of $[Co_2(\mu\text{-}CO)_2(CO)_2(\mu\text{-}dmpm)_2]$, 4.1a and $[Co_2(CO)_4(\mu\text{-}dmpm)_2]$, 4.1b.

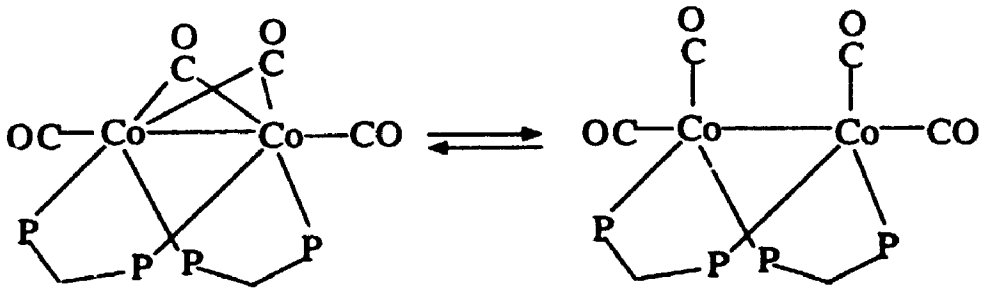

(4.4)

4.1a 4.1b

4.2.3. Variable Temperature ^{1}H,^{13}C and ^{31}P NMR Investigation

The ^{31}P NMR spectrum of **4.1a** and **4.1b** exhibits only a single resonance indicating an equilibrium between the two limiting structures which is rapid on the NMR time scale. Similarly, the ^{1}H NMR of mixtures reveal only a singlet in the CH_2P_2 regions of the spectrum. Thus a variable temperature multinuclear NMR study was pursued in order to establish the mechanism of fluxionality.

The ^{13}C NMR spectrum on ^{13}CO enriched samples at -92°C shows two resonances at δ= 203.5 ppm, assigned to the terminal CO groups, and at δ= 265.5 ppm due to the bridging carbonyl groups. This assignment is based on the tendency of bridging carbonyls to be shifted downfield relative to terminal carbonyls and the similarity to shifts observed for μ-CO groups in related molecules such as $[Co_2(CO)_6(\mu\text{-PP})]$[5] (PP=dmpm, dppm), $[Co_4(CO)_{12}]$,[17e] and $[Co_4(CO)_8(\mu\text{-PP})_2]$.[5] In addition, the ^{13}C NMR spectrum also shows two peaks at δ= 19.0 and 19.5 ppm due to the MeP carbon atoms. However, at room temperature the ^{13}C NMR could not be resolved. No ^{13}C resonances for 4.1b were resolved even at temperatures when it is known to be present and when resonances for 4.1a were resolved.

Similarly the ^{1}H NMR spectrum at room temperature gave a single broad

resonance due to the CH_2P_2 protons, but gave two broad resonances due to the non-equivalent protons CH^aH^b at low temperatures. Two resonances were also observed due to the non-equivalent Me^aP and Me^bP groups at low temperature, but a single resonance was seen at room temperature. The decoalescence of ^{31}P NMR spectra in acetone-d_6 is shown in Figure 4.4. At room temperature it shows a single broad resonance at $\delta = 14.4$ ppm with width at half height ca. ~80 Hz. This resonance was assigned to the fluxional mixture of isomers but, at room temperature, solutions contain mostly the non bridged isomer. At -65°C this resonance was sharpened and shifted to $\delta = 33.2$ ppm, that is ~19 ppm downfield compared to room temperature, and this resonance is attributed to the carbonyl bridged isomer. The solid state structure of the unbridged form of analogous dppm complex, $[Co_2(CO)_4(\mu\text{-dppm})_2]$, clearly indicates chemical inequivalence of the carbonyl groups occupying axial and equatorial sites on the TBP coordinated cobalt atoms and, therefore, more than one resonance is expected for the $CH^aH^bP_2$ protons and the carbonyl carbon atoms but this non-equivalence was not observed. Moreover, the reaction shown in equation 4.4 for the equilibrium between **4.1a** and **4.1b** which most likely involves the windshield wiper type motion exchanging terminal carbonyls on one cobalt atom to the other cobalt atom via a CO bridged intermediate like that in **4.1a**, does not of itself lead to equivalence of carbonyl groups or the CH^aH^b protons of the bridged form. This confirms that a second form of fluxionality with a much lower activation energy must occur within the non-bridged form 4.1b. A reasonable mechanism for this fluxional process making all carbonyls and CH_2P_2 protons equivalent is illustrated by equation 4.5. The structures are shown as Newman projections along the Co-Co bond.

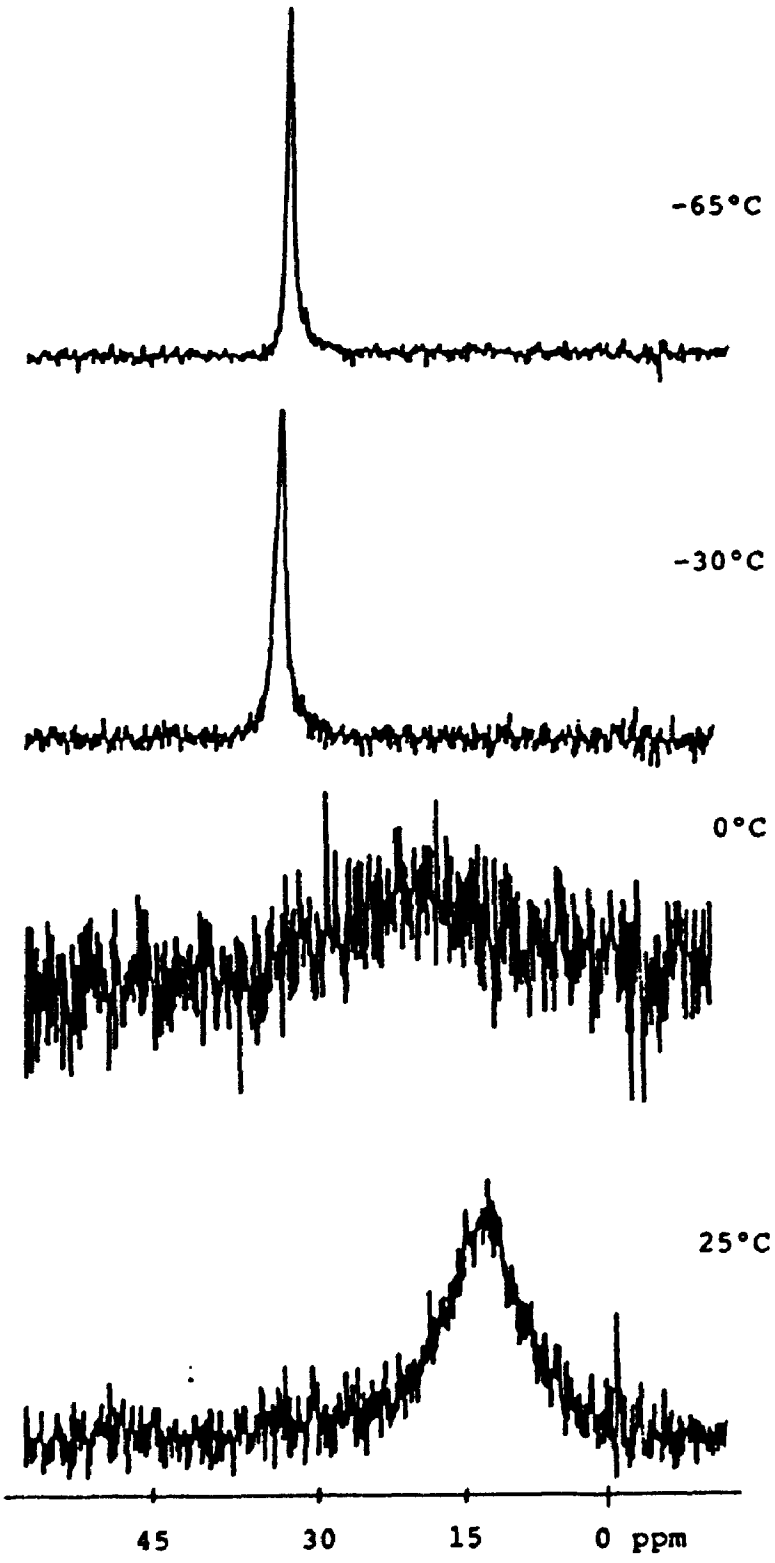

Figure 4.4: Variable temperature ^{31}P NMR spectra of 4.1 in C_3D_6O.

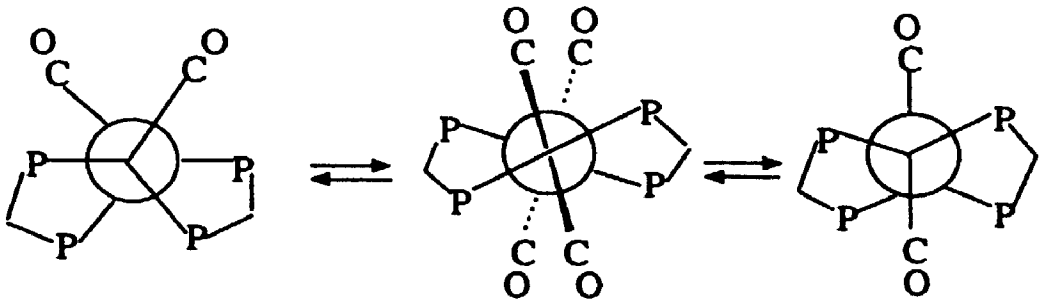

b c b' (4.5)

The reversible reaction b⇌c is most reasonable as structure c is analogous to the structure of the D_{2d} isomer of $[Co_2(CO)_8]$ (isomer c in eqn 4.2). The formation of a third isomer b' through c is possible but not necessary to explain the NMR data. A variable temperature, multinuclear NMR investigation of $[Co_2(CO)_4(\mu\text{-dppm})_2]$ isomers[21] has produced results consistent with those found for **4.1**.

4.2.4. Variable Temperature IR Study of 4.1

The thermodynamics of the equilibrium **4.1a**⇌**4.1b** were determined by variable temperature solution FTIR spectroscopy (Figure 4.5). The room temperature spectrum exhibits strong terminal ν(CO) stretches with increasing amounts of ν(μ-CO) signals at lower temperatures, demonstrating that the unbridged form is favoured at higher temperatures. Equilibrium constants, K, were determined from these spectra over the temperature range 190-301 K and a plot of *ln*K vs 1/T resulted in a good linear fit giving an estimate of ΔH and ΔS according to the equation 4.6.

$$\mathit{ln}K = -\Delta H/RT + \Delta S/R \qquad (4.6)$$

Figure 4.5: Variable temperature solution FTIR spectra of 4.1 in CH_2Cl_2.

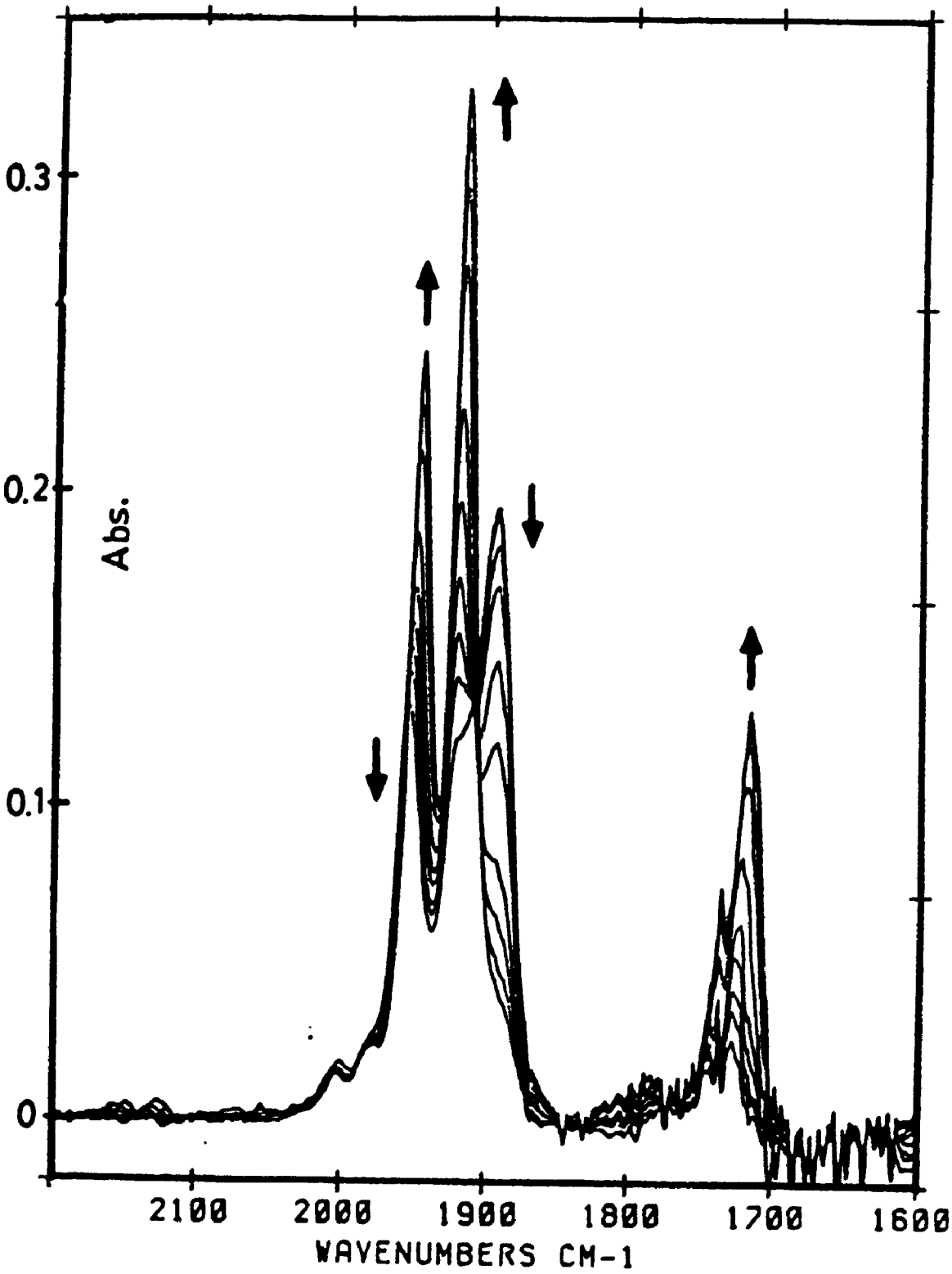

The thermodynamic data for **4.1**, analogous dppm isomers, and $[Co_2(CO)_8]$ are presented in Table 4.1. The enthalpy term strongly favours the bridged form while the entropy term strongly favours the unbridged form in each case. However the effect is much lower for the parent $[Co_2(CO)_8]$.

In Table 4.1 ΔG^* values were estimated from the coalescence temperatures of NMR chemical shifts by using the Eyring equation and were unchanged over the temperature range 233-275°K. This suggests that ΔS^* is small and hence $\Delta G^* \sim \Delta H^*$. The entropy term favors unbridged form because of the greater mobility compared to bridged form, but libration about Co-Co bond is not expected to be possible until the μ-CO bonds in the bridged isomer are completely broken, and so the entropy of activation term is not expected to be an important contributor to ΔG^*. If it were otherwise, the observed correlation of ΔH° and ΔG^* would not be expected. The entropy term is probably also responsible for the relative instability of isomer **b'** in equation 4.5. Molecular models indicate that **b'** is strain free but the conformation is rigid, whereas in **b** libration about the Co-Co bond is possible.

4.2.5. Solution Magnetic Properties of 4.1

Organometallic complexes possess not only unusual structural properties and chemical reactivities but also interesting spectroscopic and magnetic properties as well. The magnetic properties of metal complexes are usually investigated in the solid state using the traditional Gouy balance method. One disadvantage of using this method is in cases where the solid state structures of the metal complexes are not retained in solution, since magnetic moments for the solution species can not be

Table 4.1. Thermodynamic and Kinetic Data for the Carbonyl-Bridged = Nonbridged Isomers.

complex	ΔH/kJ mol^{-1}	ΔS/J K^{-1}mol^{-1}	ratio b:nb 298K	190K	ΔG*/kJ mol^{-1}
$[Co_2(CO)_8]$	+5.6	+21	44:56	74:26	27
$[Co_2(CO)_4(dmpm)_2]$	+26.3(2.1)	+107(13)	9:91	98:2	47(1)
$[Co_2(CO)_4(dppm)_2]$	+22.1(1.5)	+102(8)	3:97	85:15	41.5(1)

estimated accurately. In order to overcome this problem Evans developed a technique which involves ^{1}H NMR to determine the magnetic properties of metal complexes in solution.[22] There are two major advantages with this technique. Firstly, using variable temperature NMR methods, magnetic moments at several different temperatures can be estimated fairly accurately. Secondly, the traditional solid state methods require large quantities of metal salts, whereas Evans's method requires only a few milligrams of sample to study the magnetic properties accurately.

The unusually large temperature dependence of the chemical shifts exhibited in the ^{31}P NMR by the two isomers of $[Co_2(CO)_4(\mu\text{-dmpm})_2]$, 4.1a and 4.1b, were suspected to be partly due to different magnetic properties of these isomers rather than simply due to the presence of two isomeric forms. This was further supported by the fact that the crystal structure of the nonbridged form of the dppm analogue reveals an unusually large Co-Co distance at 2.809(6) Å, suggesting a very weak Co-Co bond and possible paramagnetism. Therefore, solution magnetic properties of complexes 4.1a and 4.1b were investigated using variable temperature ^{1}H NMR. The results of these studies are shown in Figure 4.6. This clearly shows that the species predominant at room temperature in solution is paramagnetic in nature while the carbonyl bridged complex at low temperatures is diamagnetic. It is therefore, suggested that the transformation of 4.1a into 4.1b involves in addition to migration of CO groups from bridging to terminal positions, a reversible rupture of the Co-Co bond.

4.3. Synthesis of $[Co_4(CO)_8(\mu\text{-dmpm})_2]$ (4.2).

When the stoichiometry of the reaction which produces $[Co_2(CO)_4(dmpm)_2]$

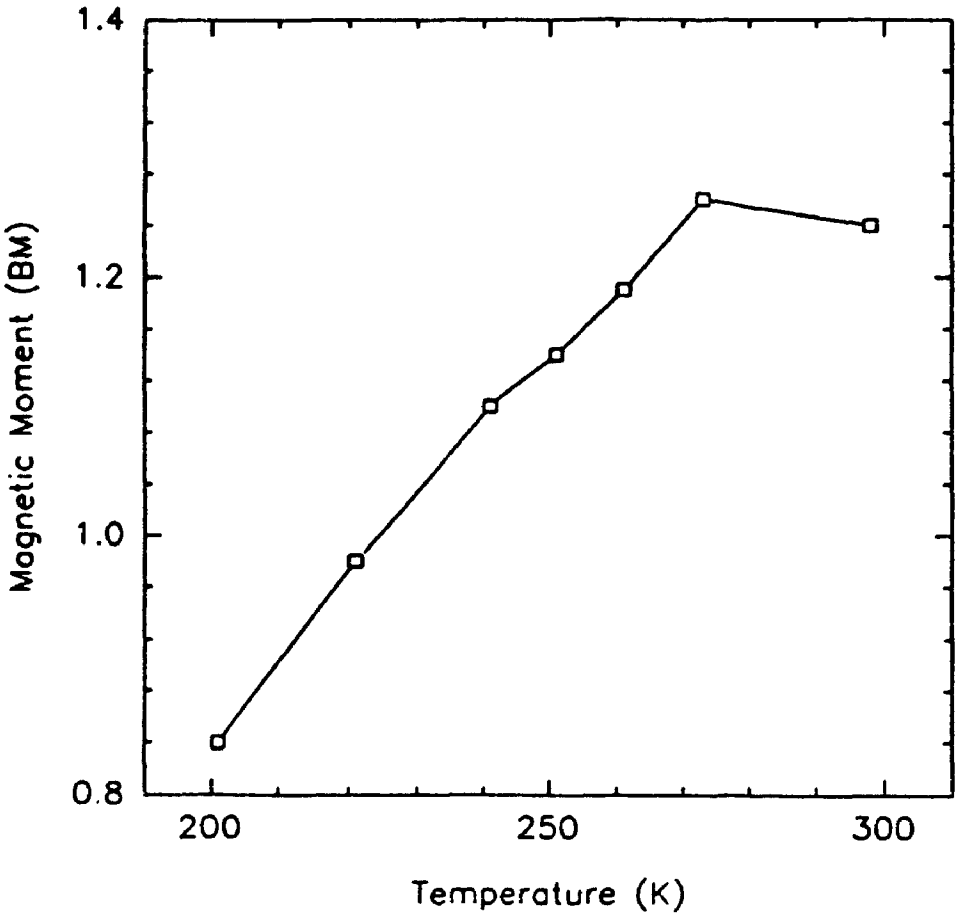

Figure 4.6: Plot of magnetic moment vs temperature of 4.1 measured in CH_2Cl_2 solutions by ^1H NMR using Evans method.

complexes is changed from Co:dmpm = 1:2.5-3 to 1:1, the reduction with $NaBH_4$ in the presence of CO yields a black crystalline complex with chemical composition $Co_4(CO)_8(dmpm)_2$. The complex may have been formed according to the following equation 4.7.

$$4Co^{2+} + 2dmpm + 8BH_4^- + 8CO \rightarrow Co_4(CO)_8(dmpm)_2 + 4B_2H_6 + 4H_2 \quad (4.7)$$

The black crystals can be precipitated from benzene solution by adding n-heptane. The complex is stable in the solid state, but it decomposes slowly in solution at room temperature.

4.3.1. The Molecular Structure of $[Co_4(CO)_8(\mu\text{-dmpm})_2]$ (4.2).

The solid state molecular structure of 4.2 is determined by single crystal X-ray diffraction analysis carried out by Dr. Muir at the University of Glasgow. The ORTEP diagram is shown in Fig.4.7 and the bond distances and angles produced in this analysis are listed in Table 4.2. This reveals that the molecule contains four cobalt atoms bonded to each other forming a distorted tetrahedron, with two edges spanned by two dmpm ligands and one face edge-bridged by three carbonyl groups. The remaining five carbonyl groups are essentially linear [Co-C-O 171.2(10) - 179.3(9)°] and terminally bound to cobalt atoms. Thus, the molecular geometry of 4.2 can be derived from the C_{3v} structure of the parent $[Co_4(CO)_{12}]$[15,18,23] by substituting one apical and one equatorial carbonyl group with one dmpm ligand, and two axial carbonyl groups with another dmpm ligand.

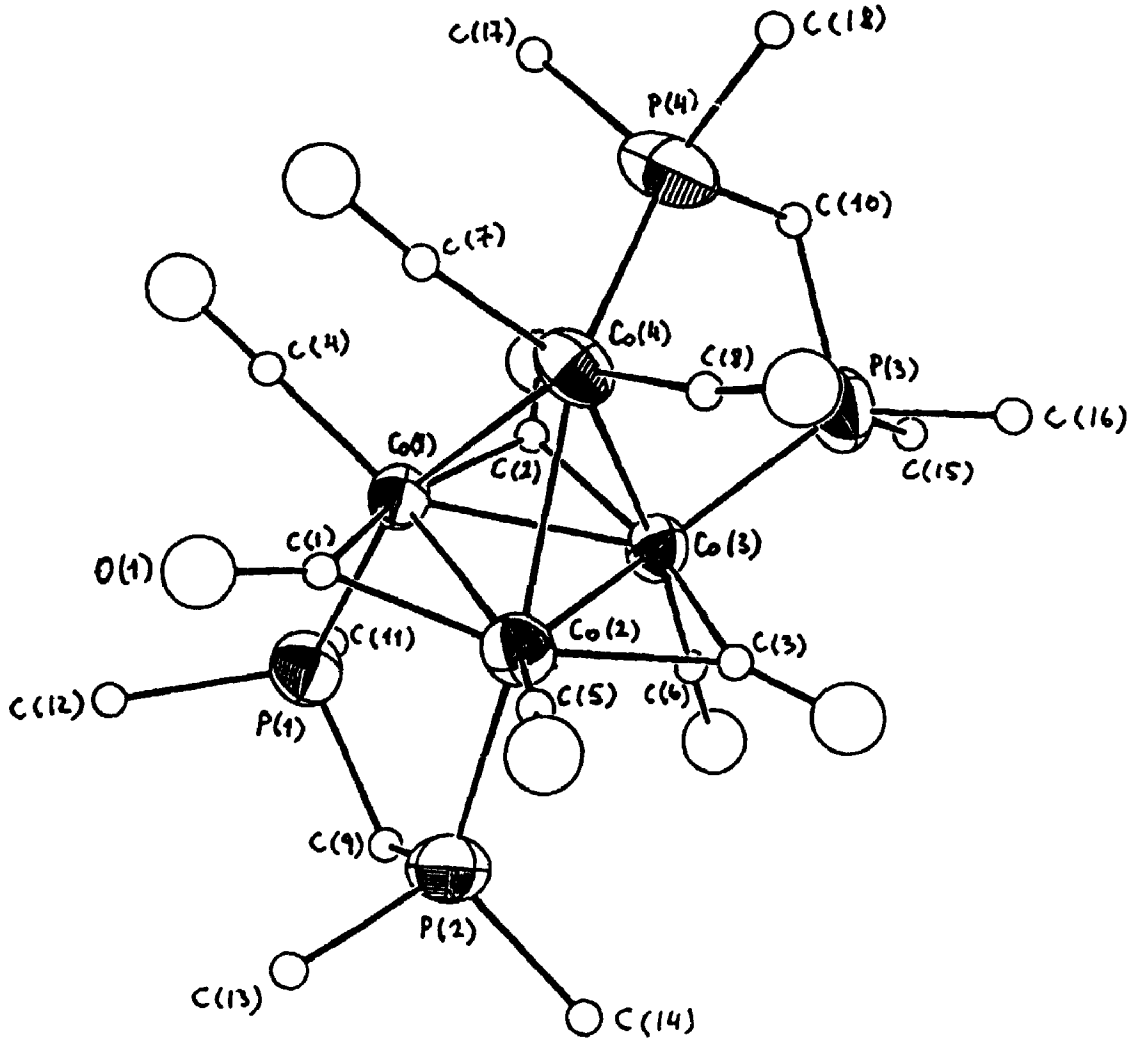

Figure 4.7: The ORTEP diagram of $[Co_4(CO)_8(\mu\text{-dmpm})_2]$, 4.2.

Table 4.2. Selected Interatomic Distances (Å) and Angles (°) in $[Co_4(CO)_8(\mu\text{-dmpm})_2]$.

Co(1) - Co(2)	2.426(1)	Co(1) - Co(3)	2.452(2)
Co(1) - Co(4)	2.503(2)	Co(1) - P(1)	2.180(2)
Co(1) - C(1)	1.910(6)	Co(1) - C(2)	1.868(7)
Co(1) - Co(4)	1.730(7)	Co(2) - Co(3)	2.451(2)
Co(2) - Co(4)	2.510(2)	Co(2) - P(2)	2.187(2)
Co(2) - C(1)	1.880(7)	Co(2) - C(3)	1.978(8)
Co(2) - C(5)	1.741(7)	Co(3) - Co(4)	2.541(2)
Co(3) - P(3)	2.177(2)	Co(3) - C(2)	1.890(7)
Co(3) - C(3)	1.888(7)	Co(3) - C(6)	1.734(8)
Co(4) - P(4)	2.202(3)	Co(4) - C(7)	1.753(8)
Co(4) - C(8)	1.751(9)	P(1) - C(9)	1.841(7)
P(2) - C(9)	1.842(8)	P(3) - C(10)	1.842(7)
P(4) - C(10)	1.867(8)		

Bond angle (°):

Co(2)-Co(1)-Co(3)	60.3(1)	Co(2)-Co(1)-Co(4)	61.2(1)
Co(2)-Co(1)-P(1)	98.1(1)	Co(2)-Co(1)-C (1)	49.7(2)
Co(2)-Co(1)-C(2)	109.9(2)	Co(2)-Co(1)-C (4)	146.1(3)
Co(3)(Co(1)-Co(4)	61.7(1)	Co(3)-Co(1)-P(1)	102.0(1)
Co(3)-Co(1)-Co(1)	109.6(2)	Co(3)-Co(1)-C(2)	49.7(2)
Co(3)-Co(1)-C(4)	143.9(3)	Co(4)-Co(1)-P(1)	157.7(1)
Co(4)-Co(1)-C(1)	78.7(3)	Co(4)-Co(1)-C(2)	82.7(2)
Co(4)-Co(1)-C(4)	104.9(3)	P(1)-Co(1)-C(1)	94.4(2)
P(1)-Co(1)-C(2)	98.2(3)	P(1)-Co(1)-C(4)	97.1(3)
C(1)-Co(1)-C(2)	157.6(3)	C(1)-Co(1)-C(4)	99.1(3)
C(2)-Co(1)-C(4)	97.6(3)	Co(1)-Co(2)-Co(3)	60.4(1)

Co(1)-Co(2)-Co(4)	60.9(1)	Co(1)-Co(2)-P(2)	97.8(1)
Co(1)-Co(2)-C(1)	50.7(2)	Co(1)-Co(2)-C(3)	109.3(2)
Co(1)-Co(2)-C(5)	147.1(3)	Co(3)-Co(2)-Co(4)	61.1(1)
Co(3)-Co(2)-C(2)	101.6(1)	Co(3)-Co(2)-C(1)	110.7(2)

It is apparent from Table 4.2 that the tetrahedron formed by the four cobalt atoms is not symmetrical and the apical Co(4) atom is displaced more towards Co(1), Co(2) and away from Co(3). Thus, the Co(3)-Co(4) bond distance at 2.541(2) Å is significantly longer than the distances of Co(1)-Co(4) and Co(2)-Co(4) at 2.503(2) and 2.510(2) Å respectively. This is further supported by the bond angle data which reveals smaller bond angles for Co(1)-Co(3)-Co(4) at 60.2(1)° and Co(2)-Co(3)-Co(4) at 60.3(1)° compared to Co(3)-Co(1)-Co(4) and Co(3)-Co(2)-Co(4) at 61.7(1) and 61.6(1)° respectively.

The disposition of the dmpm ligands along the edges of the Co_4 tetrahedron is such as to yield the isomeric form 4.2. The five-membered Co_2P_2C ring containing the axial dmpm ligand adopts an envelope conformation, with the CH_2 group at the flap, the conformation of the ring incorporating the C(3) and C(4) atoms is puckered, as is evident form the torsion angles shown in Table 4.2. The molecular structure of 4.2 is therefore asymmetrical and closely similar to that of the rhodium cluster $[Rh_4(CO)_8(\mu\text{-dppm})_2]$, dppm = $Ph_2PCH_2PPh_2$.[15]

The Co-Co bond lengths in 4.2 vary from 2.426(1) to 2.541(2)Å and can be compared with those of 2.438(3) - 2.717(1)Å observed in other crystallographically characterised cobalt complexes.[15,18,23-27] They follow the trend displayed by tetrahedral cluster complexes of the type $[Co_4(CO)_{12-n}L_n]$, n=1-5, in which the metal-metal bonds in the basal plane are shorter, and presumably stronger, than the bonds involving the apical cobalt atom.[18,24-27] In 4.2 the basal-basal and basal-apical Co-Co distances average at 2.443 and 2.518 Å respectively. Of the three basal-apical bonds the one spanned by the dmpm ligand [Co(3)-Co(4) 2.541(2)Å] is slightly longer

than the two unsupported bonds [Co(1)-Co(4) 2.503(2), Co(2)-Co(4) 2.510(2)Å]. In the basal plane, however, the bond bridged by the dmpm ligand [Co(1)-Co(2) 2.426(1)Å] is shorter than the other two [Co(2)-Co(3) 2.451(2), Co(1)-Co(3) 2.452(2)Å]. This indicates that the dmpm ligand can span disparate distances. Thus, the bite distance for the dmpm ligand bridging the apical-basal cobalt atoms Co(3)-Co(4) is 0.115 Å larger than the dmpm ligand bridging basal-basal cobalt atoms Co(1)-Co(2).

All the terminal Co-C distances (axial, equatorial and apical) are approximately equal [1.730(7)-1.753(8)Å] and they are substantially shorter than the bridging Co-C distances [1.868(7)-1.978 (8) Å]. Only one carbonyl bridge is slightly asymmetrical [Co(3)-C(3) 1.888(7), Co(2)-C(3) 1.978(8)Å].

The Co-P bond lengths are within the range of those observed in phosphine and phosphite derivatives of the $[Co_4(CO)_{12}]$ cluster [2.156(2)-2.266(6)Å].[18,26] In the axial dmpm ligand the Co-P bonds are equal [2.180(2) and 2.187(2)Å], while in the other one the apical bond [Co(4)-P(4) 2.202(3)Å] is substantially longer than the equatorial bond [Co(3)-P(3) 2.177(2)Å]. The lengthening of the Co(4)-P(4) bond may be attributed to the trans-influence of the axial phosphine transmitted through the metal-metal bond [P(2)-Co(2)-Co(4) 157.0(1), Co(2)-Co(4)-P(4) 154.0(1)°].

4.3.2. Spectroscopic Characterization of 4.2

The solid state IR spectrum of 4.2 as shown in Figure 4.8 exhibits carbonyl stretching frequencies at 1989, 1963, 1946, 1930 and 1893 cm^{-1} consistent with terminal CO groups, and stretching frequencies at 1810, 1773 and 1743 cm^{-1} for

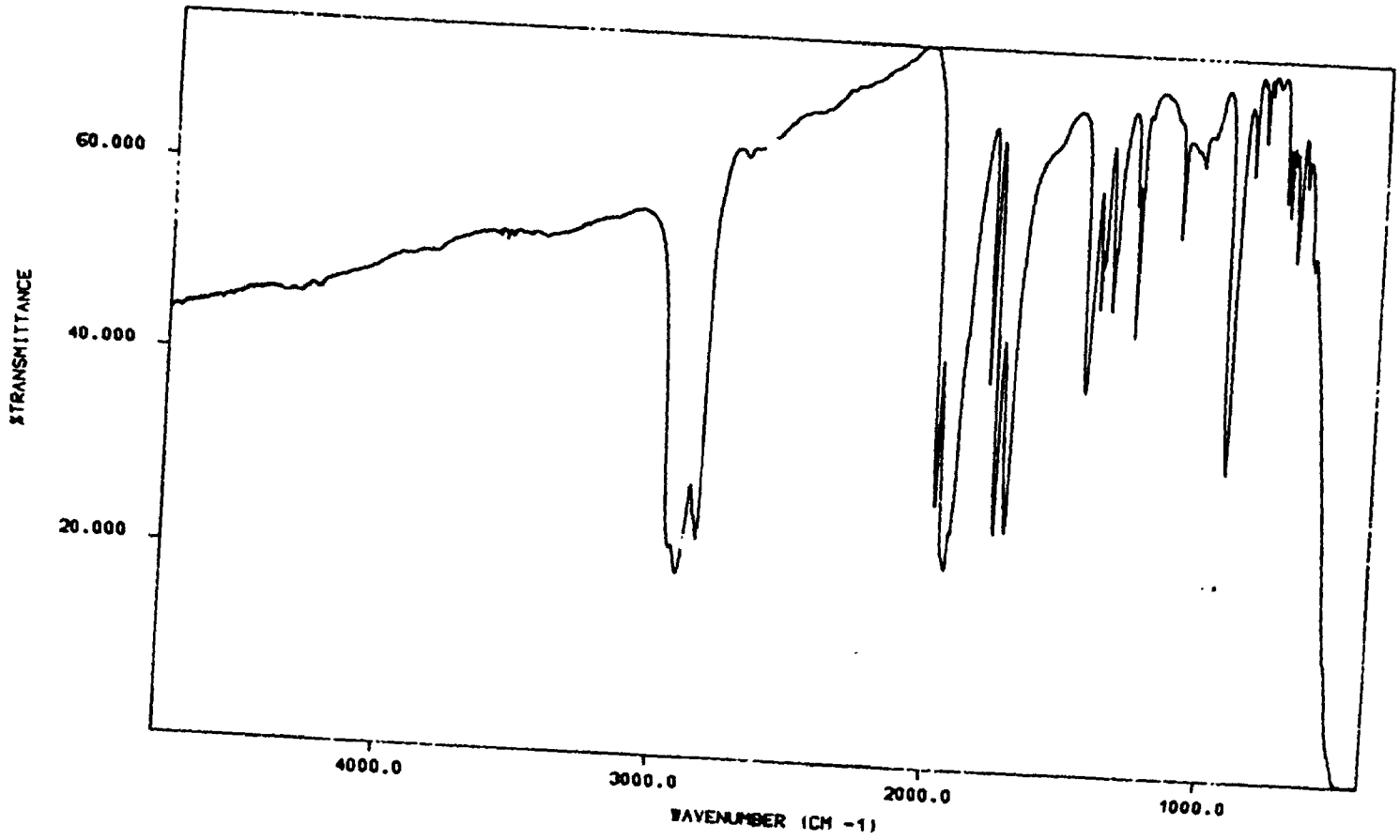

Figure 4.8: The IR spectrum (Nujol) of $[Co_4(CO)_8(\mu\text{-dmpm})_2]$, 4.2.

bridging carbonyl groups. This complex is derived from the parent $[Co_4(CO)_{12}]$ cluster which shows IR stretches at 2065, 2060, 2040, 2030 and 1879 cm^{-1} in hexane.[16,17e] The decrease in the stretching frequencies in 4.2 compared to the parent complex $[Co_4(CO)_{12}]$ is consistent with the enhanced back donation of electronic charge from metal atom to the π^* orbitals of CO groups. The substitution of very basic dmpm ligands for CO groups makes the metal atoms more electron rich, and thus better π-donors.

At room temperature the ^{31}P NMR shows a broad resonance centred at -0.9 ppm. On cooling solutions to -90°C this splits into three resonances with an intensity ratio of 2:1:1. The latter pattern is consistent with the solid state structure of complex 4.2. The lowest field doublet at δ = 6.8 ppm, J(PP)= 50.4 Hz could be assigned to the equivalent phosphorus atoms P^aP^b bound to the basal cobalt atoms Co(1) and Co(2). The phosphorus atom P^d bound with the apical cobalt atom Co(4) appears as a featureless broad resonance at δ = -11 ppm. This signal should be coupled to the basal phosphorus atom P^c, which appears as a doublet, but the apical position is severely broadened by the cobalt quadrupole even at low temperature. The remaining phosphorus atom P^c appears as a partially resolved doublet at δ = -4.8 ppm, J(PP)= 33.6 Hz. Similar spectral patterns have been observed in other related complexes.[5]

The ^1H NMR spectrum of 4.2 is also temperature dependent. Thus, at room temperature, it shows a broad resonance for the PMe protons centred at δ =1.47 ppm. However, at -90°C a spectrum consistent with the static structure was obtained. For this type of molecule, three resonances for the CH_2P_2 protons with an intensity ratio of 2:1:1, each split into a triplet due to coupling with two equivalent phosphorus

atoms of the dmpm ligand are expected. However, the ^1H NMR shows only two partially resolved resonances in the CH_2P_2 region of the spectrum. The partially resolved triplet resonance at $\delta = 3.17$ ppm, $^2J(PH) = 9.5$ Hz was assigned due to the $CH^cH^dP_2$ protons of one dmpm ligand and the resonance at $\delta = 2.05$ ppm was assigned to H^b of $CH^aH^bP_2$ protons, while the other half of the resonance due to H^a of $CH^aH^bP_2$ of the other dmpm ligand is not apparent. This resonance may have been buried under the methyl resonances of the dmpm ligand. The expected intensity ratio is however, observed in those methylene resonances which appeared in the ^1H NMR spectrum. From the solid state structure, four methyl resonances are expected each splitting into a doublet by coupling with a phosphorus atom of a dmpm ligand. The spectrum indeed shows four resonances for CH_3 protons with partially resolved doublet patterns at $\delta = 1.64$ ppm, J(obs) =7.0 Hz; 1.49 ppm (unres.); 1.34 ppm (unres.) and 1.23 ppm, J(obs) =7.5 Hz. Thus, all this evidence clearly shows that the spectroscopic data obtained is consistent with the solid state structure obtained by diffraction methods and shown in Fig.4.7.

4.3.3. Mechanism of Fluxionality in 4.2:

The above NMR studies shows that, like the parent $[Co_4(CO)_{12}]$, the dmpm substituted derivative 4.2 exhibits stereochemical non-rigidity in solution. The ^1H and ^{31}P NMR spectral data clearly show that at room temperature the molecule is fluxional on the NMR time scale, while at -90°C fluxionality can be frozen out. The mechanism of this fluxionality is investigated. It has been suggested, for the parent $[Co_4(CO)_{12}]$ complex, that in solution the CO groups migrate around the Co_4

tetrahedron, and this bridging-terminal merry-go-round type of motion causes each cobalt atom to become equivalent at higher temperature. However, at lower temperature, ^{13}C NMR and ^{57}Co NMR results show that there are indeed three different CO groups and two distinct Co atoms present.[17] The fluxionality has also been explained in terms of a structure containing an icosahedron of twelve CO groups with a tetrahedron of four cobalt atoms inside. It has been suggested that the inner Co_4 tetrahedron can rotate around each neighbouring face of the icosahedron, thus, making all cobalt atoms equivalent at higher temperatures.[17b]

Variable temperature ^{31}P NMR spectra of complex 4.2 are illustrated in Figure 4.9. This clearly shows that at room temperature all the phosphorus atoms appear to be equivalent. However, on cooling the sample to -10°C, decoalescence of ^{31}P NMR resonance is observed. This on further cooling to -90°C splits into three resonances, indicating three different sites for phosphorus atoms. Similarly, the ^{1}H NMR also exhibits temperature dependence as shown in Figure 4.10. Thus, at room temperature only one resonance each for the CH_2P_2 and PMe_2 protons was observed. This splits into three resonances for CH_2P_2 and four for PMe_2 at -92°C. On the basis of this information, a possible mechanism is shown in Figure 4.11 which involves the migration of carbonyl groups from terminal→bridging→terminal on each face of the triangle which will make all the phosphorus atoms, CH_2P_2 and PMe_2 protons equivalent at higher temperature. At lower temperatures this exchange process is much slower and the spectra are then consistent with the solid state structure.

Figure 4.9: Variable temperature ^{31}P NMR spectra of $[Co_4(CO)_8(\mu\text{-dmpm})_2]$, 4.2.

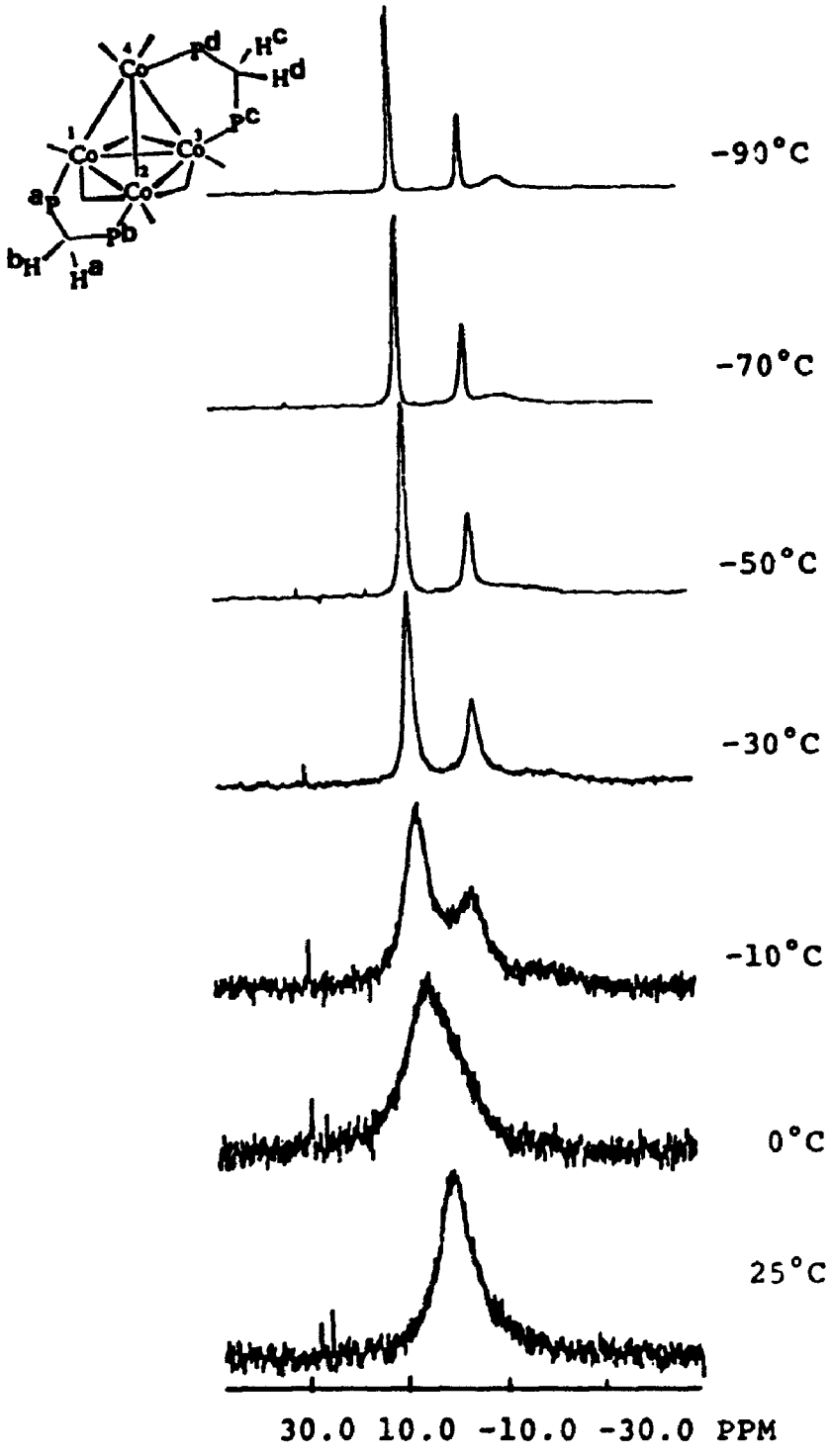

Figure 4.10: Variable temperature ^1H NMR spectra of $[Co_4(CO)_8(\mu\text{-dmpm})_2]$, 4.2.

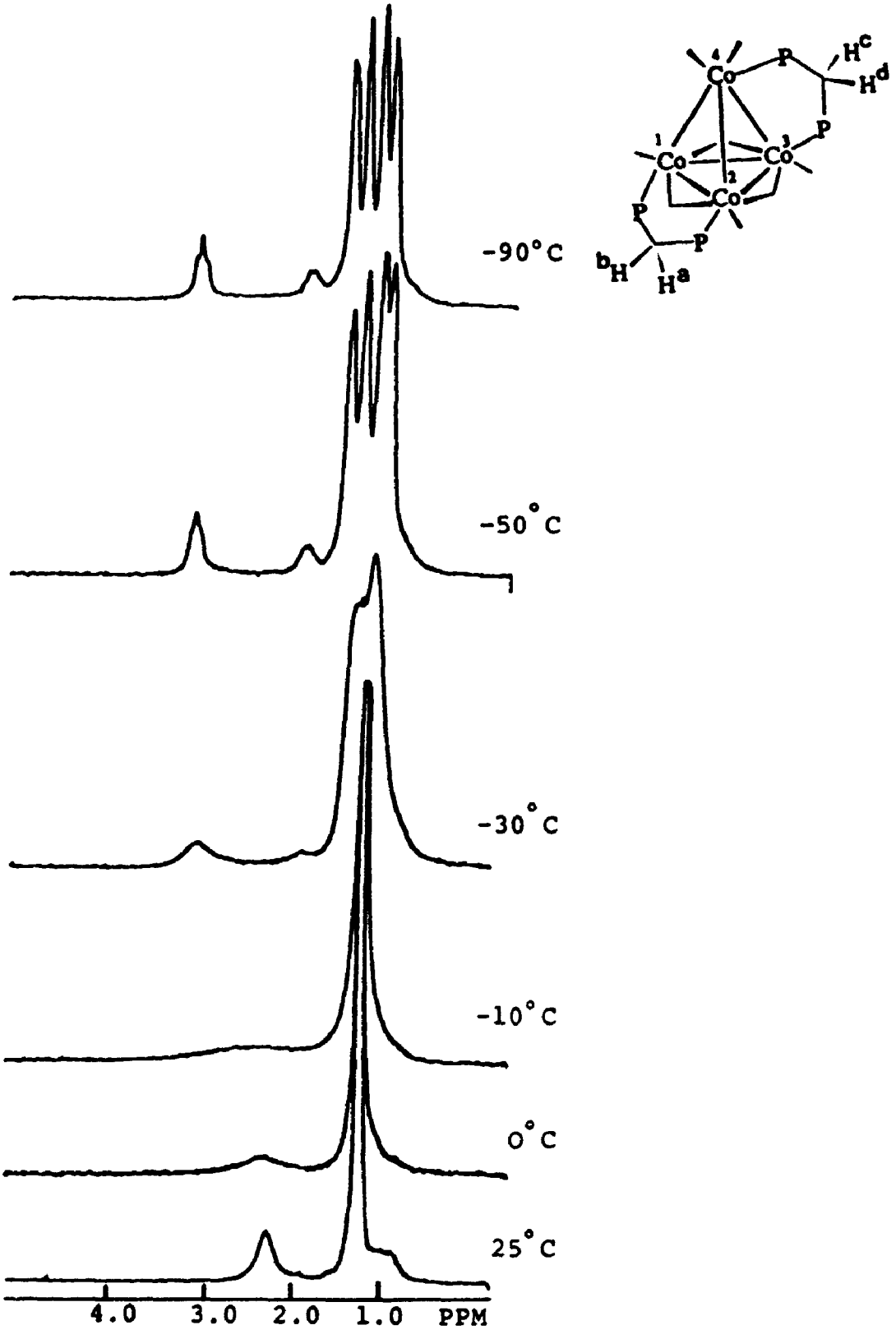

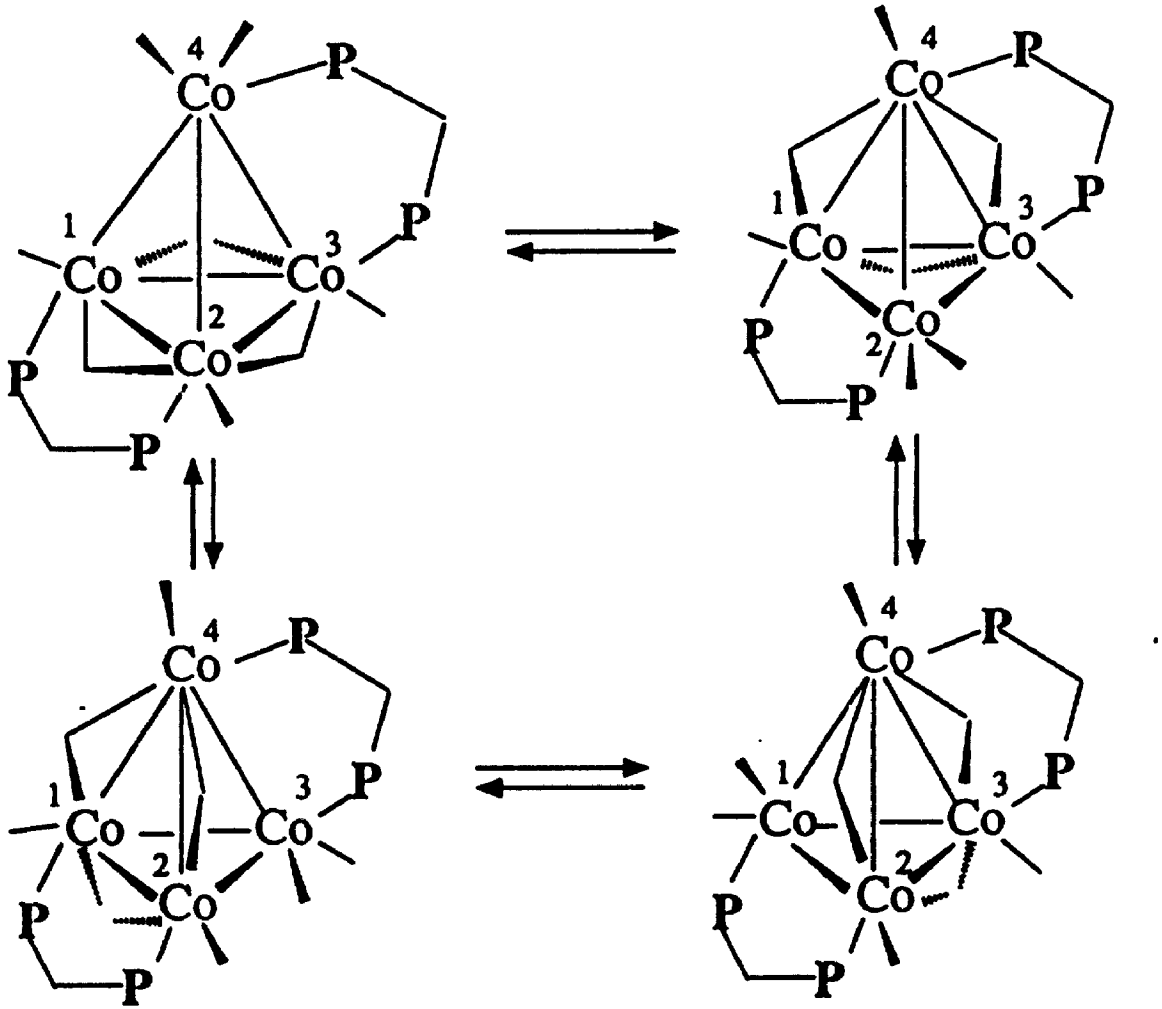

Figure 4.11: Mechanism of fluxional process in $[Co_4(CO)_8(\mu\text{-dmpm})_2]$, 4.2.

4.4. Reaction Chemistry of Complex 4.1 $[Co_2(CO)_4(dmpm)_2]$.

Complexes with M-M bonds are often reactive. Dinuclear complexes have been extensively studied in this regard. Although dinuclear cobalt complexes with bridging dppm and other related phosphines have been investigated in detail,[5,7,28] dmpm bridged complexes have not been explored much.[5] Metal complexes bridged by the highly basic and sterically less demanding dmpm ligand are particularly interesting, since they are envisaged to provide accessibility to the electron-rich metal centres and so promote reactivity towards substrates, particularly in oxidative addition reactions.[29] Earlier work with metal complexes of the dmpm ligand indicated that the smaller steric effect of methyl substituents can lead to different, and in some ways enhanced, reactivity compared to similar dppm complexes.[30] On the basis of a systematic study on platinum complexes with diphospnine ligands $R_2PCH_2PR_2$ (R=Me,Et,OEt,Ph), it was suggested that the structures and reactivities of these platinum diphosphine complexes are chiefly governed by steric effects.[31]

A literature survey reveals that metal complexes of dmpm appear to be more air sensitive than analogous metal carbonyl complexes of most other tertiary phosphines.[5,32-34] The increased air sensitivity of metal carbonyl complexes of dmpm is attributed to the presence of sterically unencumbered and relatively electron-rich metal atoms in these metal carbonyl complexes compared with analogous metal carbonyl complexes of other phosphorus ligands (e.g. dppm). This enhanced reactivity is observed despite the tendency of these metal carbonyls to favour an 18 electron rare gas electronic configuration and despite the presence of several π- accepting carbonyl ligands to remove excess metal electron density.

Several reactions were attempted with these dinuclear species. Reactions in which products were successfully isolated will be discussed here.

4.4.1. Reactions with Group 11 Metal Complexes.

In an attempt to prepare heterometallic complexes several reactions were carried out with copper(I), silver(I) and gold(I) reagents. Analytically pure products were only obtained from the reaction with copper(I). Details of this together with characterization work are discussed below.

4.4.1.1. Reaction of 4.1 with $[Cu(MeCN)_4]BF_4$ with the Formation of $[Co_4Cu_3(CO)_8(dmpm)_4][BF_4]$ (4.3).

When a solution of $[Co_2(CO)_4(dmpm)_2]$ in CH_2Cl_2 was treated with $[Cu(MeCN)_4]BF_4$, a deep green solution was obtained from which black crystals of $[Co_4Cu_3(CO)_8(dmpm)_4]BF_4$ 4.3 were isolated in low yield. In the solid state, these crystals are air stable. It dissolves only in highly polar solvents such as DMF, solutions of which decomposes rapidly on exposure to air.

The complex may have been formed according to the following equation.

$$2[Co_2(CO)_4(dmpm)_2] + 3[Cu(MeCN)_4]^+ + 2e^- \rightarrow [Co_4Cu_3(CO)_8(dmpm)_4]^+ + 12MeCN \quad (4.8)$$

4.4.1.2. Molecular Structure of 4.3.

A crystal obtained by slow diffusion of n-pentane to a CH_2Cl_2 solution of

complex 4.3 was found to be suitable for an X-ray diffraction analysis, which was carried out by Dr. Vittal at UWO. The molecular structure of this complex is illustrated by the ORTEP diagram in Figure 4.12 and bond distances and angles are given in Table 4.3. This reveals that the cluster cation contains two triangles of metal atoms Co(1)Co(2)Cu(2) and Co(3) Co(4) Cu(3) bridged by a central copper atom Cu(1). Each Co_2Cu triangle has three edge-bridging carbonyl ligands of which one [e.g. C(3)O(3)] bridges a Co-Co bond and two [e.g. C(5)O(5) and C(7)O(7)] are semibridging between cobalt and copper.[35,36] The two Co_2Cu triangles are bridged by two dmpm ligands, of which one bridges between equivalent copper atoms Cu(2)P(1)P(2)Cu(3) and one bridges between cobalt atoms Co(1)P(3)P(4)Co(3), while the remaining dmpm and carbonyl ligands are terminally bound to cobalt. The two Co_2Cu triangles lean towards one another such that the non-bonded distance Cu(2)Cu(3) 3.211(4)Å is much shorter than the corresponding distances Co(1)Co(3) 4.248(4)Å and Co(2)Co(4) 4.24(4)Å. In order to span the long Co(1)-Co(3) distance the μ-dmpm ligand has bond angles which are significantly distorted from the normal tetrahedral values: Co(1)P(3)C(20), 112.2(1.2)°; P(3)C(20)P(4), 121.8(2.1)°; Co(3)P(4)C(20) = 121.5(1.4)°, indicating considerable strain. Indeed the cluster is remarkable in having the versatile μ-dmpm ligands spanning pairs of metal atoms separated by the disparate distances of 2.51, 2.52, 3.21 and 4.25Å.

The most remarkable feature of the structure of 4.3 is the geometry of the bridging copper atom Cu(1). It does not bridge symmetrically between the faces of the Co_2Cu triangles but is displaced towards the cobalt atoms such that the Cu(1)Co distances 2.458(4)-2.474(4)Å are significantly shorter than the Cu(1)Cu distances

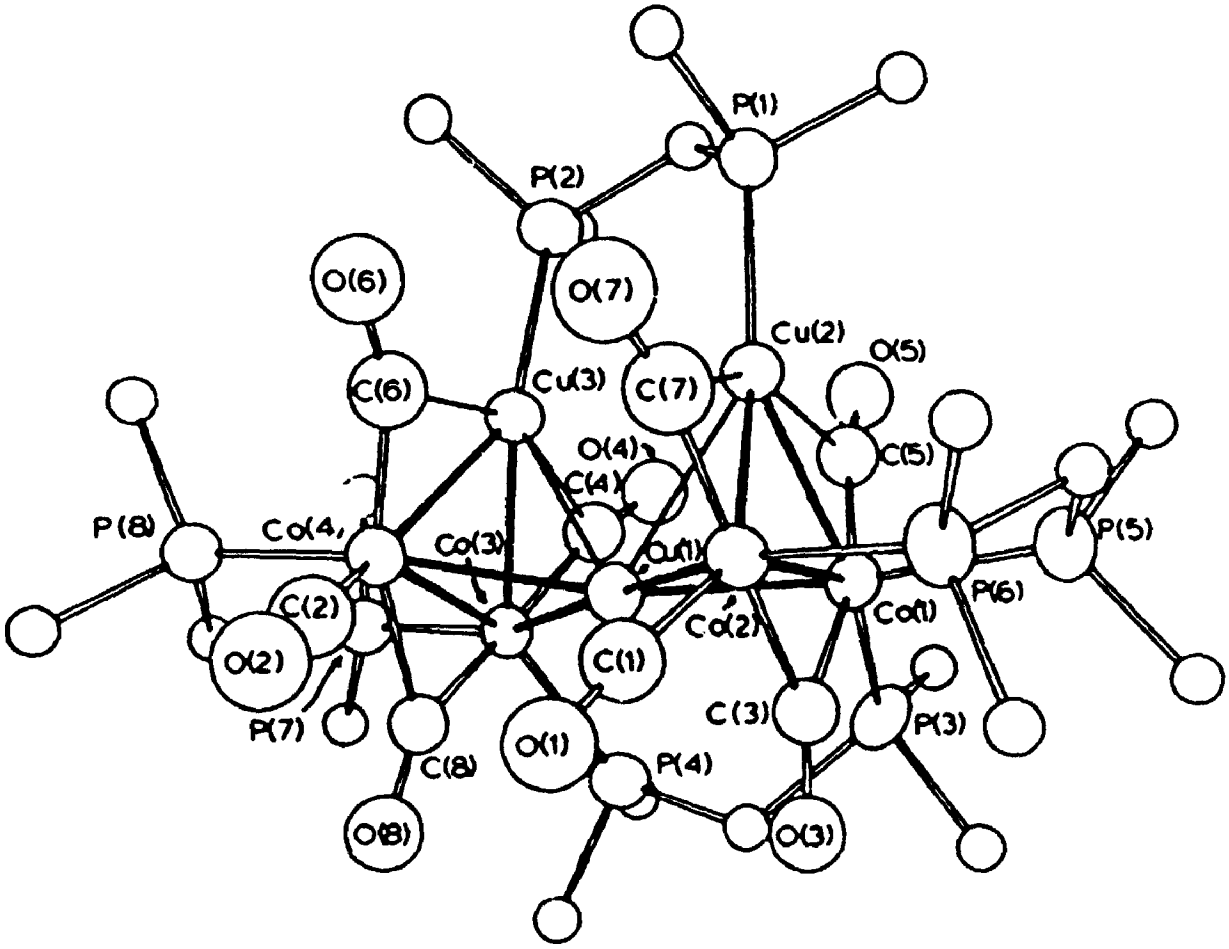

Figure 4.12a: The ORTEP diagram of the cation $[Co_4Cu_3(CO)_8(\mu\text{-dmpm})_4]^+$ 4.3.

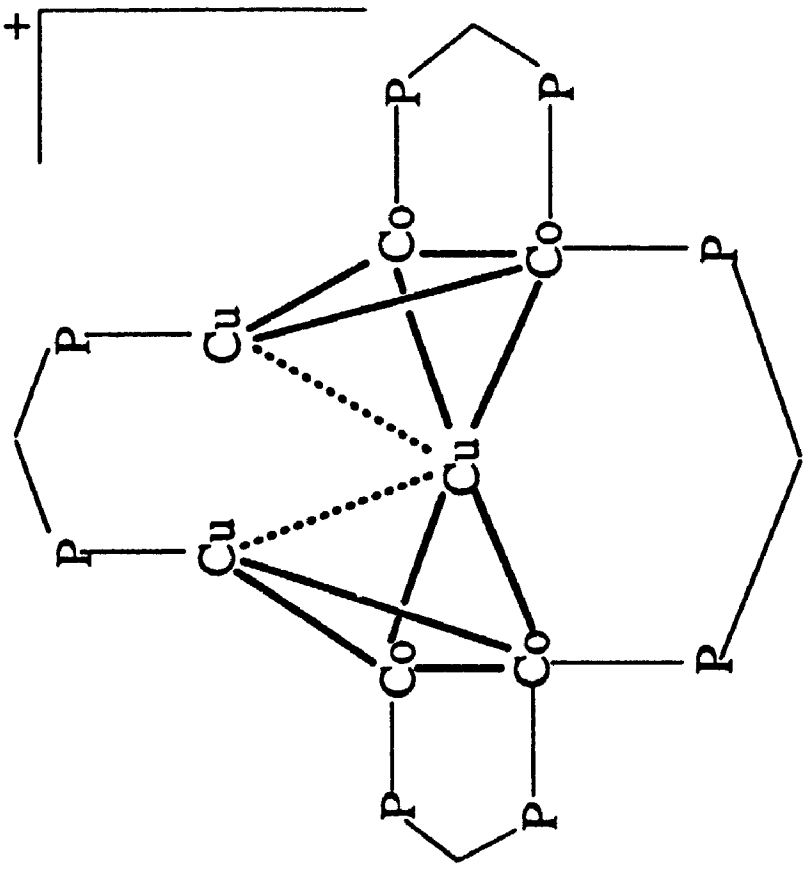

Figure 4.12b: A simplified structural diagram of 4.3, carbonyl groups are omitted for clarity.

Table 4.3: Bond Distances (Å) and Angles (°) of $[Co_4Cu_3(CO)_8(\mu\text{-dmpm})_4]BF_4$.

Cu(2)---Cu(1)	2.683(4)	Cu(3)---Cu(1)	2.624(3)
Co(1)---Cu(1)	2.466(4)	Co(2)---Cu(1)	2.463(4)
Co(3)---Cu(1)	2.458(4)	Co(4)---Cu(1)	2.474(4)
Cu(3)...Cu(2)	3.221(4)	Co(1)---Cu(2)	2.450(4)
Co(2)---Cu(2)	2.422(4)	Co(3)---Cu(3)	2.443(3)
Co(4)---Cu(3)	2.442(4)	Co(2)---Co(1)	2.523(4)
Co(4)---Co(3)	2.509(4)	P(1) ---Cu(2)	2.223(6)
P(2)---Cu(3)	2.229(6)	C(5) ---Cu(2)	2.187(20)
C(7)---Cu(2)	2.146(24)	C(4)---Cu(3)	2.203(20)
C(6)---Cu(3)	2.116(23)	P(3)---Co(1)	2.196(6)
P(5)---Co(1)	2.219(6)	C(3)---Co(1)	1.839(20)
C(5)---Co(1)	1.734(21)	P(6)---Co(2)	2.196(6)
C(1)---Co(2)	1.735(24)	C(3)---Co(2)	1.934(19)
C(7)---Co(2)	1.735(26)	P(4)---Co(3)	2.209(6)
P(7)---Co(3)	2.228(6)	C(4)---Co(3)	1.729(22)
C(8)---Co(3)	1.867(20)	P(8)---Co(4)	2.202(6)
C(2)---Co(4)	1.748(24)	C(6)---Co(4)	1.733(23)
C(8)---Co(4)	1.923(20)	C(10)---P(1)	1.871(22)
C(11)---P(1)	1.738(25)	C(12)---P(1)	1.791(23)
C(10 ---P(2)	1.793(22)	C(21)---P(2)	1.790(25)
C(22)---P(2)	1.779(21)	C(20)---P(3)	1.938(36)
C(31)---P(3)	1.773(23)	C(32)---P(3)	1.653(30)
C(20)---P(4)	1.710(34)	C(41)---P(4)	1.708(29)
C(42)---P(4)	1.714(37)	C(30)---P(5)	1.846(19)
C(51)---P(5)	1.862(20)	C(52)---P(5)	1.786(23)
C(30)---P(6)	1.829(20)	C(61)---P(6)	1.790(21)
C(62)---P(6)	1.798(21)	C(40)---P(7)	1.824(19)
C(71)---P(7)	1.826(20)	C(72)---P(7)	1.833(19)
C(40)---P(8)	1.858(20)	C(81)---P(8)	1.817(19)

C(82)---P(8)	1.838(20)	C(1)---O(1)	1.168(23)
C(2)---O(2)	1.134(24)	C(3)---O(3)	1.196(20)
C(4)---O(4)	1.191(21)	C(5)---O(5)	1.202(21)
C(6)---O(6)	1.220(23)	C(7)---O(7)	1.88(25)
C(8)---O(8)	1.206(20)		

Angles (°):

Cu(3)-Cu(1)-Cu(2)	74.5(1)	Co(1)-Cu(1)-Cu(2)	56.6(1)
Co(1)-Cu(1)-Cu(3)	112.1(1)	Co(2)-Cu(1)-Cu(2)	55.96(9)
Co(2)-Cu(1)-Cu(3)	124.3(1)	Co(2)-Cu(1)-Co(1)	61.6(1)
Co(3)-Cu(1)-Cu(2)	126.1(1)	Co(3)-Cu(1)-Cu(3)	57.35(9)
Co(3)-Cu(1)-Co(1)	119.3(1)	Co(3)-Cu(1)-Co(2)	178.0(1)
Co(4)-Cu(1)-Cu(2)	112.6(1)	Co(4).Cu(1)-Cu(3)	57.2(1)
Co(4)-Cu(1)-Co(1)	168.1(1)	Co(4)-Cu(1)-Co(2)	118.4(1)
Co(4)-Cu(1)-Co(3)	61.2(1)	Co(1)-Cu(2)-Cu(1)	57.2(1)
Co(2)-Cu(2)-Cu(1)	57.4(1)	Co(2)-Cu(2)-Co(1)	62.4(1)
P(1)-Cu(2)- Cu(1)	140.0(2)	P(1)-Cu(2)-Co(1)	144.2(2)
P(1)-Cu(2)-Co(2)	150.1(2)	C(5)-Cu(2)-Cu(1)	78.4(5)
C(5)-Cu(2)-Co(1)	43.5(5)	C(5)-Cu(2)-Co(2)	105.8(6)
C(5)-Cu(2)-P(1)	102.5(6)	C(7)-Cu(2)-Cu(1)	82.8(7)
C(7)-Cu(2)-Co(1)	106.4(7)	C(7)-Cu(2)-Co(2)	44.1(7)
C(7)-Cu(2)-P(1)	107.1(7)	C(7)-Cu(2)-C(5)	149.9(9)
Co(3)-Cu(3)-Cu(1)	57.90(9)	Co(4)-Cu(3)-Cu(1)	58.3(1)
Co(4)-Cu(3)-Co(3)	61.8(1)	P(2) -Cu(3)-Cu(1)	141.0(2)
P(2) -Cu(3)-Co(3)	146.8(2)	P(2) -Cu(3)-Co(4)	146.7(2)
C(4) -Cu(3)-Cu(1)	80.4(5)	C(4) -Cu(3)-Co(3)	43.3(6)
C(4) -Cu(3)-Co(4)	105.1(6)	C(4) -Cu(3)-P(2	105.3(6)
C(6) -Cu(3)-Cu(1)	81.0(6)	C(6) -Cu(3)-Co(3)	105.8(6)
(6) -Cu(3)-Co(4)	44.0(6)	C(6) -Cu(3)-P(2)	104.7(7)
C(6) Cu(3)-C(4)	149.1(9)	Cu(2)-Co(1)-Cu(1)	66.2(1)
Co(2)-Co(1)Cu(1)	59.2(1)	Co(2)-Co(1)-Cu(2)	58.3(1)

P(3) -Co(1)-Cu(1)	100.2(2)	P(3) -Co(1)-Cu(2)	148.7(2)
P(3) -Co(1)-Co(2)	140.4(2)	P(5) -Co(1)-Cu(1)	156.0(2)
P(5) -Co(1)-Cu(2)	99.1(2)	P(5) -Co(1)-Co(2)	97.2(2)
P(5) -Co(1)-P(3)	101.5(2)	C(3) -Co(1)-Cu(1)	69.7(6)
C(3) -Co(1)-Cu(2)	107.1(6)	C(3) -Co(1)-Co(2)	49.7(6)
C(3) -Co(1)-P(3)	92.8(6)	C(3) -Co(1)-P(5)	98.9(6)
C(5) -Co(1)-Cu(1)	93.6(7)	C(5) -Co(1)-Cu(2)	60.2(7)
C(5) -Co(1)-Co(2)	118.4(7)	C(5) -Co(1)-P(3)	94.6(7)
C(5) -Co(1)-P(5)	94.9(7)	C(5) -Co(1)-C(3)	162.8(9)
CU(2)-Co(2)-Cu(1)	66.6(1)	Co(1)-Co(2-Cu(1)	59.3(1)
Co(1)-Co(2)-Cu(2)	59.4(1)	P(6) -Co(2)-Cu(1)	154.6(2)
P(6) -Co(2)-Cu(2)	106.0(2)	P(6) -Co(2)-Co(1)	95.7(2)
C(1) -Co(2)-Cu(1)	97.2(7)	C(1) -Co(2)-Cu(2)	146.2(7)
C(1) -Co(2)-Co(1)	138.8(7)	C(1) -Co(2)-P(6)	100.2(7)
C(3) -Co(2)-Cu(1)	68.5(6)	C(3) -Co(2)-Cu(2)	105.0(6)
C(3) -Co(2)-Co(1)	46.4(6)	C(3) -Co(2)-P(6)	91.6(6)
C(3) -Co(2)-C(1)	95.2(9)	C(7) -Co(2)-Cu(1)	98.7(8)
C(7) -Co(2)-Cu(2)	59.5(8)	C(7) -Co(2)-Co(1)	118.7(8)
C(7) -Co(2)-P(6)	97.5(8)	C(7) -Co(2)-C(1)	96.5(1.1)
C(7) -Co(2)-C(3)	163.7(1)	Cu(3)-Co(3)-Cu(1)	64.7(1)
Co(4)-Co(3)-Cu(1)	59.8(1)	Co(4)-Co(3)-Cu(3)	59.1(1)
P(4) -Co(3)-Cu(1)	95.8(2)	P(4) -Co(3)-Cu(3)	143.3(2)
P(4) -Co(3)-Co(4)	139.0(2)	P(7) -Co(3)-Cu(1)	156.2(2)
P(7) -Co(3)-Cu(3)	101.3(2)	P(7) -Co(3)-Co(4)	96.8(2)
P(7) -Co(3)-P(4)	105.7(2)	C(4) -Co(3)-Cu(1)	95.2(7)
C(4) -Co(3)-Cu(3)	61.0(7)	C(4) -Co(3)-Co(4)	120.0(7)
C(4) -Co(3)-P(4)	92.5(7)	C(4) -Co(3)-P(7)	93.9(7)
C(8) -Co(3)-Cu(1)	72.2(6)	C(8) -Co(3)-Cu(3)	107.9(6)
C(8) -Co(3)-Co(4)	49.5(6)	C(8) -Co(3)-P(4)	93.7(6)
C(8) -Co(3)-P(7)	96.0(6)	C(8) -Co(3)-C(4)	166.5(9)
Cu(3)-Co(4)-Cu(1)	64.5(1)	Co(3)-Co(4)-Cu(1)	59.1(1)

Co(3)-Co(4)-Cu(3)	59.1(1)	P(8) -Co(4)-Cu(1)	156.3(2)
P(8) -Co(4)-Cu(3)	105.0(2)	P(8) -Co(4)-Co(3)	97.2(2)
C(2) -Co(4)-Cu(1)	99.1(7)	C(2) -Co(4)-Cu(3)	147.8(8)
C(2) -Co(4)-Co(3)	138.0(8)	C(2) -Co(4)-P(8)	99.4(7)
C(6) -Co(4)-Cu(1)	93.3(7)	C(6) -Co(4)-Cu(3)	58.0(7)
C(6) -Co(4)-Co(3)	117.1(8)	C(6) -Co(4)-P(8)	98.6(7)
C(6) -Co(4)-C(2)	98.2(1)	C(8) -Co(4)-Cu(1)	71.0(6)
C(8) -Co(4)-Cu(3)	106.0(6)	C(8) -Co(4)-Co(3)	47.6(6)
C(8) -Co(4)-P(8)	93.4(6)	C(8) -Co(4)-C(2)	93.1(1)
C(8) -Co(4)-C(6)	162.0(9)	C(10)-P(1) -Cu(2)	112.8(8)
C(11)-P(1) -Cu(2)	119.3(9)	C(11)-P(1) -C(10)	105.1(1.1)
C(12)-P(1) -Cu(2)	116.5(8)	C(12)-P(1) -C(10)	98.8(1.1)
C(12)-P(1) -C(11)	101.7(1.2)	C(10)-P(2) -Cu(3)	118.4(8)
C(21)-P(2) -Cu(3)	114.6(1)	C(21)-P(2) -C(10)	98.0(1.2)
C(22)-P(2) -Cu(3)	115.0(9)	C(22)-P(2) -C(10)	106.6(1.1)
C(22)-P(2) -C(21)	101.8(1.2)	C(20)-P(3) -Co(1)	112.2(1.2)
C(31)-P(3) -Co(1)	118.9(9)	C(31)-P(3) -C(20)	88.5(1.3)
C(32)-P(3) -Co(1)	118.8(1.2)	C(32)P(3) -C(20)	114.4(1.7)
C(32)-P(3) -C(31)	99.9(1.4)	C(20)-P(4) -Co(3)	121.5(1.4)
C(41)-P(4) -Co(3)	119.6(1.1)	C(41)-P(4) -C(20)	110.4(1.7)
C(42)-P(4) -Co(3)	116.6(1.3)	C(42)-P(4) -C(20)	91.7(1.7)
C(42)-P(4) -C(41)	88.9(1.7)	C(30)-P(5) -CO(1)	110.6(7)
C(51)-P(5) -Co(1)	122.7(8)	C(51)-P(5) -C(30)	101.5(1)
C(52)-P(5) -Co(1)	118.3(8)	C(52)-P(5) -C(30)	100.2(1)
C(52)-P(5) -C(51)	100.2(1.1)	C(30)-P(6) -Co(2)	110.2(7)
C(61)-P(6) -Co(2)	120.1(8)	C(61)-P(6) -C(30)	100.2(1)
C(62)-P(6) -Co(2)	115.2(8)	C(62)-P(6) -C(30)	106.6(1)
C(62)-P(6) -C(61)	102.8(1.1)	C(40)-P(7) -Co(3)	110.8(7)
C(71)-P(7) -Co(3)	126.5(7)	C(71)-P(7) -C(40)	98.9(9)
C(72)-P(7) -Co(3)	113.2(7)	C(72)-P(7) -C(40)	104.9(9)
C(72)-P(7) -C(71)	99.9(1)	C(40)-P(8) -Co(4)	111.9(7)

C(81)-P(8) -Co(4)	119.0(7)	C(81)-P(8) -C(40)	99.2(9)
C(82)-P(8) -Co(4)	117.4(7)	C(82)-P(8) -C(40)	104.7(1)
C(82)-P(8) -C(81)	102.3(9)	P(2) -C(10)-P(1)	115.4(1.2)
P(4) -C(20)-P(3)	121.8(2.1)	P(6) -C(30)P(5)	111.5(1.2)
P(8) -C(40)-P(7)	111.9(1.1)	O(1) -C(1) -Co(2)	174.1(2)
O(2) -C(2) -Co(4)	177.3(2.2)	Co(2)-C(3) -Co(1)	83.9(8)
O(3) -C(3) -Co(1)	142.7(1.6)	O(3) -C(3) -Co(2)	133.4(1.6)
Co(3)-C(4) -Cu(3)	75.7(8)	O(4) -C(4) -Cu(3)	120.1(1.6)
O(4) -C(4) -Co(3)	164.2(1.8)	Co(1)-C(5) -Cu(2)	76.4(8)
O(5) -C(5) -Cu(2)	119.9(1.5)	O(5) -C(5) -Co(1)	163.8(1.8)
Co(4)-C(6) -Cu(3)	78.1(9)	O(6) -C(6) -Cu(3)	124.0(1.7)
O(6) -C(6) -Co(4)	157.7(2)	Co(2)-C(7) -Cu(2)	76.4(1)
O(7) -C(7) -Cu(2)	123.9(1.9)	O(7) -C(7) -Co(2)	159.7(2.2)
Co(4)-C(8) -Co(3)	82.9(8)	O(8) -C(8) -Co(3)	141.9(1.7)
O(8) -C(8) -Co(4)	134.9(1.6)		

2.683(4) and 2.624(3)Å. The latter distances are in the range found for weak lateral forces between copper(I) atoms,[37,38] but the Cu-Cu bonding is still presumably partly responsible for the tilting of the Co_2Cu triangles described above. The four cobalt atoms and Cu(1) are approximately coplanar [dihedral angle between planes Cu(1)Co(1)Co(2) and Cu(1)Co(3)Co(4) 14.8(3)°; ∠Co(2)Cu(1)Co(3) 178.0(1)°; ∠Co(1)Cu(1)Co(4) 168.1(1)°]. Although at least one group 11 cluster complex is known to contain an approximately square-planar metal centre in oxidation state (I),[39] this stereochemistry is much more typical of these metals in oxidation state (III). Furthermore, formal removal of the central copper atom Cu(1) as Cu^+ leaves each Co_2Cu triangle with an odd electron count, whereas its removal as Cu^{3+} and other copper atoms as LCu^+ leaves two $[Co_2L_6(\mu\text{-}CO)]^{2-}$ units (where L= terminal CO or phosphine donor atoms) in which each cobalt has an 18 electron configuration and thus, each Co_2Cu triangle has its favoured electron count.[38] Although the use of oxidation states in clusters is fraught with problems, it is used here to indicate that the atom Cu(1) probably uses dsp^2 hybrid orbitals in bonding and has the stereochemistry expected for this bonding state. Together these factors suggest that the cluster contains a formally d^8 copper(III) atom Cu(1). This is an unprecedented electron configuration in copper clusters.[38] Since this is a unique electron configuration, the possible presence of hydride ligands has been considered. It should be noted that a formulation as $[Co_4Cu_3H_2(CO)_8(\mu\text{-dmpm})_4]^+$ would require Cu(1) to have oxidation state (I). However, no evidence for hydride was observed in the ^1H NMR spectrum (no signals from δ 0 to -50 ppm) nor from final difference Fourier maps in the X-ray structure determination. Dissolution of the cluster in a $[^2H_7]$ dimethylformamide-CCl_4 mixture

failed to give any trace of $CHCl_3$. This reduction of CCl_4 to $CHCl_3$ is a sensitive test for transition metal hydrides. The mass spectrum gave a peak at m/z= 1195 as expected for the cluster cation without hydride ligands.

4.4.1.3. Spectroscopic Characterization of 4.3.

The infrared spectrum (Nujol) of complex 4.3 is shown in Figure 4.13. This reveals three different sets of bands, the highest energy bands at 1981, 1946 and 1917 cm^{-1} are assigned to the terminally bound CO groups while the lowest energy band at 1713 cm^{-1} is typical of bridging carbonyl groups. The remaining bands at 1879, 1860, 1838, 1833 and 1803 cm^{-1} are assigned to the semi-bridging carbonyl groups. Similar stretching frequencies for terminal and bridging carbonyl groups have been observed in $[Co_2(CO)_4(dmpm)_2]$ and $[Co_4(CO)_8(dmpm)_2]$, as discussed earlier, and other phosphine substituted cobalt carbonyl complexes.[5,28,40] Similar stretching frequencies for semibridging carbonyls were earlier reported in other mixed metal cobalt complexes such as $[(tmed)CuCo(CO)_4]$ (tmed= N,N,N',N'-tetramethylethylenediamine),[41] $[Cu(dmpe)_2][Cu(Co(CO)_4)_2]$[35] and $[CoRh(CO)_3(dppm)_2]$.[42]

From the X-ray structure it is apparent that there are three distinct sites for phosphorus atoms. In agreement, the ^{31}P NMR in DMF solution shows three resonances with an intensity ratio of 1:2:1 at δ = 3.66, 3.28 and -31.19 ppm respectively. The lowest field resonance may be assigned to the dmpm ligand bridging cobalt atoms between the two Co_2Cu triangles, while the highest field resonance is attributed to the phosphorus atoms of the dmpm ligand bridging the two copper

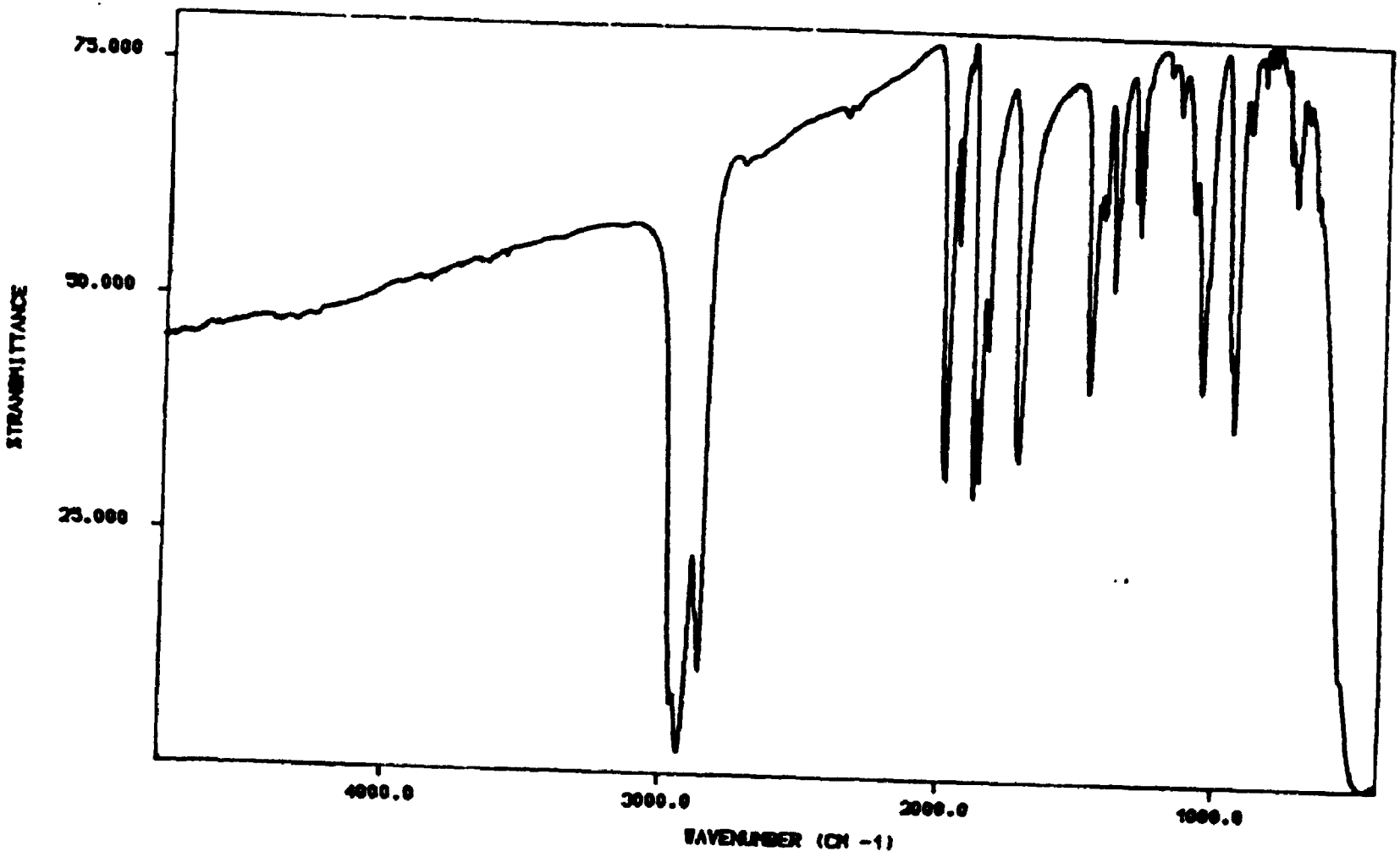

Figure 4.13: The IR spectrum (Nujol) of $[Co_4Cu_3(CO)_8(\mu\text{-dmpm})_4]BF_4$, 4.3.

atoms. The remaining resonance at $\delta = 3.28$ ppm, which is twice as intense as the other two resonances, is attributed to the dmpm ligands bridging the Co-Co bonds in each Co_2Cu triangle. Similarly, the ^1H NMR exhibits six resonances for PMe protons with an intensity ratio of 1:1:1:2:1:2 at $\delta = 1.04$, 1.18, 1.24, 1.42, 1.64 and 1.68 ppm respectively, consistent with the solid state structure. Only one broad resonance at $\delta = 2.7$ ppm for CH_2P_2 protons was observed.

The FAB mass spectrum gave a parent ion peak for $Co_4Cu_3(CO)_8(dmpm)_4^+$ at m/e 1195, with an excellent agreement between observed and calculated isotope patterns. In addition EDX analysis reveals cobalt to copper ratio of 4:3 atom percent. Thus, all of this evidence is fully consistent with the solid state structure established by the single crystal X-ray diffraction studies and shown in Figure 4.12.

4.4.2. Reactions of 4.1 with Ag(I) and Au(I).

In addition to reaction of 4.1 with Cu^+ several reactions with $Ag(CH_3CO_2)$ and $AuCl(SMe_2)$ were attempted to prepare analogous Co-Ag and Co-Au clusters. Although in some of the reactions involving Au^+, spectroscopic evidence indicated the formation of similar species to the Co-Cu cluster discussed above, these complexes could not be isolated in pure form from the reaction solutions. There was no evidence for the formation of analogous Co-Ag cluster species, from the Co-Ag reaction solutions.

4.4.3. Reaction of 4.1 with NaI and I_2

When a solution of $[Co_2(CO)_4(dmpm)_2]$ in $C_2H_4Cl_2$ was treated with NaI in a

1:2 molar ratio a red solution was formed which, on precipitation with $NaBPh_4$ yielded the bright red crystalline complex $[Co_2(\mu\text{-}I)(CO)_3(\mu\text{-}dmpm)_2][BPh_4]$, 4.4. This product could also be prepared by treating $[Co_2(CO)_4(dmpm)_2]$ with I_2, followed by precipitation with $NaBPh_4$.

The IR spectrum of this complex shows carbonyl stretching frequencies due to terminal CO groups at 2018, 1939 and 1901 cm^{-1} while a strong band at 1804 cm^{-1} is due to bridging CO. These frequencies are significantly shifted towards higher energy compared to the parent complex $[Co_2(CO)_4(dmpm)_2]$ indicative of diminishing M→CO back bonding. This is consistent with the oxidation of cobalt atoms by iodine, thus leading to a reduction of electron density on cobalt.

The ^{31}P NMR spectrum shows a sharp singlet resonance at $\delta = 29$ ppm and no change was observed in this resonance at -90°C. This suggests that there is a mirror plane bisecting the dmpm ligands through the methylene carbons, thus, making all the phosphorus atoms chemically equivalent. The large downfield shift observed in ^{31}P NMR is consistent with the deshielding of the ^{31}P nucleus concurrent with the increase in the oxidation state of the metal which results in reduced electron density on the phosphorus atom, either through reduced M → Pπ back bonding or increased polarization of the phosphorus lone pair by the more electronegative metal centre. However, the influence of ring size on the chemical shift can not be ruled out.

The ^1H NMR spectrum of 4.4 is shown in Figure 4.14. The resonance for the methylene protons $CH^aH^bP_2$ of dmpm was clearly resolved into an AB pattern. The asymmetry observed is consistent with the formation of a $Co_2(\mu\text{-}I)(\mu\text{-}CO)$ double bridged structure, which would make the methylene protons inequivalent. Similarly,

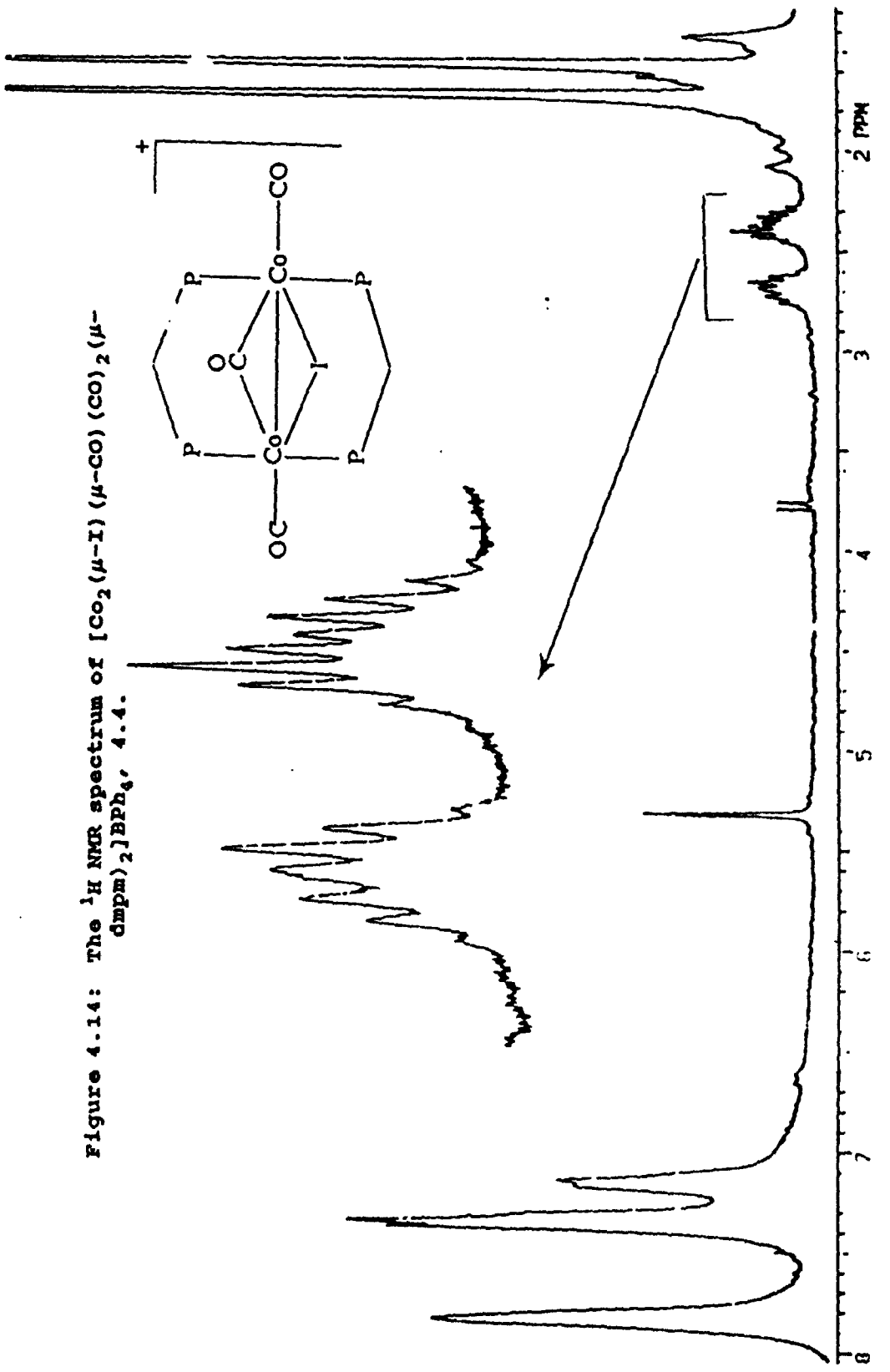

Figure 4.14: The ^1H NMR spectrum of $[Co_2(\mu\text{-}I)(\mu\text{-}CO)(CO)_2(\mu\text{-}dmpm)_2]BPh_4$, 4.4.

two resonances in a 1:1 intensity ratio were expected and observed at $\delta = 1.56$ and 1.71 ppm for the PMe_2 protons of the dmpm ligands. In addition, the ^1H NMR shows resonances due to the BPh_4^- protons in the region 7.0-7.6 ppm. The integration of the phenyl protons of BPh_4^- ion compared with that of the CH_2P_2 or PMe_2 protons of the dmpm ligand shows that only one BPh_4^- is present. The structure of 4.4 is thus proved to be $[Co_2(\mu\text{-}I)(\mu\text{-}CO)(CO)_2(\mu\text{-dmpm})_2]BPh_4$.

4.4.4. Reaction of 4.1 with HBF_4

When a solution of $[Co_2(CO)_4(dmpm)_2]$ in CH_2Cl_2 was reacted with excess HBF_4, it immediately formed a bright red solution from which the bright red solid 4.5 was isolated. The Infrared spectrum of solid 4.5, shown in Figure 4.15, reveals carbonyl stretches for both terminal and bridging carbonyl groups. The frequencies for these bands are shifted significantly towards higher energy relative to $[Co_2(CO)_4(dmpm)_2]$. This clearly indicates that the electronic population on the cobalt atoms has been reduced due to oxidation. Similar behaviour was observed when $[Co_2(CO)_4(dmpm)_2]$ was treated with I_2 and NaI as discussed in section 4.4.2.

The variable temperature ^{31}P NMR spectra are illustrated in Figure 4.16. At room temperature there is a single resonance at $\delta = 30.9$ ppm, but this decoalesces and splits at -90°C into two apparent triplets, centred at $\delta = 34.7$ and 30.6 ppm with $^2J(PP) = 38$ Hz. This clearly indicates that the molecule is fluxional at room temperature. However at lower temperatures fluxionality is slower and the limiting spectrum is obtained.

The ^1H NMR also exhibits temperature dependent behaviour. Thus at room

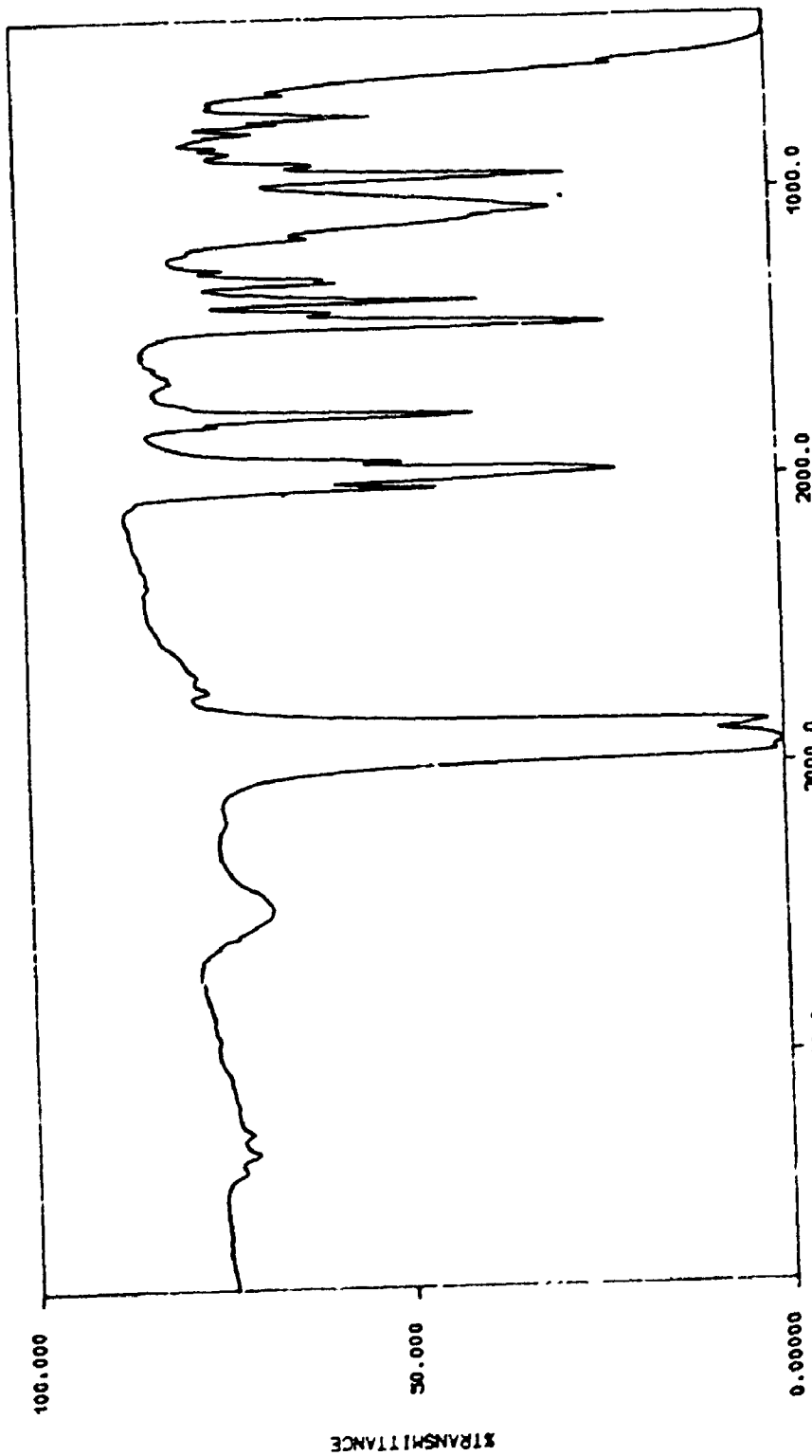

Figure 4.15: The IR spectrum (Nujol) of 4.5.

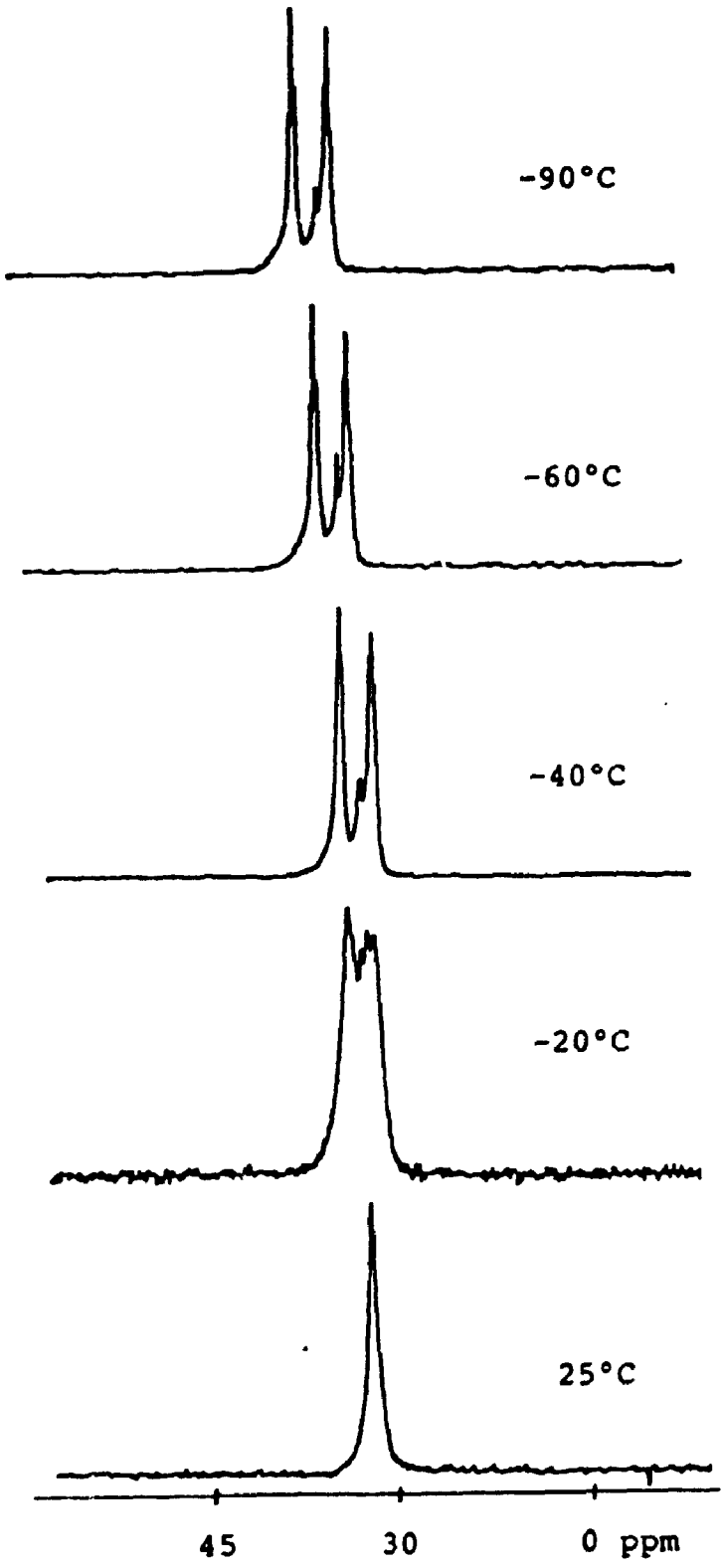

Figure 4.16: Variable temperature ^{31}P NMR spectra of 4.5 in CD_2Cl_2.

temperature it shows a partially resolved quintet resonance at $\delta = 2.9$ ppm for the CH_2P_2 protons with $^2J(PH) = 5.5$ Hz., which slightly broadened at -90°C. In addition an unresolved broad resonance at $\delta = 1.8$ ppm was observed for the PMe protons. This resonance is further broadened on cooling the sample to -90°C. No hydride resonance was observed in the region $\delta = 0$-30 ppm. In addition the chemical analysis suggest a formulation of $[Co_2(CO)_3Cl(dmpm)_2]BF_4$.

4.4.5. Reaction of 4.1 with CO.

When CD_2Cl_2 solutions of 4.1 were treated with CO gas, red coloured solutions were produced with identical IR, ^{31}P and ^1H NMR spectroscopic properties as exhibited by the complex produced in the reactions of 4.1 with HBF_4 discussed earlier in section 4.4.3. Clearly the same complex is formed in both reactions but it has not yet been fully characterzied.

4.5. Conclusions:

From the reactions of cobalt halide salts with $NaBH_4$ in the presence of dmpm, two products were isolated. This route to obtain phosphine substituted metal carbonyl complexes is novel, and by adjusting reaction conditions, it gave two remarkably different products. Thus when the metal to dmpm ratio was 1:2.5 or higher it produced the binuclear complex $[Co_2(CO)_4(\mu\text{-dmpm})_2]$ (4.1). This dinuclear complex exhibits unusual solution properties. In solution, it exists as a mixture of isomers $[Co_2(\mu\text{-CO})_2(CO)_2(\mu\text{-dmpm})_2]$ 4.1a, and $[Co_2(CO)_4(\mu\text{-dmpm})_2]$ 4.1b. It is shown that these species are fluxional in solution, with the carbonyl groups migrating

easily from terminal to bridging positions. There is evidence that complex 4.1b is paramagnetic. The details of the mechanisms were investigated using variable temperature multinuclear NMR and FT-IR techniques. The results obtained show that there is very small activation energy involved for the interconversion of these isomers.

When the cobalt : dmpm ratio was approximately 1:1, the reduction with $NaBH_4$ in the presence of CO resulted in the formation of a tetranuclear cluster, $[Co_4(\mu\text{-}CO)_3(CO)_5(\mu\text{-}dmpm)_2]$. The formation of an analogous tetranuclear cluster with dppm, using the same route has not been observed. This indicates that the steric bulk of the ligand plays an important role in determining the products formed by this synthetic route. This observation is further supported from the fact that with dmpm only one dimeric isomer can be isolated, while with dppm both isomeric species were isolated. Steric bulk of the ligand also influences the reactivity of the products formed. Thus, while the dppm bridged dinuclear complex is easily protonated to produce a symmetrical addition product, $[Co_2(\mu\text{-}H)(CO)_3(\mu\text{-}dppm)_2]^+$,[20] this was not observed with the dmpm analogue. Thus, reaction of $[Co_2(CO)_4(\mu\text{-}dmpm)_2]$ with HBF_4 produced a species without any metal hydride and which exhibits an NMR pattern consistent with an unsymmetrical product. Similarly, the dppm dimer $[Co_2(CO)_4(\mu\text{-}dppm)_2]$ did not react with group 11 metal complexes, whereas $[Co_2(CO)_4(\mu\text{-}dmpm)_2]$ reacted with $[Cu(MeCN)_4]BF_4$ to produce a remarkable mixed metal cluster $[Co_4Cu_3(CO)_8(dmpm)_4]BF_4$. This cluster is unique since it contains a copper atom, which has an unprecedented square planar stereochemistry in cluster complexes. This study also indicates that the dimeric products formed with dppm and

dmpm are paramagnetic in solution at room temperature and diamagnetic in the solid state and at lower temperature in solutions. Thus the metal-metal bond in the isomer of $[Co_2(CO)_4(\mu\text{-dppm})_2]$ and $[Co_2(CO)_4(\mu\text{-dmpm})_2]$ with no carbonyl bridges may not exist or is perhaps very weak.

4.6. Experimental

4.6.1. Synthesis of $[Co_2(CO)_4(dmpm)_2]$ (4.1)

$CoCl_2.6H_2O$ (0.5 g, 2.1 mmol) was dissolved in EtOH (60 mL). To this was added dmpm (0.8 mL, 6.95 mmol). The resulting yellowish-brown mixture was stirred under a slow stream of CO gas for 1 h. An ethanolic suspension (20 mL) of $NaBH_4$ (0.35 g, 9.25 mmol) was than added dropwise over a period of 15 min. The deep brown mixture so formed was stirred for a further 2.5 h under a slow stream of CO gas. The yellowish-orange suspension so formed was than filtered off. This was redissolved in CH_2Cl_2 (10 mL) and a layer of n-pentane (20 mL) was carefully added to it. The yellowish-orange microcrystalline product, which formed over a one week period, was filtered off, washed with EtOH (7 mL) and dried under reduced pressure. A second batch of product could be obtained by evaporating the solvent from the mother liquor and recrystallizing the residue from CH_2Cl_2 and n-pentane.

Yield: 20 % M.P. 135-137°C

Anal. Calc. for $C_{14}H_{28}O_4P_4Co_2$: C, 33.53; H, 5.59%; Found: C, 32.85; H, 5.71%.

IR (CH_2Cl_2): 4.1a, 1945, 1916, 1735; 4.1b, 1953, 1920, 1893.

NMR at -92°C in CD_2Cl_2: 4.1a: ^1H, δ 1.93[$CH^aH^bP_2$, H^a], 2.75[$CH^aH^bP_2$, H^b], 1.50[MeP]; ^{13}C, -82°C, δ 203.5[terminal CO], 265.5[μ-CO], 19.5, 19.0[MeP]; ^{31}P, -62°C, δ 29.85(s).

4.1b: ^1H, -90°C, δ 2.19[CH_2P_2], 1.34[MeP]; ^{13}C, not resolved; ^{31}P, -62°C, δ 19.3(s).

FAB-MS: m/z 502; Calc. for $Co_2(CO)_4(dmpm)_2^+$ = 502

4.6.2. Synthesis of $[Co_4(CO)_8(dmpm)_2]$ (4.2)

To a stirring solution of $CoCl_2.6H_2O$ (0.90 g, 2.75 mM) in EtOH (60 mL) was added dmpm (0.40 mL, 3.47 mmol). This solution was than saturated with CO gas for about 0.5 h, and a suspension of $NaBH_4$ (0.40 g, 10.57 mmol) in EtOH (20 mL) was then added over a period of 15 min. The mixture turned blackish in colour. This was stirred under a slow stream of CO gas for a further 2.5 h. Solvent was than removed to dryness under vacuum. The black solid was dissolved in C_6H_6 (30 mL), the solution was filtered, some of the solvent (~30-40%) was evaporated by vacuum and a layer of n-heptane (30 mL) was added to the remaining solution, which was then set aside for a period of two weeks. The black crystalline complex so formed was filtered off, washed with n-heptane (10 mL) and dried under reduced pressure.

Yield: 15%

Anal. Calc. for $C_{18}H_{28}O_8P_4Co_4.0.5C_7H_{16}$: C, 33.0; H, 4.6%

Found: C, 33.7; H, 3.3%

IR: ν(CO), terminal CO's, 1989, 1963, 1946, 1930, 1893 cm^{-1} and bridging CO's, 1810, 1773, 1743 cm^{-1}.

NMR in CD_2Cl_2; ^1H, 25°C δ 2.45[br, CH_2P_2]; 1.47[d, $J(PH)_{obs}$ = 8 Hz., PMe_2]; -90°C δ 3.17[br,t, $CH^cH^dP_2$, $^2J(PH)$=9.5 Hz.]; 2.05[br, $CH^aH^bP_2$, H^b]; The resonance due to H^a is buried under PMe_2 peaks; 1.64[br,d PMe_2, $J(PH)_{obs}$ = 7 Hz.]; 1.49[br, PMe_2]; 1.34[br, PMe_2]; 1.23[br,d, PMe_2, $J(PH)_{obs}$ = 7.5 Hz.]; ^{31}P, 25°C δ -0.9 (br); -90°C δ 6.8[d, J(PP) = 50.4 Hz., P^aP^b]; -4.8[br,d, J(PP) = 33.6 Hz., P^c]; -11[br, P^d].

4.6.3. Synthesis of $[Co_4Cu_3(CO)_8(dmpm)_4]BF_4$ (4.3)

To a stirring solution of $[Co_2(CO)_4(dmpm)_2]$ (0.70 g, 0.14 mmol) in CH_2Cl_2 (10 mL) was added a suspension of $[Cu(MeCN)_4]BF_4$ (0.05 g, 0.14 mM) in CH_2Cl_2 (5 mL). The original dark brown solution immediately turned deep green. The mixture was stirred for a further 4 h under N_2 atmosphere. The intensely green solution so formed was decanted off and a layer of n-pentane was carefully added to it. This was then allowed to stand over a period of 3 weeks. The mother liquor was than decanted off and the intensely green crystalline product (large crystals appear black) was washed with n-pentane and dried under reduced pressure.

Yield: 5% M.P. 174-175°C (decomp.)

IR (Nujol): $\nu(CO)/cm^{-1}$ 1981 (vs), 1946 (m), 1917 (sh), 1879 (vs), 1860 (vs), 1838 (m), 1833 (m), 1803 (sh), 1713(vs).

NMR at 25°C in DMF-d_7: ^1H, δ 1.04 (1 Me), 1.18 (1 Me), 1.24 (1 Me), 1.42 (2 Me), 1.64 (1 Me), 1.68 (2 Me), 2.7 (CH_2P_2); ^{31}P, δ 3.66 (1 P), 3.28 (2 P), -31.19 (1 P).

FAB-MS: m/z 1195; calc. for $Co_4Cu_3(CO)_8(dmpm)_4^+$ 1195, with excellent agreement between observed and calculated isotope patterns. Accurate mass: found, 1194.708; calc. 1194.715.

4.6.4. Synthesis of $[Co_2(\mu\text{-}I)(CO)_3(dmpm)_2]BPh_4$ (4.4)

$Co_2(CO)_4(dmpm)_2$ (0.16 g, 0.32 mmol) was dissolved in $C_2H_4Cl_2$ (~7 mL) and stirred under N_2 gas. An ethanolic solution (~3mL) of NaI (0.1 g, 0.67 mmol) was than added to it, forming some suspension. The mixture was stirred overnight,

forming a red solution and some white precipitate. The solution was filtered and excess $NaBPh_4$ in ethanol (~2 mL) was added to the filtrate. A layer of ethanol (~15 mL) was then carefully added and this was then left aside over a period of 4 days. The red crystalline complex so formed was filtered off, washed with n-pentane (~10 mL) and dried under reduced pressure.

Yield; 20 % M.P 133-135°C (dec)

Anal: Calc. for $C_{37}H_{48}BIO_3P_4Co_2.1.25CH_2Cl_2$: C, 44.73; H, 4.92. Found: C, 44.74; H, 5.37.

IR: ν(CO): 2018 (vw), 1937 (vs), 1901 (sh), 1804 (vs)

NMR at 25°C in CD_2Cl_2: ^1H, δ 1.7 [d, PMe]; 2.4 [m, $CH^aH^bP_2$, $^2J(PH)$= 5.5 Hz.]; 2.68 [m, $CH^aH^bP_2$, $^2J(PH)$= 5.5 Hz.]; 7.4 [m, BPh]; ^{31}P, δ 29.3 (s)

4.6.5. Synthesis of $[Co_2(CO)_3Cl(dmpm)_2]BF_4$ (4.5).

To a stirring solution of $Co_2(CO)_4(dmpm)_2$ (0.25 g; 0.50 mmol) in CH_2Cl_2 (10 mL) was added aqueous HBF_4 in excess. The solution immediately turned from dark brownish black to red. The mixture was then stirred for a further 5-7 min. under N_2. The aqueous layer was than removed and extracted twice with CH_2Cl_2 (~10 mL). The organic layers were combined and a layer of n-pentane (~20 mL) was added to it carefully. This was left aside over a period of two weeks. The red rod like crystals so formed were filtered off, washed with n-pentane (~10 mL) and dried under reduced pressure.

Yield: 60 % Anal. Calc. for $C_{13}H_{28}ClBF_4O_3P_4Co_2$: C, 26.16; H, 4.70; Found: C, 26.84; H, 4.97%

IR= 2026 (m), 1973 (vs), 1936 (vs), 1806 (w), 1767 (vs).

NMR in CD_2Cl_2: ^1H, 25°C δ 2.9[q,br, CH_2P_2, $^2J(PH)$ = 5.5 Hz.]; 1.8[br, PMe_2]; ^{31}P, 25°C δ 30.9(s); -90°C δ 34.7 [t, $^2J_{AB}$=38 Hz] , 30.6 [t, $^2J_{AB}$=38 Hz].

4.6.6. Solution Magnetic Moment Studies of 4.1

A sample of $[Co_2(CO)_4(\mu\text{-dmpm})_2]$ (6.1 mg; 0.01 mmol) was dissolved in CD_2Cl_2 (0.5 mL) containing 5% CH_2Cl_2 and 5% TMS. This solution was then transferred into a 5 mm NMR tube. A 3 mm sealed capillary containing 5% CH_2Cl_2 and 5% TMS in CD_2Cl_2 was than inserted into it as inner reference and the cap was closed. ^1H NMR measurements were than recorded from 298°K to 183°K. At the end of the experiment the inner capillary was removed and another spectrum was recorded at 298°K.

4.7. References

1. L. Mond; H. Hirzt and M.D. Cowap; J. Chem. Soc. 798 (1910).

2. R.F. Heck, "Organotransition Metal Chemistry" Academic Press, Toronto, (1974).

3. G.G. Summer; H.P. Klug and L.E. Alexander; Acta Crystallogr. *17*, 732 (1964).

4a. G. Bor and K. Noack; J. Organomet. Chem. *64*, 367 (1974).

b. G. Bor; U.K. Dieter and K. Noack; J. Chem. Soc., Chem. Comm. 914 (1976).

c. S. Onaha and D.F. Shriver; Inorg. Chem. *15*, 915 (1976).

5. E.C. Lisic and B.E. Hanson; Inorg. Chem. *25*, 812 (1986).

6.(a). S. Attali and R. Poilblanc; Inorg. Chim. Acta. *6*, 475 (1972).

(b). E. Mantasti; E. Pelizzetti; R. Rossetti and P.L. Stanghellini; Inorg. Chim. Acta. *25*, 7 (1977).

7. G. Wilkinson, Ed., "Comprehensive Organometallic Chemistry" Vol. 5, Pergamon Press, Toronto, 1982.

8a. W. Harrison and J. Trotter; J. Chem. Soc.A 1607 (1971).

b. W.R. Cullen; J. Crow; W. Harrison and J. Trotter; J. Am. Chem. Soc. *92*, 6339 (1970).

c. D.J. Thornhill and A.R. Manning; J. Chem. Soc., Dalton Trans. 2086 (1973).

d. T. Fukumoto; Y. Matsumura ard R. Okawara; J. Organomet. Chem. *69*, 437 (1978).

9. G. de Leeuw; J.S. Field and R.J. Haines; J. Organomet. Chem. *359*, 245 (1989).

10. G.M. Brown; J.E. Finholt; R.B. King and J.W. Bibber; Inorg. Chem. *21*, 2139 (1982).

11. S.A. Laneman; F.R. Fronczek and G.G. Stanley; Inorg. Chem. *28*, 1207 (1989).

12. M.G. Newton; R.B. King; M. Chang; N.S. Pantaleo and J. Gimeno; J. Chem. Soc., Chem. Comm. 531 (1977).

13. L.S. Chai and W.R. Cullen; Inorg. Chem. *14*, 482 (1975).

14. R.L. Sweany and T.L. Brown; Inorg. Chem. *16*, 415 (1977).

15. F.H. Carré; F.A. Cotton and B.A. Frenz; Inorg. Chem. *15*, 380 (1976).

16. B.F.G. Johnson and R.E. Benfield; J. Chem. Soc. Dalton Trans. 1554 (1978).

17.(a). S. Aime; D. Osella; L. Milone; G.E. Hawkes and E.W. Randall; J. Am. Chem. Soc. *103*, 5920 (1981).

(b). B.E. Hanson and E.C. Lisic; Inorg. Chem. *25*, 715 (1986).

(c). S. Aime; M. Botta; R. Gobetto and B.E. Hanson; Inorg. Chem. *28*, 1196 (1989).

(d). B.T. Heaton; J. Sabounchei; S. Kernaghan; H. Nakayama; T. Eguchi; S. Takeda; N. Nakamura and H. Chihara; Bull. Chem. Soc. Jpn. *63*, 3019 (1990).

(e). Ibid.; J. Organomet. Chem. *428*, 207 (1992).

18. D.J. Darensbourg and M.J. Incorvia; Inorg. Chem. *20*, 1911 (1981).

19. R.B. King; J. Gimeno and T.J. Lotz; Inorg. Chem. *17*, 2401 (1978).

20. D.J. Elliot; Ph.D. Thesis UWO; (1991).

21. D.J. Elliot; H.A. Mirza; R.J. Puddephatt; D.G. Holah, A.N. Hughes; R.H. Hill and W. Xia; Inorg. Chem. *28*, 3282 (1989).

22.(a) D.F. Evans; J. Chem. Soc. 2003 (1959).

(b) D. Ostfeld; I.A. Cohen; J. Chem. Edu. *49*, 829 (1972).

(c) G.V.D. Tiers; J. Phys. Chem. *62*, 1151 (1958).

(d) E.W. Washburn; International Critical Tables, vol. III, p 27 and vol. IV, p 361, McGraw-Hill Book Co. Inc., N.Y. (1929).

(e) B.N. Figgis; J. Lewis; Modern Coord. Chem., ed. J. Lewis; R.G. Wilkins; Interscience, N.Y. (1960).

23. C.H. Wei; Inorg. Chem. *8* 2384 (1969); C.H. Wei, G.R. Wilkes and L.F. Dahl; J. Am. Chem. Soc. *89*, 4792 (1967); C.H.Wei and L.F. Dahl; ibid. *88*, 1821 (1966).

24. A.A. Bahsoun, J.A. Osborn; C. Voelken; J. Bonnet and G. Lavigne; Organometallics *1*, 1114 (1982).

25. D.J. Darenbourg; D.J. Zalewski and T. Delord; Organometallics *3*, 1210 (1984).

26. D.J. Darensbourg; D.J. Zalewski; R.L. Rhenigold and R.L. Durney; Inorg. Chem. *25*, 3281 (1986).

27. M.G. Richmond and J.K. Kochi; Organometallics *6*, 777 (1987).

28. B.E. Hanson; P.E. Fanwick and J.S. Mancini; Inorg. Chem. *21*, 3811 (1982).

29. R.J. Puddephatt; M.A. Thompson; Lj. Manojlovic-Muir; K.W. Muir; A.A. Frew and M.P. Brown; J. Chem. Soc. Chem. Commun. 805 (1981).

30. S.S.M. Ling; R.J. Puddephatt; Lj. Manojlovic-Muir; K.W. Muir; Inorg. Chim. Acta. *77*, L95 (1983).

31. S.S.M Ling; I.R. Jobe; A.J. McLennan; Lj. Manojlovic-Muir; K.W. Muir and R.J. Puddephatt; J. Chem. Soc. Chem. Commun. 566 (1985).

32. R. B. King and K.S. RaghuVeer; Inorg. Chem. *23*, 2482 (1984).

33. K.S. RaghuVeer; Ph.D. Thesis U. Of Georgia (1982).

34. R.J Puddephatt; Chem. Soc. Rev. 99 (1983).

35. D.J. Darensbourg; C.-S. Chao; J.H. Reibenspies and C.J. Bischoff; Inorg. Chem. *29*, 2153 (1990).

36. M. Achternbosch; H. Braun; R. Fuchs; P. Klufers; A. Selle and V. Wilhelm;

Angew. Chem. Int. Ed. Engl. ***29***, 783 (1990).

37. S.W. Lee and W.C. Trogler; Inorg. Chem. ***29***, 1659 (1990).

38. I. Salter, Adv. Organomet. Chem. 249 (1989).

39. B.F.G. Johnson; D.A. Kaner; J. Lewis and P.R. Raithby; J. Chem. Soc. Chem. Commun. 753 (1981).

40. D.J. Darensbourg, D.J. Zalewski and T. Delord; Organomet. *3*, 1210 (1984).

41. G. Doyle; K.A. Eriksen and D. VanEngen; Organomet. *4*, 877 (1985).

42. D.J Elliot; G. Ferguson; D.G. Holah; A.N. Hughes; M.C. Jennings; V.R. Magnuson; D. Potter and R.J. Puddephatt; Organomet. *9*, 1336 (1990).

Chapter 5

Syntheses and Structural Characterization of Monomeric Nickel(II) Complexes Stabilized with the Ligand Bis(diphenylphosphino)methane.

5.1 Introduction

Nickel, palladium and platinum all form square planar complexes with $Ph_2PCH_2PPh_2$ (dppm) of stoichiometry $[MCl_2(dppm)]$, 5.1a, and $[M(dppm)_2]^{2+}$.[1-4] However, while the palladium and platinum complexes of formula $MCl_2(dppm)_2$ are formulated as ionic complexes with chelate dppm ligands $[M(dppm)_2]Cl_2$, 5.1b, the nickel complex has been formulated as the non-ionic complex with monodentate ligands cis-$[NiCl_2(dppm\text{-}P)_2]$, 5.1c.[5-7] The cationic $[Ni(dppm)_2]^{2+}$ and $[NiCl(dppm)_2]^{+}$, 5.1d, which is thought to have a square pyramidal stereochemistry at nickel, are only formed to a significant extent with non-coordinating anions such as perchlorate and tetraphenylborate.[5,6] Earlier, it had been thought that dppm would not chelate to nickel because of the ring strain in the resultant 4-membered ring.[5,6] The structures of the complexes 5.1a-d were proposed on the basis of analytical data, magnetic properties, and IR and UV-visible spectroscopy.

More recently, $[NiCl_2(dppm)_2]$ has been found very useful as a reagent for synthesis of homonuclear and heteronuclear dppm-bridged complexes containing nickel, and also as a catalyst precursor for the stereospecific cross-coupling of alkenyl halides and alkenyl Grignard reagents to give dienes or of alkyl halides with Grignard reagent in the presence of CO to give ketones, and also as a catalyst for the coupling of ethylene and butadiene to give 1,4,9- decatriene.[9-13]

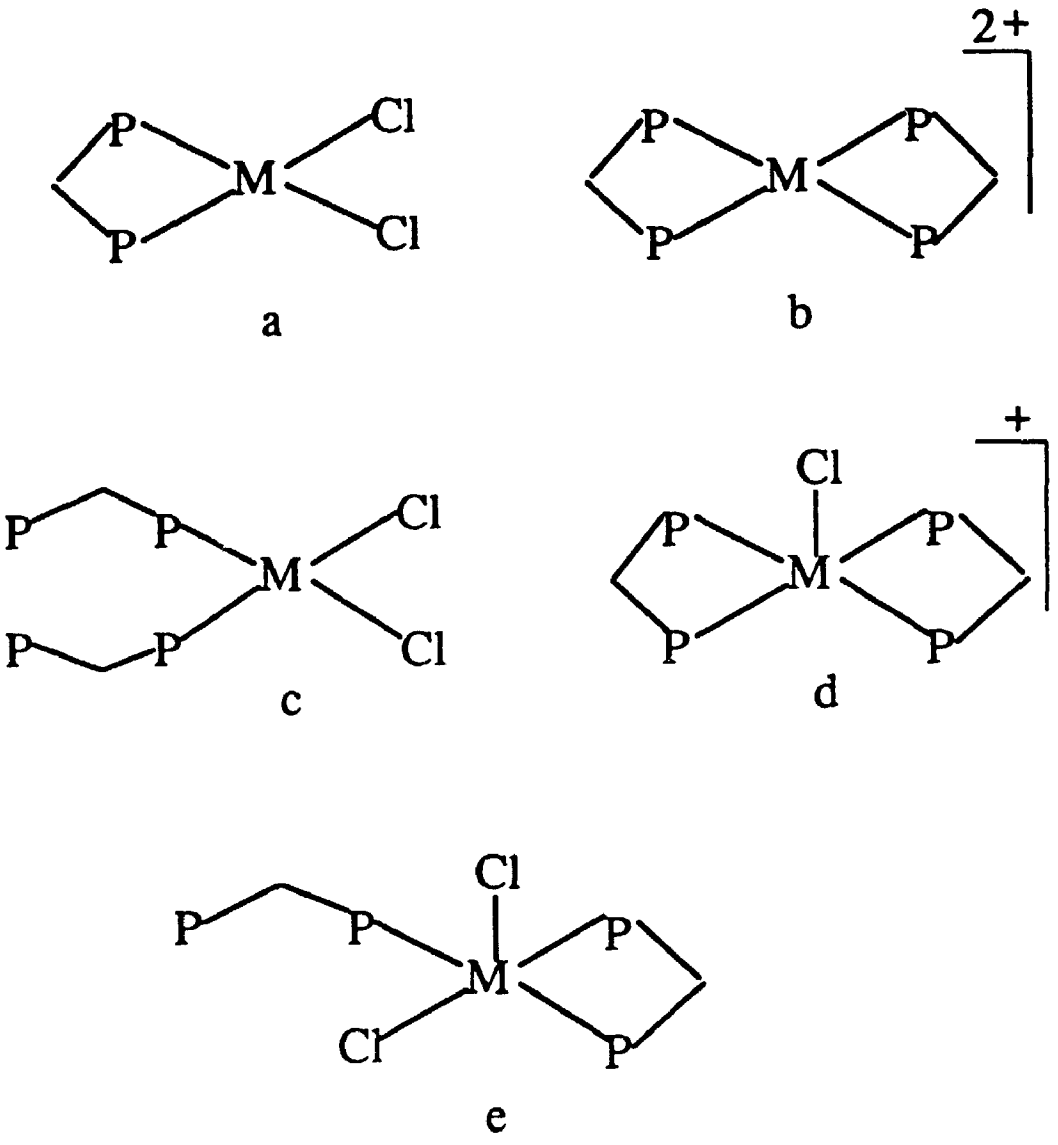

Figure 5.1: The geometries of dppm complexes of M(II), (M = Ni, Pd, Pt).

We have used $[NiCl_2(dppm)_2]$ as a precursor to dinickel complexes and noted that recrystallization led to partial dissociation of dppm with formation of a mixture of large crystals of $[NiCl_2(dppm)]$, which are red-brown in colour, and of $[NiCl_2(dppm)_2]$, which are black. Since both complexes had been formulated with square planar cis-$NiCl_2P_2$ chromophores, the great difference in appearance was surprising. The structure was, therefore, reinvestigated and the spectroscopic and crystallographic details of the structure are discussed in the following pages.

This chapter describes the first example of a crystallographically characterized nickel complex of a chelating dppm ligand. Nickel complexes with chelating dppm ligands were proposed earlier but the structure was never established with single crystal X-ray diffraction studies.

5.2 Crystal Structure of $[NiCl_2(dppm)_2]$

The solid state structure of $[NiCl_2(dppm)_2]$ was determined to be $[NiCl_2(\eta^1\text{-dppm})(\eta^2\text{-dppm})]$, 5.1e, by an X-ray crystallographic study of its solvate 5.1e.C_6H_5Me. This was carried out by Dr. Muir at the University of Glasgow. In the crystal structure, molecules of the nickel complex are separated from those of solvent by normal van der Waals distances.

The molecular structure of 5.1e is shown in Figure 5.2 and is characterized by bond lengths and angles in Table 5.1. It is apparent from the Table 5.1 that the Ni-Cl(2) bond distance at 2.527(2)Å is significantly longer than the Ni-Cl(1) bond at 2.228(2)Å, however, these distances are within the expected range for Ni-Cl bonds. Similarly it could also be noted that the bond length Ni-P(1) at 2.192(2)Å is

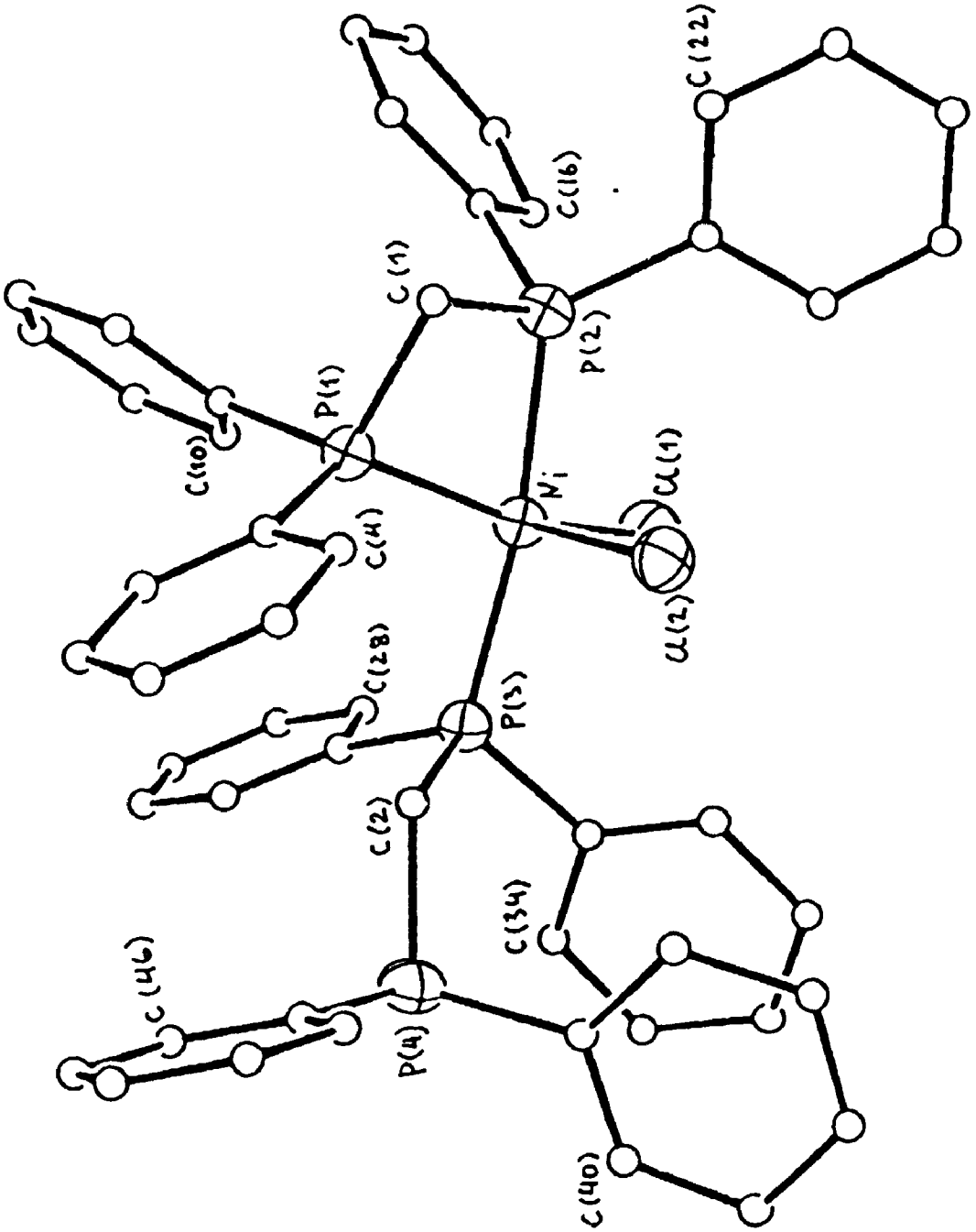

Figure 5.2: The molecular structure of $[NiCl_2(\eta^1\text{-dppm})(\eta^2\text{-dppm})]$, 5.1e.

Table 5.1: Selected Bond distances (Å) and Bond Angles (°) for [$NiCl_2(\eta^1$-dppm) (η^2-dppm)]

Ni - Cl(1)	2.228(2)	Ni - Cl(2)	2.527(2)
Ni - P(1)	2.192(2)	Ni - P(2)	2.210(2)
Ni - P(3)	2.218(2)	P(1) - C(1)	1.834(6)
P(1) - C(3)	1.803(6)	P(1) - C(9)	1.813(6)
P(2) - C(1)	1.834(6)	P(2) - C(15)	1.820(6)
P(3) - C(21)	1.818(6)	P(3) - C(2)	1.824(6)
P(3) - C(27)	1.815(6)	P(3) - C(33)	1.821(6)
P(4) - C(2)	1.854(6)	P(4) - C(39)	1.843(6)
P(4) - C(45)	1.831(6)		

Bond Angles (deg.)

Cl(1)-Ni-Cl(2)	107.2(1)	Cl(1)-Ni-P(2)	94.8(1)
Cl(2)-Ni-P(1)	93.5(1)	Cl(2)-Ni-P(3)	93.2(1)
P(1)-Ni-P(3)	97.9(1)	Ni-P(1)-C(1)	93.1(2)
Ni-P(1)-C(9)	114.2(2)	C(1)-P(1)-C(9)	106.3(3)
Ni-P(2)-C(1)	92.5(2)	Ni-P(2)-C(21)	122.4(2)
C(1)-P(2)-C(21)	110.2(3)	Ni-P(3)-C(2)	112.9(2)
Ni-P(3)-C(33)	117.2(2)	C(2)-P(3)-C(33)	102.2(3)
C(2)-P(4)-C(39)	104.4(3)	C(39)-P(4)-C(45)	102.4(3)
P(1)-Ni-P(2)	73.3(1)	P(1)-C(1)-P(2)	91.5(3)
P(3)-C(2)-P(4)	117.1(3)	P(1)-C(3)-C(8)	122.2(5)
P(1)-C(9)-C(14)	120.3(5)	P(2)-C(15)-C(20)	122.3(5)
P(2)-C(21)-C(26)	121.0(5)	P(3)-C(27)-C(32)	123.9(5)
P(3)-C(33)-C(38)	119.9(5)	P(4)-C(39)-C(44)	125.2(5)
P(4)-C45)-C(50)	125.7(5)		

significantly shorter than the distances Ni-P(2) and Ni-P(3) at 2.210(2) and 2.218(2)Å respectively. This may be attributed to the higher trans influence of the phosphine ligand compared to the chloride, thus causing lengthening in the distances Ni-Cl(2), Ni-P(2) and Ni-P(3). It is also apparent from Table 5.1 that the bond angle P(2)-Ni-P(3) at 171.1° deviates slightly from the ideal 180°, while significant deviation from the ideal geometry was observed for Cl(1)-Ni-P(1)at 156.1(1)°. The bond angles Cl(2)-Ni- P(1), Cl(2)-Ni-P(2) and Cl(2)-Ni-P(3) at 93.5(1), 88.9(1) and 93.2(1)° respectively are close to the ideal 90°. However, the bond angle Cl(2)-Ni-Cl(1) at 107.2(1)° deviates by approximately 17° from the ideal geometry of 90°. The coordination geometry around nickel is thus best described as intermediate between trigonal bipyramidal [with P(2) and P(3) atoms at the axial sites] and square pyramidal [with the Cl(2) atom at the axial site. In the low spin, square pyramidal nickel(II) complex $[NiCl(CH_2\{P(Ph)CH_2CH_2NH_2\}_2]^+$ an even longer Ni-Cl bond [2.699(7)Å] has been observed and its elongation has been ascribed to electronic effects.[14] A detailed inspection of the non-bonding intramolecular distances in 5.1e however, suggests that steric effects may also be a factor in lengthening the Ni-Cl(2) bond.

In the four-membered $NiP_2C(1)$ chelate ring the methylene carbon atom is displaced from the NiP_2 plane by 0.672(5) Å, to afford the C(1)...Ni separation of 2.934(6) Å. All internal ring angles (Table 5.1) are about 16° less than the ideal values for unconstrained P-Ni-P (90°), Ni-P-C and P-C-P (ca.109°) angles. Similar severe angular distortions have also been observed in other dppm chelates such as tetrahedral $[Ni(dchp)_2]$ dchp = bis(dicyclohexylphosphino)methane,[15] square planar

$[PdCl_2(dppm)]$,[1b] $[PtPh_2(dppm)]$[16] and $[Au(C_6F_5)_2(dppm)]^+$,[17] five-coordinate $[Fe(CO)_3(dppm)]$[18] and octahedral $[Mo(CO)_4(dppm)]$[19] and $[RhHCl(dppm)_2]^+$ complexes.[20]

The molecular structure of 5.1e reflects the stereochemical flexibility of the dppm ligands arising, in particular, from their ability to distort substantially the bond angles subtended at phosphorus and the methylene carbon atoms, and to adopt different conformations about the P-CH_2 bonds. This flexibility, demonstrated in the present structure by the very different bond angles and conformations associated with the η^1- and η^2-dppm ligands, makes dppm a highly versatile ligand, capable of coordinating the metal atoms in η^1-terminal, η^2-chelate and η^2-bridging modes and thus efficiently stabilizing mononuclear, binuclear and cluster complexes.[21]

5.3 Spectroscopic Characterization

The diffuse reflectance spectra of $[NiCl_2(dppm)]$ and $[NiCl_2(dppm)_2]$, as shown in Figure 5.3, gave a single band at 19,800 cm^{-1} and two band at 20,100 cm^{-1} and 13,500 cm^{-1} respectively. Clearly the extra ligand field band for $[NiCl_2(dppm)_2]$ at low energy (13,500 cm^{-1}) is responsible for its darker colour in the solid state. Both $[NiCl_2(dppm)]$ and $[NiCl_2(dppm)_2]$ gave orange-red solutions in dichloromethane and the UV-visible spectra as 1-2x10^{-4}M solutions were essentially identical, both containing a ligand field band at 21,200 cm^{-1}(ϵ = 2.3x10^3L mol^{-1} cm^{-1}), and two other bands at 29,600 cm^{-1} (shoulder) and 33,300 cm^{-1} . Addition of excess dppm to either solution caused a shift of the band to 21,100 cm^{-1}, but no new band appeared. This suggests that $[NiCl_2(dppm)_2]$ in dilute solution is essentially completely

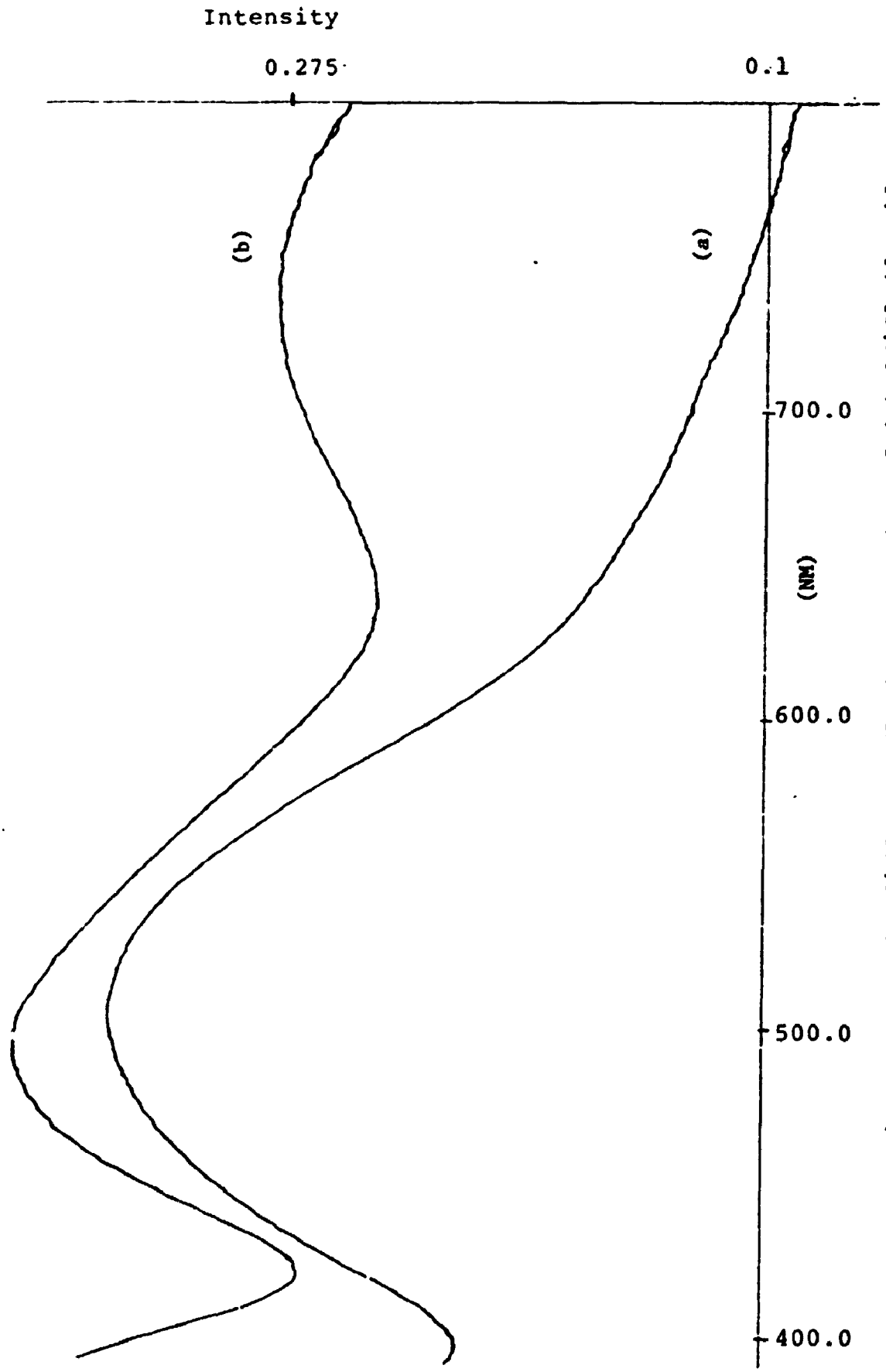

Figure 5.3: The diffuse reflectance spectra of (a) $[NiCl_2(dppm)]$; (b) $[NiCl_2(\eta^1\text{-dppm})(\eta^2\text{-dppm})]$.

dissociated to $[NiCl_2(dppm)]$ and free dppm and clearly shows that the solid state structure of $[NiCl_2(dppm)_2]$ is not retained in dilute solution.

The ^{31}P NMR spectrum of $[NiCl_2(dppm)]$ in CD_2Cl_2 solution at room temperature contained a broad singlet at δ = -51.0 ppm, (width at half height 30 Hz) and at -90°C this sharpened but the chemical shift was not significantly changed (δ = -50.4 ppm, width at half height 2 Hz). At room temperature $[NiCl_2(dppm)_2]$ failed to give a ^{31}P NMR resonance but, at -90°C, a sharp singlet at -39.7 ppm was observed. When both complexes were present, two sharp resonances at δ = -50.4 and -39.7 ppm were observed at -90°C showing that no exchange between the complexes was occurring at this temperature. The ^1H NMR spectrum of $[NiCl_2(dppm)]$ contained a broad resonance at δ = 3.62 ppm due to the CH_2 protons of dppm at both room temperature and at -90°C. The CH_2 protons of dppm in $[NiCl_2(dppm)_2]$ gave two broad resonances at δ = 4.20 and 4.45 ppm, with partially resolved coupling J(HH) = ca. 15 Hz, at -90°C but only an extremely broad peak at δ = ca. 4 ppm at room temperature. The phenyl ^1H resonances are also temperature dependent. At room temperature there are three resolved resonances at δ = 7.26 (para), 7.50 and 7.58 ppm (ortho and meta), but at -90°C there are at least four resonances between 6.78-7.40 ppm. The average chemical shift changes from 7.5 ppm at room temperature to 7.2 ppm at -90°C. The NMR data, for solutions of $[NiCl_2(dppm)_2]$ are not consistent with a static structure 5.1e, as determined in the solid state. Thus, in 5.1e all phosphorus atoms are non-equivalent but only one resonance, with a chemical shift consistent with chelating dppm, is observed in the ^{31}P NMR spectrum of $[NiCl_2(dppm)_2]$ at -90°C. It is, of course, possible that the molecule is fluxional even

at -90°C such that all phosphorus atoms become effectively equivalent, but we note that the ^1H NMR spectrum at -90°C contains two resonances for the CH_2P_2 protons. Any form of fluxionality which leads to equivalence of all phosphorus atoms is expected to lead to equivalence of the CH_2P_2 protons also. Rapid reversible dissociation of dppm to give $[NiCl_2(dppm)]$ at -90°C is also shown not to occur, since separate resonances are observed when mixtures of the two complexes are present. Dissociation of dppm from $[NiCl_2(dppm)_2]$ is negligible at low temperature at the concentrations used for NMR, since no signal due to $[NiCl_2(dppm)]$ is observed in solutions of $[NiCl_2(dppm)_2]$ under these conditions. The static structure 5.1d is consistent with the NMR data at -90°C, since in this structure all ^{31}P atoms are equivalent but the CH_2P_2 protons are not. The cause of the loss of the ^{31}P signal in the ^{31}P NMR and the extreme broadening of the CH_2P_2 signal in the ^1H NMR at room temperature is not clear.

5.4 Conclusions:

The work described in this chapter has given a definitive solution to the structure of $[NiCl_2(dppm)_2]$ in the solid state. The X-ray diffraction studies have shown that the structure is 5.1e, where nickel has the unexpected coordination number of five and contains both monodentate and bidentate dppm ligands. The earlier formulation as structure 5.1c,[5,6] which has not been questioned in later papers ,[1c] is therefore incorrect. This work thus shows that dppm can chelate to nickel by forming a four membered strained ring and is the first example of a structurally characterized nickel complex with a chelating dppm ligand. Although the complex is fully

characterized in the solid state, the structure in solution is still to be settled. In the concentrated solutions required for NMR, the structure is clearly neither 5.1c nor 5.1e, but is perhaps $5.1d^{+}Cl^{-}$. In dilute solution, as required for studies of the UV-visible spectra, it is likely that dissociation of dppm to give [$NiCl_2$(dppm)] occurs to a major extent. The chemistry is much more complex than was previously thought.

5.5 Experimental Section

The complex $[NiCl_2(dppm)_2]$ was prepared by the literature method,[5] by mixing solutions of $NiCl_2.6H_2O$ (2.0g; 8.42 mmol) in ethanol (30 mL) with dppm (6.40g; 16.65 mmol) in toluene (40 mL). The volume of solvent was reduced, CH_2Cl_2 (20 mL) was added to redissolve some precipitate and the mixture was layered with pentane (40 mL). A mixture of red-brown crystals of $[NiCl_2(dppm)]$ and black crystals of $NiCl_2(dppm)_2$.toluene were formed over a period of one week. Solvent was than decanted off and the crystalline product was washed with n-pentane (30 mL) and dried under reduced pressure. The compl[illegible]s were separated by hand picking large crystals and the pure compounds were used for characterization purposes. Both complexes were diamagnetic in the solid state (Gouy method) at room temperature.

5.5.1 $[NiCl_2(\eta^2\text{-dppm})]$, 5.1a

Anal. Calcd. for $C_{25}H_{22}Cl_2NiP_2$: C, 59.4; H, 4.0. Found: C, 58.35; H, 4.3%; mp 284-285°C; UV-Vis (CH_2Cl_2): a band at 21,200 cm^{-1} ($\epsilon = 2.3x10^3$ L mol^{-1} cm^{-1}), and two other bands at 29,600 cm^{-1} (shoulder) and 33,300 cm^{-1}; UV-VIS (solid state, diffuse reflectance) a band at 19,800 cm^{-1}. NMR at 25°C in CD_2Cl_2: ^1H, δ 3.62 [br, 2H]; 7.50 [br, 12H]; 7.98 [s, 8H]; at -90°C the spectrum obtained was essentially the same except that the resonances for the phenyl protons were broader with an additional shoulder peak at δ 7.26. ^{31}P (25°C) δ = -51.0 ppm (width at half height = 30 Hz.); at -90°C δ = -50.4 ppm (width at half height = 2 Hz.);

5.5.2 [$NiCl_2(\eta^1$-dppm)(η^2-dppm)], 5.1e

Anal.Calc. for $C_{50}H_{44}Cl_2NiP_4$.toluene: C, 69.05; H, 5.25. Found: C, 68.1; H, 5.25%; mp 170-173°C UV-VIS in CH_2Cl_2 is identical to the solution UV-VIS of $NiCl_2(\eta^2$-dppm).; UV-VIS (solid state, diffuse reflectance): two bands at 20,100 cm^{-1} and 13,500 cm^{-1}. NMR at 25°C in CD_2Cl_2, ^1H δ = 4 [br, 4H]; 7.26[s, 8H]; 7.50[s, 16H]; 7.58[s, 16H]; at -90°C δ = 4.20[br, 2H]; 4.45[br, 2H]; J(HH) = ca. 15 Hz.; 6.78-7.40[br, 40H]; ^{31}P at -90°C = -39.7 ppm

5.6 References:

1.(a) J. Chatt; F.A. Hart; H.R. Watson; J. Chem. Soc. 2537 (1962).

(b) W.L. Steffen; G.J. Palenik; Inorg. Chem. *15*, 2432 (1976).

(c) For an excellent review of related complexes of nickel(II), see L. Sacconi; F. Mani; A. Bencini "Comprehensive Coordination Chemistry," G. Wilkinson; R.D. Gillard; J.A. McCleverty eds., Pergamon, Oxford, vol.*5*, chp. 50, (1987).

2. M.P. Brown; R.J. Puddephatt; M. Rashidi; K.R. Seddon; J. Chem. Soc. Dalton Trans. 951 (1977).

3. C. Ercolani; J.V. Quagliano; L.M. Vallarino; Inorg. Chem. Acta. *7*, 413 (1973).

4. W.W. Fogleman; H.B. Jonassen; J.Inorg. Nucl. Chem. *31*, 1536 (1969).

5. G.R. van Hecke; W.D. Horrocks Jr.; Inorg. Chem. *5*, 1968 (1966).

6. G. Booth; J. Chatt; J. Chem. Soc. 3238 (1965).

7. P.M. Boorman; A.J. Carty; Inorg. Nucl. Chem. Lett. *4*, 101 (1968).

8. K.K. Chow; C.A. McAuliffe; Inorg. Chim. Acta. *10*, 197 (1974).

9. Z. Zhang; H. Wang; H. Wang; R. Wang; W. Zhao; L Yang; J. Organomet. Chem. *347*, 269 (1988).

10. X.L.R. Fontaine; S.J. Higgins; C.R. Langrick; B.L. Shaw; J. Chem. Soc., Dalton Trans. 777 (1987).

11. T. Yamamoto; Y. Ehara; A. Yamamoto; Nippon Kagaku Kaishi 310 (1982).

12. Y. Inoue; T. Kagawa; Y. Ichuda; H. Hashimoto; Bull. Chem. Soc. Jpn. *45*, 1996 (1972).

13. V. Fiandanese; G. Marchese; G. Mascolo; F. Naso; L. Ronzine; Tet. Lett. *29*, 3705 (1988).

14. L.G. Scanlon; Y.-Y. Tsao; K. Toman; S.C. Cummings; D.W. Meek; Inorg. Chem. ***21***, 2707 (1982).

15. C. Kruger; Yi-H. Tsay; Acta. Cryst. ***B28***, 1941 (1972).

16. P.S. Braterman; R.J. Cross; Lj. Manojlovic-Muir; K.W. Muir; G.B. Young; J. Organomet. Chem. ***85***, C40 (1975).

17. R. Uson; A. Laguna; M. Laguna; E. Fernandez; M.D. Villacampa; P.G. Jones; G. Sheldrick; J. Chem. Soc. Dalton Trans. 1679 (1983).

18. F.A. Cotton; K.I. Hardcastle; G.A. Rusholme; J. Coord. Chem. ***2***, 217 (1973).

19. K.K. Cheung; T.F. Lai; K.S. Mok; J. Chem. Soc. (A) 1644 (1971).

20. M. Cowie; S.K. Dwight; Inorg. Chem. ***18***, 1209 (1979).

21.(a) R.J. Puddephatt; Chem. Soc. Rev. 99 (1983).

(b) R.J. Puddephatt; Lj. Manjlovic-Muir; K.W. Muir; Polyhedron ***9***, 2767 (1990).

Chapter 6

Synthesis, Characterization and Reactivity Studies of Di and Trinuclear Nickel Complexes Bridged by Bis(diphenylphosphino)methane.

6.1. Introduction

Many catalytic transformations using mononuclear transition metal complexes have been established now. There is, however, growing interest in binuclear transition metal complexes due to the anticipation that they will allow for increased versatility in catalyst design.[1] There has also been a considerable amount of research effort directed towards the synthesis and characterization of transition metal cluster compounds. It is believed that they may also play a role as homogeneous catalysts or as precursors for catalytically active species.[2-5] Diphosphine ligands of the type dppm and dmpm are often used to stabilize these binuclear and polynuclear metal complexes. These ligands are very versatile and not only stabilize metals in negative and zero oxidation states but also in low positive oxidation states. In addition they yield products with unusual structural properties.[6-8]

Over the last several years a considerable amount of work has been done on the binuclear and cluster chemistry of the group 10 metals palladium and platinum. In contrast, nickel has received relatively little attention. There are only a few reports on binuclear nickel complexes stabilized with diphosphine ligands and their structural properties are even less studied. Thus, it has been shown for group 10 metals that certain d^9-d^9 dimers may exist in two structural forms depicted in Figure 6.1 as 6.1, 6.3 and 6.2, 6.4 respectively, in which LL is the binucleating ligand dppm

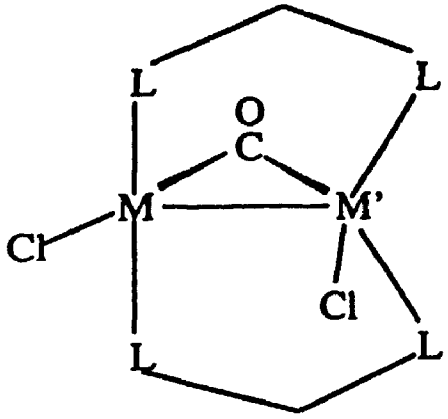

6.1a, M = M' = Ni
6.1b, M = Pt, M' = Ni

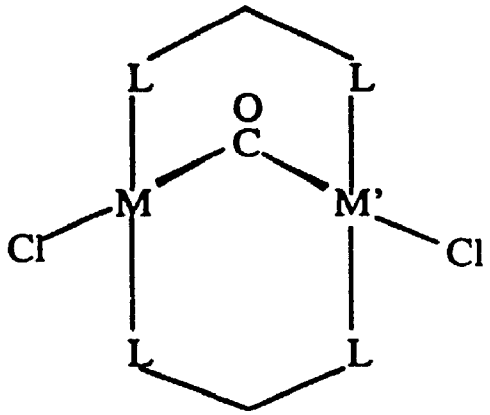

6.2a, M = M' = Pd
6.2b, M = M' = Pt
6.2c, M = Pd, M' = Pt

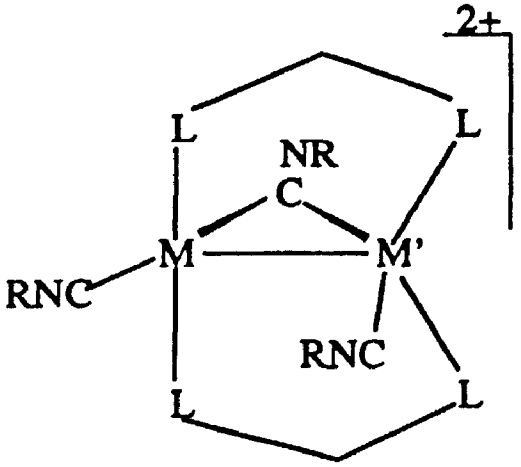

6.3a, M = M' = Ni
6.3b, M = Pd, M' = Ni
6.3c, M = Pt, M' = Ni

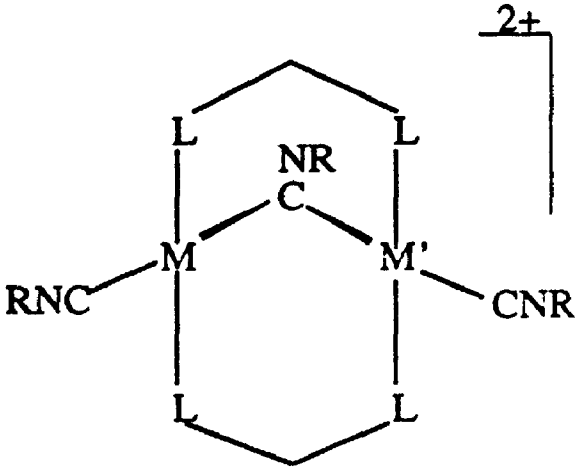

6.4a, M = M' = Pd
6.4b, M = M' = Pt
6.4c, M = Pd, M' = Pt

Figure 6.1: Structures of certain d^9-d^9 dimers of nickel group metals.

($Ph_2PCH_2PPh_2$) or dpam ($Ph_2AsCH_2AsPh_2$). In the complexes 6.2, 6.4 and several related "A-frame" complexes, there is no metal-metal bonding and each metal atom has square planer stereochemistry.[9] However, in 6.1, 6.3 and related complexes the metal centres are not equivalent, and the metal-metal distance is in the range expected if there is a metal-metal bond.[10] These have been formulated as mixed oxidation state complexes with a coordinate metal-metal bond, formed by donation of an electron pair from a tetrahedral M(0) centre to a T-shaped M(II)centre.[10] In the nickel group, structure 6.1 or 6.3 has only been observed if one of the metal centres is nickel and, in heteronuclear complexes, the nickel is present as the tetrahedral Ni(0) donor M' in 6.1 or 6.3. The A-frame structure analogous to 6.2 or 6.4 has been found for nickel in $[Ni_2Cl_2(\mu\text{-SO})(\mu\text{-dppm})_2]$,[11] and it is not obvious why the different structures are adopted. Another aspect of the chemistry of this type of dinuclear complex is the reactivity towards the addition of another metal atom across metal-metal bond, thus forming trinuclear metal complexes.[12,13] In recent years there has been considerable research impetus towards the synthesis, structural characterization and reactivity studies of trinuclear metal clusters, since they provide an opportunity to study the insight of reactions occurring on the metal surfaces in heterogeneous catalysis. A large number of such cluster complexes has already been made and their properties have been investigated.[2,3,5] From group 10, the metals Pd and Pt have been extensively studied and several coordinatively unsaturated trinuclear metal clusters of palladium and platinum have been characterized.[14-17] The reactivity of several of these clusters has also been explored. Thus for example, the coordinatively unsaturated cluster cations $[M_3(\mu\text{-CO})(\mu\text{-dppm})_3]^{2+}$, M=Pd, Pt, have been shown to

add small ligands in a way which often mimics chemisorption on a metal surface.[18] The scheme 6.1 shows one such example where the addition of halide ions X^- gives the corresponding clusters $[M_3(\mu_3\text{-}X)(\mu_3\text{-}CO)(\mu\text{-}dppm)_3]^+$.[18,19]

The analogous nickel complexes have not been reported, although there is a similar cluster $[Ni_3(\mu_3\text{-}I)(\mu_3\text{-}CNMe)(\mu\text{-}dppm)_3]^+$, and there appears to be no complete triad of nickel group clusters of any kind.[20] It was therefore of interest to synthesize trinuclear nickel clusters stabilized by diphosphine ligands and thus compare their properties with those of the known palladium and platinum complexes.

This chapter gives details of the synthesis and structural characterization of di- and trinuclear nickel complexes bridged by the diphosphine ligand dppm. To understand the unusual structure of the dinuclear nickel complex $[Ni_2Cl_2(\mu\text{-}CO)(\mu\text{-}dppm)_2]$, Extended Huckel Molecular Orbital (EHMO) calculations were carried out by W. Davis. A summary of these calculations is also given in this chapter.

6.2. Synthesis of $[Ni_2Cl_2(\mu\text{-}CO)(\mu\text{-}dppm)_2]$ 6.1.

The complex $[Ni_2Cl_2(\mu\text{-}CO)(\mu\text{-}dppm)_2]$, 6.1, was prepared by reaction of the nickel(0) and nickel(II) complexes $[Ni_2(CO)_2(\mu\text{-}CO)(\mu\text{-}dppm)_2]$[21] and $[NiCl_2(dppm)_2]$[22] according to equation (6.1).

$$[Ni_2(CO)_2(\mu\text{-}CO)(\mu\text{-}dppm)_2] + 2[NiCl_2(dppm)_2] \rightarrow 2[Ni_2Cl_2(\mu\text{-}CO)(\mu\text{-}dppm)_2] + CO + 2dppm \quad (6.1)$$

Complex 6.1 was also obtained by reaction of $[Ni(CO)_2(dppm\text{-}P)_2]$ with nickel(II)

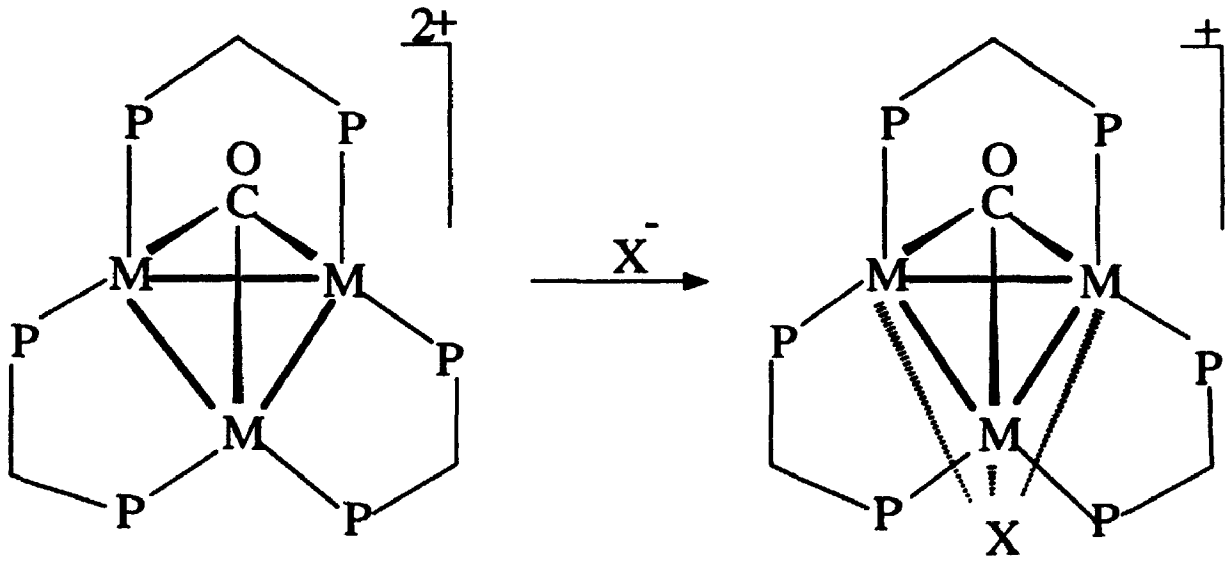

Scheme 6.1: Addition of a halide ion to a trinuclear cluster cation.

chloride. Both synthetic methods are variations of comproportionation of Ni(0) with Ni(II) to give $Ni(I)_2$. The complex 6.1 was obtained as deep green-black crystals. Solutions or powdered samples of 6.1 are green while large crystals appear black. In solution the complex was very sensitive to oxygen, but the solid complex was oxidized only slowly by air.

6.2.1. The Structure of $[Ni_2Cl_2(\mu\text{-CO})(\mu\text{-dppm})_2]$ 6.1

The structure of the product was determined by an X-ray crystal structure analysis of its solvate $[Ni_2Cl_2(\mu\text{-CO})(\mu\text{-dppm})_2].CH_2Cl_2$ which was carried out by Dr. Lj. Manojlovic-Muir at the University of Glasgow. The molecular structure of 6.1 is shown in Figure 6.2 and is characterized by bond lengths and angles listed in Table 6.1. It comprises two NiCl fragments held together by an unsymmetrically bridging carbonyl [Ni(2)-C(3) 1.790(4), Ni(1)-C(3) 1.926(4) Å, Ni(1)-C(3)-Ni(2) 89.5(2)°] and by two bridging dppm ligands providing a trans, cis-configuration around the metal centres. The NiCl fragments also appear to be linked directly by a Ni-Ni bond [2.617(1)Å] comparable in length with the metal-metal single bonds observed in other dppm bridged dinickel complexes [Ni-Ni 2.439(1)-2.694(1)Å].[10,21,23] It is apparent from Table 6.1 that the bond angle Ni(1)-Ni(2)-C(3) at 47.4° is approximately 4° larger than the angle Ni(2)-Ni(1)-C(3) at 43.1°, confirming that CO is more strongly bonded to Ni(2). This is further supported by the fact that the bond distance of Ni(2)-C(3) at 1.790(4)Å is significantly shorter than the distance of Ni(1)-C(3) at 1.926(4)Å, although both distances are within the expected range for Ni-C single bonds. Table 6.1 also shows that the CO bond is bent towards the Ni(1) center

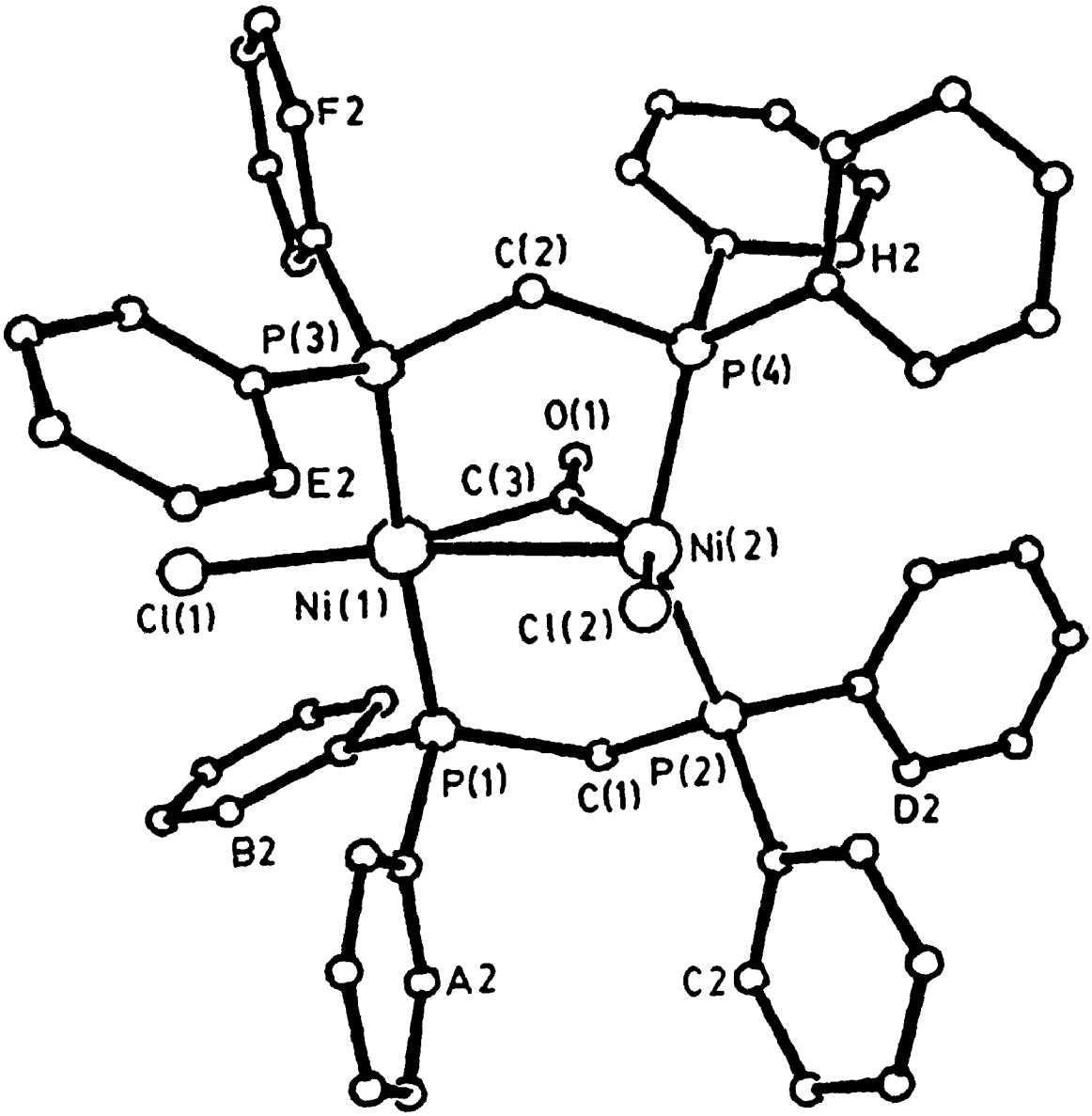

Figure 6.2: The ORTEP diagram of $[Ni_2Cl_2(\mu\text{-}CO)(\mu\text{-}dppm)_2]$, 6.1.

Table 6.1: Selected Bond Lengths (Å) and Angles (deg) for $[Ni_2Cl_2(\mu\text{-}CO)(\mu\text{-}dppm)_2]$

Ni(1) - Ni(2)	2.617(1)	Ni(1) - C1(1)	2.225(2)
Ni(1) - P(1)	2.231(1)	Ni(1) - P(3)	2.242(1)
Ni(1) - C(3)	1.926(4)	Ni(2) - C1(2)	2.262(2)
Ni(2) - P(2)	2.221(1)	Ni(2) - P(4)	2.214(1)
Ni(2) - C(3)	1.790(4)	P(1) - C(1)	1.848(4)
P(1) - C(A1)	1.826(4)	P(1) - C(b1)	1.825(4)
P(2) - C(1)	1.844(4)	P(2) - C(c1)	1.822(4)
P(2) - C(D1)	1.824(4)	P(3) - C(2)	1.861(4)
P(3) - C(E1)	1.833(4)	P(3) - C(F1)	1.826(4)
P(4) - C(2)	1.844(4)	P(4) - C(G1)	1.827(4)
P(4) - C(H1)	1.820(4)	O(1) - C(3)	1.177(5)

Bond Angles (°)

Ni(2) - Ni(1) - C1(1)	162.0(1)	Ni(2) - Ni(1) - P(1)	88.3(1)
Ni(2) - Ni(1) - P(3)	86.0(1)	Ni(2) - Ni(1) - C(3)	43.1(2)
C1(1) - Ni(1) - P(1)	92.2(1)	C1(1) - Ni(1) - P(3)	91.3(1)
C1(1) - Ni(1) - C(3)	156.8(2)	P(1) - Ni(1) - P(3)	171.6(1)
P(1) - Ni(1) - C(3)	87.5(2)	P(3) - Ni(1) - C(3)	92.5(2)
Ni(1) - Ni(2) - C1(2)	103.7(1)	Ni(1) - Ni(2) - P(2)	102.2(1)
Ni(1) - Ni(2) - P(4)	103.6(1)	Ni(1) - Ni(2) - C(3)	47.4(2)
C(1) - Ni(2) - P(2)	105.3(1)	C1(2) - Ni(2) - P(4)	92.6(1)
C1(2) - Ni(2) - C(3)	150.0(2)	P(2) - Ni(2) - P(4)	144.0(1)
P(2) - Ni(2) - C(3)	91.0(2)	P(4) - Ni(2) - C(3)	88.2(2)
Ni(1) - P(1) - C(1)	115.4(2)	Ni(1) - P(1) - C(A1)	115.4(2)
Ni(1) - P(1) - C(B1)	113.8(2)	C(1) - P(1) - C(A1)	102.9(2)
C(1) - P(1) - C(B1)	102.7(2)	C(A1) - P(1) - C(B1)	105.1(2)
Ni(2) - P(2) - C(1)	107.4(2)	Ni(2) - P(2) - C(C1)	122.7(2)
Ni(2) - P(2) - C(D1)	115.1(2)	C(1) - P(2) - C(C1)	106.7(2)

C(1) - P(2) - C(D1) 102.0(2)
Ni(1) - P(3) - C(2) 119.8(2)
Ni(1) - P(3) - C(F1) 113.6(2)
C(2) - P(3) - C(F1) 102.5(2)
Ni(2) - P(4) - C(2) 101.4(2)
Ni(2) - P(4) - C(H1) 118.9(2)
C(2) - P(4) - C(H1) 108.0(2)
P(1) - C(1) - P(2) 110.6(2)
Ni(1) - C(3) - Ni(2) 89.5(2)
Ni(2) - C(3) - O(1) 148.2(3)
C(C1) - P(2) - C(D1) 100.8(2)
Ni(1) - P(3) - C(E1) 110.9(2)
C(2) - P(3) - C(E1) 102.2(2)
C(E1) - P(3) - C(F1) 106.4(2)
Ni(2) - P(4) - C(O1) 124.5(2)
C(2) - P(4) - C(O1) 102.6(2)
C(O1) - P(4) - C(H1) 99.6(2)
P(3) - C(2) - P(4) 144.2(2)
Ni(1) - C(3) - O(1) 122.4(3)

as indicated by the bond angles Ni(1)-C(3)-O = 122.4° and Ni(2)-C(3)-O = 148.2°. The two 5-membered Ni_2P_2C rings adopt distorted envelope conformations as shown in Figure 6.3. The metal atoms display significantly different coordination geometries. Around the Ni(1) atom the geometry is approximately square planar with bond angles from 87.5-92.5° with maximum deviation of 2.5° from the ideal 90° and with one coordination site being spanned by the Ni(2)-C(3) bond. In contrast, the geometry around the Ni(2) atom can be described as highly distorted trigonal bipyramidal, with the Ni(1),P(2) and P(4) atoms at equatorial and the Cl(2) and C(3) atoms at axial sites. The complex 6.1 is therefore isostructural with 6.1b and 6.3a[10a], in which the bridging CO [Pt-C 2.03(1), Ni-C = 1.77(2)Å, Ni-C-O = 145(1)°] in 6.1 or bridging MeNC [Ni-μC 2.19(1) and 1.824(9)Å] in 6.3a respectively is considered semi-bridging.[10a,10c] The structure is also similar to those of the complexes $[RhM(CO)_2(\mu\text{-dppm})_2]$, M = Rh, Ir or Co,[24] into which it would transform by a Berry pseudorotation interchanging the position of the equatorial Ni-Ni and axial Ni-μC bonds around Ni(2).

Complex 6.1 can be considered to be formed from $[Ni_2(CO)_2(\mu\text{-CO})(\mu\text{-dppm})_2]$, 6.6, by a 2-electron oxidation with substitution of the terminal carbonyl groups in 6.6 by chloride ligands but with retention of the μ-CO group. Opening of the P-Ni-P angles from 106° in 6.6 to 172 and 142° in 6.1[21] leads to conversion of the cis,cis W-frame[25] or cradle type structure[10,21,23] of 6.6 into the trans,cis-structure of 6.1. The major difference between the structures of 6.1 and its palladium and platinum congeners,[9] which have symmetrical A-frame structures, is thus the cis and trans- geometry of the nickel atoms in the former.

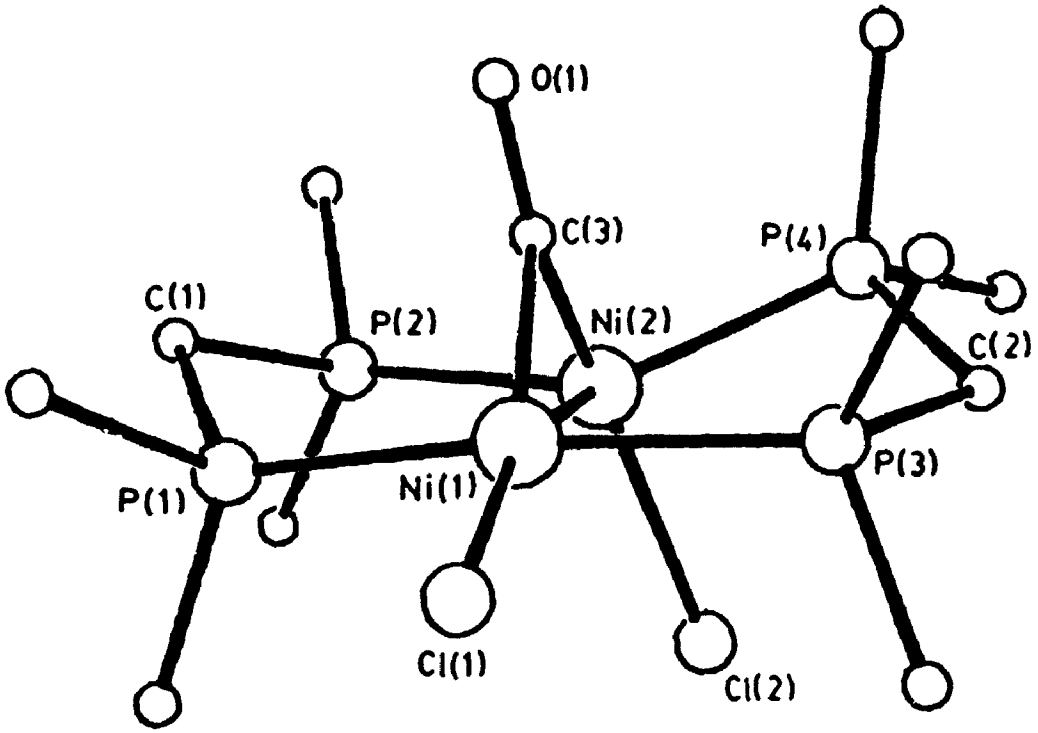

Figure 6.3: Molecular structure of 6.1 viewed approximately along the Ni-Ni bond. Phenyl carbon atoms are omitted except those bonded to phosphorus.

6.2.2. Spectroscopic Properties of $[Ni_2Cl_2(\mu\text{-}CO)(\mu\text{-}dppm)_2]$

The carbonyl stretching frequency in the IR spectrum of 6.1 was at 1763 cm^{-1} in the solid state and at 1765 cm^{-1} in CH_2Cl_2 solution. The close similarity indicates that the solid state structure with a semi-bridging carbonyl ligand is retained in solution. For comparison the ν(CO) values for 6.2a and 6.2b are 1705 and 1638 cm^{-1} respectively.[9] In the nickel group backbonding is usually weakest for palladium so the higher value of ν(CO) for the nickel complex can be attributed to the different structures, with the ketonic carbonyl in 6.2 giving lower ν(CO) values than the semi-bridging carbonyl in 6.1 [ν(CO)=1763 cm^{-1}] or 6.1b [ν(CO) 1756 cm^{-1}]. The FAB mass spectrum of 6.1 gave an envelope at m/e=925 corresponding to $(M+H)^+$, (figures given for ^{35}Cl,^{58}Ni isotopes), and the most intense envelope was at m/e=889 corresponding to $(M\text{-}Cl)^+$. There was no peak corresponding to loss of CO from 6.1, indicating that the carbonyl group is strongly bound. This is consistent with our observation that CO is not easily lost from 6.1 by thermolysis, whereas similar heating of 6.2a or 6.2b easily gives CO and $[M_2Cl_2(\mu\text{-}dppm)_2]$.[9]

The ^{31}P NMR spectrum of 6.1 gives a singlet at δ=17.1 at 20°C and this shifts only slightly to δ=17.8 ppm at -90°C in CH_2Cl_2 solution. Since the ground state structure as shown in Figure 6.1 has two very different phosphorus environments, it is clear that the complex must be fluxional even at low temperature. Some further information is obtained from the ^1H NMR spectra. At 20°C the CH_2P_2 protons of the dppm ligands gave an "AB" pattern [$\delta(H^a)$ 2.96, $\delta(H^b)$ 3.33, $^2J(H^aH^b)$ = 14Hz], with further unresolved splitting due to $^{31}P^1H$ coupling, and the spectrum was essentially the same at -90°C. These data show that the fluxionality creates an

effective plane of symmetry perpendicular to the Ni-Ni axis, thus making the two nickel atoms and four phosphorus atoms equivalent but does not create a plane of symmetry containing the $Ni_2P_4C_2$ skeleton. Hence the NMR properties are those expected for an A-frame structure 6.2,[9] and the fluxional process is defined as the carbonyl migrating between the nickel atoms, with accompanying changes in stereochemistry at each nickel as shown in scheme 6.2, perhaps by way of the A-frame structure 6.2. The NMR data indicate that 6.1 is diamagnetic and this has been confirmed for solutions in CH_2Cl_2 at 20°C and at -90°C by Evans method.[26]

6.2.3. Theoretical Studies on $[Ni_2Cl_2(\mu\text{-}CO)(\mu\text{-}dppm)_2]$

There have been several studies of bonding in dppm-bridged dimers, including $[M_2X_2(\mu\text{-}dppm)_2]$ and their derivatives of the A-frame type.[25,27,28] In the present work, the dppm ligands have been substituted by carbonyl ligands. This is, of course, a gross approximation which is justified by the need to modify the distances and angles between donor atoms in order to model both structures 6.1 and 6.2, which would lead to complications if a model bidentate ligand such as $H_2PCH_2PH_2$ or multi-atom ligand such as PH_3 were used to model the dppm donors. The results will only be used in a qualitative way. The formation of complexes 6.1 or 6.2 can be modelled in a number of ways. When M=Pt or Pd, complexes 6.2 may be formed by addition of CO to the d^9-d^9 dimers $[M_2X_2(\mu\text{-}dppm)_2]$, X=Cl, 6.7 and this approach is summarized in Figure 6.4. Approach of the carbonyl ligand in the centre of the M-M bond of 6.7 (with X groups bent back but maintaining the M-M distance as expected for a single bond)[27] leads to strong interaction between the filled σ-donor orbital of

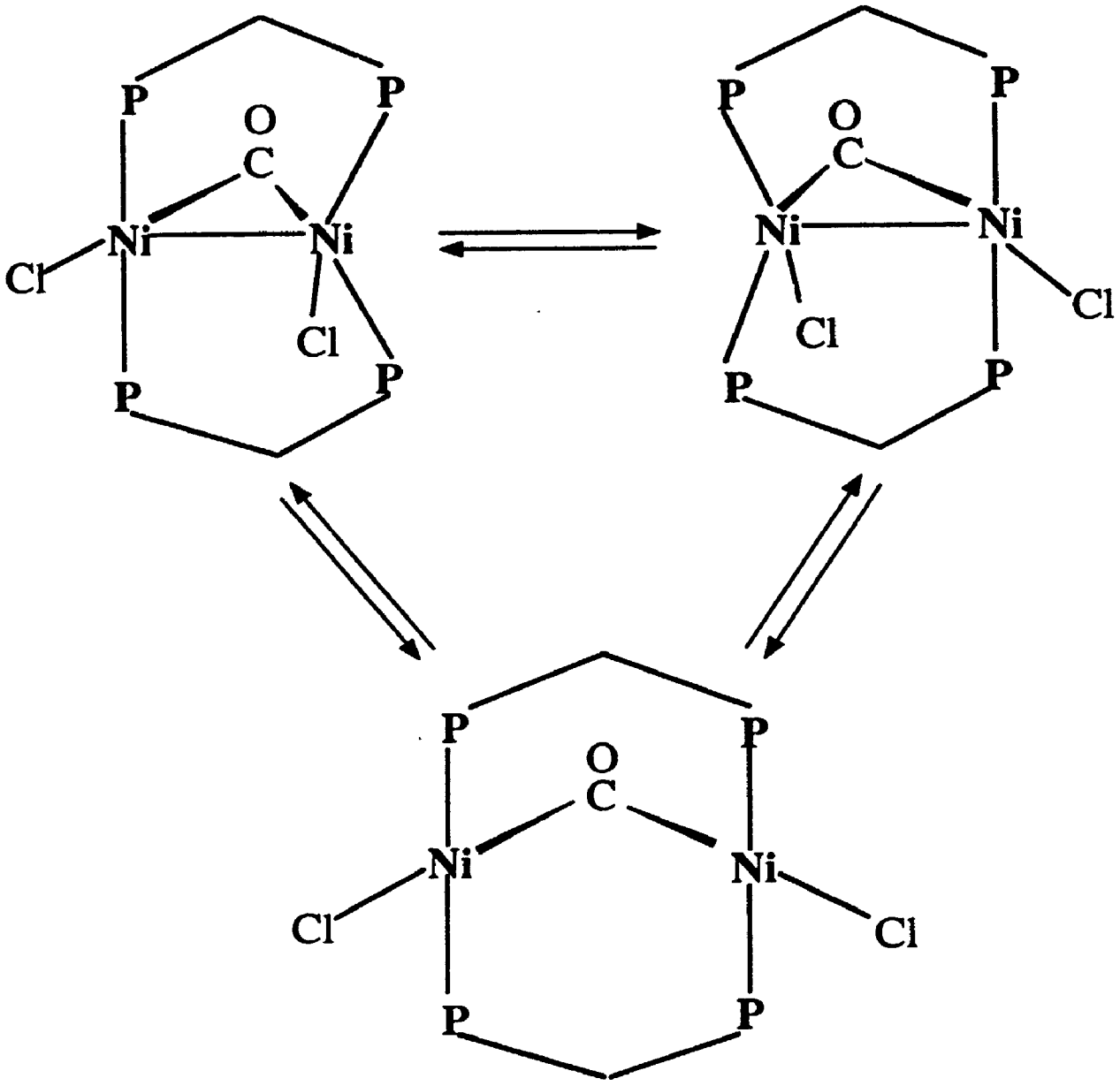

Scheme 6.2: The mechanism of fluxional process of $[Ni_2(\mu\text{-}CO)Cl_2(\mu\text{-}dppm)_2]$ 6.1

CO and M-M σ-bonding orbital of 6.7 to give a strongly bonding and strongly antibonding combination as described previously.[27] In addition the M-M antibonding orbital interacts with π^*(CO) and is sufficiently stabilized that it becomes the HOMO, shown as b_2 in column B of Figure 6.4.[27] There are eight roughly non-bonding 5d-orbitals in a block below b_2 and a series of vacant $2p\pi^*$(CO) orbitals above, of which the lowest is a_1 in Figure 6.4. The HOMO is at high energy and the HOMO-LUMO gap b_2-a_1 is low so the molecule is not expected to be stable in this geometry. The obvious stabilizing distortion of B as shown in Figure 6.4 is to move the metal atoms apart to give A as depicted in Figure 6.4; the antibonding interactions between the metal atoms in b_2 is then minimized as mutual overlap of the metal orbitals decreases. Of course, A is the observed structure for the complexes when M,M'=Pt or Pd and the HOMO really is greatly stabilized by the B to A distortion as shown in Figure 6.4. The distortion of B to give the observed structure 6.1 (M,M'=Ni) is less obvious. The carbonyl carbon slips towards M' to give the semi-bridging CO and the halide ligand X moves below M', as shown in C in Figure 6.4. The HOMO is stabilized, partly because the MM' interaction is less antibonding, as the lower symmetry at M' allows more mixing of d-orbitals. Bending the ligands L back from the Y-axis to change the stereochemistry of M' from pseudo-square pyramidal to pseudo-trigonal bipyramidal as shown in D of Figure 6.4 causes further stabilizing of the orbital derived from b_2 while the d_{xy} orbital on M' is destabilized and becomes the HOMO. The HOMO energy and HOMO-LUMO gap are now similar for D and A. Of course, D approximates the observed structure 6.1 (M=Ni).

The above calculations indicate that A=6.2 and D=6.1 are both viable

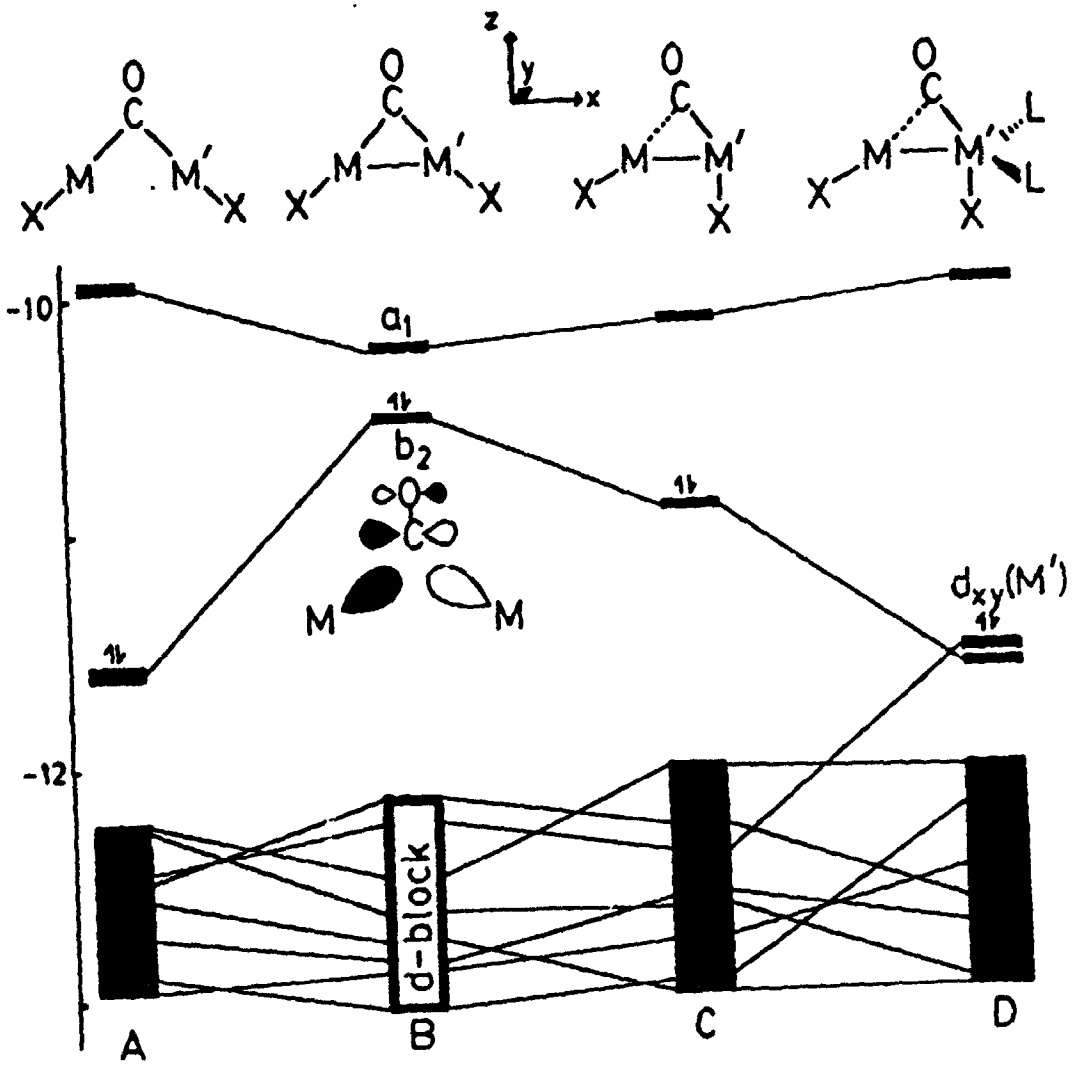

Figure 6.4: Key orbital energy changes as complex B undergoes distortion toward the stable structures A and D. The major factor influencing overall stability is the energy of the HOMO (b_2 in B).

structures, but can they explain why A is preferred for Pt and Pd but D is better for Ni? The calculations were carried out for both Pt and Ni complexes and some results are shown in Table 6.2. In both cases, A is calculated to be slightly more stable than D. The only indication that D might be preferable for M=Ni is that the HOMO is at marginally lower energy and the HOMO-LUMO gap is slightly higher for D when M=Ni but for A when M=Pt as shown in Table 6.2. Given that the LUMO is π^*(L), where L is a CO substituting for dppm phosphorus donor, it is clear that this is of limited significance and no further speculation is warranted. In both forms, A and D, the HOMO-LUMO gap as listed in Table 6.2 is sufficient that the compounds are expected to be diamagnetic for both Pt and Ni, in agreement with our experimental data.[29]

Formation of 6.1=D as shown in Figure 6.4 can also be considered to occur by addition of CO to only one metal centre of $[M_2X_2(\mu\text{-dppm})_2]$, whereupon that centre would attain an 18-electron configuration and its stereochemistry would change from square planar (dsp^2) to trigonal bipyramidal (dsp^3), as shown in structure F of Figure 6.5. Complex F could also be formed by donation of electron density from an 18-electron M(0) fragment $[M'(CO)XL_2]^-$ (with geometry distorted from tetrahedral as in G, Figure 6.5, so as to give a filled metal-based orbital directed along the x-axis) to a T-shaped 14-electron fragment $[M(CO)L_2]^+$, E depicted in Figure 6.5, which has a vacant acceptor orbital directed along the x-axis. It will be instructive to carry out calculations using the latter model since this may give insight into the proposed donor-acceptor metal-metal bonding in 6.1 and related compounds.[9] A correlation diagram is shown in Figure 6.5. It can be seen that a strong interaction is

Table: 6.2 Selected Parameters (E, energy, eV; Q, charge, e) from the EHMO Calculations.

Complex	E(total)	E(H)[a]	E(H-L)[b]	M-M'overlap	Q(M)
Q(M')(M,M')					
(M,M')					
5 (Pt)	-1309.8	-11.85 1082	0.28	0.24	0.24
B (Pt)	-1510.2	-10.56 0.31	0.00	0.52	0.52
A (Pt)	-1511.6	-11.62 1.67	-0.05	0.42	0.42
C (Pt)	-1510.4	-11.22 0.80	0.04	0.33	0.29
D (Pt)	-1510.6	-11.59 1.56	0.12	0.44	0.70
F (Pt)	-1509.2	-11.10 1.23	0.27	0.10	0.75
5 (Ni)	-1326.4	-12.09 2.04	0.10	0.10	0.10
B (Ni)	-1525.4	-10.63 0.44	-0.14	0.43	0.43
A (Ni)	-1526.8	-11.49 1.54	-0.11	0.37	0.37
C (Ni)	-1526.0	-11.29 1.35	-0.11	0.45	0.35
D (Ni)	-1526.4	-11.75 1.94	-0.05	0.46	0.38
F (Ni)	-1525.0	-11.26 1.59	0.09	0.04	0.55

[a] E(H) = Energy of the HOMO

[b] E(H-L)= HOMO-LUMO gap

Figure 6.5: Molecular orbital correlation diagram for formation of the idealized square planar-trigonal bipyramidal complex F, from the fragments $[MXL_2]^+$ (14 electron) and $[MX(CO)L_2]^-$ (18 electron), with formation of a σ(M-M')-bonding MO.

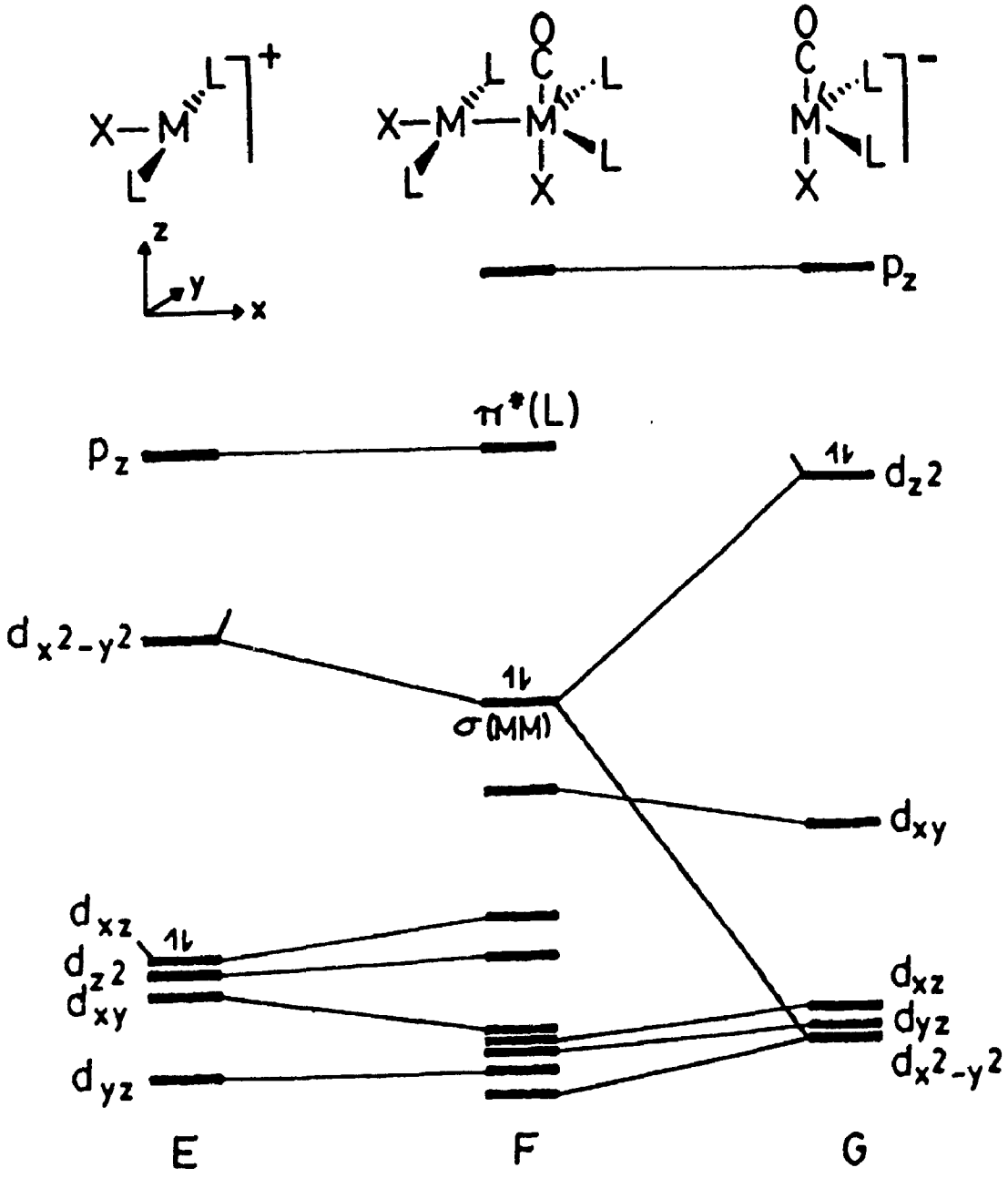

predicted between the HOMO of G, having mostly M' d_z^2, p_z character, and the LUMO of E, having mostly M d_{x2-y2} character, to give a σ(M-M') bonding orbital. In the process, d_{x2-y2} character of M' is mixed in as shown in Figure 6.5. This donation of charge from G to E is calculated to be sufficiently great that, when charge in F is apportioned to each fragment from which it was derived, fragment E is negatively (-0.25 e when M, M' = Pt) and G positively (+0.25 e when M, M' = Pt) charged. This is a classic situation for formation of a semi-bridging carbonyl since sliding the carbonyl ligand of F towards M would allow it to remove charge from M by backbonding.[30]

This then leads naturally to structure D = 6.1. A series of calculations were made as the angle θ (angle M-M'-CO, Figure 6.6) decreased from 90° to 50° and some results are shown in Figure 6.6. As θ decreases, the orbital σ(M-M') is stabilized while other orbitals are not much changed, and hence this distortion leads to net stabilization. The orbital character becomes complex, and includes much mixing with π^*(CO), such that in D (θ ca. 50°) it is best considered as a 3-centre 2-electron bond with little computed metal-metal bonding character.[31] In addition, the computed charges on the two fragments E and G shown in Figure 6.6 decrease and then reverse as θ decreases as depicted in Figure 6.6. This is consistent with the expected effect of the semibridging carbonyl in removing electron density from fragment E. However, there is an equally valid way of rationalizing this effect. As θ is reduced from 90° the fragment G moves towards its more stable tetrahedral geometry (sp^3 for a 4-coordinate d^{10} complex) and the HOMO is stabilized (moving the CO ligand away from the z-axes reduces the σ- antibonding character of d_z2 and allow d_z2 to CO π^*

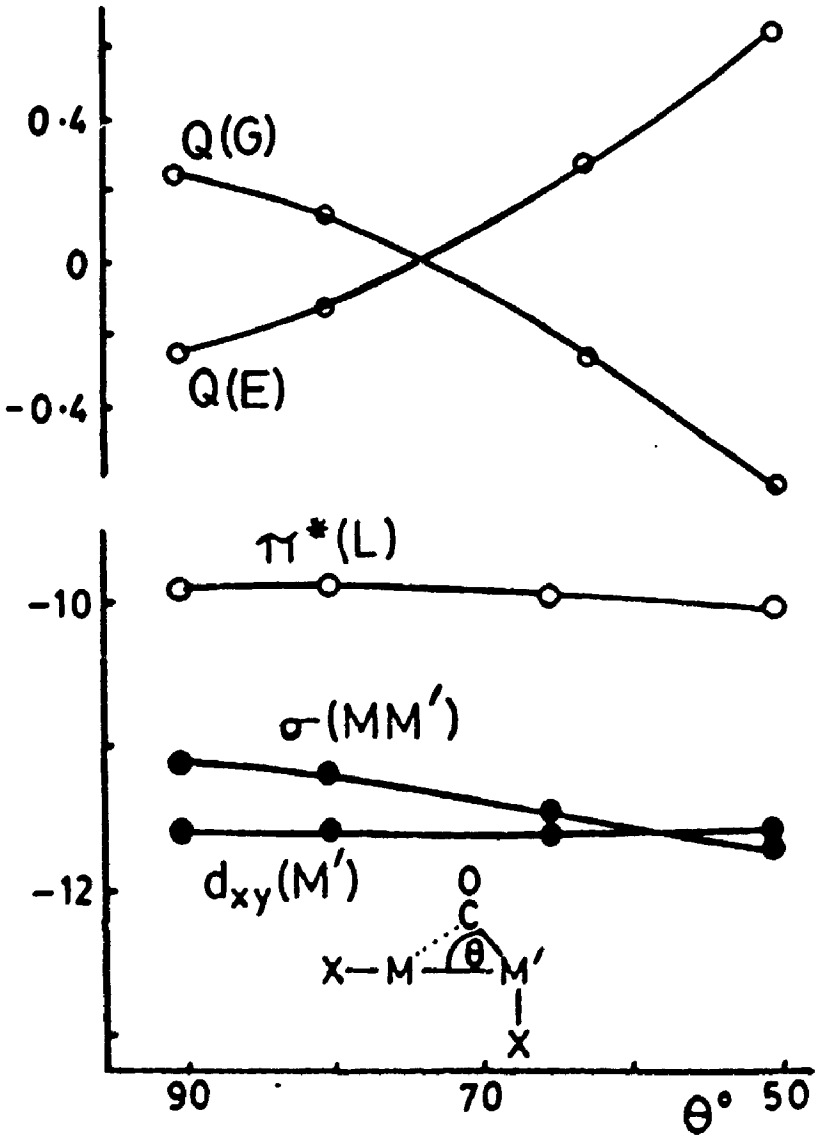

Figure 6.6: Bottom: Changes in the energies of three frontier orbitals {π^*(L), σ(M-M), and d_{xy}(M′) in figure 6.5}. Top: Changes in the charges on the fragments E and G, as the angle θ is reduced from the value of 90° in structure F.

backbonding, both of which effects stabilize the HOMO of fragment G). The result is that the distorted fragment G is a poorer donor and donates less charge to fragment E. The donor orbital of the distorted fragment G backbonds strongly to CO and so becomes a mixed M'C donor rather than a more pure metal-centred donor. Whichever way one looks at this, the result is that in the case with θ ca. 50° the computed charge on fragment E is +0.63 e (M, M' = Pt) and +0.44 e (M, M' = Ni).[32] Thus, the original charge of -1 e on the distorted (θ = 50°) fragment G is only partly donated to fragment E and so, given the reservations outlined above,[31,32] it is reasonable, although over simplified, to regard the complex 6.1 as containing a donor-acceptor metal-metal bond with some residual polarity $\{MXL_2\}^{\delta+}\{M'(CO)XL_2\}^{\delta-}$. Thus all the theoretical and experimental results clearly show that the structure shown in Figure 6.2 is the most reasonable for the $[Ni_2Cl_2(\mu\text{-}CO)(\mu\text{-}dppm)_2]$.

6.3. Synthesis of $[Ni_3(\mu_3\text{-}Cl)(\mu_3\text{-}CO)(\mu\text{-}dppm)_3]Cl$, 6.5

The formal oxidation state of the metal atoms in $[M_3(\mu_3\text{-}CO)(\mu\text{-}dppm)_3]^{2+}$ or $[M_3(\mu_3\text{-}Cl)(\mu_3\text{-}CO)(\mu\text{-}dppm)_3]^{+}$ is +2/3 and there are a number of logical ways to prepare such complexes. For example, 2Ni(0) + Ni(II) or Ni(0) + 2Ni(I) might give 3Ni(2/3). A number of such reactions, for example, $[Ni_2(\mu\text{-}CO)(CO)_2(\mu\text{-}dppm)_2]$[21] with $[NiCl_2(dppm)]$, $[NiCl_2(dppm)_2]$[33] or $[Ni_2Cl_2(\mu\text{-}CO)(\mu\text{-}dppm)_2]$[29,34] in the required ratio, were attempted unsuccessfully. The clusters $[M_3(\mu_3\text{-}CO)(\mu\text{-}dppm)_3]^{2+}$ with M=Pd or Pt are most easily prepared by reduction of $[M(O_2CCF_3)_2(dppm)]$ with CO/H_2O[18] but this route was also unsuccessful when M=Ni. Finally, the cluster

$[Ni_3(\mu_3\text{-}Cl)(\mu_3\text{-}CO)(\mu\text{-}dppm)_3]Cl$ was prepared by reaction of $[Ni_2(\mu\text{-}CO)(CO)_2(\mu\text{-}dppm)_2]$[21] with refluxing 1,2-dichloroethane. This reaction uses the solvent 1,2-dichloroethane as both oxidant and source of chloride, according to equation 6.2. A similar reaction using 1,2-dibromoethane as oxidant was unsuccessful since oxidation to nickel(II) appeared to occur.

$$3[Ni_2(\mu\text{-}CO)(CO)_2(\mu\text{-}dppm)_2] + 2C_2H_4Cl_2 \rightarrow 2\{[Ni_3(\mu_3\text{-}Cl)(\mu_3\text{-}CO)(\mu\text{-}dppm)_3]^+Cl^-\} + 7CO + 2C_2H_4 \quad (6.2)$$

The complex $[Ni_3(\mu_3\text{-}Cl)(\mu_3\text{-}CO)(\mu\text{-}dppm)_3]Cl$ was also prepared by heating $[Ni_2Cl_2(\mu\text{-}CO)(\mu\text{-}dppm)_2]$, 6.1, briefly to 100°C under vacuum. The intention was to drive off CO and form $[Ni_2Cl_2(\mu\text{-}dppm)_2]$, by analogy with the corresponding reactions when M=Pd or Pt,[9] but the only product was $[Ni_3(\mu_3\text{-}Cl)(\mu_3\text{-}CO)(\mu\text{-}dppm)_3]Cl$. A possible stoichiometry is shown in equation 6.3, though the volatile product was not characterized.

$$3[Ni_2Cl_2(\mu\text{-}CO)(\mu\text{-}dppm)_2] \rightarrow 2[Ni_3(\mu_3\text{-}Cl)(\mu_3\text{-}CO)(\mu\text{-}dppm)_3]Cl + COCl_2 \quad (6.3)$$

6.3.1. X-ray Diffraction Studies of $[Ni_3(\mu_3\text{-}Cl)(\mu_3\text{-}CO)(\mu\text{-}dppm)_3]$

The reaction product, $[Ni_3(\mu_3\text{-}Cl)(\mu_3\text{-}CO)(\mu\text{-}dppm)_3]Cl$, was crystallized from a dichloroethane/pentane mixture in the presence of $NaBPh_4$, and the identity of the product was then established by an X-ray diffraction study of $[Ni_3(\mu_3\text{-}Cl)(\mu_3\text{-}CO)(\mu\text{-}dppm)_3][BPh_4]\cdot C_2H_4Cl_2$, which was carried out at the University of Glasgow,

Scotland.

In the crystal structure of the salt, the solvent molecules $C_2H_4Cl_2$ are loosely entrapped in what would have been voids and their relatively high atomic displacement parameters suggest that they may be somewhat disordered. The geometry of the $[BPh_4]^-$ ions is as expected [B-C 1.631(9)-1.654(9)Å, C-B-C 104.0(5) - 112.7(5)°]. The stucture of the molecule is shown in Figure 6.7 and the bond distances and angles are listed in the Table 6.3.

The structure of the cationic cluster 6.5, as shown in Figure 6.7, is closely similar to those of the complexes $[Pd_3(\mu_3\text{-}X)(\mu_3\text{-}CO)(\mu\text{-}dppm)_3]^+$, X=Cl or I,[18,19] and $[Ni_3(\mu_3\text{-}I)(\mu_3\text{-}CNMe)(\mu\text{-}dppm)_3]^+$.[20] It contains a triangular Ni_3 cluster, with Ni-Ni distances [2.381(1)-2.418(1)Å] indicative of nickel-nickel single bonds [2.37-2.69 Å].[20,29,33] The edges of the Ni_3 triangle are bridged by three dppm ligands to form a roughly planar $[Ni_3P_6]^{2+}$ skeleton, with the Ni-P bond lengths [2.195(2) - 2.214(2)Å] lying within the range of those previously observed (2.18-2.26Å).[10c,20,23b,35,36] The capping sites above the opposite faces of the Ni_3 cluster are occupied by triply bridging Cl and CO ligands, forming a distorted trigonal bipyramidal $[Ni_3(\mu_3\text{-}Cl)(\mu_3\text{-}CO)]^+$ unit. The data from Table 6.3 show that the CO ligand is distorted towards the Ni(1)-Ni(2) bond; thus the distance Ni(2)-C at 1.956(15)Å is significantly longer than the distances Ni(1)-C and Ni(3)-C at 1.913(15) and 1.908(16)Å respectively. This is further supported by the fact that the bond angles C-Ni(1)-Ni(2) at 52.5(4)° and C-Ni(3)-Ni(2) at 52.9(4)° are slightly larger than the angles C-Ni(2)-Ni(1) and C-Ni(2)-Ni(3) at 50.9(5) and 51.1(5)° respectively. The distortion of the CO ligand also affected the binding of the chloride ion. Thus, the Cl atom appears to be more weakly

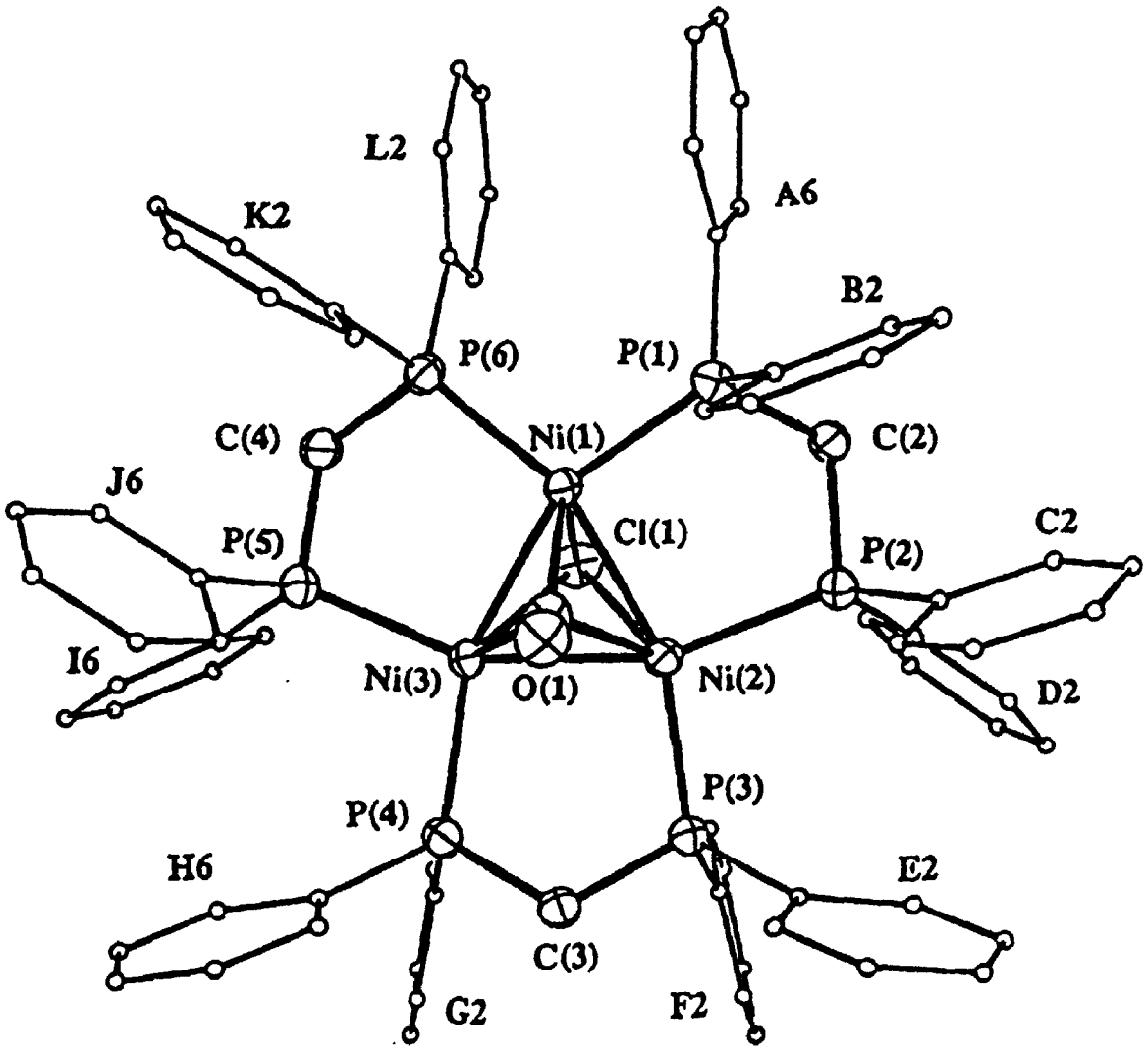

Figure 6.7: The X-ray structure of the cation $[Ni_3(\mu_3\text{-}Cl)(\mu_3\text{-}CO)(\mu\text{-}dppm)_3]^+$, 6.5.

Table 6.3: Selected bond lengths (Å) and angles (°) in $[Ni_3(\mu_3\text{-}Cl)(\mu_3\text{-}CO)(\mu\text{-}Ph_2PCH_2PPh_2)_3]^+$

Ni(1) - Ni(2)	2.400(1)	Ni(1) - Ni(3)	2.418(1)
Ni(1) - Cl(1)	2.497(16)	Ni(1) - C1(1')	2.690(28)
Ni(1) - P(1)	2.207(2)	Ni(1) - P(6)	2.210(2)
Ni(1) - C(1)	1.913(15)	Ni(1) - C(1')	1.900(38)
Ni(2) - Ni(3)	2.381(1)	Ni(2) - Cl(1)	2.605(16)
Ni(2) - Cl(1')	2.598(30)	Ni(2) - P(2)	2.205(2)
Ni(2) - P(3)	2.195(2)	Ni(2) - C(1)	1.956(15)
Ni(2) - C(1')	1.847(37)	Ni(3) - Cl(1)	2.563(16)
Ni(3) - Cl(1')	2.549(32)	Ni(3) - P(4)	2.214(2)
Ni(3) - P(5)	2.196(2)	Ni(3) - C(1)	1.908(16)
Ni(3) - C(1')	1.819(34)	P(1) - C(2)	1.838(5)
P(1) - C(A1)	1.829(5)	P(1) - C(B1)	1.824(6)
P(2) - C(2)	1.833(5)	P(2) - C(C1)	1.808(6)
P(2) - C(D1)	1.819(6)	P(3) - C(3)	1.828(5)
P(3) - C(E1)	1.825(6)	P(3) - C(F1)	1.816(6)
P(4) - C(3)	1.832(5)	P(4) - C(G1)	1.815(6)
P(4) - C(H1)	1.822(6)	P(5) - C(4)	1.830(5)
P(5) - C(I1)	1.822(5)	P(5) - C(J1)	1.810(6)
P(6) - C(4)	1.830(5)	P(6) - C(K1)	1.814(6)
P(6) - C(L1)	1.826(6)	O(1) - C(1)	1.102(37)

Bond Angles (°)

Ni(2)-Ni(1)-Ni(3)	59.2(1)	Ni(2)-Ni(1)-Cl(1)	64.2(4)
Ni(2)-Ni(1)-Cl(1')	61.1(6)	Ni(2)-Ni(1)-P(1)	95.4(1)
Ni(2)-Ni(1)-P(6)	156.2(1)	Ni(2)-Ni(1)-C(1)	52.5(4)
Ni(2)-Ni(1)-C(1')	49.2(12)	Ni(3)-Ni(1)-Cl(1)	62.8(4)
Ni(3)-Ni(1)-Cl(1')	59.6(6)	Ni(3)-Ni(1)-P(1)	154.6(1)
Ni(3)-Ni(1)-P(6)	98.6(1)	Ni(3)-Ni(1)-C(1)	50.7(5)

Ni(3)-Ni(1)-C(1')	48.0(10)	Cl(1)-Ni(1)-P(1)	110.0(4)
Cl(1)-Ni(1)-P(6)	99.1(4)	Cl(1)-Ni(1)-C(1)	103.4(6)
Cl(1')-Ni(1)-P(1)	108.5(6)	Cl(1')-Ni(1)-P(6)	117.6(5)
Cl(1')-Ni(1)-C(1')	95.7(13)	P(1) -Ni(1)-P(6)	106.7(1)
P(1)-Ni(1)-C(1)	114.0(5)	P(1) -Ni(1)-C(1')	118.2(9)
P(6)-Ni(1)-C(1)	122.1(4)	P(6) -Ni(1)-C(1')	110.4(11)
Ni(1)-Ni(2)-Ni(3)	60.8(1)	Ni(1)-Ni(2)-Cl(1)	59.7(4)
Ni(1)-Ni(2)-Cl(1')	65.0(6)	Ni(1)-Ni(2)-P(2)	98.6(1)
Ni(1)-Ni(2)-P(3)	156.9(1)	Ni(1)-Ni(2)-C(1)	50.9(5)
Ni(1)-Ni(2)-C(1')	51.1(10)	Ni(3)-Ni(2)-Cl(1)	61.7(4)
Ni(3)-Ni(2)-Cl(1')	61.4(6)	Ni(3)-Ni(2)-P(2)	157.4(1)
Ni(3)-Ni(2)-P(3)	97.1(1)	Ni(3)-Ni(2)-C(1)	51.1(5)
Ni(3)-Ni(2)-C(1')	49.0(10)	Cl(1)-Ni(2)-P(2)	100.9(4)
Cl(1)-Ni(2)-P(3)	118.1(4)	Cl(1)-Ni(2)-C(1)	98.5(6)
Cl(1')-Ni(2)-P(2)	120.9(6)	Cl(1')-Ni(2)-P(3)	99.5(5)
Cl(1'(-Ni(2)-C(1')	100.2(13)	P(2)-Ni(2) -C(1')	104.2(1)
P(2)-Ni(2)-C(1)	124.7(4)	P(2)-Ni(2) -C(1')	111.7(10)
P(3)-Ni(2)-C(1)	111.0(4)	P(3)-Ni(2)-C(1')	120.8(10)
Ni(1)-Ni(3)-Ni(2)	60.0(1)	Ni(1)-Ni(3)-Cl(1)	60.1(4)
Ni(!)-Ni(3)-Cl(1')	65.5(5)	Ni(1)-Ni(3)-P(4)	157.2(1)
Ni(1)-Ni(3)-P(5)	96.5(1)	Ni(1)-Ni(3)-C(1)	50.8(5)
Ni(1)-Ni(3)-C(1')	50.9(11)	Ni(2)-Ni(3)-Cl(1)	63.5(4)
Ni(2)-Ni(3)-Cl(1')	63.5(6)	Ni(2)-Ni(3)-P(4)	98.4(1)
Ni(2)-Ni(3)-P(5)	156.1(1)	Ni(2)-Ni(3)-C(1)	52.9(4)
Ni(2)-Ni(3)-C(1')	50.0(12)	Cl(1)-Ni(3)-P(4)	119.3(4)
Cl(1)-Ni(3)-P(5)	102.1(4)	Cl(1)-Ni(3)-C(1)	101.3(6)
Cl(1')-Ni(3)-P(4)	99.5(5)	Cl(1')-Ni(3)-P(5)	113.3(6)
Cl(1')-Ni(3)-C(1')	102.8(14)	P(4)-Ni(3) -P(5)	105.5(1)
P(4)-Ni(3)-C(1)	111.5(5)	P(4)-Ni(3) -C(1')	122.3(10)
P(5)-Ni(3)-C(1)	117.5(4)	P(5)-Ni(3)-C(1')	112.8(11)
Ni(1)-Cl(1)-Ni(2)	56.1(4)	Ni(1)-Cl(1)-Ni(3)	57.1(4)

Ni(2)-Cl(1)-Ni(3)	54.9(4)	Ni(1)-Cl(1')-Ni(2)	53.9(6)
Ni(1)-Cl(1')-Ni(3)	54.9(7)	Ni(2)-Cl(1')-Ni(3)	55.1(7)
Ni(1)-P(1)-C(2)	107.0(2)	Ni(1)-P(1)-C(A1)	122.0(2)
Ni(1)-P(1)-C(B1)	117.7(2)	Ni(2)-P(2)-C(2)	108.9(2)
Ni(2)-P(2)-C(C1)	119.2)	Ni(2)-P(2)-C(D1)	113.7(2)
Ni(2)-P(3)-C(3)	110.0(2)	Ni(2)-P(3)-C(E1)	116.2(2)
Ni(2)-P(3)-(F1)	118.2(2)	Ni(3)-P(4)-C(3)	108.6(2)
Ni(3)-P(4)-C(G1)	118.8(2)	Ni(3)-P(4)-C(H1)	117.5(2)
Ni(3)-P(5)-C(4)	108.3(2)	Ni(3)-P(5)-C(I1)	118.3(2)
Ni(3)-P(5)-C(J1)	117.5(2)	Ni(1)-P(6)-C(4)	107.7(2)
Ni(1)-P(6)-C(K1)	121.3(2)	Ni(1)-P(6)-C(L1)	118.8(2)
Ni(1)-C(1)-Ni(2)	76.7(6)	Ni(1)-C(1)-Ni(3)	78.5(7)
Ni(1)-C(1)-O(1)	138.9(18)	Ni(2)-C(1)-Ni(3)	76.1(6)
Ni(2)-C(1)-O(1)	128.8(19)	Ni(3)-C(1)-O(1)	133.6(17)
Ni(1)-C(1')-Ni(2)	79.7(17)	Ni(1)-C(1')-Ni(3)	81.1(15)
Ni(1)-C(1')-O(1')	127.7(51)	Ni(2)-C(1')-Ni(3)	81.0(17)
Ni(2)-C(1')-O(1')	135.5(50)	Ni(3)-C(1')-O(1')	131.6(52)
P(1)-C(2)-P(2)	108.3(3)	P(3)-C(3)-P(4)	108.9(3)
P(5)-C(4)-P(6)	110.4(3)		

bound to Ni(2) compared to Ni(1) and Ni(3) as is evident from the bond distance data which show that the Ni(2)-Cl distance at 2.605(16)Å is longer than the Ni(1)-Cl and Ni(3)-Cl distances at 2.497(16) and 2.563(16)Å respectively. This is also apparent from the bond angles Cl-Ni(1)-Ni(2) at 64.2(4)° and Cl-Ni(3)-Ni(2) at 63.5(4)° which are slightly longer than the angles Cl-Ni(2)-Ni(1) and Cl-Ni(2)-Ni(3) at 59.7(4) and 61.7(4)° respectively. The close similarity of 6.5 with its palladium analogue, $[Pd_3(\mu_3\text{-}Cl)(\mu_3\text{-}CO)(\mu\text{-}dppm)_3]^+$,[18,19b] extends to the observed Cl/CO disorder, each ligand spanning the capping sites on both sides of the Ni_3 cluster as shown in Figure 6.8. The two resulting orientations of the $[Ni_3(\mu_3\text{-}Cl)(\mu_3\text{-}CO)]^+$ unit occur with 70:30 occupancy. Although the accuracy of the bond lengths and angles in the $[Ni_3(\mu_3\text{-}Cl)(\mu_3\text{-}CO)]^+$ unit (Table 6.3) is somewhat lowered by the Cl/CO disorder, the Ni-C distances [1.82(4) - 1.96(2)Å] are in accord with those [1.77 - 2.203 Å] found in the $[Ni_3(\mu_3\text{-}CO)(\mu\text{-}Me_2PCH_2PMe_2)_4]^{2+}$ cluster and in some carbonyl bridged binuclear complexes.[10a,21,29,34,37] The Ni-Cl distances [2.50(2) - 2.60(3) Å] can be compared with long Ni-Cl bonds of 2.527(2) Å in $[NiCl_2(dppm)_2]$[38] and 2.699(7) Å in $[NiCl(CH_2\{CH_2P(Ph)CH_2CH_2CH_2NH_2\}_2)]$,[39] but they are substantially longer than the distances [2.22 - 2.27 Å] considered typical of normal covalent Ni-Cl bonds.[10a,11,29,37] In the closely related complexes $[Pd_3(\mu_3\text{-}X)(\mu_3\text{-}CO)(\mu\text{-}dppm)_3]^+$, X=Cl or I, and $[Ni_3(\mu_3\text{-}X)(\mu_3\text{-}CNMe)(\mu\text{-}dppm)_3]^+$, X=I, the metal-halogen bonds are also abnormally long [Pd-Cl 2.74 - 3.16, Pd-I 2.95 - 3.03, Ni-I 2.73 - 2.78 Å].[18-20] It thus appears that weak covalent character of the $M_3(\mu_3\text{-}X)$ interaction is a common feature of the halide adducts of the $[M_3(\mu_3\text{-}CO)(\mu\text{-}dppm)_3]^{2+}$ (M=Ni or Pd) and $[Ni_3(\mu\text{-}CNMe)(\mu\text{-}dppm)_3]^{2+}$ clusters.

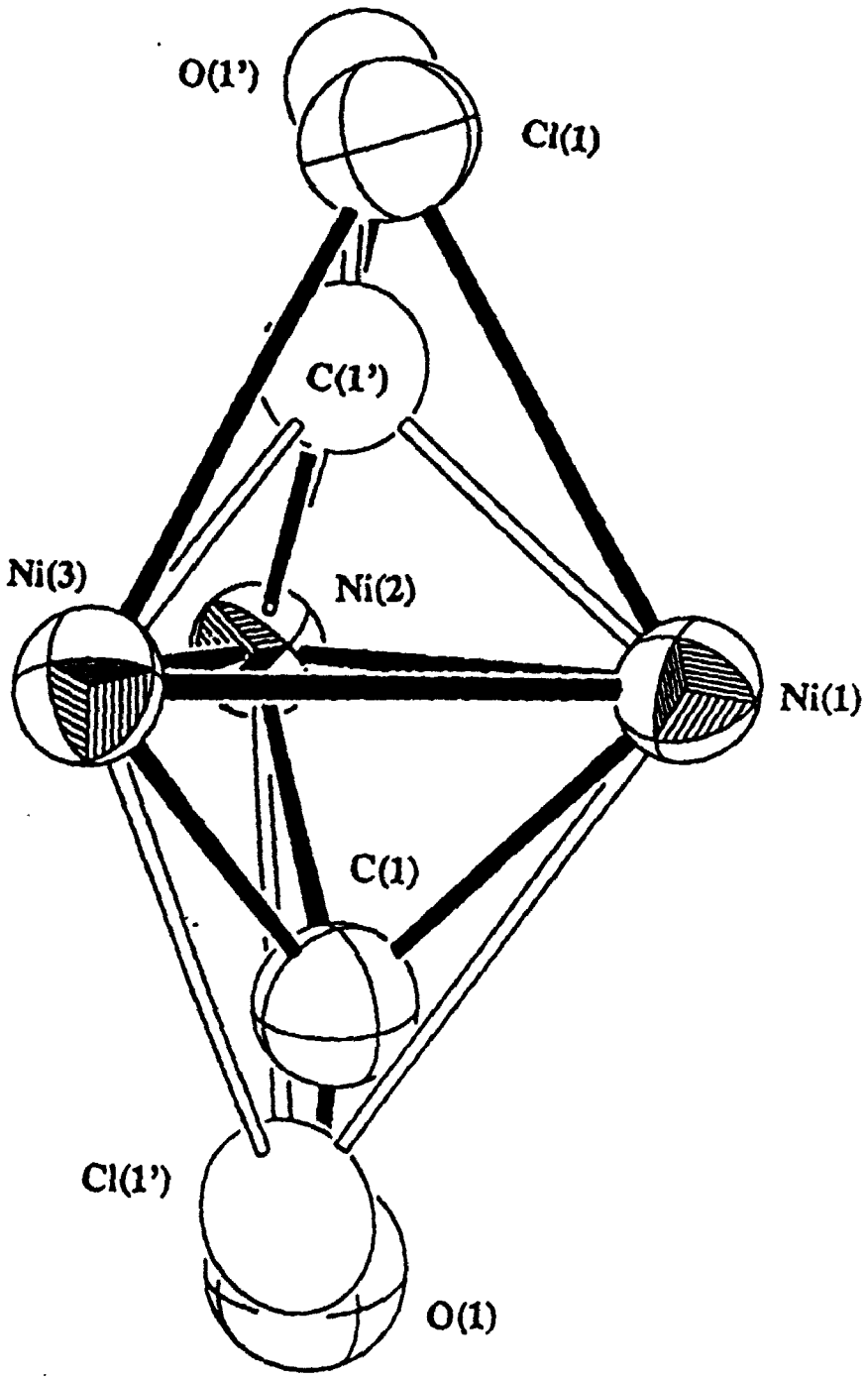

Figure 6.8: Molecular structure of 6.5 showing the disorder of CO and Cl. The dppm ligands are omitted for the sake of clarity.

In 6.5 and in the other crystallographically characterized $[M_3(\mu_3\text{-}X)(\mu_3\text{-}CO)(\mu\text{-}dppm)_3]^+$ complexes (M = Pd, X = Cl^-, I^- or CF_3COO^-; M = Pt, X = SnF_3^-),[18,19,40,41] the three M_2P_2C rings adopt envelope shapes, two with the CH_2 groups at the flaps lying above, and the third with the CH_2 group at the flap lying below, the M_3P_6 Plane. Thus one CH_2 group and four axial plus two equatorial phenyl groups form a fence around one, and two CH_2 groups and two axial plus four equatorial phenyl groups around the other face of the M_3P_6 skeletons as shown in Figure 6.7. In such a conformation of the $[M_3(\mu\text{-}dppm)_3]^{2+}$ fragment the two faces of the M_3 cluster are exposed to sterically different environments, the steric hindrance being larger within the fence comprising four axial phenyl groups. The Cl/CO disorder observed in 6.5 and in its palladium analogue, resulting in two different orientations of the $[M_3(\mu_3\text{-}Cl)(\mu_3\text{-}CO)]^+$ unit with respect to the $[M_3(\mu_3\text{-}dppm)_3]^{2+}$ skeleton, shows that small ligands, such as Cl and CO, can bind to either face of the M_3 cluster. The ligands with higher steric requirements, such as I^-, CF_3COO^- and SnF_3^-, display a preference for the face of the M_3 cluster surrounded by the smaller number of the axial phenyl groups.

6.3.2. Spectroscopic Studies of $[Ni_3(\mu_3\text{-}Cl)(\mu_3\text{-}CO)(\mu\text{-}dppm)_3]^+$

The infrared spectrum of $[Ni_3(\mu_3\text{-}Cl)(\mu_3\text{-}CO)(\mu\text{-}dppm)_3]Cl$ shows a carbonyl stretching frequency at 1717 cm^{-1}, and the low energy shift of this band is indicative of carbonyl being triply bridging. Analogous $[Pd_3(\mu_3\text{-}CO)(Cl)(dppm)_3]PF_6$ and $[Pt_3(\mu_3\text{-}CO)(Cl)(dppm)_3]PF_6$ complexes exhibit ν(CO) stretches at 1820 and 1767 cm^{-1} respectively. This clearly indicates that backbonding to CO is strongest for Ni

and weakest for Pd, which is the usual trend in this triad.

The ^{31}P NMR spectrum of 6.5 in CD_2Cl_2 solution shows a singlet resonance at δ = -3.0 ppm. This suggests that all the phosphorus atoms are equivalent. For bridging dppm complexes of nickel the phosphorus shift in the NMR spectrum is usually in the region δ = 15-30 ppm.[10-12] The high field shift for 6.5 indicates higher shielding of phosphorus in the cluster. Similar higher field chemical shifts have also been reported for $[Ni_3(\mu_3\text{-}CNMe)(\mu_3\text{-}I)(dppm)_3]I$, δ = 0.02 ppm and $[Ni_3(\mu_3\text{-}CNMe)(CNMe)_2(\mu_3\text{-}I)(dppm)_2]I$, δ = 0.5 ppm.[35,42]

The ^1H NMR spectrum of 6.5 from room temperature to -90°C remains unchanged except for a slight broadening. The spectrum shows only a broad resonance at δ = 3.86 ppm attributed to the CH_2 protons of the dppm ligands and multiplet resonances spanning in the range of 6.6-7.4 ppm for phenyl protons of dppm. For this type of complex, two resonances are expected for the P-CH_2-P protons. However, no such observation was made which suggests that there is a rapid fluxional process occurring in solution or that there is accidental degeneracy of the chemical shifts. The latter is more probable since no very easy mechanism for Cl/CO exchange can be envisaged.

6.4. Miscellaneous Reactions:

In recent years studies to investigate the reactivities of binuclear and cluster complexes towards different metal reagents have received considerable attention. One of the prime objectives of such studies is to make heteronuclear complexes which might be useful in catalysis. We also investigated in this regard our dinuclear and

trinuclear complexes. Some of the results which were obtained in these studies are summarized here.

6.4.1. Reactions of $[Ni_2(\mu\text{-}CO)(CO)_2(\mu\text{-}dppm)_2]$.

Reactions of this complex with many reagents were attempted, but in most cases mixtures were obtained which could not be purified. Only those reactions which gave clean products are discussed here.

6.4.1.1. Reaction with HPF_6:

When cold solutions of $[Ni_2(\mu\text{-}CO)(CO)_2(\mu\text{-}dppm)_2]$ in CH_2Cl_2 were reacted with HPF_6, a light yellow complex was formed. The infrared spectrum of this complex shows both bringing and terminal carbonyl stretches [ν(CO) = 2049(s), 2035(vs), 1998(vw), 1993(vw), 1858(vs) cm^{-1}] and the frequencies were shifted to higher energy region compared to the parent $[Ni_2(\mu\text{-}CO)(CO)_2(\mu\text{-}dppm)_2]$ complex [ν(CO) = 2000(w), 1972(vs), 1955(vs), 1915(sh), 1790(vs) cm^1]. A single resonance was observed in the ^{31}P NMR at δ = 26 ppm suggesting that all phosphorus atoms are in equivalent environments. The ^1H NMR spectrum of this complex shows, in addition to the resonances for the CH_2 protons of the dppm at δ = 2.56 and 3.06 ppm, an upfield quintet resonance at δ = -11.05 ppm with $J(PH)_{obs}$ = 28Hz., attributed to a hydride ligand bound symmetrically to the two nickel atoms. Thus, on the basis of these data the complex was characterized as the known $[Ni_2(\mu\text{-}CO)(CO)_2(\mu\text{-}H)(\mu\text{-}dppm)_2]PF_6$.[43]

6.4.1.2. Reaction with $[Cu(MeCN)_4]BF_4$

The reaction of $[Ni_2(\mu\text{-}CO)(CO)_2(\mu\text{-}dppm)_2]$ with $[Cu(MeCN)_4]BF_4$ in MeCN solution produced a yellowish green complex, which can also be readily prepared by the addition of $[Cu(MeCN)_4]BF_4$ to a cold solution of $[Ni(CO)_2(\eta^1\text{-}dppm)_2]$. The ^{31}P NMR spectrum of this complex along with a possible structure is shown in Fig 6.9.

6.4.1.3. Reaction with Ag^+

The reaction of $[Ni_2(\mu\text{-}CO)(CO)_2(\mu\text{-}dppm)_2]$ with Ag^+ in MeCN solution produced a dark solution. The ^{31}P NMR spectrum shows a very similar pattern as found for the Cu^+ reaction product discussed above. However, the product could not be isolated to do further analysis.

6.5. Conclusions:

The chemistry of metal-metal bonds has been shown to be important in organometallic chemistry. A large number of di and polynuclear complexes have been prepared and studied in this regard. It has also been shown that reactions of these metal-metal bonded complexes produce a large variety of products with unusual physical and structural properties. In recent years, numerous theoretical studies have also been carried out to understand the mechanism of the formation and stability of the products.

This chapter gives details of one such study where experimental, spectroscopic and theoretical tools were collectively used in an attempt to get insight into the mechanism of formation and the unusual structure of nickel- nickel bonded

Figure 6.9: The ^{31}P NMR spectrum of $[NiCu(CO)_2(MeCN)(\mu\text{-dppm})_2]^+$.

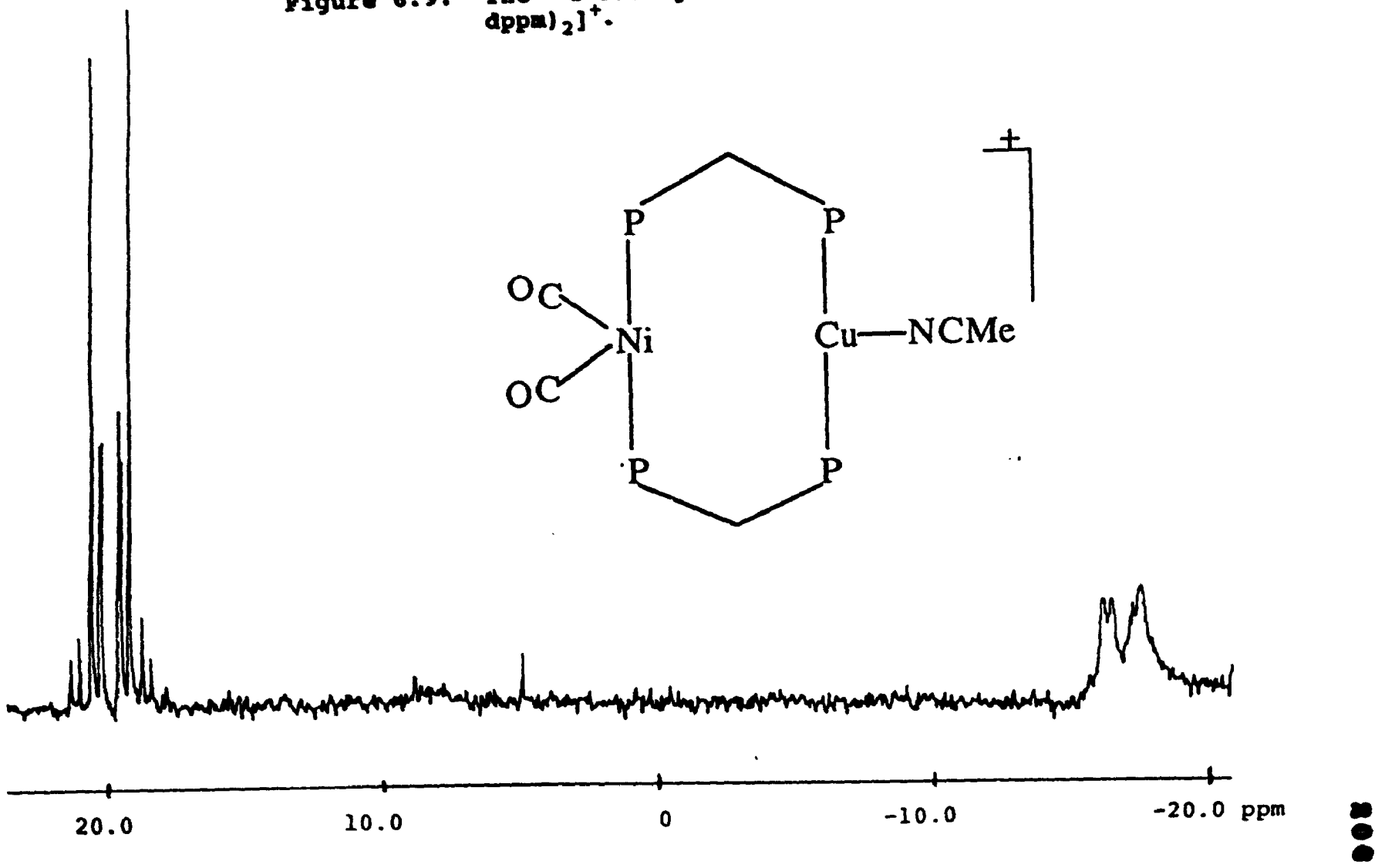

complexes. Thus, the dinuclear nickel complex $[Ni_2(\mu\text{-}CO)(Cl)_2(\mu\text{-}dppm)_2]$, 6.1, which is synthesized from the reaction of $[Ni_2(\mu\text{-}CO)(CO)_2(\mu\text{-}dppm)_2]$ and $[NiCl_2(dppm)_2]$ exhibits very unusual structural properties. The MO calculations performed on this complex and the platinum analogue show that the observed structures 6.1 or 6.2 are more stable than other possible structures such as B (Figure 6.4) or F (Figure 6.5). However, the calculations gave very similar results for the Pt and Ni derivatives and so do not explain why the different structures 6.2 and 6.1 respectively are adopted. For both metals, the energies of 6.1 and 6.2 are calculated to be very similar and so easy interconversion between these structures might be predicted. Since the Pt or Pd complexes 6.2 have high symmetry, it is not easy to determine if conversion to 6.1 is facile. However, the NMR data discussed above show clearly that the less symmetrical nickel complex 6.1 is fluxional and, on the NMR time scale, has the symmetry characteristic of 6.2. The fluxionality is still rapid at -90°C as evidenced by the observation of a sharp singlet in the ^{31}P NMR spectrum at this temperature. It was also shown that the fluxionality requires an intermediate or transition state with a symmetrical bridging CO ligand and B (Figure 6.4) is the most likely candidate, as suggested in equation 6.2. Thus there is experimental as well as theoretical evidence that structures 6.1 and 6.2 may readily interconvert.

The heating of complex 6.1 is shown to yield rather unexpectedly a trinuclear cluster $[Ni_3(\mu_3\text{-}CO)(\mu_3\text{-}Cl)(\mu\text{-}dppm)_3]^+$ which could also be readily prepared in high yield by refluxing $[Ni_2(\mu\text{-}CO)(CO)_2(\mu\text{-}dppm)_2]$ in $C_2H_4Cl_2$. The cluster has unsymmetrically triply bridging carbonyl and chloride ligands. This cluster, which is characterized by X-ray crystallography, completes the first triad of trinuclear clusters

of the type $[M_3(CO)(Cl)(dppm)_3]^+$ of group 10 metals. The structural properties of this cluster are shown to be very similar to that of the analogous Pd and Pt clusters. However, in contrast to the palladium and platinum clusters which have been shown to react readily with many small molecules, this nickel cluster is found to be rather inert towards the few reactions which were attempted to determine its reactivity for example MeI, I_2, CH_2I_2, PhC≡CPh, AgO_2CMe and $AuCl(SMe_2)$.

The reactions of $[Ni_2(\mu\text{-}CO)(CO)_2(\mu\text{-}dppm)_2]$ with other metal complexes, such as complexes of Cu, Ag and Au, have been shown to produce heteronuclear complexes, although these complexes have not been fully characterized yet.

6.6. Experimental

Nickel complexes were handled under an atmosphere of dry nitrogen by using standard Schlenk tube and drybox techniques.

6.6.1. $[Ni_2Cl_2(\mu\text{-}CO)(\mu\text{-}dppm)_2]$, 6.1

A solution of $[NiCl_2(dppm)_2]$ (0.04 g) in CH_2Cl_2 (5 mL) was added to a solution of $[Ni_2(CO)_2(\mu\text{-}CO)(\mu\text{-}dppm)_2]$ (0.03 g) in CH_2Cl_2 (10 mL) at room temperature. Over a period of 4 h., the colour of the solution changed from red-brown to green. The solution was layered with EtOH and left for 2 days, whereupon deep green-black crystals of the product precipitated. This was separated by filtration, washed with EtOH (10 mL), then pentane (10 mL) and dried under vacuum. Yield 89%.

The same product was obtained by reaction of $NiCl_2.6H_20$ (0.55 g) in EtOH

(10 mL) with $[Ni(CO)_2(dppm\text{-}P)_2]$ (2.0 g) in CH_2Cl_2 (25 mL) at -78°C. The mixture was stirred at -70°C for 0.5 h. then at 20°C for 0.5 h. The product was obtained by precipitation with n-pentane (30 mL), and a further crop was obtained by reducing the volume of the filtrate and adding more pentane (20 mL). Yield 91%.

IR(Nujol): $\nu(CO) = 1763\ cm^{-1}$; $(CH_2Cl_2) = 1765\ cm^{-1}$;

NMR CD_2Cl_2: ^1H; δ = 2.96[br, $CH^aH^bP_2$, CH^a], 3.33[br, $CH^aH^bP_2$, CH^b, $^2J(H^aH^b)$]; ^{31}P, 20°C δ = 17.1(s); -90°C δ 17.7(s).

6.6.2. $[Ni_3(\mu_3\text{-}Cl)(\mu_3\text{-}CO)(\mu\text{-}dppm)_3]Cl$,6.5

A solution of $[Ni_2(\mu\text{-}CO)(CO)_2(\mu\text{-}dppm)_2]$ (0.31 g) in $C_2H_4Cl_2$ (10 mL) was heated under reflux for 2 h. The colour changed from orange to brown-black during this period. The solution was cooled to room temperature and pentane (25 mL) was added to precipitate the product. Yield 92%. Anal.Calc. For $C_{76}H_{66}Cl_2Ni_3OP_6$: C,63.9;H,4.7. Found: C,63.9;H,4.7%. IR(Nujol): $\nu(CO) = 1726\ cm^{-1}$. NMR in CD_2Cl_2:(^1H), δ = 3.86[br.s., CH_2P_2]; ^{31}P, δ = -2.9[s, dppm].

The same complex could be prepared by heating $[Ni_2Cl_2(\mu\text{-}CO)(\mu\text{-}dppm)_2]$ under vacuum at 100°C for 5 min., followed by extraction into CD_3CN. The NMR and IR parameters were identical to those reported above.

6.6.3. $[Ni_3(\mu_3\text{-}Cl)(\mu_3\text{-}CO)(\mu\text{-}dppm)_3]BPh_4$,6.6.

To a solution of $[Ni_3(\mu_3\text{-}Cl)(\mu_3\text{-}CO)(\mu\text{-}dppm)_3]Cl$ in $C_2H_4Cl_2$(10 mL), prepared as above, was added $NaBPh_4$ (0.2g) in ethanol (3 mL). This solution was layered with pentane (20 mL) and set aside for 2 weeks, after which time the black

crystals of the product were filtered off and washed with cold ethanol and then ether. Anal Calc. for $C_{100}H_{86}BClNi_3OP_6$: C, 70.1; H, 5.0. Found: C, 69.5; H, 5.0%. The NMR parametcrs were identical to those of the chloride salt listed above.

IR(Nujol): ν(CO) = 1717 cm^{-1}.

6.6.4. Synthesis of $[Ni_2(\mu\text{-H})(\mu\text{-CO})(CO)_2(\mu\text{-dppm})_2]PF_6$

To a stirring solution of $Ni_2(\mu\text{-CO})(CO)_2(\mu\text{-dppm})_2$ (0.12 g; 0.12 mmol) in CH_2Cl_2 (10 mL) was added excess HPF_6 (7 drops). The solution immediately turned from yellowish-orange to green and then greenish-brown. The mixture was stirred for a further 7-10 min and solvent was removed to dryness by vacuum. The yellowish-orange crude product was washed with n-hexane (10 mL) and dried under reduced pressure. Yield: 95%

IR: ν(CO); 2048.7(vs), 2035.2(vs), 1997.6(sh), 1992.5(sh), 1942.6(v.CO) 1857.7(vs). In addition it shows broad stretch due to water.

NMR in CD_2Cl_2: ^1H, δ -11.1[q, Ni_2H, $^2J(PH)$ = 28Hz.]; 2.56[br, $CH'H^bP'_2$, H^a]; 3.1[br, $CH^aH^bP_2$, H^b]; 6.85-7.5[m, Ph, 40 H]; ^{31}P, δ = 26.0 (s)

6.6.5. EHMO Calculations.

Molecular orbital calculations of the extended Huckel type[44] were carried out using ICONS, with fragment MO analysis [Program ICON8,QCPE No. 517, *6*, 100 (1986)]. Weighted Hij were used throughout. Distances used were Ni-Ni 2.62, Pt-Pt 2.64, Ni-C 1.79, Pt-C 1.90, Ni-Cl 2.40, C-O 1.10 Å. These being averaged values from X-ray structures of molecules 6.1 and 6.2.[9,10]

6.7. References:

(1) A.L. Balch in Homogeneous Catalysis with Metal Phosphine Complexes; Ed. by L.H. Pignolet, Plenum Press N.Y. (1983).

2. Yu. L. Slovokhotov and Yu. T. Struchkov; Russ. Chem. Rev. (Engl.) ***54***, 323 (1985).

3. E. L. Muetterties; Chem. Eng. News, Aug. (1982).

4. R. J. Puddephatt; Lj. Manojlovic-Muir and K. W. Muir; Polyhedron ***9***, 2767 (1990)

5. E. L. Muetterties; T. N. Rhodin; E. Bands; C.F. Brucker and W.R. Pretzer; Chem. Rev. ***79***, 91 (1979)

6. R.J. Puddephatt; Chem. Soc. Rev. 99 (1983)

7. K.S. Raghuveer; Ph.D. Thesis, University of Georgia (1983).

8. B. Chaudret; B. Delavaux and R. Poilblanc; Coord. Chem. Rev. ***86***, 91 (1988).

9.(a) R. Colton; M.J. McCormick; C.D. Pannan; Aust. J. Chem. ***31***, 1425 (1978).

(b) M.P. Brown; A.N. Keith; Lj. Manojlovic-Muir; K.W. Muir; R.J. Puddephatt; K.R. Seddon; Inorg. Chim. Acta. ***34***, L223 (1979).

(c) P.. Pringle; B.L. Shaw; J. Chem. Soc. Dalton Trans. , 889 (1983).

(d) C.-L.Lee ; B.R. James ; D.A. Nelson ; R.T. Hallen; Organometallics ***3***, 1360 (1984).

(e) L.S. Benner; A.L. Balch; J. Am. Chem. Soc. ***100***, 6099, (1978).

(f) M.P. Browm; R.J. Puddephatt; M. Rashidi; K.R. Seddon; J. Chem. Soc. Dalton Trans. 1540. (1978).

(g) K.R. Grundy; K.N. Robertson; Organometalics ***2***, 1736 (1983).

10 (a) D.G. Holah; A.N. Hughes; V.R. Magnuson; H.A. Mirza; K.O. Parker; Organometallics *7*, 1233 (1988).

(b) K.S. Ratliff; P.E. Fanwick; C.P. Kubiak; Polyhedron, *9*, 2651 (1990).

(c) D.L. DeLaet; R. del Rosario; P.E. Fanwick ; C.P. Kubiak J. Am. Chem. Soc. *109*, 754 (1987).

(d) J. Ni; C.P. Kubiak; Inorg. Chem. *29*, 4345 (1990).

(e) J. Ni; P.E. Fanwick; C.P. Kubiak; Inorg. Chem. *27*, 2020 (1988).

11. J.K. Gong; P.E. Fanwick; C.P. Kubiak; J. Chem. Soc. Chem. Comm. 1190 (1990).

12. (a) J. Ni; C.P. Kubiak; Inorg. Chem. Acta. *127*, L37 (1987).

(b) J. Ni; P.E. Fanwick; C.P. Kubiak; Inorg. Chem. *27*, 2017 (1988).

13. G.J. Arsenault; Lj. Manojlovic-Muir; K.W. Muir; R.J. Puddephatt; I. Treurnichat; Angew. Chem. Int. Ed. Engl. *26*, 86 (1987).

14. D.M.P. Mingos and R.W.M. Wardle; Trans. Met. Chem. *10*, 441 (1985).

15. N.K. Eremko; E.G. Mednikov; S.S. Kuresove; Russ. Chem. Rev. (Engl. Transl.) *54*, 394 (1985).

16. H.C. Clark; V.K. Jan; Coord. Chem. Rev. *55*, 151 (1984).

17. C.P. Horwitz; D.F. Shriver; Adv. Organomet. Chem. *23*, 219 (1984).

18. R.J. Puddephatt; Lj. Manojlovic-Muir; K.W. Muir; Polyhedron *9*, 2767 (1990).

19. (a) Lj. Manojlovic-Muir; K.W. Muir; unpublished work.

(b) Lj. Manojlovic-Muir; K.W. Muir; B.R. Lloyd; R.J. Puddephatt, J. Chem. Soc. Chem. Commun. 536 (1985).

(c) B.R. Lloyd; A. Bradford; R.J. Puddephatt; Organometallics *6*, 424 (1987).

(d) G. Ferguson; B.R. Lloyd; R.J. Puddephatt. Organometallics.

20. K.S. Ratliff; P.E. Fanwick; C.P. Kubiac; Polyhedron *9*, 1487 (1990).

21. (a) D.G. Holah; A.N.Hughes; H.A.Mirza; J.D. Thompson; Inorg. Chim. Acta. *126*, L7 (1987).

(b) Z.-Z. Zang; H.-K. Wang; H.-G. Wang; R.-J. Wang; W.-J. Zhao; L.-M. Yang; J. Organomet. Chem. *347*, 269 (1988).

(c) J.A. Obsorn; G.G. Stanley; P.H. Bird. J. Am. Chem. Soc. *110*, 2117.(1988)

22. G.R. Van Hecke; W.D. Horrocks. Jr.; Inorg. Chem. *5*, 1968 (1966).

23. (a) H. Einspahr; J. Donohue; Inorg. Chem. *13*, 1839 (1974).

(b) D.L. DeLaet; D.R. Powell; C.P. Kubiak; Organometallics, *4*, 954 (1985).

(c) D.L. Delaet; P.E. Fanwick; C.P. Kubiak; Organometallics *5*, 1807 (1986).

24. (a) C. Woodcock; R. Eisenberg; Inorg. Chem. *24*. 1285, (1985).

(b) R. McDonald; M. Cowie; Inorg. Chem. *29*, 1564,(1990).

(c) D.J. Elliot; G. Ferguson; D.G. Holah; A.N. Hughes; M.C. Jennings; V.R. Magnuson; D. Potter; R.J. Puddephatt; Organometallics; *9*, 1336 (1990).

25. H.H. Karsch; B. Milewski-Mahrla; J.O. Besenhard; P. Hofmann; P. Stauffert; T.A. Albright; Inorg. Chem. *25*, 3811 (1986).

26. D.F. Evans; J. Chem. Soc. 2003 (1959).

27. D.M. Hoffman; R. Hoffman; Inorg. Chem. *20*, 3543 (1981).

28. K.S. Ratliff; D.L. DeLaet; Gao; P.E. Fanwick; C.P. Kubiak; Inorg. Chem. *29*, 4022 (1990).

29. After this work was completed we learned that Kubiak and coworkers have reported complex 6.1 in a conference abstract. Few details were given. There is

agreement on the structure of 6.1a [Ni-Ni 2.614(2), compared to 2.617(1) in the present work] but not on the magnetic properties. J. Gong; D. Morgenstern; P.E. Fanwick; C.P. Kubiak; Abstr. 198'th ACS National Meeting, Miami Beach, (1989), Abstr. 281, mentioned in ref. 11.

30. F.A. Cotton; G. Wilkinson. " Advanced Inorganic Chemistry," Fifth Ed., Wiley, New York, 1030-1031,

(1988).

31. Metal-Metal bond character in carbonyl-bridged complexes is debatable, and has been much debated. For a recent discussion see: A.A. Low; K.L. Kunze; P.J. Mac Dougall; M.B. Hall; Inorg. Chem. *30*, 1079 (1991).

32. Figure 6.6 overemphasizes the true polarity in the bridged forms ($\theta < 90°$) since the charge on the μ-CO group is attributed to fragment G only. The two metal atoms are predicted to be equally charged at θ ca. 63°, M,M'= Pt (charge ca. +0.5 e) and at θ ca. 52°, M,M'= Ni (charge ca. +0.4 e).

33. G. Booth; J. Chatt; J. Chem. Soc. 3238, (1965).

34. Lj. Manojlovic-Muir; K.W. Muir; W.M. Davis; H.A. Mirza; R.J. Pudddephatt; Inorg. Chem. *31*, 904 (1992).

35. (a) J. Gong; J. Huang; P.E. Fanwick; C.P. Kubiak; Angew. Chem. Int. Ed. Engl. *29*, 396 (1990).

(b) K.S. Ratliff; G.K. Broeker; P.E. Fanwick; C.P. Kubiak; Angew. Chem. Int. Ed. Engl. *29*, 395 (1990).

36. D.L. DeLaet; P.E. Fanwick; C.P. Kubiak; Organometallics *5*, 1807 (1986).

37. (a) G. Ferguson; M.C. Jennings; H.A. Mirza; R.J. Puddephatt; Organometallics

9, 1576 (1990).

(b) S. Schreiner; M.M. Setzer; T.N. Gallaher; Inorg. Chim. Acta. *188*, 131 (1991).

38. Lj.Manojlovic-Muir; H.A. Mirza; R.J. Puddephatt; N. Sadiq; Inorg. Chem. (submitted for publication).

39. L.G. Scanlon; Y.-Y. Tsao; K. Toman; S.C. Cummings; D.W. Meek; Inorg. Chem. *21*, 2707 (1982).

40. Lj. Manojlovic-Muir; K.W. Muir; B.R. Lloyd; R.J. Puddephatt; J. Chem. Soc. Chem. Commun. 1336 (1983).

41. G. Douglas; M.C. Jennings; Lj. Manojlovic-Muir; K.W. Muir; R.J. Puddephatt; J. Chem. Soc. Chem. Commun. 159 (1989).

42. K.S. Ratliff; P.E. Fanwick; C.P. Kubiak; Polyhedron *9*, 1487 (1990).

43. J.K. Gong; C.P. Kubiak; Inorg. Chem. Acta. *162*, 19 (1989).

44. (a) R. Hoffman; J. Chem. Phys. *39*, 1397 (1963).

(b) A. Rossi; J. Howell; D. Wallace; K. Harki; R. Hoffmann; J. Am. Chem. Soc. *100*, 3686 (1978).

(c) J.H. Ammeter; H.-B. Burgi ; J.C. Thibault; R. Hoffmann, J. Am. Chem. Soc. *98*, 3686.(1976).

(d) R.H. Summerville; R. Hoffmann; J. Am. Chem. Soc. *98*, 7240 (1976).

Chapter 7

Synthesis and Characterization of Di- and Trinuclear Nickel Complexes with Bis(dimethylphosphino)methane Bridging Ligands.

7.1 Introduction

For group 10 metals two areas of chemical research have received considerable attention in recent years. First is the formation of binuclear metal complexes stabilized by diphosphine ligands. When the diphosphine ligand has the ability to form binuclear complexes, the strong metal-phosphorus bonds lock together the two metal centres in close proximity and hence can promote organometallic reactions involving two metal centres.[1]

A large number of such binuclear complexes involving palladium and platinum have been prepared and their reactivity has been investigated. However, analogous nickel complexes have not been studied in such depth. Recently it has been shown that di- and trinuclear metal complexes of the type $[M_2(L\text{-}L)_2X_4]$ (Where L-L = bidentate ligand such as dppm, dpam) and $[M_3(dppp)_2X_4]$ exhibit luminescent properties.[2-4] These findings have generated considerable interest in the photochemical nature of these species with the aim of developing model photocatalysts based on homo- and heteronuclear complexes.

The second area which has been the centre of focus for the last several years is the synthesis of trinuclear metal complexes. This is primarily because of the potential of these systems to serve as models for catalysis, and due to the idea that trinuclear metal clusters mimic the smallest fragment of a metal surface.[5] Thus, reaction

occurring on trinuclear clusters would mimic the reactions on metal surfaces. In this regard the group 10 metals have received considerable attention. Most of the work is, however, directed on the synthesis and reactivity studies of complexes of palladium and platinum. In contrast, nickel has not been explored much. There are only a few trinuclear nickel clusters with bridging diphosphine ligands and their chemistry has not been investigated. Almost all of these clusters are electronically saturated.

One of the objectives of cluster synthesis is to make coordinatively unsaturated complexes and then to investigate their reactivity in comparison to metal surfaces. In this regard, when one compares the cluster complexes of Ni, Pd and Pt, it can be easily noticed that the chemistry of Pd and Pt is quite different than Ni.[6] Thus, for triangulo-M_3 clusters when M=Pd or Pt, the complexes are typically coordinatively unsaturated with 42-electrons {e.g. $[M_3(\mu\text{-}CO)_3(PR_3)_3]$, $[M_3(\mu_3\text{-}CO)(\mu\text{-}dppm)_3]^{2+}$},[6,7] 44-electrons {e.g. $[M_3(\mu_2\text{-}CO)_3(PR_3)_4]$[6], $[M_3(\mu_3\text{-}CO)(\mu\text{-}dppm)_3(PR_3)]^{2+}$},[7] or 46-electrons {e.g. $[Pt_3(\mu_2\text{-}CO)(\mu\text{-}dppm)_4]^{2+}$}[8] configurations. However, when M = Ni, most examples are coordinatively saturated with 48e {e.g. $[Ni_3(CO)_6\{\mu_3\text{-}HC(PPh_2)_3\}]$[9], $[Ni_3(\mu_3\text{-}CPh)(C_5H_5)_3]$[6] or 49-53e {e.g. $[Ni_3(\mu_3\text{-}CO)_2(C_5H_5)_3]$, $[Ni_3(\mu_3\text{-}S)_2(C_5H_5)_3)]$}[6,10] configurations. Despite these differences there are connections between Ni and Pt in the cluster anions derived from $[M_3(CO)_6]^{2-}$; however, the parent is not known when M = Ni. In addition, there are interesting structural differences in the higher nuclearity clusters.[6,11] Therefore, the synthesis of new Ni_3 complexes in this work offers an unusual opportunity to compare the structures and properties of trinickel complexes bridged by diphosphine ligands with the properties of analogous palladium and platinum complexes.

This chapter describes the syntheses of di- and trinuclear nickel complexes stabilized by the ligand dmpm, which is a less bulky and better σ-donor than dppm. It was found that the reactions of metal halide salts with BH_3CN^- a mild reducing agent, leads to B-C bond cleavage and to dimer or cluster formation. The reactions were found to be dependent on the experimental conditions. Details of these reactions are described in the following pages.

7.2 Synthesis of $[Ni_2(CN)_4(\mu\text{-dmpm})_2]$, 7.1

The complex $[Ni_2(CN)_4(\mu\text{-dmpm})_2]$ is a minor product in the synthesis of $[Ni_3(\mu\text{-CO})(\mu\text{-dmpm})_4]^{2+}$ which will be discussed later in this chapter. It forms according to the equation 7.1,

$$2Ni(II) + 2dmpm + 4BH_3CN^- \rightarrow [Ni_2(CN)_4(\mu\text{-dmpm})_2] + 2B_2H_6 \qquad (7.1)$$

The complex is precipitated out as a yellow-orange microcrystalline solid from the reaction solution and it can be recrystallized from methylene chloride/acetone solution by adding a layer of ethanol.

7.2.1. The Structure of $[Ni_2(CN)_4(\mu\text{-dmpm})_2]$, 7.1

The ORTEP diagram of complex 7.1 is depicted in Figure 7.1. The molecule, like $[Pd_2(CN)_4(\mu\text{-dppm})_2]$, 7.2, and $[Pt_2(CN)_4(\mu\text{-dppm})_2]$, 7.3[2,3], has a crystallographically imposed centre of symmetry. It consists of two nickel atoms bridged by two dmpm groups and two cyanide ligands are bonded to each nickel

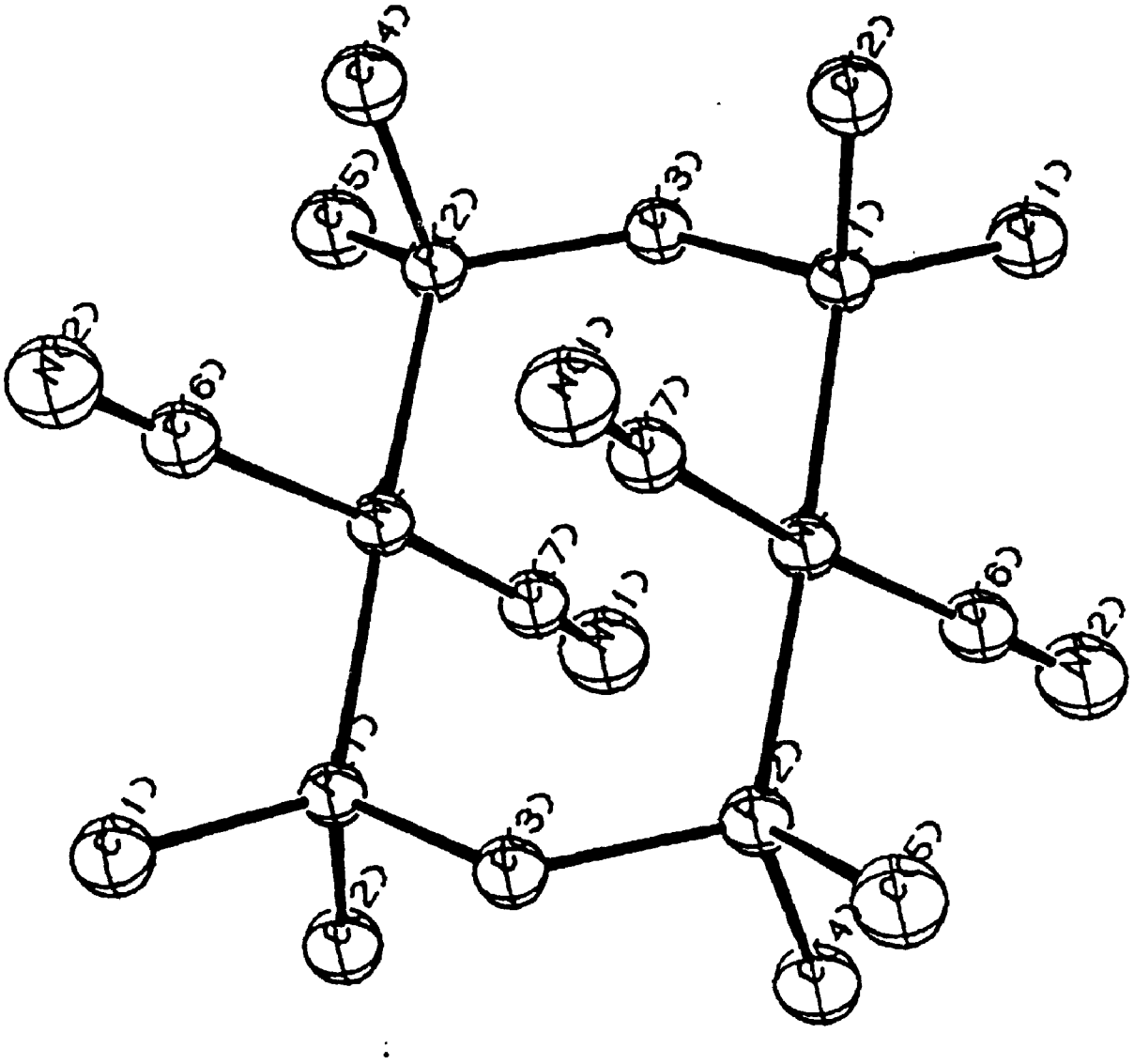

Figure 7.1: The ORTEP diagram of $[Ni_2(CN)_4(\mu\text{-dmpm})_2]$, 7.1.

atom. Each nickel atom exhibits approximately square planar coordination, with two trans cyano groups and two trans phosphorus atoms from the dmpm ligands, thus giving each nickel a 16 electron count. Selected bond distances and angles are given in Table 7.1. It can be seen that the P-Ni-P angles of 178.1(1)° are very close to that of rectilinear geometry. It is also apparent from Table 7.1 that the C(6)-Ni-C(7) angles of 170.5(3)° are significantly distorted from 180°, suggesting the presence of a weak interunit Ni...CN bonding interactions as in 7.2 and 7.3.[2,3] The coordination planes of the nickel atoms are parallel to each other with the Ni-Ni vector approximately perpendicular to the P-Ni-P axis. The measured Ni-C distances of 1.870(7)Å and 1.898(7)Å are slightly longer then the average values of Ni-C bond distances at 1.85Å in the compounds containing the ion $[Ni(CN)]_4^{2-}$. They are however, close to the Ni-C(CN) distances of 1.873Å in trans-$[Ni(CN)_2(PPh_3)_2].C_2N_2$.[4]

An important structural feature of the $[Ni_2(CN)_4(\mu\text{-dmpm})_2]$ molecule is the intramolecular Ni...Ni separation of 3.209(1)Å which suggests a weak Ni...Ni interaction. Direct Ni-Ni bonds are usually in the range of 2.29-2.59Å[12] whereas non bonded separations have been reported to occur in the range of 3.3-4.4Å.[13,14] This separation in $[Ni_2(CN)_4(\mu\text{-dmpm})_2]$ is in the middle of these two ranges although close to the non bonded separation. Another interesting feature to be noted here is the bond angles Ni-C(7)-N(1) 173.2(7)° and Ni-C(6)-N(2) 178.6(7)° which indicate that one of the cyano group on each nickel bends away from the adjacent group possibly as a result of non bonded repulsive interactions, which is in contrast to palladium and platinum analogues where both groups bend back.[2,3] The structures of

Table 7.1: Selected Bond Lenghts (Å) and Angles (°) For $[Ni_2(CN)_4(\mu\text{-dmpm})_2]$.

Ni - P(1)	2.198(2)	Ni - P(2)	2.190(2)
Ni - C(6)	1.870(7)	Ni - C(7)	1.898(7)
P(1) - C(1)	1.813(8)	P(1) - C(2)	1.820(8)
P(1) - C(3)	1.838(7)	P(2) - C(3)	1.832(7)
P(2) - C(4)	1.816(8)	P(2) - C(5)	1.833(9)
N(1) - C(7)	1.071(11)	N(2) - C(6)	1.414(11)
Ni ... Ni'	3.209(1)	P(1)...P(2')	3.144(2)

Bond Angles (°)

P(1)-Ni-P(2)	178.1(1)	P(1)-Ni-C(6)	91.4(3)
P(1)-Ni-C(7)	89.1(3)	P(2)-Ni-C(6)	90.4(3)
P(2)-Ni-C(7)	89.3(3)	C(6)-Ni-C(7)	170.5(3)
Ni-P(1)-C(1)	119.3(3)	Ni-P(1)-C(2)	117.5(3)
Ni-P(1)-C(3)	109.1(3)	C(1)-P(1)-C(2)	101.6(4)
C(1)-P(1)-C(3)	101.5(4)	C(2)-P(1)-C(3)	106.0(4)
Ni-P(2)-C(3)	115.6(3)	Ni-P(2)-C(4)	116.3(3)
Ni-P(2)-C(5)	113.1(3)	C(3)-P(2)-C(4)	105.0(4)
C(3)-P(2)-C(5)	100.7(4)	C(4)-P(2)-C(5)	104.4(4)
P(1)-C(3)-P(2')	117.9(4)	Ni-C(6)-N(2)	178.6(7)
Ni-C(7)-N(1)	173.2(7)		

the palladium and platinum analogues (with dppm ligands in place of dmpm) have also been established by X-ray crystallography[2,3], and are shown in Figure 7.2.

7.2.2. Spectroscopic Characterization

The infrared spectrum of complex 7.1 shows a stretch at 2120 cm^{-1} attributed due to ν(CN) in addition to a weak band at 2102 cm^{-1}. The single strong stretch at 2120 cm^{-1} indicates that the two cyano groups have trans geometry. Both the Pd and Pt analogues, $[M_2(CN)_4(\mu\text{-dppm})_2]$, also exhibit a single ν(CN) stretch at 2130 cm^{-1}.[2,3,15] The 10 cm^{-1} decrease in energy of the IR frequency in complex 7.1 compared to the palladium and platinum complexes may be due to the greater basicity of dmpm in the case of the nickel compared to dppm in the palladium and platinum complexes. Thus, the effect will cause more back bonding and therefore weakening of the C≡N bonds for the nickel complex.

The $^{31}P\{^1H\}$NMR spectrum of 7.1 shows a single resonance as expected at δ = 34 ppm . This suggests that all four phosphorus atoms are in equivalent positions, and hence that the solid state structure is maintained in solution. Again this is in complete agreement with the $^{31}P\{^1H\}$NMR of $[Pd_2(CN)_4(\mu\text{-dppm})_2]$ and $[Pt_2(CN)_4(\mu\text{-dppm})_2]$; in both cases a single resonance was observed.[15] The ^1H NMR spectrum of $[Ni_2(CN)_4(\mu\text{-dmpm})_2]$ shows a triplet at δ = 2.3 ppm due to the P-CH_2-P protons. Usually for this type of molecule a quintet is expected due to virtual coupling. Indeed, for the palladium analogue a quintet was observed for the methylene protons. However, in the case of platinum, the ^1H NMR spectrum shows only a triplet. For the dmpm ligand, the ^1H NMR spectrum shows a doublet centered at δ = 1.65 ppm,

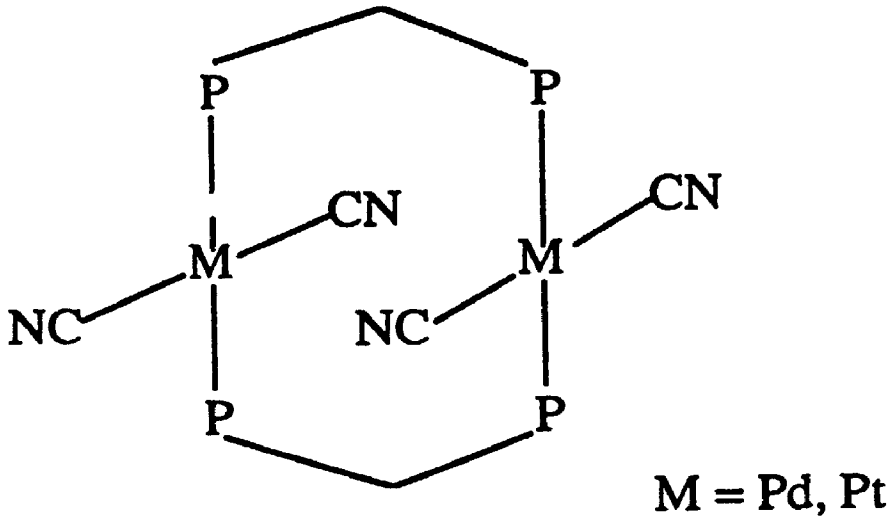

Figure 7.2: The structure of $[M_2(CN)_4(\mu\text{-dppm})_2]$ complexes, (M = Pd, Pt).

with $^2J(PH)$ = 12.5Hz, for the Me-P protons.

Therefore, all the analytical and spectroscopic results are in complete agreement with the structure established by X-ray diffraction studies and shown in Figure 7.1

7.3. Synthesis of $[Ni_3(\mu_3\text{-}CO)(\mu\text{-}dmpm)_4][X]_2$ X_2 = $[Na(NCBH_3^-)_3]$, $[PF_6^-]_2$, $[BPh_4^-]_2$, 7.4

The complex $[Ni_3(\mu_3\text{-}CO)(\mu\text{-}dmpm)_4][Na(NCBH_3)_3]$ 7.4 was prepared by reduction of nickel(II) chloride with $Na[BH_3CN]$ in the presence of dmpm and CO according to the following equation,

$$3Ni(II) + 4dmpm + 4e^- + CO \rightarrow [Ni_3(\mu_3\text{-}CO)(\mu\text{-}dmpm)_4]^{2+} \quad (7.2)$$

Large black crystals (smaller crystals are purple) formed in the reaction solution. The cation $[Ni_3(\mu_3\text{-}CO)(\mu\text{-}dmpm)_4]^{2+}$ could also be precipitated as the BPh_4^-, 7.4b, and PF_6^-, 7.4c, salts. Purple solutions of the cation 7.4 are easily oxidized by air but the solid complexes are air-stable.

7.3.1. Crystal Structure of $[Ni_3(\mu_3\text{-}CO)(\mu\text{-}dmpm)_4][Na(NCBH_3)_3]$ 7.4

The structure of 7.4 was established by a single crystal X-ray diffraction study. This reveals that the dication consists of three nickel centres bonded to each other forming a triangle. Each edge of the triangle is bridged by a dmpm ligand thus forming a roughly planar $Ni_3(\mu\text{-}dmpm)_3$ unit, with a μ_3-CO ligand and a μ_2-dmpm

ligand axially bound on either side of the Ni_3 triangle. Figure 7.3 shows the ORTEP diagram of complex 7.4; selected bond lengths and bond angles are given in Table 7.2. The overall cluster electron count is 46e, and this appears to be unique in Ni_3 clusters.[6,9,10] The centre of coordinative unsaturation is clearly at Ni(3), since the extra axially bound μ-dmpm ligand coordinates to Ni1 and Ni2. The Ni-Ni distances (as given in Table 7.2) are in the expected range for single bonds.[6,10,11] Coordinatively unsaturated clusters sometimes take part in metal-metal multiple bonding, but these Ni-Ni bond distances do not suggest such an effect since they are very similar to values in 48-electron Ni_3 clusters.[6,10,11] The Ni(3) centre differs both sterically and electronically from Ni(1) and Ni(2). This difference has, however, little influence on the Ni-Ni bond distances. Thus, the Ni(1)-Ni(2) distance of 2.4596(5)Å is slightly longer than Ni(2)-Ni(3) and Ni(1)-Ni(3) at 2.4360(4) and 2.3756(5) Å respectively. This lengthening of the Ni(1)-Ni(2) bond may be due to steric effects. From Table 7.2 it is also apparent that the Ni-P bond distances are sensitive to their environment. Thus, the Ni(3)-P(6) and Ni(3)-P(7) bond lengths at 2.1828(9) and 2.2004(8)Å respectively are the shortest among all Ni-P bonds. Moreover, the Ni-P distances of the axially bound dmpm ligand, Ni(1)-P(3) and Ni(2)-P(4) at 2.2589(8) and 2.2544(8)Å respectively are the longest Ni-P distances. These differences may arise as a result of a rehybridization of nickel orbitals due to the higher coordination numbers of Ni(1) and Ni(3), or it could simply be the result of steric congestion at these sites. However, these distances are all in the expected range for Ni-P single bonds.

All nickel-carbonyl distances are in the bonding range, though the Ni(3)-C

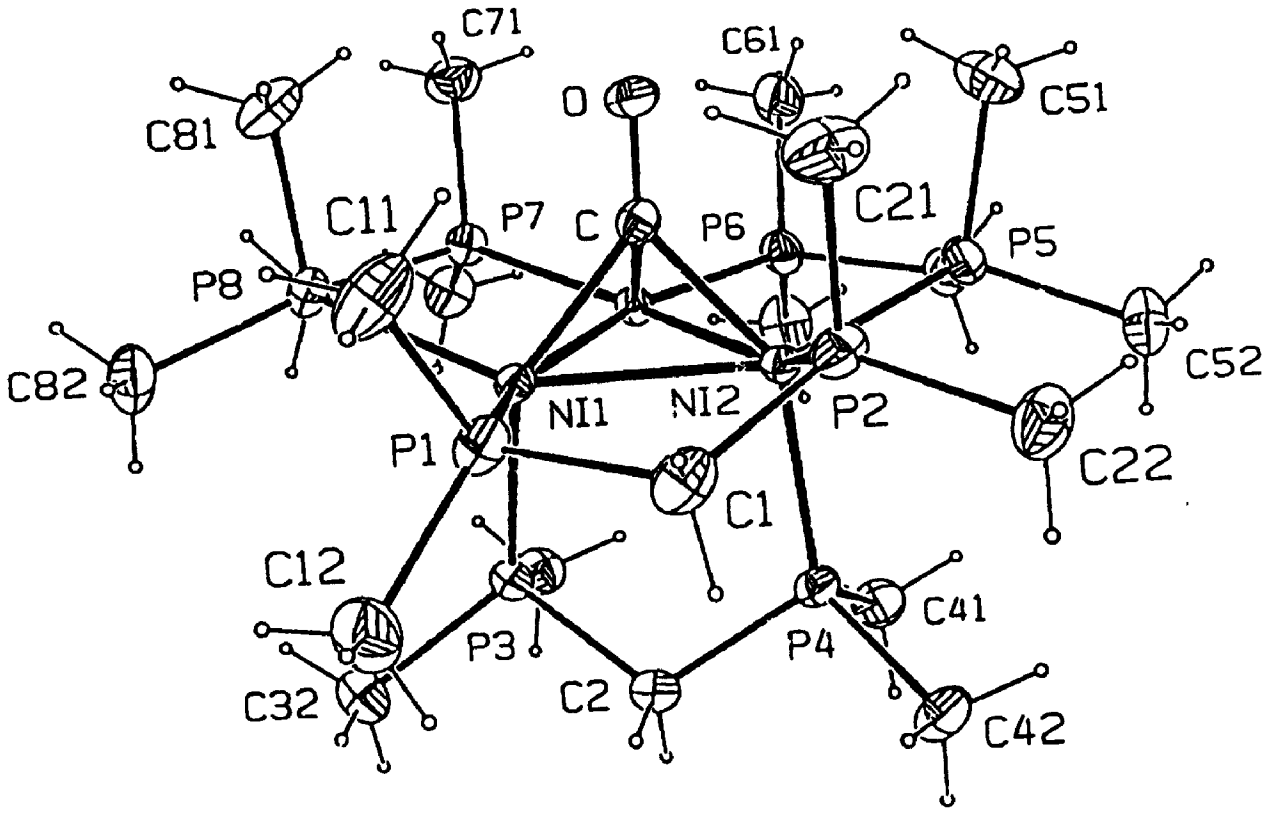

Figure 7.3: The ORTEP diagram of the cation $[Ni_3(\mu_3\text{-}CO)(\mu\text{-}dmpm)_4]^{2+}$, 7.4.

Table 7.2: Selected Bond Lengths (Å) and Bond Angles (°) For $[Ni_3(\mu_3\text{-}CO)(\mu\text{-}dmpm)_4][Na(NCBH_3)_3]$.

Ni1-Ni2	2.4596(5)	O-C	1.189(3)
Ni1-Ni3	2.3756(5)	Na-N91	2.387(3)
Ni1-P1	2.2119(8)	Na-N92	2.374(4)
Ni1-P3	2.2589(8)	Na-N93	2.370(4)
Ni1-P8	2.2043(8)	N91-C91	1.134(4)
Ni1-C	1.916(3)	C91-B91	1.561(6)
Ni2-Ni3	2.4360(4)	N92-C92	1.126(5)
Ni2-P2	2.2172(8)	C92-B92	1.567(7)
Ni2-P4	2.2544(8)	N93-C93	1.138(5)
Ni2-P5	2.1958(9)	C93-B93	1.545(6)
Ni2-C	1.906(3)	Ni3-P7	2.2004(8)
Ni3-C	2.028(3)	Ni3-P6	2.1828(9)

Bond Angles (°)

Ni2-Ni1-Ni3	60.47(1)	Ni2-Ni1-P1	95.27(3)
Ni2-Ni1-P3	95.56(2)	Ni2-Ni1-P8	149.43(3)
Ni2-Ni1-C	49.76(8)	Ni3-Ni1-P1	154.65(3)
Ni3-Ni1-P3	85.74(2)	Ni3-Ni1-P8	97.88(2)
Ni3-Ni1-C	55.16(8)	Ni1-Ni2-Ni3	58.06(1)
Ni1-Ni2-C	50.12(8)	Ni3-Ni2-C	54.05(8)
Ni1-Ni3-Ni2	61.47(1)	Ni1-Ni3-C	50.82(8)
Ni2-Ni3-C	49.51(8)	Ni1-C-O	138.7(2)
Ni2-C-O	137.6(2)	Ni3-C-O	122.9(2)
N91-Na-N92	117.8(1)	N91-Na-N93	106.7(1)
N92-Na-N93	111.6(1)	Na-N91-C91	174.2(3)
Na-N92-C92	164.3(4)	N92-C92-B92	179.2(4)
Na-N93-C93	143.6(3)	N93-C93-B93	179.5(4)

distance (2.028(3)Å) is significantly longer than the other two Ni-C distances (Ni(1)-C = 1.916(3)Å, Ni(2)-C = 1.906(3)Å). Furthermore, the Ni(3)-Ni(1)-C and Ni(3)-Ni(2)-C bond angles at 55.16(8)° and 54.05(8)° respectively compared to Ni(1)-Ni(3)-C at 50.82(8)° and Ni(2)-Ni(3)-C at 49.51(8)° suggest that the carbonyl group is not symmetrically bridging the Ni_3 triangle, but that it is distorted towards the Ni(1)-Ni(2) bond and away from the Ni(3) centre. The bond angles of Ni(3)-C-O, Ni(2)-C-O and Ni(1)-C-O at 122.9(2)°, 137.6(2)° and 138.7(2)° respectively indicate that the C-O bond is bent back towards the Ni(3) centre.

The anion also has an interesting structure containing a sodium ion trigonally coordinated to three cyanoborohydride ligands, with distances Na-N = 2.370(4), 2.374(4) and 2.387(3) Å as shown in Figure 7.4. Most coordination compounds of sodium have coordination number 6, and, although there are some with coordination number 3, they contain much more complex ligands than the present example.[16]

The major structural differences between the cation 7.4 and the analogous platinum cluster cation $[Pt_3(\mu_2\text{-CO})(\mu\text{-dmpm})_4]^{2+}$ (7.5)[8] is that in 7.4 the carbonyl ligand is best considered as a distorted μ_3-CO species, whereas in 7.5 it is more distorted toward μ_2-CO, as shown in Figure 7.5.[8] The Pt(3)-C distance is 2.47(1)Å, and the interaction with Pt(3) is therefore weak. The carbonyl bends back away from Pt(3) by only 6° in 7.5, whereas it bends away from Ni(3) by 13° in 7.4, with respect to the M(1)M(2)C plane. Thus, the M(3)-CO bonding is much weaker in 7.5 than in 7.4, but a weak semibridging interaction is still possible.

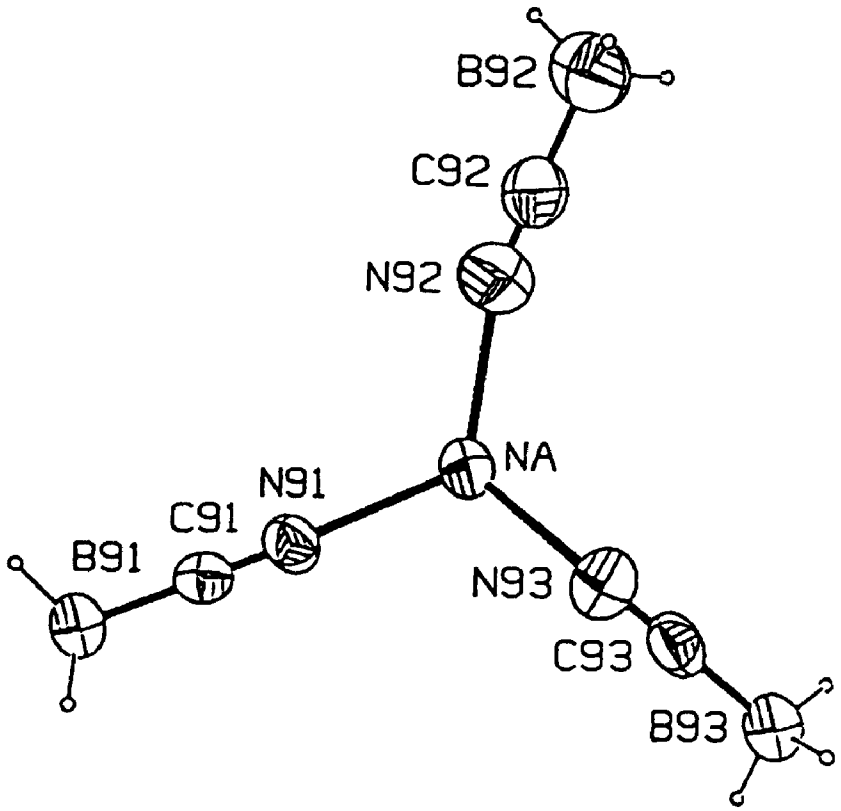

Figure 7.4: The X-ray structure of the anion $[Na(NCBH_3)_3]^{2-}$

Figure 7.5: The geometry of bridging carbonyl group in 7.4 and 7.5.

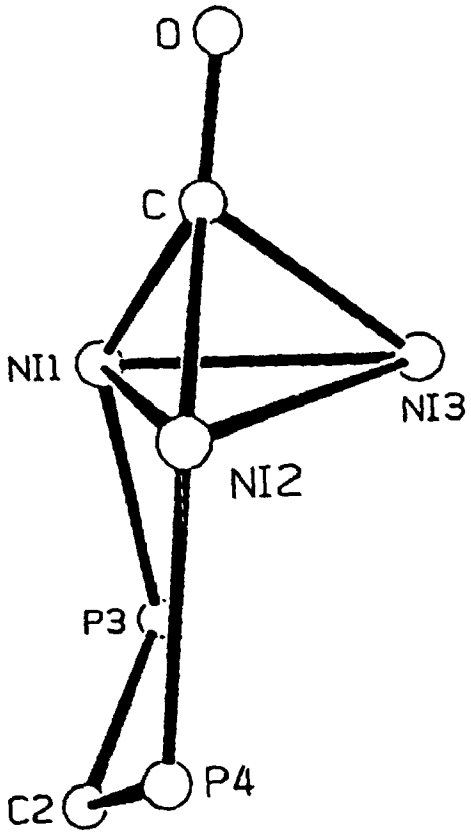

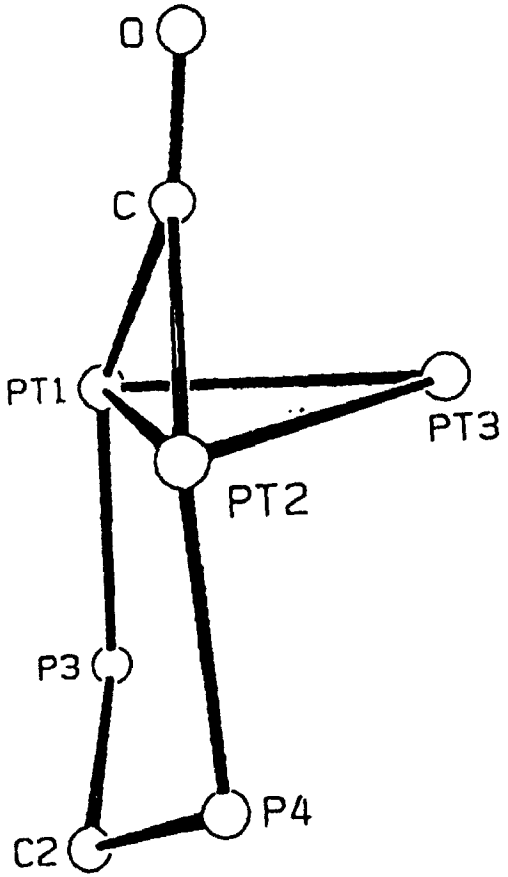

7.3.2. Spectroscopic Characterization

The IR spectrum shows a carbonyl stretching frequency for 7.4 at 1700 cm^{-1}, consistent with a triply bridging carbonyl.[17] The CO stretching frequencies for doubly bridging carbonyl groups in nickel complexes are usually higher in energy. For example doubly bridging CO group in $[Ni_2(\mu\text{-}CO)(CO)_2(\mu\text{-}dppm)_2]$ appears at 1790 cm^{-1}.[18] Similarly, the analogous $[Pt_3(\mu_2\text{-}CO)(dmpm)_4]^{2+}$ cluster exhibits an IR stretch at 1730 cm^{-1}, in accordance with the doubly bridging CO group.[6]

The room temperature $^{31}P\{^1H\}$ NMR spectrum of 7.4 contains only two resonances, a triplet and septet with an intensity ratio of 3:1, respectively, each with J(PP)=7 Hz. Thus, each of the phosphorus atoms P3 and P4 couples equally to the other six phosphorus atoms, implying rapid rotation of the axial dmpm ligand about the Ni_3 triangle and indicating that the molecule is fluxional. The resonance at δ = -29 ppm is due to the equatorial phosphorus atoms P^aP^b and P^c while the resonance at δ = -11 ppm is due to phosphorus atoms P^d, the axially bound dmpm ligand. However, at lower temperature this fluxionality was slower and the expected spectrum for the static structure 7.4 was obtained. Both room temperature and low temperature $^{31}P\{^1H\}$ NMR spectra of complex 7.4 are shown in Figure 7.6.

In clusters of this kind, there is a large coupling $^3J(PP)$ for the roughly linear PMMP units.[7,8] In complex 7.4, such couplings are $^3J(P^bP^b)$and $^3J(P^aP^c)$ (Figure 7.6) and it follows that the singlet resonances at δ = -26.3 ppm is due to P^b while the "AB" doublets at δ = -29.2 and -32.6 ppm are due to P^a and P^c with $^3J(PP)$ = 138 Hz. The assignment of P^a and P^c to individual resonances is arbitrary and is based on a comparison with the spectrum of 7.5, in which couplings to ^{195}Pt permit a more

Figure 7.6: The ^{31}P NMR spectra of complex 7.4, (a) at 25°C and (b) at -90°C.

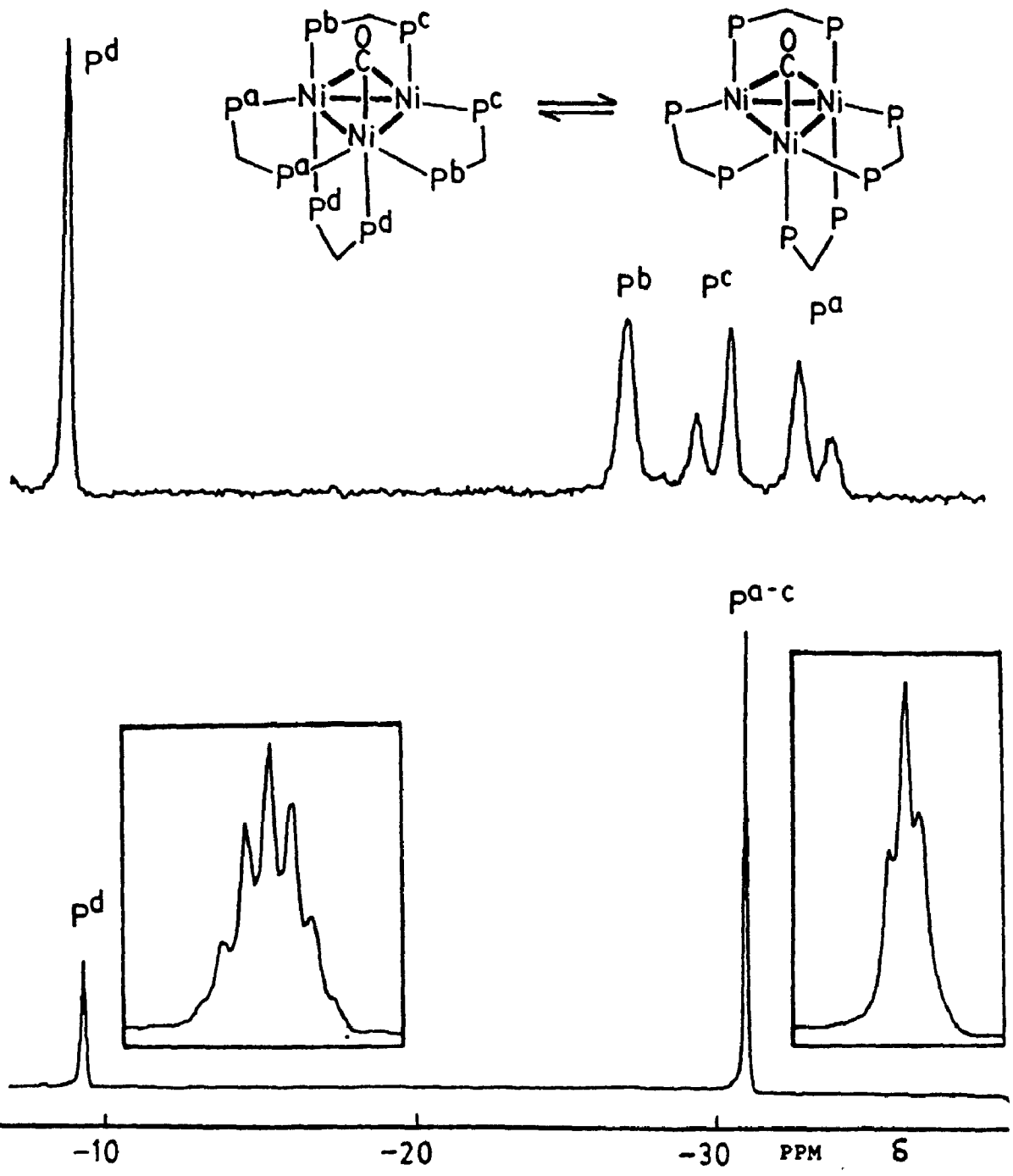

complete assignment.[8] The ^{31}P resonances are broad, at least partly due to the presence of unresolved PP couplings. This leads to the second difference between 7.4 and 7.5, namely that 7.4 is fluxional but 7.5 is not. Thus, while the NMR data for 7.5 at 25°C are fully consistent with the structure determined crystallographically,[8] this is not the case for 7.4.

The fluxionality of 7.4 also leads to equivalence of the $CH^aH^bP_2$ and Me_2P protons of the axial dmpm ligand in the room temperature ^1H NMR spectrum. The equatorial dmpm ligands give two resonances for the CH^aH^b and Me^aMe^bP protons, since these ligands are effectively equivalent due to the fluxionality, but this fluxional process does not lead to an effective plane of symmetry containing the Ni_3P_6 plane. The corresponding fluxionality of 7.5 would require a greater motion of the carbonyl ligand as well as the axial dmpm ligand, and so the structural difference between 7.4 and 7.5 could be a contributing factor to the higher activation energy for fluxionality of 7.5. We note, however, that the complex $[Pt_3(\mu\text{-CO})(\mu\text{-dppm})_4]^{2+}$ (7.6; dppm = $Ph_2PCH_2PPh_2$) does exhibit fluxionality similar to that of 7.4 and that the fluxionality is not frozen out at -80°C.[8] In complex 7.6 the fourth dppm ligand is weakly bound due to steric hindrance and the fluxionality is evidently faster due to this effect.[8]

7.3.3. Mechanism of Fluxionality

As mentioned above, the complex 7.4 is fluxional and the axially bound fourth dmpm ligand can migrate around the triangular face of the nickel cluster. This form of fluxionality was earlier observed only in the case of $[Pt_3(CO)(\mu\text{-dppm})_4]^{2+}$ and its derivatives.[19] The fluxional process is shown in Figure 7.7a and it involves an

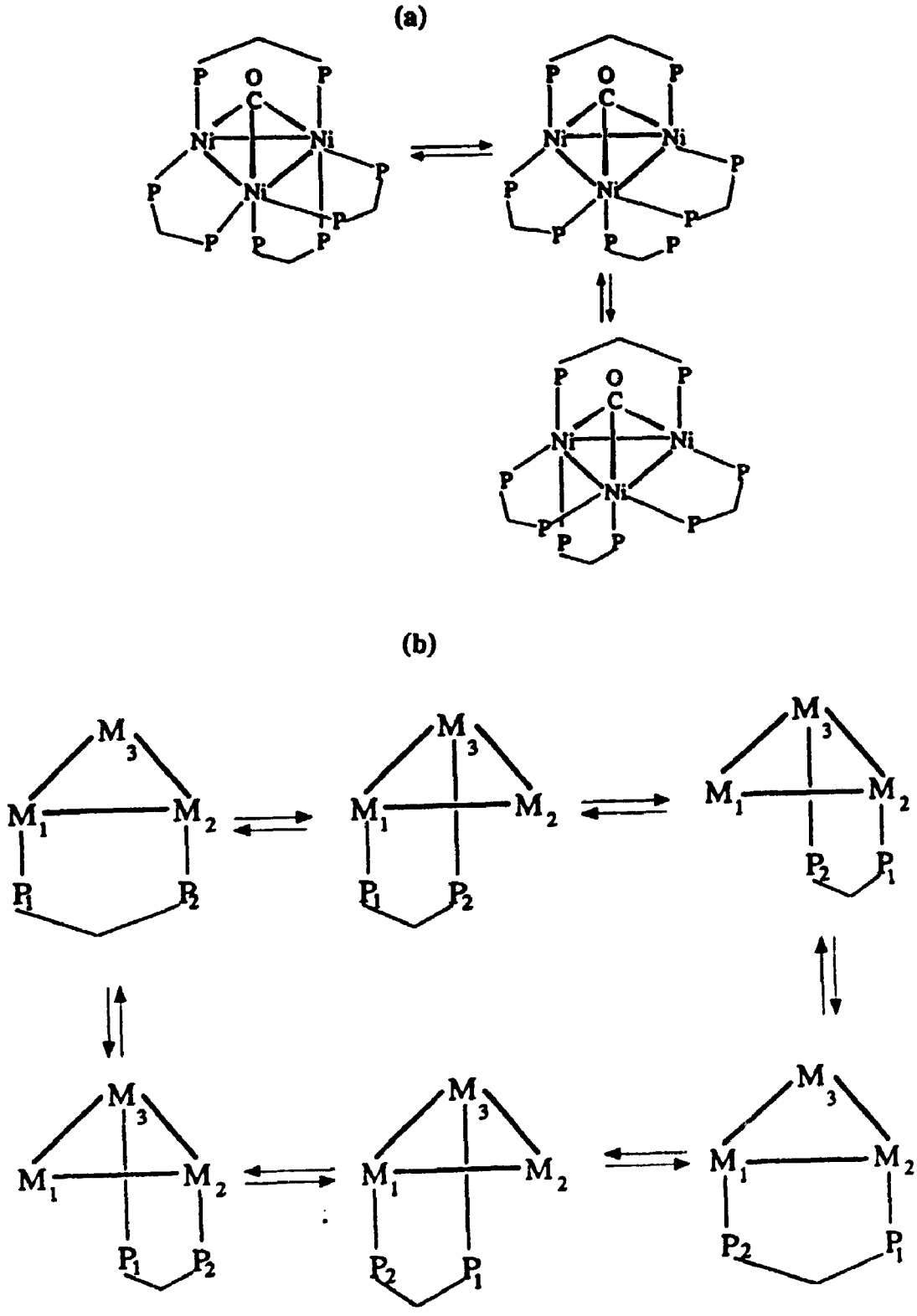

Figure 7.7: (a) Mechanism of fluxionality of dmpm ligand in 7.4, (b) six contributing structures for the complete fluxional process.

intermediate with a monodentate dmpm, although a concerted phosphorus shift is also possible. The complete fluxional process must include the six contributing species as shown in Figure 7.7b in simplified form. A fluxional process involving complete dissociation of dmpm is precluded by the NMR data. Such a mechanism which clearly can occur, although slowly on the NMR time scale, would lead to coalescence of resonances due to P^d and free dmpm. The type of fluxional process exhibited by complex 7.4 is possible only for coordinatively unsaturated clusters.

7.4. Reactivity Studies:

The reaction chemistry of trinuclear palladium and platinum clusters with 42 and 44 electron configurations has been extensively explored and it has been found that these complexes are very reactive towards a variety of small molecules.[20] However, a very limited amount of work has been done on 46 electron clusters.[21] In view of the theory that 42e configuration is favoured for group 10 M_3 clusters, it was considered that for these 46 electron clusters it may be possible to displace one of the bridging phosphine ligands or the μ-CO group rather readily.[21] Alternatively, it was thought that coordination of small molecules to the vacant coordination site of the nickel cluster may occur and stop the fluxional process. Therefore, the reactivity of 7.4 towards several small molecules was investigated. However, in most cases cluster fragmentation was observed. The results of these investigations are described below.

7.4.1. Reaction with CH_2I_2:

The reaction of 7.4 with CH_2I_2 is very slow, and leads to the fragmentation of

the cluster. The $^{31}P\{^{1}H\}$ NMR spectrum of the reaction solution monitored over a one week period shows the appearence of two resonances at δ = -6.7 ppm and -26 ppm with an intensity ratio of approximately 1:1. The reaction solution turned slowly to a green colour from the original purple colour over a one week period . No pure product could be isolated. Similar reactions with $PhPH_2$ and KCN also led to mixtures of products which could not be separated.

7.4.2. Reaction with MeNC:

When a solution of the hexafluorophosphate salt of 7.4 was treated with a large excess of MeNC, the $^{31}P\{^{1}H\}$ NMR spectrum showed the appearance of a new signal at δ = 13.5 ppm in addition to signals due to the starting complex 7.4. After a two week period, the resonances due to the complex 7.4 had disappeared and the only observed resonance was due to the species with chemical shift at δ = 13.5 ppm. Efforts to isolate this product in pure form were unsuccessful.

7.4.3. Reaction with $CO_{(g)}$:

When CO was bubbled in a solution of 7.4 and $^{31}P\{^{1}H\}$NMR was observed for the resulting solution. It shows resonances only due to the starting complex 7.4. Thus, indicating that further coordination of CO or displacement of the fourth dmpm with CO does not occur even with the excess of CO.

7.4.4. Reaction with $^{13}CO_{(g)}$

When a solution of 7.4 is exposed to excess of $^{13}CO_{(g)}$, over a period of one

day, an exchange of ^{12}CO by ^{13}CO took place, yielding 7.4*. This was characterized by ^{13}C NMR and IR spectroscopy. [IR: $\nu(^{13}CO)$ = 1645.5 cm^{-1}, ^{13}C NMR $\delta(^{13}CO)$ = 207.3 ppm].

7.5. Conclusion:

The reaction of metal salts with BH_4^- or BH_3CN^- to give useful new complexes has been known for some time. The mechanism of reaction is fairly complex and is not fully understood yet. A large variety of products have been observed to be formed by this route. Although in most cases simple reduction of the metal salt occurs, hydride and cyanide complexes have also been observed in these reactions. Ready cleavage of the B-C bond of BH_3CN^- has been seen before.[17] Very recently, coordination of a BH_2 group to the metal has also been observed in these laboratories.[22]

It is shown in the present work that reduction of metal salts with BH_3CN^-, a mild reducing agent, can lead to B-C bond cleavage as well as to cluster formation. The reaction product has been found to be dependent on the experimental conditions. Thus, if reaction is stopped within a few minutes after the addition of BH_3CN^-, then the cyano complex $[Ni_2(CN)_4(\mu\text{-dmpm})_2]$ is predominant. However, if the reaction is carried out over longer time periods after the addition of BH_3CN^-, then the trinuclear cluster $[Ni_3(\mu\text{-CO})(\mu\text{-dmpm})4]^{2+}$ is the dominant species formed.

There is an interesting difference between this reaction and the reaction carried out using Co(II) halide salts (chapter 4), in that when ligand to metal ratio was 1:1, the reaction of cobalt(II) formed a tetranuclear cluster and increasing the ligand to

metal ratio facilitated the formation of a dinuclear complex. In contrast, for nickel(II) salts, when the ligand to metal ratio was increased the trinuclear cluster was formed and lower ratios resulted in the formation of a dinuclear complex predominantly.

The dinuclear nickel complex $[Ni_2(CN)_4(\mu\text{-dmpm})_2]$ has the same trans geometry as that of the dppm bridged palladium and platinum analogues. However, luminescent properties have not been observed in the nickel complex. There are two major differences between $[Ni_3(\mu_3\text{-CO})(\mu\text{-dmpm})_4]^{2+}$ and its platinum analogue. The first major difference is that the CO group is triply bridging in the case of nickel while it is doubly bridging in the platinum cluster. Secondly, the nickel cluster is fluxional at room temperature while the platinum cluster is not. Thus, while the room temperature ^{31}P NMR spectrum of the platinum cluster is in agreement with its static structure, this is not the case for the nickel cluster.

There are also differences observed in terms of reactivity. The platinum cluster is found to be inert to most reagents.[21] However, fragmentation of the nickel cluster was observed in almost all reactions, which indicates that the nickel cluster is more reactive than the platinum analogue. This difference may be due to steric reasons, since nickel is small compared to platinum and therefore, addition of another ligand to the coordinatively unsaturated site may cause greater steric congestion in the nickel cluster. In turn, this leads to fragmentation of the nickel cluster, while platinum has less steric congestion and therefore is more stable. Both the nickel and platinum clusters undergo exchange with ^{13}CO to give $[M_3(^{13}CO)(\mu\text{-dmpm})_4]^{2+}$.

7.6. Experimental Section

All manipulations were carried out under an atmosphere of dry nitrogen.

7.6.1. $[Ni_2(CN)_4(dmpm)_2$

To an ethanolic solution (40 mL) of $NiCl_2.6H_2O$ (0.5g; 2.10 mmol) was added dmpm (1.18g; 8.69 mmol) dropwise. The resulting deep red solution was stirred under a slow stream of CO gas for a period of 30-40 min. $NaBH_3CN$ (0.5g; 8.10 mmol) in ethanol (15mL) was then added dropwise over a period of 15 min. forming a greenish-blue solution with a yellow suspension. CO gas was bubbled for a further 5-7 min. and the resulting mixture was then filtered. The yellow solid was washed with n-pentane (10mL) and dried under vacuum. Yield: 40%

The solid product can be recrystallized from CH_2Cl_2 and ethanol to yield an orange crystalline product.

Anal.Calc. for $C_{14}H_{28}N_4P_4Ni_2.2CH_2Cl_2$

C, 28.9; H, 4.8; N, 8.5% Found: C, 28.9; H, 4.9; N, 9.3%.

IR: ν(CN) 2120 cm^{-1}, 2103 cm^{-1}(w); NMR (CD_2Cl_2) ^1H: δ = 2.3[t, 4H, CH_2P_2]; 1.67[d, 12H, MeP]; ^{31}P: δ = 31.6ppm .

7.6.2. $[Ni_3(\mu_3\text{-}CO)(\mu\text{-}dmpm)_4][Na(BH_3CN)_3]$.

To a solution of $NiCl_2.6H_2O$ (0.50g; 2.10 mmol) in ethanol (30mL) was slowly added $Me_2PCH_2PMe_2$(1.18g; 8.69 mmol), and the dark brown solution was stirred under a slow stream of CO for 0.5 h. A solution of $NaBH_3CN$ (0.50g; 8.10 mmol), in ethanol (15mL) was then added slowly (15min), and the purple reaction

mixture was stirred under CO for 2h. The solution was filtered, the volume of solvent was reduced to ca. 7mL, and the solution was layered with ether (10mL) and allowed to stand at 0°C for 1 week. The intensely purple crystals (large crystals appeared black) of the product that formed were washed with pentane and dried under vacuum: Yield 35%; mp 203-204°C. An analytically pure sample was obtained from CH_2Cl_2 and was shown by ^1H NMR spectroscopy to contain occluded CH_2Cl_2. Anal. Calc for $C_{24}H_{65}B_3N_3NaNi_3OP_8.CH_2Cl_2$: C, 30.8; H, 6.9; N, 4.3%. Found, C, 29.6; H, 6.8; N, 4.6%. IR (Nujol): ν(CO) 1700, 1688cm^{-1}; ν(BH) and ν(CN) 2319, 2270, 2253, 2178, 2169 cm^{-1}. NMR at 25°C in CD_3OD: ^1H, δ 3.07[d, 3H, $^2J(HH)$ = 14Hz, $CH^aH^bP_2$]; 2.89[d, 3H, $^2J(HH)$ = 14Hz, $CH^aH^bP_2$]; 2.56[t, 2H, $^2J(PH)$ = 10Hz, $CH_2P^d_2$]; 1.83[12H, MeP^d]; 1.53, 1.39[each 18H, MeP^{a-c}]; 1.84[1:1:1:1 q, 9H, $^1J(BH)$ = 88Hz, BH_3CN]; ^{31}P, δ -9.3 [septet, 2P, $^2J(PP)$ = 7Hz, P^d]; -31.1 [t, 6P, $^2J(PP)$ = 7Hz, P^{a-c}]; ^{31}P (at -80°C): δ = -7.9[s, 2P, P^d]; -26.3[s, 2P, P^b]; -29.2[d, 2P, $^3J(PP)$ = 138Hz, P^c]; -32.6[d, 2P, $^3J(PP)$ = 138Hz, P^a]; ^{13}C (at -80°C): δ = 207.3[s, CO]. A limiting low temperature ^1H NMR spectrum was not obtained at -90°C, and the resonances were too broad to be useful.

7.6.3. $[Ni_3(\mu_3\text{-}CO)(\mu\text{-}dmpm)_4][PF_6]_2$.

To a solution of $[Ni_3(\mu_3\text{-}CO)(\mu\text{-}dmpm)_4][Na(BH_3CN)_3]$ (0.3g) in acetone (10 mL) was added excess NH_4PF_6 (0.2g) in ethanol (8 mL). After 5 min, pentane (20mL) was added to precipitate the product as a purple solid, which was washed with ether and pentane and dried under vacuum: Yield 90%; mp 303-306°C. Anal. Calc for $C_{21}H_{56}F_{12}Ni_3OP_{10}$: C, 24.3; H, 5.4%. Found: C, 23.9; H, 5.5%. The

NMR data for the cation were the same as for complex 7.4; IR.: ν(CO) 1694 cm^{-1}; $\nu(^{13}CO)$ = 1646 cm^{-1} (obtained as a Nujol mull from a sample enriched in ^{13}CO).

$[Ni_3(\mu_3\text{-}CO)(\mu\text{-}dmpm)_4][BPh_4]_2$, 7.4c, was prepared in a similar manner as for 7.4b, and the spectroscopic data for the cation were the same as that of 7.4.

7.7. References:

1.(a) R.J.Puddephatt; Chem. Soc. Rev. 99 (1983)

(b) B. Chaudret; B. Delavaux and R. Poilblanc; Coord. Chem. Rev. ***86***, 191 (1988).

2. H.K. Yip; T.F. Lai and C.M. Che; J. Chem. Soc. Dalton Trans. 1639 (1991).

3. C.M. Che; V.W.W. Yam; W.T. Wong and T.F. Lai; Inorg. Chem. ***28***, 2908 (1989).

4. H.K. Yip; C.M. Che and S.M. Peng; J. Chem. Soc. Chem. Commun. 1626 (1991).

5. D.J. Underwood; R. Hoffman; K. Tatsumi; A. Nakamura and Y. Yamamoto; J. Am. Chem. Soc. ***107***, 5968 (1985).

6.(a) P.W. Jolly; Comprehensive Organometallic Chemistry; G. Wilkinson; F.G.A. Stone; Eds.; Pergamon: Oxford. England, Vol.***6***, Chp. 37.7 (1982).

(b) D.M.P. Mingos; R.W.M. Wardle; Transition Met. Chem. ***10***, 441 (1985).

(c) N.K. Eremko; E.G. Mednikov; S.S. Kurasov; Russ. Chem. Rev. (Engl. Transl.) ***54***, 394 (1985).

(d) H.C. Clark; V.K. Jain; Coord. Chem. Rev. ***55***, 151 (1984). (e) C.S. Browning; D.H. Farrar; R.R. Gukathasan; S.A. Morris; Organometallics ***4***, 1750 (1985).

(f) Y. Yamamoto; K. Takahashi; H. Yamazaki; J. Am. Chem. Soc. ***108***, 2458 (1986).

(g) G. Longoni; P. Chini; J. Am. Chem. Soc. ***98***, 7225 (1976). (h) C.P. Horwitz; D.F. Shriver; Adv. Organomet. Chem. ***23***, 219 (1984).

7.(a) G. Ferguson; B.R. Lloyd; R.J. Puddephatt; Organometallics ***5***, 344 (1986).

(b) A.M. Bradford; M.C. Jennings; R.J. Puddephatt; Organometallics ***7***, 792 (1988).

8.(a) S.S.M. Ling; N. Hadj-Bagheri; Lj. Manojlovic-Muir; K.W. Muir; R.J. Puddephatt; Inorg.Chem. *26*, 231 (1987).

(b) A.M. Bradford; R.J. Puddephatt; New J. Chem. *12*, 427 (1988).

9. J.A. Osborn; G.G. Stanley; Angew. Chem. Int. Ed. Engl. *19*, 1025 (1980).

10. J.J. Maj; A.D. Rae; L.F. Dahl; J. Am. Chem. Soc. *104*, 3054 (1982) and references therein.

11.(a) A. Ceriotti; P. Chini; R.D. Perrgola; G. Longoni; Inorg. Chem. *22*, 1595 (1983).

(b) D.J. Underwood; R. Hoffmann; K. Tatsumi; A. Nakamura; Y. Yamamoto; J. Am. Chem. Soc. *107*, 5968 (1985).

12. D.L. DeLeat; D.R. Powell; C.P. Kubiak; Organomet. *4*, 954 (1985).

13. J.K. Gong; P.E. Fanwick and C.P. Kubiak; J. Chem. Soc. Chem. Commun. 1190 (1990).

14. K.R. Pörschke; Y.H. Tsay & C. Krüger; Inorg. Chem. *25*, 2097 (1986).

15. F.S.M. Hassan; D.P. Markham; P.G. Pringle; B.L. Shaw; J. Chem. Soc. Dalton Trans. 279 (1985).

16.(a) D.E. Fenton; Comprehensive Coordination Chemistry; G. Wilkinson; R.D. Gillard; J.A. McCleverty; Eds.; Pergamon: Oxford, England, Vol *3*, Chp. 23 (1987).

(b) A.S.C. Chan; H.-S. Shieh; J.R. Hill; J. Organomet. Chem. *279*, 171 (1985).

17. (a) H.A. Mirza; M.Sc. Thesis, Lakehead University (1988).

(b) D.J. Elliot; S. Haukilahti; D.G. Holah; A.N. Hughes; S. Maciaszek; R.J. Barton; Y. Luo; B.E. Robertson; Can. J. Chem. *66*, 1770 (1988).

18. D.G. Holah; A.N. Hughes; H.A. Mirza; J.D. Thompson; Inorg. Chemica. Acta

126, L7 (1987).

19. A.M. Bradford; Ph.D. Thesis, University of Western Ontario (1990).

20.(a) M. Rashidi and R.J. Puddephatt; J. Am. Chem. Soc. *108*, 7111 (1986).

(b) R.J. Puddephatt; Lj. Manojlovic-Muir; K.W. Muir; Polyhedron *9*, 2767 (1990).

(c) M.C. Jennings; N.C. Payne & R.J. Puddephatt; J. Chem. Soc. Chem. Commun. 1809 (1986).

(d) R.J. Puddephatt; M. Rashidi & J.J. Vittal; J. Chem. Soc. Dalton 2835 (1991).

21. N. Hadj-Bagheri; Ph.D. Thesis, University of Western Ontario (1988).

22. D.J. Elliot; C.J. Levy; R.J. Puddephatt; D.G. Holah; A.N. Hughes; V.R. Magnuson; I.R. Moser; Inorg. Chem. *29*, 5014 (1990).

Chapter 8

Global Summary

This thesis documents the synthesis and chemistry of binuclear and cluster complexes of Ru, Co and Ni. The main synthetic approach was to reduce metal halide salts with $NaBH_4$ or $NaBH_3CN$ in the presence of dppm and dmpm under an atmosphere of CO gas. This resulted in the production of several new complexes with interesting structural features. These complexes were characterized by using a variety of spectroscopic and analytical techniques and several of the structures were established by single crystal X-ray diffraction methods.

The reaction of metal salts with BH_4^- or BH_3CN^- to give useful new complexes has been known for some time. The mechanism of reaction is however fairly complex and is not fully understood yet. Several types of products have been observed to be formed by this route. Although in most cases simple reduction of the metal salt occurs, hydride and cyanide complexes have also been observed in several instances.

In chapter 2 reactions of Ru(III) with $NaBH_4$ are outlined. It was shown that easy reduction of ruthenium(III) to ruthenium(0) can occur, in the presence of CO and dppm, producing mainly $[Ru_2(\mu\text{-}CO)(CO)_4(\mu\text{-}dppm)_2]$, 2.1 in high yield, if good leaving groups are present on ruthenium(III) but not if chloride ligands are present. The easier reduction of metal carboxylates than metal halides should be a general effect for soft metal ions, but its success is still difficult to predict. For example, the attempted reduction of ruthenium(III) in the presence of CO and bis(dimethylphosphino)methane, dmpm, gave $[Ru(dmpm)_2(BH_3CN)_2]$ but failed to

give any ruthenium(0) carbonyl even though both $[Ru_2(CO)_5(\mu\text{-dmpm})_2]$ and $[Ru_3(CO)_{8-2n}(\mu\text{-dmpm})_n]$ (n = 1,2) are stable complexes. Similarly, attempted reduction of osmium(III) chloride in the presence of silver acetate, dppm and CO failed to give any osmium(0) carbonyls. The chemistry of the electron rich $[Ru_2(\mu\text{-CO})(CO)_4(\mu\text{-dppm})_2]$, 2.1, was also explored and it was found that the complex 2.1 is remarkably reactive towards sterically less demanding unsaturated organic reagents and forms several interesting new products. Whereas these reactions were only exploratory in nature, the evidence indicates that simple alkynes react with 2.1 in steps to forms several new species.

Chapter 3 described the synthesis of highly substituted ruthenium carbonyl cluster $[Ru_3(CO)_6(\mu\text{-dppm})_3]$, 3.1, from the reduction of Ru(III) with $NaBH_4$ in the presence of dppm under an atmosphere of CO gas. The structure of 3.1 was established by single crystal X-ray diffraction studies. It is also shown that this electron rich cluster complex is very reactive towards small molecules. For example, HBF_4 yielded the protonated adduct $[Ru_3(\mu\text{-H})(CO)_6(\mu\text{-dppm})_3]^+$, 3.2, whose structure was also established using X-ray crystallography. The presence of hydride was confirmed by spectroscopic means and it was also correctly located from the difference Fourier map and by comparison of the structures of 3.1 and 3.2. Spectroscopic data also indicate that the hydride is fluxional and the mechanism of fluxionality was proposed.

Chapter 4 documents reactions of cobalt halide salts with $NaBH_4$ in the presence of dmpm and CO. Two remarkably different products were isolated by adjusting reaction conditions. Thus when the metal to dmpm ratio was 1:2.5 or

higher it produced the binuclear complex $[Co_2(CO)_4(\mu\text{-dmpm})_2]$ (4.1). In solution, it exists as a mixture of isomers $[Co_2(\mu\text{-CO})_2(CO)_2(\mu\text{-dmpm})_2]$ 4.1a, and $[Co_2(CO)_4(\mu\text{-dmpm})_2]$ 4.1b and these species are fluxional, with the carbonyl groups migrating from terminal to bridging positions. The details of the mechanisms were investigated using variable temperature multinuclear NMR and FT-IR techniques which shows that there is very small activation energy involved for the interconversion of these isomers. These studies also indicates that the dimeric products of cobalt formed with dppm and dmpm are paramagnetic in solution at room temperature and diamagnetic in the solid state and at lower temperature in solutions.

When the cobalt : dmpm ratio was approximately 1:1, the reduction with $NaBH_4$ in the presence of CO resulted in the formation of a tetranuclear cluster, $[Co_4(\mu\text{-CO})_3(CO)_5(\mu\text{-dmpm})_2]$. The formation of an analogous tetranuclear cluster with dppm, using the same route has not been observed. This indicates that the steric bulk of the ligand plays an important role in determining the products formed by this synthetic route. Steric bulk of the ligand also influences the reactivity of the products formed. Thus, the dppm complex $[Co_2(CO)_4(\mu\text{-dppm})_2]$ did not react with group 11 metal complexes, whereas $[Co_2(CO)_4(\mu\text{-dmpm})_2]$ reacted with $[Cu(MeCN)_4]BF_4$ to produce a remarkable mixed metal cluster $[Co_4Cu_3(CO)_8(dmpm)_4]BF_4$. This cluster is unique since it contains a copper atom which has an unprecedented square planar stereochemistry in cluster complexes.

The work described in chapter 5 gives a definitive solution to the structure of $[NiCl_2(dppm)_2]$ in the solid state. The X-ray diffraction studies have shown that one of the dppm ligands is coordinated in a chelating fashion while the other is acting as

monodentate ligand and that the nickel has the unexpected coordination number of five and contains both monodentate and bidentate dppm ligands. This work thus shows that dppm can chelate to nickel by forming a four membered strained ring and is the first example of a structurally characterized nickel complex with a chelating dppm ligand.

Chapter 6 outlines the details of the experimental, spectroscopic and theoretical tools used collectively to get insight into the mechanism of formation and the unusual structure of binuclear nickel complexes. Thus, the MO calculations performed on the dinuclear nickel complex $[Ni_2(\mu\text{-}CO)(Cl)_2(\mu\text{-}dppm)_2]$, 6.1 and the platinum analogue 6.2, shows that the observed structures 6.1 or 6.2 are more stable than other possible structures. However, the calculations gave very similar results for the Pt and Ni derivatives and so easy interconversion between these structures might be predicted. The NMR data show that the less symmetrical nickel complex 6.1 is fluxional and, on the NMR time scale, has the symmetry characteristic of 6.2. The fluxionality is rapid even at -90°C and requires an intermediate or transition state with a symmetrically bridging CO ligand. The complex 6.1 on heating yielded rather unexpectedly a trinuclear cluster $[Ni_3(\mu_3\text{-}CO)(\mu_3\text{-}Cl)(\mu\text{-}dppm)_3]^+$ which could also be readily prepared in high yield by refluxing $[Ni_2(\mu\text{-}CO)(CO)_2(\mu\text{-}dppm)_2]$ in $C_2H_4Cl_2$. As shown by X-ray crystallography, the cluster contains unsymmetrically bridging carbonyl and chloride ligands. This cluster completes the first triad of trinuclear clusters of the type $[M_3(\mu_3\text{-}CO)(\mu_3\text{-}Cl)(dppm)_3]^+$ of group 10 metals.

Finally, chapter 7 described the reduction of nickel salts with BH_3CN^-, a mild reducing agent, in the presence of dmpm and CO gas, which produced two markedly

different products, a dinuclear complex, which resulted from the B-C bond cleavage of BH_3CN^-, and a trinuclear cluster complex. The reaction products were found to be dependent on the experimental conditions such as the duration of the reaction and the metal : ligand ratio. The dinuclear nickel complex $[Ni_2(CN)_4(\mu\text{-dmpm})_2]$, 7.1 has the same trans geometry as that of the dppm bridged palladium and platinum analogues. There are two major differences between $[Ni_3(\mu_3\text{-CO})(\mu\text{-dmpm})_4]^{2+}$, 7.2 and its platinum analogue. Firstly, the CO group is triply bridging in the case of nickel while it is doubly bridging in the platinum cluster. Secondly, the nickel cluster is found to be fluxional at room temperature while the platinum cluster is a non fluxional species. In conclusion, reactions of metal salts with $NaBH_4$ or $NaBH_3CN$ in the presence of dppm, dmpm, and CO have been studied. The one step synthesis of electron-rich carbonyl complexes from cheaply available metal halides is very attractive and the high yield synthesis of new complexes by this method is reproducible and convenient. However, the unpredictability of the reduction is certainly a major problem in further extension of the synthetic method. The electron rich complexes have shown remarkable reactivity and several interesting new clusters have been formed.

APPENDIX 1

Details of Instruments and Chemicals Used in Experiments.

Nuclear Magnetic Resonance Spectroscopy:

^{1}H NMR spectra were recorded on a Varian XL-200 or Gemini-200 spectrometer. $^{13}C\{^{1}H\}$ and $^{31}P\{^{1}H\}$ spectra were recorded on a Varian XL-300 or Gemini-300 spectrometers. ^{1}H and $^{13}C\{^{1}H\}$ chemical shifts were measured relative to Me_4Si. $^{31}P\{^{1}H\}$ chemical shifts were measured relative to 85% H_3PO_4.

IR Spectroscopy:

All IR spectra were run as Nujol mulls (unless otherwise mentioned) between NaCl plates on a Bruker IR/32 FT-IR spectrometer equipped with an IBM 9000 computer.

UV-Visible Spectroscopy:

Ultraviolet and visible spectra were recorded on a Varian Cary 2290 spectrometer. The diffuse reflectance spectra were obtained on a UV-260 Shimadzu Double Beam spectrophotometer.

Mass Spectrometery:

Mass spectra were obtained from a Finnigan MAT 8230 mass spectrometer.

Elemental Analyses:

Elemental analyses were carried out either at Guelph Chemical Laboratories or at Galbraith Laboratories Inc.

Magnetic Moment:

The magnetic susceptibility of solid samples were recorded on a MSB-1 Magnetic Susceptibility Balance by Johnson and Matthey Inc.

Melting Point:

The melting points of new compounds were determined using a Fisher Scientific Electrothermal Melting Point Apparatus.

Glove Box:

A Vacuum Atmospheres Company HE-43-2 DRI-LAB was used to handle various air sensitive reagents.

Sources of Chemicals:

All metal salts, phosphines, solvents, deuterated solvents, ^{13}CO and miscellaneous chemicals were purchased from Aldrich, Strem, Fischer or BDH and used without further purification (unless otherwise mentioned).